Proceedings of the

Thirty-First DOE Solar Photochemistry Research Meeting

Solar Photo chemistry

MS&E Solar

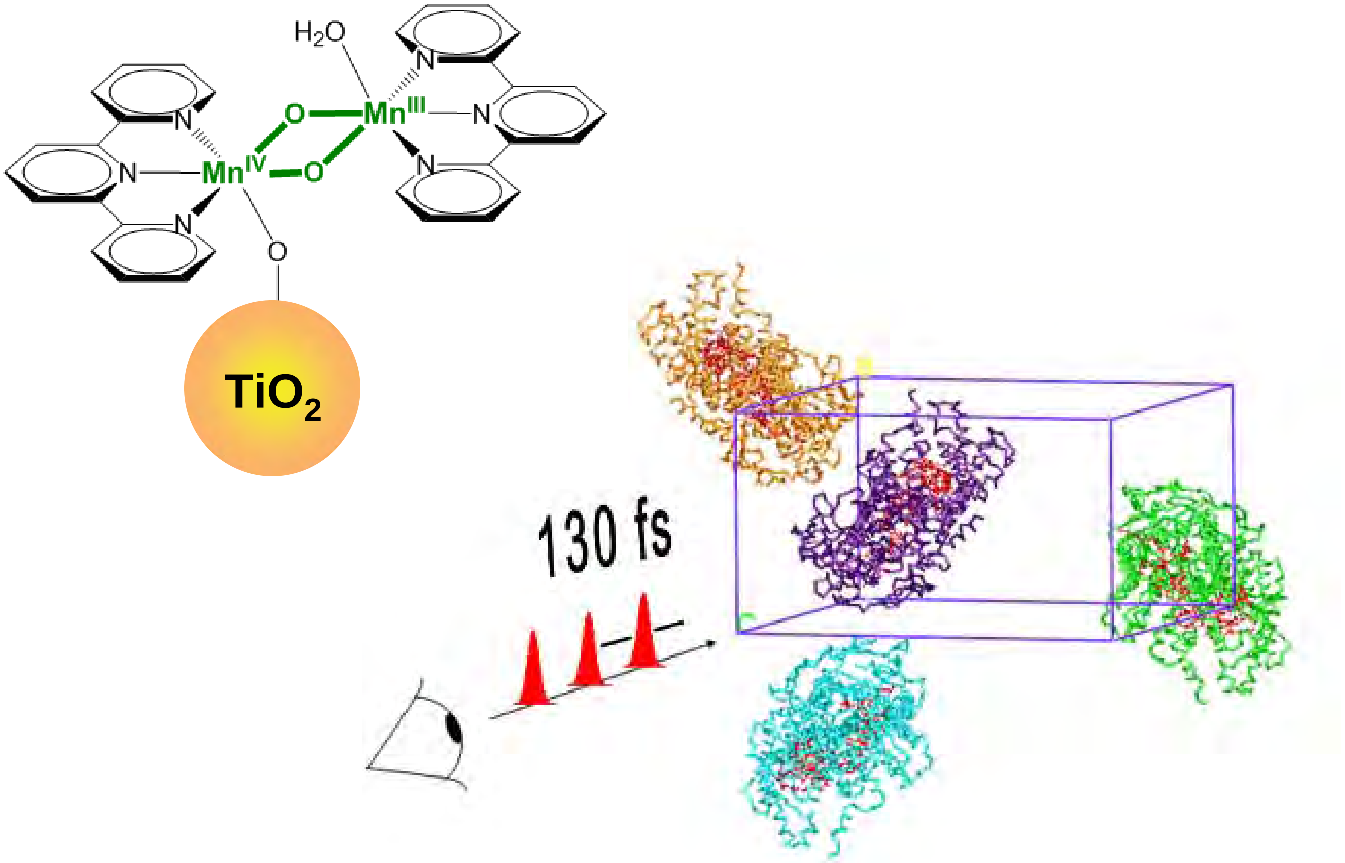

Westin Annapolis Hotel Annapolis, MD June 7-10, 2009

Sponsored by:

Chemical Sciences, Geosciences, and Biosciences Division
U.S. Department of Energy

Program and Abstracts

Solar Photochemistry Program
Research Meeting

Westin Annapolis Hotel
Annapolis, Maryland
June 7-10, 2009

Chemical Sciences, Geosciences, and Biosciences Division
Office of Basic Energy Sciences
Office of Science
U.S. Department of Energy

Cover Graphics:
The cover figures are drawn from the abstracts of this meeting. One represents the function of oxomanganese catalysts attached to TiO_2 for solar fuel production (Brudvig et al.). Another depicts the ultrafast imaging of photosynthetic solar energy at nanometer resolution (Tiede et al.). A third shows the exciton localization within long chain fluorine oligomers (Miller).

This document was produced under contract number DE-AC05-06OR23100 between the U.S. Department of Energy and Oak Ridge Associated Universities.

The research grants and contracts described in this document are supported by the U.S. DOE Office of Science, Office of Basic Energy Sciences, Chemical Sciences, Geosciences and Biosciences Division and their invited

FOREWORD

The 31st Department of Energy Solar Photochemistry Research Meeting, sponsored by the Chemical Sciences, Geosciences, and Biosciences Division of the Office of Basic Energy Sciences, is being held June 7-10, 2009 at the Westin Annapolis Hotel in Annapolis, Maryland. These proceedings include the meeting agenda, abstracts of the formal presentations and posters of the conference, and an address list for the participants.

This Conference is composed of the grantees who do research in solar photochemical energy conversion with the support of the Chemical Sciences, Geosciences, and Biosciences Division. The purpose of the meeting is to foster collaboration, cooperation, and the exchange of new concepts and ideas between these researchers. The resultant synergy is a major strength of this Program and engenders the standard of excellence in research required to sustain this Program over the years. With this fiscal year comes the arrival of Energy Frontier Research Centers to Basic Energy Sciences which will provide a renewed and expanded source of funding for research in solar photoconversion. Many of these Centers are chaired by members of this program.

The Solar Photochemistry Research Meeting will have a number of guests this year from sibling programs in Basic Energy Sciences. For the most part, these are the researchers who won grant awards in the Basic Research Needs solicitation for Solar Energy Utilization in 2007 from the Materials Science and Engineering Division. They will present posters and talks on their approaches to research in solar photoconversion. One of their members will serve as the special guest lecturer for this conference, Professor Xiaoyang Zhu from the University of Minnesota who will present his research on charge separation from excitons in junctions of quantum dots. In the conference sessions that follow there will be presentations on both homogeneous and heterogeneous splitting of water, photosynthetic photoconversion, photophysics of nanostructures, and on organic molecular junctions and systems.

I would like to express my appreciation to Larry Rahn for his help in the assembly of this abstract book, to Diane Marceau of the Division of Chemical Sciences, Geosciences, and Biosciences, Margaret Lyday, and Connie Langston of the Oak Ride Institute of Science and Education for their assistance with the preparation of this volume and the coordination of the logistics of this meeting. I must also thank all of the researchers whose enthusiasm, energy, and dedication to scientific inquiry have enabled these advances in solar photoconversion and made this meeting possible.

Mark T. Spitler
Chemical Sciences, Geosciences,
and Biosciences Division
Office of Basic Energy Sciences

Solar Photochemistry Research Conference Overview

Time	Sunday, June 7	Monday, June 8	Tuesday, June 9	Wednesday, June 10	
7:00		Continental Breakfast	Continental Breakfast	Continental Breakfast	7:00
8:00					8:00
8:30		Opening Remarks	Session V	SessionVIII	8:30
8:45		Session I *Opening Speaker*			8:45
9:00					9:00
9:30					9:30
9:45		Break			9:45
10:00				Break	10:00
10:15		Session II	Break		10:15
10:30			Session VI	Session IX	10:30
11:00					11:00
11:30					11:30
11:50					11:50
12:20		Lunch	Lunch	Lunch	12:20
12:30					12:30
12:45					12:45
1:00			Free Afternoon	Session X	1:15
1:30		Session III			1:30
2:00					2:00
2:30		Free Time			2:30
2:45				Closing Remarks	2:45
3:00	Registration (3:00 - 6:00 P.M.) No Host Reception				3:00
3:30					3:30
4:00					4:00
4:30					4:30
5:00		Session IV			5:00
5:30			Session VII		5:30
6:00					6:00
6:30	Dinner	Dinner	Social Hour Dinner		6:30
7:00					7:00
7:30					7:30
8:00		Posters (odd numbers) Refreshments			8:00
8:30	Reception (cont.)		Posters (even numbers) Refreshments		8:30
9:00					9:00
9:30					9:30

Table of Contents

TABLE OF CONTENTS

Foreword iii

Overview iv

Program xv

Abstracts of Oral Presentations

Session I – Opening Session

The Coulomb Barrier in Excitonic Charge Separation
Xiaoyang Zhu, University of Minnesota 3

Session II – Mechanistic Aspects of Homogeneous Solar Photochemistry

Thermal and Photodriven Water Oxidation Catalyzed by an All-Inorganic Tetra-Ruthenium Polyoxometalate
Yurii V. Geletii, Claire Besson, Zhuangqun Huang, Yu Hou, Qiushi Yin, Alexsey Kuznetsov, Rui Cao, Kenneth I. Hardcastle, Alexey L. Kaledin, Djamaladdin G. Musaev, Tianquan Lian and **Craig L. Hill,** Emory University 7

Ru(II) Complexes that Catalyze Water Oxidation
Ruifa Zong, Huan-Wei Tseng, Zeping Deng, Gang Zhang and **Randolph Thummel,** University of Houston 10

Photogeneration of Hydride Donors and Their Use Toward CO_2 Reduction
Etsuko Fujita, James T. Muckerman and Dmitry E. Polyansky, Brookhaven National Laboratory 13

Highly Reducing Metal-Alkylidyne Chromophores and Assemblies
Benjamin M. Lovaasen, Daniel O'Hanlon, and **Michael D. Hopkins**, The University of Chicago 18

Session III –Theory of Electron Transfer in Donor-Acceptor Pairs

Reduced Electronic Spaces for Modelling Donor/Acceptor Interactions
Marshall D. Newton, Brookhaven National Laboratory 23

Electron-Transfer Under Dynamical Arrest
Brandon Deason, Naoki Ito, Ranko Richert, **Dmitry V. Matyushov** and **Ian R. Gould**, Arizona State University 25

Session IV – Photosynthetic Photoconversion

Mapping Structure with Function in Biomimetic and Natural Photosynthetic Architectures
David M. Tiede, Karen L. Mulfort, Jenny V. Lockard, Lisa M. Utschig, Oleg Poluektov, Lin X. Chen, Libai Huang, Shana Bender, Iltai Kim and Gary Wiederrecht, Argonne National Laboratory 31

Photosynthetic Interprotein Electron Transfer
Lisa M. Utschig, Oleg G. Poluektov, Lin X. Chen, Jenny V. Lockard, Sergey Milikisiyants and David M. Tiede, Argonne National Laboratory 35

Session V – Heterogeneous Systems for Solar Photoconversion

Chemical Control Over the Electrical Properties of GaAs and Zn_3P_2 Semiconductor Surfaces and Photoelectrodes
Gregory M. Kimball, Matthew C. Traub, and **Nathan S. Lewis**, California Institute of Technology 41

Controlled Nitrogen Doping of TiO_2 for Visible Light Photoactivity
M.A. Henderson, S.A. Chambers, T. Ohsawa, I. Lyubinetsky and Y. Du, Pacific Northwest National Laboratory 45

From Molecular to Microstructural Design of Heterometallic Oxide/Organic Solids for Visible-Light Photocatalysis
Paul A. Maggard, North Carolina State University 48

Session VI – Molecular Photocatalysis at Surfaces

Oxomanganese Catalysts for Solar Fuel Production
W. Brudvig, Victor S. Batista, Robert H. Crabtree and Charles A. Schmuttenmaer**,** Yale University 53

Heterobinuclear Units for Driving H_2O Oxidation or CO_2 Reduction Catalysts on Silica Nanopore Surfaces
Heinz Frei, Lawrence Berkeley National Laboratory 56

Toward Photochemical Water Splitting Using Band-Gap-Narrowed Semiconductors and Transition-Metal Based Molecular Catalysts
James T. Muckerman, José A. Rodriguez and Etsuko Fujita, Brookhaven National Laboratory 59

Session VII – Dye Sensitized Semiconductors

Monodispersed Zinc Oxide Nanoparticle-Dye Dyads and Triads: Characterization of the Early Events in Dye-Sensitized Semiconductor Electrodes
David A. Blank, **Wayne L. Gladfelter** and Kent R. Mann, University of Minnesota 67

First-Row Transition Metal-Based Chromophores for Dye-Sensitized Semiconductors: Fundamental Issues and Applications
Amanda Smeigh, Allison Brown, Lindsey Jamula, Dong Guo and **James K. McCusker**, Michigan State University 70

Session VIII – Photophysics of Quantum Dots

Carrier Multiplication in Semiconductor Nanocrystals: Current Status and Challenges
Victor I. Klimov, Los Alamos National Laboratory 75

Hot Electron Dynamics in Quantum Dots
Byungmoon Cho, William K. Peters, Robert J. Hill, and **David M. Jonas**, University of Colorado 77

Imaging of Energy and Charge Transport in Nanoscale Systems
Jao van de Lagemaat and Manuel Romero, National Renewable Energy Laboratory 79

Session IX – Photocatalysis in Nanostructures

Nanostructured Photocatalytic Water Splitting Systems
W. Justin Youngblood, Kazuhiko Maeda, Seung-Hyun Anna Lee, Renzhi Ma, Hideo Hata, Paul G. Hoertz, Yoji Kobayashi, Miharu Eguchi, Lucas Jellison, Thomas A. Moore, Ana L. Moore, Devens Gust and **Thomas E. Mallouk,** The Pennsylvania State University 83

"Electrochemically Wired" Semiconductor Nanoparticles: Toward Vectoral Electron Transport in Hybrid Systems
Neal R. Armstrong, Jeffrey Pyun and S. Scott Saavedra, University of Arizona 86

Insights into Redox Catalysis on Metallic Particles
Dan Meisel, University of Notre Dame 88

Session X – Charge Separation in Structural Organic Molecular Systems

Defects, Doping and Transport in Excitonic Semiconductors
Brian A. Gregg, Ziqi Liang, Dong Wang and Michael Woodhouse, National Renewable Energy Laboratory 93

Conjugated Ionomers for Photovoltaic Structures
Mark C. Lonergan, University of Oregon 96

Charge Transfer at Conjugated Polymer-Fullerene Interfaces
Garry Rumbles, Nikos Kopidakis, Andrew Ferguson, David Coffey, Jeffrey Blackburn and Michael Heben, National Renewable Energy Laboratory 99

Poster Abstracts (by poster number)

1. Organic Solar Materials: Photoconversion and Concentrators
Carlijn Mulder, Philip Reusswig, Tim Heidel, Marc Baldo, Seth Difley and Troy Van Voorhis 105

2. Single Molecule Spectroscopic Studies of Charge Separation and Charge Transfer
Rodrigo E. Palacios, Joshua C. Bolinger, Kwang Jik Lee, William M. Lackowski and Paul F. Barbara 106

3. Variations in the Quantum Efficiency of Multiple Exciton Generation for a Series of Chemically-Treated PbSe Nanocrystal Films
Matthew C. Beard, Aaron Midgett, Matt Law, Octavi Semonin, Randy J. Ellingson and Arthur J. Nozik 107

4. Theory of One- and Two-Electron Transfer between Quantum Dots
D. Balamurugan, S.S. Skourtis and D.N. Beratan 108

5. Interactions of Single-Walled Carbon Nanotubes with Polymers: Implications for Separations and Photochemistry
Jeff Blackburn, John-David Rocha, Andrew Ferguson, Brian Larsen, Pravas Deria, Michael Therien, Garry Rumbles and Michael Heben 109

6. Hole Transfer Dynamics in Tetrapyrrolic Dyads
James R. Diers, Masahiko Taniguchi, Dewey Holten, Jonathan S. Lindsey and David F. Bocian 110

7. Photoinitiated Electron Collection in Mixed-Metal Supramolecular Complexes: Development of Photocatalysts for Hydrogen Production
Karen J. Brewer, Travis White, Shamindri Arachchige, David Zigler and Krishnan Rangan 111

8. Basal Plane Chemistry of Graphene
Louis Brus 112

9. Hot Vibrational State Structures of Photoexcited State Metal Complexes Revealed by Laser-Initiated Time-Resolved X-Ray Absorption Spectroscopy
Lin X. Chen, Jenny V. Lockard, Andrew B. Stickrath, Xiaoyi Zhang, Klaus Attenkofer and Guy Jennings 113

10. Electrochemical Routes to Construct α–Fe_2O_3 Photoelectrodes
Ryan L. Spray, Kenneth J. McDonald and Kyoung-Shin Choi 114

11. The Crystalline-Nanocluster Ti-O Phase: Studying Nanoparticles with Adsorbed Molecules in Periodic Arrays
Philip Coppens and Jason Benedict 115

12. Design and Synthesis of Robust Anchors for Solar Fuel Production
Bill McNamara, Laura Allen, Victor Batista, Gary Brudvig, Charles Schmuttenmaer, Robert Crabtree 116

13. Coupled Electron and Proton Transfer? A Pulse Radiolysis Study
Diane Cabelli, Brian W. Cohen, and Carol Creutz 117

14. New Open-Loop Control Methodologies to Identify Phase Sensitivity in the Preparation of Excited State Populations: Experiments and Simulations to Explore Coherent Controllability of MEG in Lead-Selenide Quantum Dots
Niels H. Damrauer, Erik M. Grumstrup and Matthew A. Montgomery 118

15. Ultrafast Spectroscopic Studies of Charge Injection into Zeolites
Prabir Dutta, Bern Kohler 119

16. Light Driven Generation of Hydrogen from Water: New Developments, New Strategies and New Results
Pingwu Du, Theodore Lazarides, Theresa McCormick, Genggeng Luo, Jacob Schneider, Paul Jarosz, William Brennessel and Richard Eisenberg 120

17. Light-Matter Interactions in Semiconductor Nanocrystalline Absorbers
Randy J. Ellingson 121

18. Light Induced Charge Separation Employing Copper Phenanthroline Complex Chromophores
C. Michael Elliott, Megan Lazorski and Lance Ashbrook 122

19. Quantum Dynamics, Photosynthesis and its Regulation
Graham R Fleming, Akihito Ishizaki, Yuan-Chung Cheng, Tae Ahn, Tessa Calhoun and Gabriela Schlau-Cohen 123

20. Ordered Sensitized Heterojunctions: Bottom-up Electrochemical Synthesis of Copper Indium Disulfide in Oriented N-Titania Nanotube Arrays
Qing Wang, Kai Zhu, Nathan R. Neale and Arthur J. Frank 125

21. Electronic Structure Calculations on Nanostructures: Theory and Applications
Ting Wang, Louis Brus, Mike Steigerwald, Art Bovachevarov and Richard A. Friesner 126

22. Model Dyes for Study of Molecule/Metal Oxide Semiconductor Interfaces and Electron Transfer Processes
Chi Hang Lee, Artem Khvorostov, Piotr Piotrowiak and Elena Galoppini 127

23. The Photocatalytic Reduction of CO_2 in Supercritical CO_2 and Ionic Liquids
David C. Grills, Mark D. Doherty, Etsuko Fujita 128

24. Si-Doped α–Fe_2O_3 Nanotube Arrays for Efficient Water-Photoelectrolysis
Thomas J. LaTempa, Xinjian Feng, Maggie Paulose, and Craig A. Grimes 129

25. Porphyrin-Fullerene Electropolymers for Solar Energy Conversion
Devens Gust, Thomas A. Moore, Ana L. Moore, Paul A. Liddell, Miguel Gervaldo, Gerdenis Kodis, Bradley Brennan and James Bridgewater 130

26. Type-Separated Nanotube Electrodes in THz, Electrochemical, and Photoelectrochemical Investigations
Jeffrey L. Blackburn, Drazenka Svedruzic, Matthew C. Beard, Chaiwat Engtrakul, Robert C. Tenent, Paul W. King and Michael J. Heben 131

27. Excited-State Energy Transfer between Nonadjacent Sites in Multiporphyrin Arrays
Hee-eun Song, Masahiko Taniguchi, Markus Speckbacher, Lianhe Yu, Jonathan S. Lindsey, David F. Bocian and Dewey Holten 132

28. Surface Plasmon Enhancement Effect on Charge Separation in Photosynthetic Reaction Centers
Cameron Postnikoff and Libai Huang 133

29. Adventures with Porphyrinic Super-Chromophores
Joseph T. Hupp 134

30. Photoinitiated Water Oxidation by the "Blue Dimer"
Jonathan L. Cape and James K. Hurst 135

31. The Kinetics of Triplet Formation and Decay in Dimers and Solids Designed for Singlet Fission
Justin C. Johnson, Arthur J. Nozik, Akin Akdag and Josef Michl 136

32. Quantum Dot Sensitized Systems for Solar Photoconversion. A Tale of Two Semiconductor Nanocrystals: CdSe and CdTe.
Jin Ho Bang, Kevin Tvrdy, David Baker and Prashant V. Kamat 137

33. Spin State Dynamics in GaSe Nanoparticles
Hoda Mirafzal, Deborah Lair and David F. Kelley 138

34. Do Carotenoid Neutral Radicals Have a Role in LHC II?
Lowell D. Kispert, A. Ligia Focsan, Tatiana A. Konovalova, Péter Molnár and Nikolay E. Polyakov 139

35. Unusually Bright Fluorescence from Single-Walled Carbon Nanotubes
Andrea J. Lee, Xiaoyong Wang, Lisa J. Carlson, and Todd D. Krauss 140

36. Efficient Charge Transport in DNA Diblock Oligomers
Frederick D. Lewis 141

37. Interfacial Charge Transfer Processes in TiO_2-Sensitizer- Ru-POM Photocatalytic Systems for Oxygen Evolution from Water
Zhuangqun Huang, Yurii V. Geletii, Yu Hou, Djamaladdin G. Musaev, Craig L. Hill, Tianquan Lian 142

38. Chlorophylls Stripped (Almost) Naked by De Novo Synthesis
Olga Mass, Masahiko Taniguchi, Marcin Ptaszek, David F. Bocian, Dewey Holten and Jonathan S. Lindsey 143

39. Benzylidene Malononitriles as Probes of Local Solvent Friction
Hui Jin, Chet Swalina, Min Liang, Sergei Arzhantsev, Xiang Li and Mark Maroncelli 144

40. Electron Transfer Dynamics in Efficient Molecular Enhanced Semiconductors
Shane Ardo, Amanda J. Morris and Gerald J. Meyer 145

41. Surface and Solution Water Oxidation
Javier J. Concepcion, Jonah Jurss, M. Kyle Brennaman, John M. Papanikolas and Thomas J. Meyer 146

42. Fast Electrons, Faster Excitons in Conjugated "Molecular Wires"
John R. Miller, Andrew R. Cook, Paiboon Sreearunothai, Sadayuki Asaoka, Norihiko Takeda, Sean McIlroy, Julia M. Keller and Kirk Schanze, Yuki Shibano and H. Imahori 147

43. Catalyst Design and Electron Transfer Mechanism between the Multiple Components of a Solar Energy-Driven Water Splitting Nanosystem
Aleksey E. Kuznetsov, Alexey L. Kaledin, Yurii Geletii, Tianquan Lian, Craig L. Hill and Djamaladdin G. Musaev 148

44. Infrared Light Trapping in Nanocrystalline Inverse Opal Photoelectrodes
Nathan R. Neale, Arthur J. Nozik and Arthur J. Frank 149

45. Sensitization of Titanium Dioxide Single Crystals with CdSe Quantum Dots
Justin Sambur and B. A. Parkinson 150

46. Femtosecond Kerr-Gated Fluorescence Microscopy
Lars Gundlach and Piotr Piotrowiak 151

47. Photoinduced Charge Separation in Polymer-C_{70}-Fullerene Composites: High - Frequency Pulsed EPR Spectroscopy
Oleg Poluektov, Juan Delgado, Nazario Martín, Andreas Sperlich and Vladimir Dyakonov 152

48. High Level Ab Initio Calculations of Photoexcited States and Electron-Phonon Interactions in Semiconductor Quantum Dots
Oleg. V. Prezhdo 153

49. Synthesis and Photophysics of Linear, Branched and Dendrimeric Conjugated Polyelectrolytes
Seoung Ho Lee, Xiaoyong Zhao, Prasad Tarenekar, Sevnur Kumurlu, Gustavo Moriena, Quentin Bricaud, Valeria D. Kleiman, John R. Reynolds and Kirk S. Schanze 154

50. Conjugated Polyelectrolyte Films: Morphology, Energy Transport and Charge Injection
Jarrett Vella, Quentin Bricaud, Hui Jiang, Justin Sambur, Derek LaMontagne, Bruce A. Parkinson, Valeria D. Kleiman, John R. Reynolds and Kirk S. Schanze 155

51. Long Wavelength Visible Light Absorbing Chromophores with Lifetimes Extended Via Reversible Energy Transfer
Jing Gu, Jin Chen and Russell Schmehl 156

52. Probing Interfacial Electron Transfer Using THz Spectroscopy
C. P. Richter, R. L. Milot, Gonghu Li, R. H. Crabtree, G. W. Brudvig, V. S. Batista and C. A. Schmuttenmaer 157

53. Single-Chain, Helical Wrapping of Individualized, Single-Walled Carbon Nanotubes by Ionic Poly(Aryleneethynylene)s Provide Diverse Organic Solvent Solubility
Pravas Deria, Youn K. Kang, One-Sun Lee, Sang Hoon Kim, Tae-Hong Park, Dawn A. Bonnell, Jeffery G. Saven and Michael J. Therien 158

54. Nanocrystal-Based Dyads for Solar to Electric Energy Conversion
M. Wu, G. Gotesman, P. Mukherjee, R. Naaman and D.H. Waldeck 159

55. Direct Measurement of Photoinduced Charge Separation Distances in Donor-Acceptor Systems for Artificial Photosynthesis
Raanan Carmieli, Annie Butler Ricks, Qixi Mi, Emilie M. Giacobbe, Sarah M. Mickley, and Michael R. Wasielewski 160

56. Multistage Photocell for Water Splitting
Marye Anne Fox, James K. Whitesell and Xuebin Shao 161

57. Metal-Linked Artificial Oligopeptides as Photoinitiated Molecular Wires
Carl P. Myers, Lauren A. Levine, Joy A. Gallagher, Richard M. Kelly and Mary Elizabeth Williams 162

58. Exploring Complex Oxides and Graphene for Dye-Sensitized Semiconductors: Synthesis, Assembly and Photoelectrochemistry
Yiying Wu, Mario A. Alpuche, Panitat Hasin and Gayatri Natu 163

LIST OF PARTICIPANTS 165

AUTHOR INDEX 177

Program

31st DOE SOLAR PHOTOCHEMISTRY RESEARCH MEETING

June 7-10, 2009

Westin Annapolis Hotel
Annapolis, Maryland

PROGRAM

Sunday, June 7

3:00 – 6:00 p.m.	Registration
5:30 – 9:30 p.m.	Reception
6:30 – 8:00 p.m.	Dinner

Monday Morning, June 8

SESSION I
Opening Session
Mark T. Spitler, Chair

7:00 a.m. Continental Breakfast

8:00 a.m. Opening Remarks
Eric Rohlfing and **Mark Spitler**, Department of Energy

8:45 a.m. **Opening Lecture**.
The Coulomb Barrier in Excitonic Charge Separation
Xiaoyang Zhu, University of Minnesota

9:45 a.m. Coffee Break

SESSION II
Mechanistic Aspects of Homogeneous Solar Photochemistry
Thomas Meyer, Chair

10:15 a.m. Thermal and Photodriven Water Oxidation Catalyzed by an All-Inorganic Tetra-Ruthenium Polyoxometalate
Craig L. Hill, Emory University

10:45 a.m. Ru(II) Complexes that Catalyze Water Oxidation
Randolph Thummel, University of Houston

11:15 a.m. Photogeneration of Hydride Donors and Their Use Toward CO_2 Reduction
Etsuko Fujita, Brookhaven National Laboratory

11:45 a.m. Highly Reducing Metal-Alkylidyne Chromophores and Assemblies
Michael D. Hopkins, The University of Chicago

12:20 p.m. Lunch

Monday Afternoon, June 8

SESSION III
Theory of Electron Transfer in Donor-Acceptor Pairs
Oleg Prezhdo, Chair

1:30 p.m. Reduced Electronic Spaces for Modelling Donor/Acceptor Interactions
Marshall D. Newton, Brookhaven National Laboratory

2:00 p.m. Electron-Transfer Under Dynamical Arrest
Dmitry V. Matyushov, Arizona State University

SESSION IV
Photosynthetic Photoconversion
Lin Chen, Chair

5:00 p.m. Mapping Structure with Function in Biomimetic and Natural Photosynthetic Architectures
David M. Tiede, Argonne National Laboratory

5:30 p.m. Photosynthetic Interprotein Electron Transfer
Lisa M. Utschig, Argonne National Laboratory

6:30 p.m. Dinner

7:30 p.m. Posters (Odd numbers)
Refreshments

Tuesday Morning, June 9

7:30 a.m. Continental Breakfast

SESSION V
Heterogeneous Systems for Solar Photoconversion
Arthur Frank, Chair

8:30 a.m. Chemical Control Over the Electrical Properties of GaAs and Zn_3P_2 Semiconductor Surfaces and Photoelectrodes
Nathan S. Lewis, California Institute of Technology

9:00 a.m. Controlled Nitrogen Doping of TiO_2 for Visible Light Photoactivity
M.A. Henderson, Pacific Northwest National Laboratory

9:30 a.m. From Molecular to Microstructural Design of Hetetrometallic Oxide/Organic Solids for Visible-Light Photocatalysis
Paul A. Maggard, North Carolina State University

10:15 a.m. Coffee Break

SESSION VI
Molecular Photocatalysis at Surfaces
Michael Elliott, Chair

10:30 a.m. Oxomanganese Catalysts for Solar Fuel Production
W. Brudvig and **Victor S. Batista,** Yale University

11:00 a.m. Heterobinuclear Units for Driving H_2O Oxidation or CO_2 Reduction Catalysts on Silica Nanopore Surfaces
Heinz Frei, Lawrence Berkeley National Laboratory

11:30 a.m. Toward Photochemical Water Splitting Using Band-Gap-Narrowed Semiconductors and Transition-Metal Based Molecular Catalysts
James T. Muckerman, Brookhaven National Laboratory

Tuesday Afternoon, June 9

12:20 p.m. Lunch

Tuesday Evening, June 9

SESSION VII
Dye Sensitized Semiconductors
Elena Galoppini, Chair

5:30 p.m. Monodispersed Zinc Oxide Nanoparticle-Dye Dyads and Triads: Characterization of the Early Events in Dye-Sensitized Semiconductor Electrodes
Wayne L. Gladfelter, University of Minnesota

6:00 p.m. First-Row Transition Metal-Based Chromophores for Dye-Sensitized Semiconductors: Fundamental Issues and Applications
James K. McCusker, Michigan State University

6:30 p.m. Social Hour
7:30 p.m. Dinner

8:30 p.m. Posters (Even numbers)
Refreshments

Wednesday Morning, June 10

7:30 a.m. Continental Breakfast

Session VIII
Photophysics of Quantum Dots
Piotr Piotrowiak, Chair

8:30 a.m. Carrier Multiplication in Semiconductor Nanocrystals: Current Status and Challenges
Victor I. Klimov, Los Alamos National Laboratory

9:00 a.m. Hot Electron Dynamics in Quantum Dots
David M. Jonas, University of Colorado

9:30 a.m. Imaging of Energy and Charge Transport in Nanoscale Systems
Jao van de Lagemaat, National Renewable Energy Laboratory

10:00 a.m. Coffee Break

Session IX
Photocatalysis in Nanostructures
Richard Eisenberg, Chair

10:30 a.m. Nanostructured Photocatalytic Water Splitting Systems
Thomas E. Mallouk, The Pennsylvania State University

11:00 a.m. “Electrochemically Wired” Semiconductor Nanoparticles: Toward Vectoral Electron Transport in Hybrid Systems
Neal R. Armstrong, University of Arizona

11:30 a.m. Insights into Redox Catalysis on Metallic Particles
Dan Meisel, University of Notre Dame

Wednesday Afternoon, June 10

12:20 p.m. Lunch

Session X
Charge Separation in Structural Organic Molecular Systems
John Miller, Chair

1:15 p.m. Defects, Doping and Transport in Excitonic Semiconductors
Brian A. Gregg, National Renewable Energy Laboratory

1:45 p.m. Conjugated Ionomers for Photovoltaic Structures

Mark C. Lonergan, University of Oregon

2:15 p.m. Charge Transfer at Conjugated Polymer-Fullerene Interfaces
Garry Rumbles, National Renewable Energy Laboratory

2:45 p.m. Closing Remarks
Mark Spitler and **Richard Greene**, U.S. Department of Energy

Session I

Opening Session

THE COULOMB BARRIER IN EXCITONIC CHARGE SEPARATION

Xiaoyang Zhu
Department of Chemistry
University of Minnesota
Minneapolis, MN 55455

When a molecular material is electronically excited by a photon, the Coulomb attraction between the excited electron and the hole gives rise to an atomic-H-like quasi-particle called an exciton. The bound electron-hole pair also forms across a material interface, such as the donor/acceptor (D/A) interface in an organic heterojunction solar cell; the results are charge-transfer (CT) excitons. In a conventional p-n junction cell, the exciton binding energy is very small and there is a built-in potential to ensure charge separation. In contrast, there is no a priori a built-in potential in a solar cell based on organic molecules and polymers. Charge separation requires an energetic driving force provided by the differences in the electronic levels at the D/A interface. From typical dielectric constants of organic semiconductors and sizes of conjugated molecules, one can estimate that the Coulomb energy of a CT exciton across a D/A interface is more than one order of magnitude greater than k_BT at room temperature. We can also estimate this by solving the Schrödinger equation in a dielectric continuum model. The results are a series of atomic-H like states with the binding energy of the 1s state on the order of a few hundred meV, Fig. 1. How can the e-h pair escape this Coulomb trap? To answer this question, we carry out two experiments: femtosecond time-resolved two-photon photoemission (TR-2PPE) spectroscopy to probe the physical nature of the CT excitons and vibrational spectroscopy to probe charge transfer and electric field at buried interfaces.

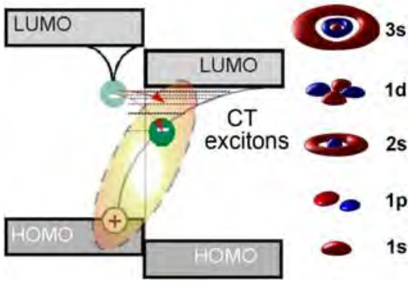

Fig. 1. Schematic illustration of charge transfer excitons at an organic donor-acceptor interface. Also shown are wavefunctions of a few CT excitons from numerical solutions to the Schrödinger equation within a dielectric continuum model.

To probe the CT excitons, we use a crystalline pentacene thin film as a model system and excite an electron above the surface [1,2]. When there is only the excess electron, the electron is bound to the surface by the positive polarization cloud in the pentacene molecules; this attractive potential leads to a bound electronic state called an image potential state. When a positive hole is present on a pentacene molecule, the electron is attracted to the surface by both the positive hole and the polarization cloud; the result of this combined attractive potential is approximately the CT exciton referenced to the image band. We observe in TR-2PPE spectroscopy a series

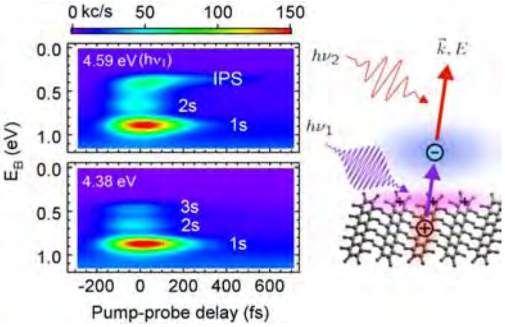

Fig. 2. Pseudo color plots of TR-2PPE spectra at different pump-probe delay times for a ~20 nm thick polycrystalline pentacene thin film grown on Si(111). The binding energy scale is referenced to the vacuum level. At $h\nu_1 = 4.38$ eV (lower panel), the 1s, 2s, & 3s CT excitons are clearly resolved. When $h\nu_1$ is increased to 4.59 eV, the delocalized image potential state (IPS) is also observed.

of CT excitons with binding energies ≤0.5 eV below the image band minimum, Fig. 2. The CT_{1s} exciton—often referred to as the exciplex—has a very low probability of dissociation. We conclude that hot CT exciton states must be involved in charge separation for three reasons. (1) Compared to CT_{1s}, hot CT excitons are more weakly bound; (2) Density-of-states of hot excitons increase with energy in the Coulomb potential; & (3) Electronic coupling from a donor exciton to a hot CT exciton can be higher than that to CT_{1s} as expected from energy resonance arguments.

Little is known about the possibility of electric field at the D/A interface. This field may come from direct charge transfer, from unintentional doping, or from charge redistribution or polarization at the D/A interface resulting from the equilibration of the charge neutrality level (similar to the Fermi level) of the two organic semiconductors [3]. Experimentally, the presence of charge transfer and interfacial field in a bulk heterojunction can be probed by vibrational spectroscopy and the Stark effect [4]. We apply this approach to a model bulk heterojunction system of poly-3-hexyl-thiophene (P3HT) and phenyl-C61-butyric acid methyl ester (PCBM) shown at the top of Fig. 3. Here, the C=O stretch vibrational peak serves as probe of charge transfer and interfacial field. We spin coat a 1:1 (weight) mixture of regio-regular P3HT and PCBM on a Ge waveguide and solvent annealed the sample overnight. Fig. 3 shows FTIR spectra in the C=O stretch region for the heterojunciton with different P3HT MW. We arrive at two conclusions: 1) there is minor peak (1720 cm^{-2}) due to charge transfer from P3HT to PCBM, leading to the formation of PCBM anions at the interface, as verified by chemically reduced PCBM (black); 2) there is Stark shift in the main peak (1738 cm^{-1}), which corresponds to an interfacial electric field of 10^6 V/cm. However, the field is in the wrong direction for charge separation and is a barrier for exciton dissociation.

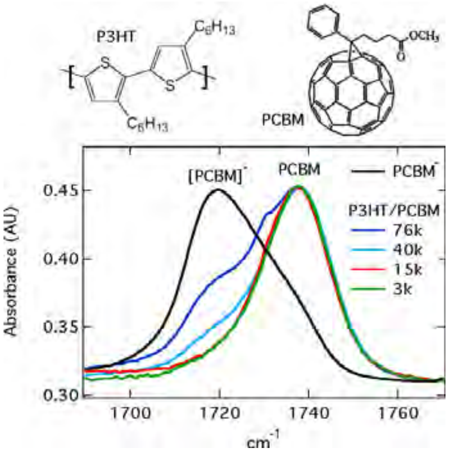

Fig. 3. FTIR spectra for P3HT/PCBM bulk heterojunctions. Also shown is a spectrum (black) for chemically reduced PCBM. The colors correspond to different P3HT molecular weight.

References

1. Muntwiler, M.; Yang, Q.; Tisdale, W. A.; Zhu, X.-Y. "Coulomb barrier for charge separation at an organic semiconductor interface," *Phys. Rev. Lett.* **2008**, *101*, 196403.

2. Zhu, X.-Y.; Yang, Q.; Muntwiler, M. "Charge transfer excitons at organic semiconductor surfaces and interfaces," *Acct. Chem. Res.* **2009**, *42*, in press.

3. Vazquez, H.; Gao, W.; Flores, F.; Kahn, A. "Energy level alignment at organic heterojunctions: role of the charge neutrality level," *Phys. Rev. B* **2005**, *71*, 041306R.

4. Barbour, L. W.; Hegadorn, M.; Asbury, J. B. "Watching Electrons Move in Real Time: Ultrafast Infrared Spectroscopy of a Polymer Blend Photovoltaic Material," *J. Am. Chem. Soc.* **2007**, *129*, 15884-15894.

5. Mills, T.; Goertz, M.; Zhu, X.-Y. "Charge transfer and interfacial electric field in polythiophene/fullerene bulk heterojunction solar cells," to be published.

Session II

Mechanistic Aspects of Homogeneous Solar Photochemistry

THERMAL AND PHOTODRIVEN WATER OXIDATION CATALYZED BY AN ALL-INORGANIC TETRA-RUTHENIUM POLYOXOMETALATE

Yurii V. Geletii, Claire Besson, Zhuangqun Huang, Yu Hou, Qiushi Yin, Alexsey Kuznetsov,
Rui Cao, Kenneth I. Hardcastle, Alexey L. Kaledin, Djamaladdin G. Musaev, Tianquan Lian,
Craig L. Hill

Department of Chemistry and Emerson Center of Scientific Computing
Emory University
Atlanta, GA 30322

The major thrusts of our integrated experimental-computational project are (1) to develop (design, prepare and characterize) fast, selective, and stable solar-driven photocatalytic systems to oxidize water to O_2 and protons; (2) to understand the structural (geometric and electronic) features central to interfacing such catalysts successfully with the principal photosensitizer materials and nanosystems available at present, and (3) to train young scholars in both the experimental and computational challenges in this multi-disciplinary solar fuel targeted effort. To date the three-PI project has yielded 5 publications[1-5] with several more in submission or about to be submitted. Progress has been made toward all three program goals and considerable progress has been made on (1).

Shortly after our grant began we developed the first molecular water oxidation catalyst (WOC), a tetraruthenium polyoxometalate, $Rb_8K_2[\{Ru_4O_4(OH)_2(H_2O)_4\}(\gamma\text{-}SiW_{10}O_{36})_2]$ (**1**), that is hydrolytically and thermally stable (X-ray structure in Figure 1).[2] More importantly, **1** contains no organic ligands or structure so it is resistant to oxidative degradation, the inevitable lifetime-limiting issue with all other homogeneous WOC systems reported to date. Complex **1** has been characterized by spectroscopic, physicochemical and other methods. Cyclic voltammetry indicates that **1** exhibits a catalytic wave for water oxidation/O_2 evolution near the thermodynamic potential for this process.[2] This complex also catalyzes the rapid totally homogeneous oxidation of water to O_2 by $[Ru(bpy)_3]^{3+}$ in pH 7 water, eq 1.[2] A joint Italian/American group prepared **1** by another method and demonstrated that it catalyzed water oxidation in strong acid by Ce(IV). DFT calculations reveal that **1** likely derives from dimerization of the oxidized, i.e. Ru^{IV}_2 form of the “monomer”.[4] Experiments and calculations indicate that the Ru^{III}_2 monomer reacts with O_2; the microscopic reverse, water oxidation, is highly endothermic.[4] This is in contrast to the structurally similar “blue dimer” WOC of Meyer and co-workers that has been carefully studied recently by multiple groups. The Ru^{III}-O-Ru^{III} moiety in the blue dimer is thermodynamically stable with respect to oxidation by O_2.

$$4\,[Ru(bpy)_3]^{3+} + 2\,H_2O \rightarrow 4\,[Ru(bpy)_3]^{2+} + O_2 + 4\,H^+ \qquad (1)$$

Most recently (work to be submitted shortly) we have established several of the oxidation and protonation states of **1**, and documented properties of different oxidation states. The initially prepared **1** (and its resting oxidation state under ambient conditions) has all the Ru centers in the 4+ oxidation state, i.e. $\{Ru^{IV}_4\}$. The one-electron-oxidized form, $\{Ru^{IV}_3Ru^{V}\}$, has been isolated and characterized by X-ray crystallography and other techniques. Thorough electrochemical studies, detailed thermodynamic analysis and kinetic studies indicate that the O_2-evolving species is $\{Ru^{V}_4\}$, and this forms upon oxidation of $\{Ru^{IV}_4\}$ by four sequential one-electron reactions by $[Ru(bpy)_3]^{3+}$. The overall reaction (followed by decay of green colored $[Ru(bpy)_3]^{3+}$ and formation of intensely orange colored $[Ru(bpy)_3]^{2+}$) proceeds quickly (within several mins) in the presence of 2-8 μM **1** with O_2 yields (quantified by GC analysis) up to 75% and turnover numbers, TON = $[O_2]$/[Ru_4-POM], up to ~10^2 .

Most recently **1** was shown to catalyze rapid, visible-light-driven water oxidation using $S_2O_8^{2-}$ and $[Ru(bpy)_3]^{2+}$ as a sacrificial electron acceptor and photosensitizer, respectively.[5] The $[Ru(bpy)_3]^{3+}$ is generated *in situ* via eq 2. The general features of the photo-driven catalytic process are summarized in Scheme 1.

$$2\,[Ru(bpy)_3]^{2+} + S_2O_8^{2-} + h\nu \rightarrow 2\,[Ru(bpy)_3]^{3+} + 2\,SO_4^{2-} \qquad (2)$$

Scheme 1. Light-induced water oxidation catalytic cycle using $[Ru(bpy)_3]^{2+}$ as a photosensitizer and persulfate as a sacrificial electron acceptor.[5] Typical experimental conditions: 0.5-1.0 mM, $[Ru(bpy)_3]^{2+}$, 2.5-10 mM $Na_2S_2O_8$, 2.5-5.0 μM Ru_4-POM, 20-50 mM sodium phosphate buffer, initial pH 7.2

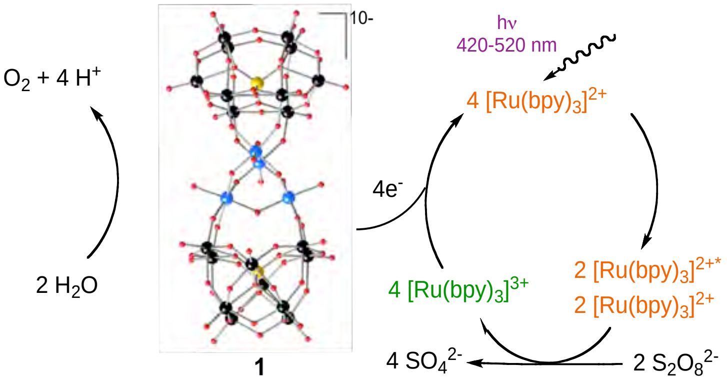

1

(atom code: Ru, O, W, Si)

In Scheme 1 and eq 2, dioxygen is formed quickly (typical reaction time is 0.5-1.0 hr) under visible light (420-520 nm) illumination. The reaction stops when all the persulfate is consumed. A gradual decrease in pH from the initial 7.2 to 6.3 and a gradual (<10-15 %) decomposition of $[Ru(bpy)_3]^{2+}$ are also observed. Under minimally optimized conditions (see Scheme 1), the O_2 yield per persulfate (eq 2) is *ca* 40% with up to ~3.5x10^2 turnovers and with a turnover frequency (TOF) up to ~8x10^{-2} s^{-1}.[5] The experimentally measured quantum yield is *ca* 9%. We also used steady-state luminescence quenching to examine the quenching of $[Ru(bpy)_3]^{2+*}$ by $S_2O_8^{2-}$ under conditions similar to those in Scheme 1. For example, 5.0 mM $Na_2S_2O_8$ in 20 mM sodium phosphate buffer solution quenches *ca.* 67% of the excited state to generate $[Ru(bpy)_3]^{3+}$.[5] The theoretical overall quantum yield is estimated to be *ca.* 26%, significantly larger than the measured value. The reason for this discrepancy is under investigation.

Detailed TD-DFT calculations, including spin-orbit coupling, and use of a simple exciton interaction model, show that electron transfer between the visible photoexcited $[Ru(bpy)_3]^{2+*}$ and $S_2O_8^{2-}$ (the first part of the process shown in Scheme 1) occurs via S_1 (MLCT state) to T_1 decay.

Most recently we have developed a tetra-cobalt polyoxometalate with WOC activity. This complex, **2**, appears to be as fast as any known homogeneous WOC. Like **1**, it is all inorganic and in preliminary experiments does not appear to degrade during turnover. Voltammetric data, kinetics behavior, SAXS and electron microscopy on both **1** and **2** indicate that neither appear to degrade to form Ru or Co oxide/hydroxide nanoparticles that are known to catalyze water oxidation. In addition, rates for water oxidation by $[Ru(bpy)_3]^{3+}$ catalyzed by either Ru and Co oxides (controls) are far lower those for **1** and **2**.

DOE Sponsored Publications 2006-2008

1. Hill, C. L.; Delannoy, L.; Duncan, D. C.; Weinstock, I. A.; Renneke, R. F.; Reiner, R. S.; Atalla, R. H.; Han, J. W.; Hillesheim, D. A.; Cao, R.; Anderson, T.; Okun, N. M.; Musaev, D. G.; Geletii, Y. "Complex catalysts from self repairing ensembles to highly reactive air-based oxidation systems" *Comptes Rendus Chimie*, **2007**, *10,* 305-312.

2. Geletii, Y. V.; Botar, B.; Kögerler, P.; Hillesheim, D. A.; Musaev, D. G.; Hill, C. L. "An all-inorganic, stable and highly active tetra-ruthenium homogeneous catalyst for water oxidation"*Angew. Chem. Int. Ed.* **2008**, *47*, 3896-3899.

3. Cao, R.; Han, J.-H.; Anderson, T. M.; Hillesheim, D. A.; Hardcastle, K. I.; Slonkina, E.; Hedman, B.; Hodgson, K. O.; Kirk, M. L.; Museav, D. G.; Morokuma, K.; Geletii, Y. V.; Hill, C. L. "Late Transition Metal Oxo Compounds and Open-Framework Materials that Catalyze Aerobic Oxidations" *Adv. Inorg. Chem.* **2008**, *60*, 245-272 (Chapter 6).

4. Kuznetsov, A. E.; Geletii, Y. V.; Hill, C. L.; Morokuma, K.; Musaev, D. G. "Mechanism of O_2-based Oxidation of the Diruthenium-substituted γ-Keggin Polyoxotungstate [γ-$Ru^{III}_2(H_2O)_2H_2SiW_{10}O_{38}]^{4-}$: Comparison with the "Blue Dimer" Water Oxidation Catalyst" *J. Am. Chem. Soc.* **2009**, *131*, ASAP.

5. Geletii, Y. V.; Huang, Z.; Hou, Y.; Musaev, D. G.; Lian, T.; Hill, C. L. "Homogeneous Light-Driven Water Oxidation Catalyzed by an Organic-Structure-Free Tetraruthenium Complex" *J. Am. Chem. Soc.* **2009**, *131* in press.

RU(II) COMPLEXES THAT CATALYZE WATER OXIDATION

Ruifa Zong, Huan-Wei Tseng, Zeping Deng, Gang Zhang, and Randolph Thummel
Department of Chemistry, 136 Fleming Building
University of Houston, Houston, TX 77204-5003

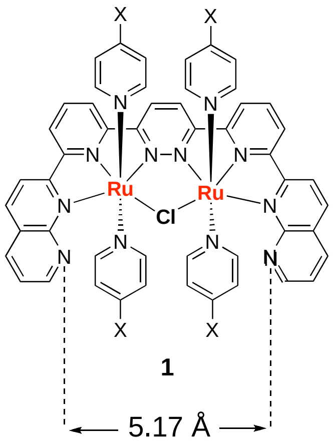

1

We have completed an initial study on a series of 13 dinuclear Ru(II) complexes such as **1** which behave as catalysts for water decomposition. The structures of these catalysts were varied in several different ways. Seven different 4-substituted pyridines as the axial ligands were examined along with variations in the peripheral naphthyridine and central pyridazine binding groups. The relative rates of oxygen evolution were measured and found to change from 1-51 while the turnover numbers (TNs) varied from 80-689. There appeared to be an approximately linear relationship between rate and TN. An x-ray structure of one of the catalysts was completed and showed considerable distortion of the bridging ligand in the equatorial plane. The distance between the two outermost nitrogens in the bridging ligand decreases from an estimated 9.50 Å in the free ligand to 5.17 Å in the complex **1**. To test the importance of the two closely situated Ru(II) centers, we examined several mononuclear complexes **2** in which the environment around the metal center was, as nearly as possible, identical to what is found in **1**. Surprisingly, these complexes were found to also be effective water oxidation catalysts (TN = 20-260).

To better understand the activity and to improve the effectiveness of these catalysts, we studied 20 other closely related mono-nuclear Ru(II) complexes which were organized into two groups. One group included complexes of the type [Ru(tpy)(NN)Cl](PF_6) (tpy = 2,2'; 6,2"-terpyridine) where NN is one of twelve different bidentate ligands. The second group included various combinations of 4-picoline, bpy (bpy = 2,2'-bipyridine), and tpy as well as the tetradentate dpp (dpp = 2,9-dipyrid-2'-yl-1,10-phenanthroline). The long wavelength MLCT absorption and the first oxidation and reduction potentials were found to be consistent with the structure of the complexes. Of the 20 complexes, 11 catalyze water oxidation and all of these

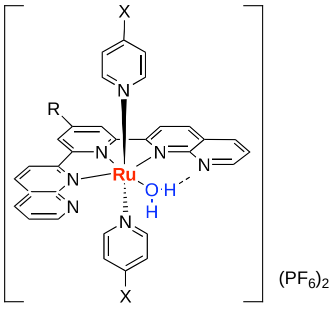

X = NMe_2, Me, CF_3
R = H, *t*-Bu, Br, CO_2H

2

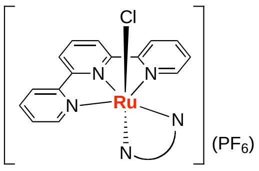

3

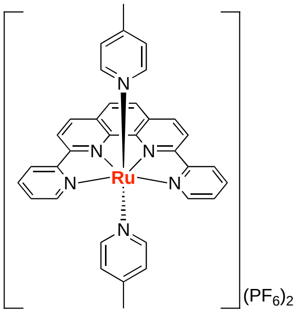

4

contain a tpy derivative or dpp. Kinetic measurements indicate a first order reaction and this fact is further verified by examination of a di-*t*-butyl substituted complex which would experience steric hindrance with respect to dimer formation.

An important issue regarding the possible involvement of RuO_2 was addressed. The kinetic profile for (slow) water oxidation by RuO_2 was compared with similar profiles for several of our catalysts. The slower catalysts are suspect in this regard, but the more active catalysts look much different (Figure 1). A catalyst recovery experiment was carried out for [Ru(bpy)(tpy)Cl]Cl which was examined by NMR after the consumption of 40 equiv. of Ce(IV). The catalyst appears to be unchanged (Figure 2) and a tentative mechanism is proposed which involves a 7-coordinate ^{VI}Ru=O species which is attacked by water to form the critical O-O bond.

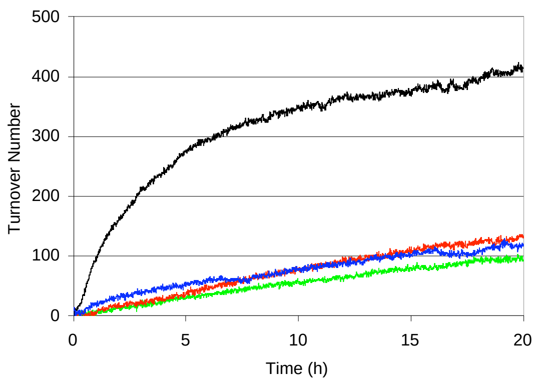

Figure 1. Kinetic plots of oxygen evolution vs time for complexes $[Ru(tpy)(4\text{-pic})_3]^{2+}$ (green), $[Ru(bpy)(tpy)(4\text{-pic})]^{2+}$ (red), $[Ru(dpp)(4\text{-pic})_2]^{2+}$ (black), and RuO_2 (blue).

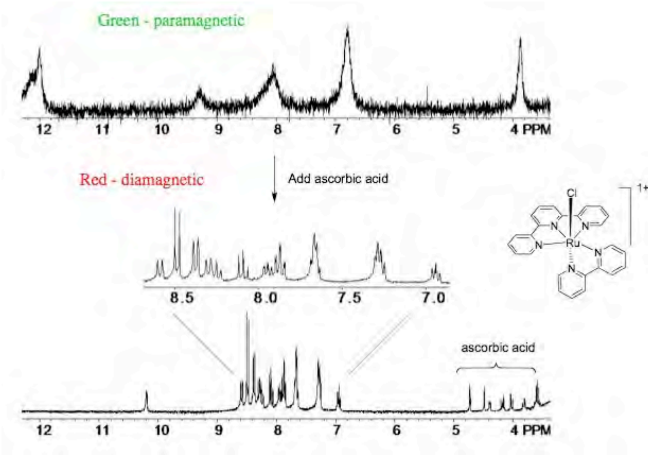

Figure 2. (top) Downfield region of the ^1H NMR spectrum in CD_3CN of the green material precipitated as a PF_6 salt from the water oxidation reaction catalyzed by [Ru(tpy)(bpy)Cl]Cl. (bottom) The same NMR spectrum after the addition of ascorbic acid (ascorbic acid peaks at 3.5-4.8 PPM).

We are currently in the process of examining other catalysts closely related to [Ru(bpy)(tpy)Cl]Cl in an effort to better understand the important features of the oxidation process and also to optimize catalyst performance. The ligand 2-(pyrid-2’-yl)-1,8-naphthyridine (pynap) is a pyrido-fused analog of bpy. The complex [Ru(pynap)(tpy)Cl]Cl shows the highest turnover (1170) of any system yet examined. Two analogous complexes involving 2,9-dimethylphenanthroline and a six-membered chelate ring help to indicate some features which may be necessary for good activity.

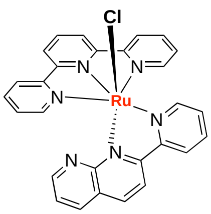

TN = 1170

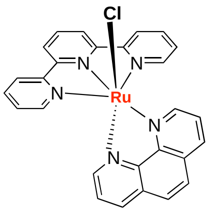

TN = 400

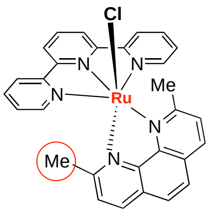

TN = 0

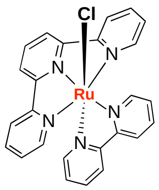

TN = 390

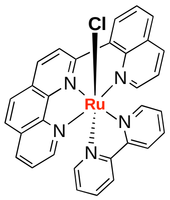

TN = 0

Publications 2005-2009

"Enhanced Luminescence in a Pt(II) Complex Involving a Six-Membered Chelate Ring" Hu, Y.-Z.; Wilson, M. H.; Zong, R.; Bonnefous, C.; McMillin, D. R.; Thummel, R. P. *JCS Dalton Trans.* **2005**, 354-358.

"A New Family of Ru Complexes for Water Oxidation," Zong, R.; Thummel, R. P. *J. Am. Chem. Soc.* **2005**, *127,* 12802-12803.

"Ruthenium(II) Complexes of 1,12-Diazaperylene and their Interactions with DNA," Chouai, A.; Wicke, S.; Turro, C.; Bacsa, J.; Dunbar, K.; Thummel, R. P. *Inorg. Chem.* **2005**, *44,* 5996-6003.

"Synthetic Approaches to Polypyridyl Bridging Ligands with Proximal Multidentate Binding Sites," Zong, R.; Wang, D.; Hammitt, R.; Thummel, R. P. *J. Org. Chem.* **2006**, *71*, 167-175.

"The Preparation and Study of a Family of Dinuclear Ru(II) Complexes which Catalyze the Decomposition of Water," Deng, Z.; Tseng, H.-W.; Zong, R.; Wang, D.; Thummel, R. *Inorg. Chem.* **2008**, *47,* 1835-1848 (invited Forum article).

"Ru(II) Complexes of Tetradentate Ligands Related to 2,9-Di(pyrid-2'-yl)-1,10-phenanthroline," Zhang, G.; Zong, R.; Tseng, H.-W.; Thummel, R. P. *Inorg. Chem.* **2008**, *47,* 990-998.

"Enhanced Metal Ion Selectivity of 2,9-Di-(pyrid-2-yl)-1,10-phenanthroline and Its Use as a Fluorescent Sensor for Cadmium(II)," Cockrell, G. M.; Zhang, G.; VanDerveer, D. G.; Thummel, R. P.; Hancock, R. D. *J. Am. Chem. Soc.* **2008**, *130,* 1420-1430.

"Mononuclear Ru(II) Complexes That Catalyze Water Oxidation," Tseng, H.-W.; Zong, R.; Muckerman, J. T.; Thummel, R. *Inorg. Chem.* **2008**, *47,* 11763-11773.

"1,5-Naphthyridine as a New Linker for the Construction of Bridging Ligands and their Corresponding Ru(II) Complexes," Singh, A. N.; Thummel, R. P. *Inorg. Chem.* **2009**, submitted.

PHOTOGENERATION OF HYDRIDE DONORS AND THEIR USE TOWARD CO_2 REDUCTION

Etsuko Fujita, James T. Muckerman, Dmitry E. Polyansky
Chemistry Department
Brookhaven National Laboratory
Upton, NY 11973-5000

Despite substantial effort, no one has succeeded in efficiently producing methanol from CO_2 using homogeneous photocatalytic systems. We are pursuing reaction schemes based on a sequence of hydride-ion transfers to carry out stepwise reduction of CO_2 to methanol. We are using hydride-ion transfer from photoproduced C–H bonds in metal complexes with bio-inspired ligands (*i.e.*, NADH-like ligands) that are known to store one proton and two electrons.

1. Photogeneration of Hydride Donors: We have shown that a polypyridylruthenium complex with an NAD^+/NADH model ligand, $[Ru(bpy)_2(pbn)]^{2+}$ ($[\mathbf{1}]^{2+}$, bpy = 2,2′-bipyridine, pbn = 2-(2-pyridyl)-benzo[*b*]-1,5-naphthyri-dine) in a wet CH_3CN/amine solution, undergoes proton-coupled two-electron reduction to give $[Ru(bpy)_2(pbnHH)]^{2+}$ ($[\mathbf{1{\bullet}HH}]^{2+}$, pbnHH = 5,10-dihydro-2-(2-pyridyl)-benzo[*b*]-1,5-naphthyridine) upon irradiation of visible light (300-600 nm). When triethylamine was used as a sacrificial electron donor, the quantum yield for $[\mathbf{1{\bullet}HH}]^{2+}$ formation is 0.21 at 355 nm. This result opens a new door to *photoinduced catalytic hydride-transfer reactions !*

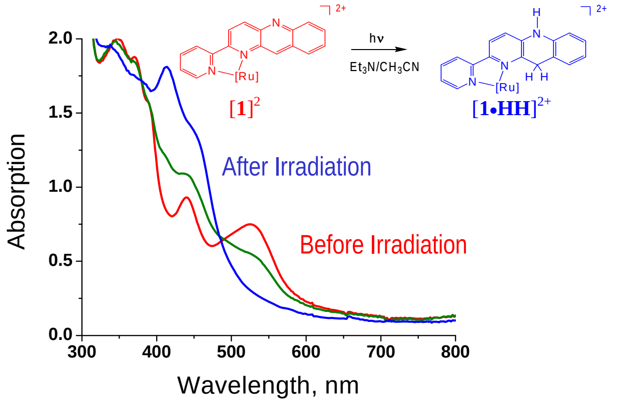

2. Kinetic and Mechanistic Investigation of Hydride Donor Generation by Pulse Radiolysis: Using the pulse radiolysis technique, we determined the mechanism of formation of $[\mathbf{1{\bullet}HH}]^{2+}$ in water. Protonation of the one-electron-reduced species [**2**] takes place below pH 11 to form [**3**] (pK_a ~11). Species [**3**] disproportionates through a π-stacked dimer at low pH (see below), and the dimer dissociates to yield $[\mathbf{1}]^{2+}$ and $[\mathbf{1{\bullet}HH}]^{2+}$. The cross reaction between [**2**] and [**3**] yields the same final products at high pH, probably by forming a N-H···N hydrogen bonding interaction between the two species, the transfer of an electron to [**3**], which subsequently acquires a proton.

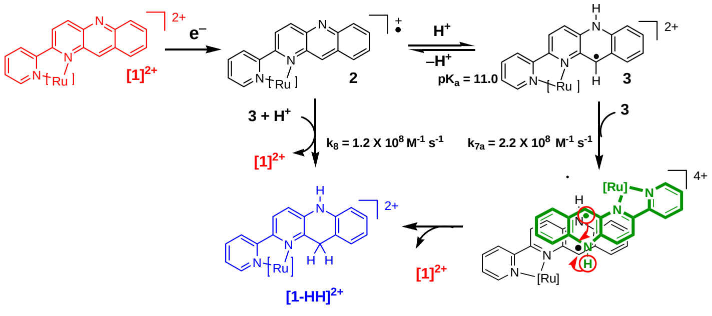

3. Stereo-Specific Photochemical Formation of a C-H Hydride: Our photolysis experiments with D_2O and H_2O solutions containing $[\mathbf{1}]^{2+}/CH_3CN$/triethanolamine produced $[\mathbf{1{\bullet}DD}]^{2+}$ (m/z 337.5838**)** and $[\mathbf{1{\bullet}HH}]^{2+}$ (m/z 336.5725**),** respectively. ^1H and ^{13}C NMR indicate that stereo-

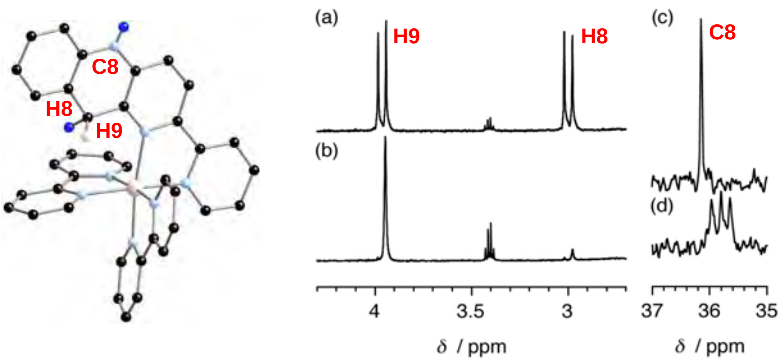

Photoproduct of $[\mathbf{1}]^{2+}$ in H_2O (a) and (c); in D_2O (b) and (d). H8 is located above the pyridine ring of bpy.

specific hydrogenation takes place at C8 (see figure at right) in the photochemical reduction of $[\mathbf{1}]^{2+}$. The reduction of $[\mathbf{1}]^{2+}$ with $Na_2S_2O_4$ in D_2O did not afford any stereospecific products in the deuterization at C8 of pbn. The stereoselective formation of *Δ*-(*S*)-$[\mathbf{1{\bullet}DD}]^{2+}$ and *Λ*-(*R*)-$[\mathbf{1{\bullet}DD}]^{2+}$, which are enantiomers with the same ^{1}H NMR spectra, clearly indicate that a π-stacked dimer is a key intermediate in the photoreduction of $[\mathbf{1}]^{2+}$. The chiral recognition reaction *via* stereospecific dimerization of a racemic mixture of monomers, followed by disproportionation, may open new directions for photochemical stereospecific hydride-transfer reactions to organic molecules.

4. Hydricity and Hydride Transfer Reactions: While $[\mathbf{1{\bullet}HH}]^{2+}$ can transfer a hydride to Ph_3C^+ ($k = 4 \times 10^{-3}\ M^{-1}\ s^{-1}$), it cannot transfer a hydride to CO_2 or M–CO. We have carried out calculations of the thermodynamic hydricity, or hydride donating power, of this photo-generated catalyst and the hydrided form of possible hydride acceptor molecules for hydride transfer reactions related to CO_2 reduction.

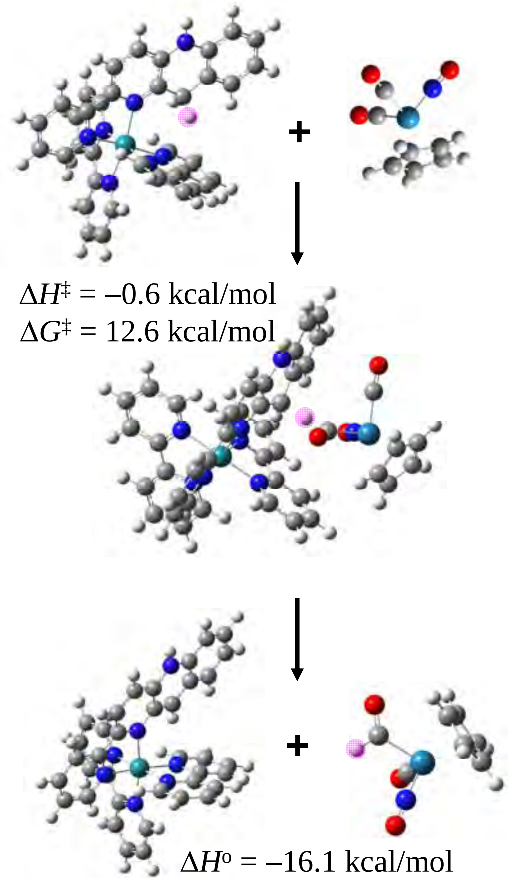

$\Delta H^{\ddagger} = -0.6$ kcal/mol
$\Delta G^{\ddagger} = 12.6$ kcal/mol

$\Delta H^{o} = -16.1$ kcal/mol
$\Delta G^{o} = -15.9$ kcal/mol

Our theoretical calculations predict that free CO is difficult to convert to the formyl anion by hydride transfer reactions, however, M–CO is much easier to convert to M–CHO. Our calculations also show that the further photoreduction of $[\mathbf{1{\bullet}HH}]^{2+}$ can create a $[\mathbf{1{\bullet}HH}]^{\bullet+}$ species with a dramatically increased hydricity that can donate its hydride to $[CpRe(NO)(CO)_2]^+$ to form CpRe(NO)(CO)(CHO), the most difficult step in CO_2 reduction to methanol. Our experiments indicate that the excited state of $[\mathbf{1{\bullet}HH}]^{2+}$ lives 70 ns and can be reductively quenched by amine to form $[\mathbf{1{\bullet}HH}]^{\bullet+}$, which is a very strong hydride donor that stores the energy of three photons. This suggests that photoinduced hydride transfer reactions to M–C_1 species are possible. In order to test this scenario we are currently carrying out experiments with $[\mathbf{1{\bullet}HH}]^{\bullet+}$. *[This work was carried out in collaboration with Koji Tanaka, Institute for Molecular Science, Japan.]*

DOE Sponsored Publications 2006-2008

Solar Energy Utilization Initiative:

1. Fujita, E.; Muckerman, J. T.; Tanaka, K. “Photochemical CO_2 Reduction by Rhenium and Ruthenium Complexes” *Am. Chem. Soc. Div. Fuel Chem.* **2008**, *53(1).*
2. Polyansky, D. E.; Cabelli, D.; Muckerman, J. T.; Fukushima, T.; Tanaka, K.; Fujita, E. “Mechanism of Hydride Donor Generation using a Ru(II) Complex Containing an NAD^+ Model Ligand: Pulse and Steady-State Radiolysis Studies” *Inorg. Chem.* **2008**, *47*, 3958-3968 (Featured as a cover article).
3. Muckerman, J. T.; Fujita, E. “Artificial Photosynthesis” In *Chemical Evolution II: From Origins of Life to Modern Society. ACS Symposium Series*; Zaikowski, L.; Friedrich, J. M., Eds.; American Chemical Society: Washington, D.C., **2009**, in press.
4. Achord, P.; Fujita, E.; Muckerman, J. T. “Theoretical Investigation of Tuning the Hydricity of Photogenerated Hydrides for Catalytic CO Reduction” in preparation.
5. Fukushima, T.; Fujita, E.; Muckerman, J. T.; Polyansky, D. E.; Tanaka, K. “Stereospecific Photogeneration of a Renewable Hydride Donor” in preparation

Hydrogen Fuel Initiative:

1. Nambu, A.; Graciani, J.; Rodriguez, J. A.; Wu, Q.; Fujita, E.; Fernandez-Sanz, J. “N-doping of TiO_2(110): Photoemission and Density Functional Studies” *J. Chem. Phys.* **2006**, *125*, 094706-1,8.
2. Chen, H.; Nambu, A.; Wen, W.; Graciani, J.; Zhong, Z.; Hanson, J. C.; Fujita, E.; Rodríguez, J. A. “Reaction of NH_3 with Titania: N-doping of the Oxide and TiN formation” *J. Phys. Chem. C* **2007**, *111*, 1366-1372.
3. Jensen, L.; Muckerman, J. T.; Newton, M. D. “First-Principles Studies of the Structural and Electronic Properties of the $(Ga_{1-x}Zn_x)(N_{1-x}O_x)$ Solid Solution Photocatalyst” *J. Phys. Chem. C* **2008**, *112*, 3439-3446.
4. Muckerman, J. T.; Polyansky, D. E.; Wada, T.; Tanaka, K.; Fujita, E. “Water Oxidation by a Ruthenium Complex with Non-Innocent Quinone Ligands: Possible Formation of an O–O Bond at a Low Oxidation State of the Metal. Forum ‘on Making Oxygen’” *Inorg. Chem.* **2008**, *47*, 1787-1802.
5. Tseng, H.-W.; Zong, R.; Muckerman, J. T.; Thummel, R. “Mononuclear Ru(II) Complexes That Catalyze Water Oxidation” *Inorg. Chem.* **2008**, *47*, 11763-11773.
6. Chen, H.; Wen, W.; Wang, Q.; Hanson, J. C.; Muckerman, J. T.; Fujita, E.; Frenkel, A.; Rodriguez, J. A. “Preparation of $(Ga_{1-x}Zn_x)(N_{1-x}O_x)$ Photocatalysts from the Reaction of NH_3 with Ga_2O_3/ZnO and $ZnGa_2O_4$: In situ Time-Resolved XRD and XAFS Studies” *J. Phys. Chem. C* **2009**, *113*, 3650-3659.
7. Shen, X.; Allen, P. B.; Hybertsen, M. S.; Muckerman, J. T. “Water Adsorption on the GaN (1010) Non-polar Surface.” (Letter) *J. Phys. Chem. C* **2009,** *113*, 3365–3368.
8. Tsai, M.-K.; Rochford, J.; Polyansky, D. E.; Wada, T.; Tanaka, K.; Fujita, E.; Muckerman, J. T. “Characterization of Redox States of $Ru(OH_2)(Q)(terpy)^{2+}$ (Q = 3,5-di-tert-butyl-1,2-benzoquinone, terpy = 2,2′:6′,2″-terpyridine) and Related Species through Experimental and Theoretical Studies” *Inorg. Chem.* **2009**, accepted.
9. Boyer, J.; Rochford, J.; Fujita, E. “Ruthenium Complexes with Redox-Active Quinone

Ligands: Electronic Properties and Catalytic Implication" (invited review) *Coord. Chem. Rev.*, submitted.

DOE Core Program:

1. Fujita, E.; Brunschwig, B. S.; Creutz, C.; Muckerman, J. T.; Sutin, N.; Szalda, D. J.; van Eldik, R. "Transition State Characterization for the Reversible Binding of Dihydrogen to Bis(2,2'-bipyridine)rhodium(I) from Temperature- and Pressure-Dependent Experimental and Theoretical Studies" *Inorg. Chem.* **2006**, *45*, 1595-1603.
2. Grills, D. C.; Huang, K.-W.; Muckerman, J. T.; Fujita, E. "Kinetic Studies of the Photoinduced Formation of Transition Metal-Dinitrogen Complexes Using Time-Resolved Infrared and UV-vis Spectroscopy" *Coord. Chem. Rev.* **2006**, *250*, 1681-1695.
3. Grills, D. C.; van Eldik, R.; Muckerman, J. T.; Fujita, E. "Direct Measurements of Rate Constants and Activation Volumes for the Binding of H_2, D_2, N_2, C_2H_4 and CH_3CN to $W(CO)_3(PCy_3)_2$: Theoretical and Experimental Studies with Time-Resolved Step-Scan FTIR and UV-vis Spectroscopy" *J. Am. Chem. Soc.* **2006**, *128*, 15728-15741.
4. Huang, K.-W.; Han, J. H.; Musgrave, C. B.; Fujita, E. "Carbon Dioxide Reduction by Pincer Rhodium η^2-Dihydrogen Complexes: Hydrogen Binding Modes and Mechanistic Studies by Density Functional Theory Calculations" *Organometallics* **2007**, *26*, 508-513.
5. Miyasato, Y.; Wada, T.; Muckerman, J. T.; E. Fujita; Tanaka, K. "Generation of Ru(II)-Semiquinone-Anilino Radical through Deprotonation of Ru(III)-Semiquinone-Anilido Complex" *Angew. Chem. Int. Ed.* **2007**, *46*, 5728-5730.
6. Muckerman, J. T.; Fujita, E.; Hoff, C. D.; Kubas, G. J. "Theoretical Investigation of the Binding of Small Molecules and the Intramolecular Agostic Interaction at Tungsten Centers with Carbonyl and Phosphine Ligands" *J. Phys. Chem. B* **2007**, *111*, 6815-6821.
7. Polyansky, D.; Cabelli, D.; Muckerman, J. T.; Fujita, E.; Koizumi, T.-a.; Fukushima, T.; Wada, T.; Tanaka, K. "Photochemical and Radiolytic Production of Organic Hydride Donor with Ru(II) Complex Containing an NAD^+ Model Ligand" *Angew. Chem. Int. Ed.* **2007**, *46*, 4169-4172.
8. Shinozaki, K.; Hayashi, Y.; Brunschwig, B. S.; Fujita, E. "Characterization of transient species and products in photochemical reactions of $Re(dmb)(CO)_3$ Et with and without CO_2" *Res. Chem. Intermed.* **2007**, *33*, 27-36.
9. Fujita, E.; Muckerman, J. T. "Catalytic Reactions Using Transition-Metal-Complexes toward Solar Fuel Generation" (Invited Review Article) *Bull. Jpn. Soc. Coord. Chem.* **2008**, *51*, 41-54.
10. Huang, K.-W.; Grills, D. C.; Han, J. H.; Szalda, D. J.; Fujita, E. "Selective Decarbonylation by a Pincer PCP-Rhodium(I) Complex" *Inorg. Chim. Acta* **2008**, *361*, 3327-3331.
11. Doherty, M. D.; Grills, D. C.; Fujita, E. "Synthesis and Photophysical Characterization of Fluorinated $Re(4,4'\text{-}X_2\text{-}2,2'\text{-bipyridine})(CO)_3Cl$ Complexes in CH_3CN and $scCO_2$" *Inorg. Chem.* **2009**, *48*, 1796-1798.

12. Achord, P.; Fujita, E.; Muckerman, J. T.; Scott, B.; Fortman, G. C.; Temprado, M.; Xiaochen, C.; Captain, B.; Isrow, D.; Weir, J. J.; McDonough, J. E.; Hoff, C. D. “Experimental and Computational Studies of Binding of Dinitrogen, Nitriles, Azides, Diazoalkanes, Pyridine and Pyrazines to $M(PR_3)_2(CO)_3$ (M = Mo,W; R = Me, ^{i}Pr)” *Inorg. Chem.*, submitted.
13. Doherty, M. D.; Grills, D. C.; Huang, K.-W.; Polyansky, D.; Fujita, E. “Kinetics and Thermodynamics of Small Molecule Binding to a PCP-Pincer Rhodium(I) Complex: Direct Addition to a Three-Coordinate Intermediate” *J. Am. Chem. Soc.*, to be submitted.

HIGHLY REDUCING METAL–ALKYLIDYNE CHROMOPHORES AND ASSEMBLIES

Benjamin M. Lovaasen, Daniel O'Hanlon, and Michael D. Hopkins
Department of Chemistry
The University of Chicago
Chicago, IL 60637

The objective of this project is to develop photochemical energy-storing assemblies with highly reducing excited states capable of activating inert solar-fuel feedstocks such as CO_2. We have focused particularly on the development of luminescent metal–alkylidyne complexes as building blocks for these systems because they possess an unusual combination of desirable features: their redox, optical and photophysical properties are broadly tunable; they participate in proton-coupled electron-transfer reactions, affording potential pathways to catalyst regeneration that do not rely on conventional sacrificial donors; and they are "drop-in" structural/electronic components for oligo and polymeric phenylene-ethynylenes, which are extensively developed materials for molecular electronics, luminescence-based sensing, and photochemical energy conversion applications. This talk will describe progress over the first 18 months of the project directed toward developing each of the above aspects of these compounds, including their integration into strongly reducing charge-separation assemblies of the types shown below.

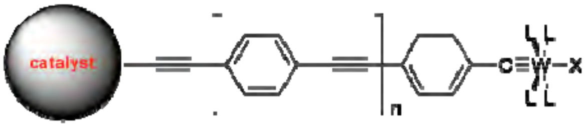

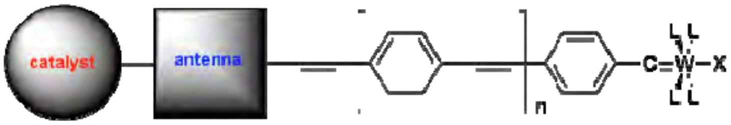

Synthesis and properties of luminescent conjugated metal–alkylidyne complexes. We have developed synthetic methods that enable site-selective metal-for-carbon substitution at any triply bonded site within a phenylene-ethynylene chain, providing hybrid metallo-phenylene-ethynylenes. Examples of this class of compounds that contain terminal tungsten centers (**1**) have been found to be especially well suited for incorporation into reducing photoassemblies. Electronic-spectroscopic, photophysical, and transient-absorption studies, together with DFT calculations, on derivatives of **1** with systematically varied ancillary ligands (e.g., L = PR_3, $P(OR)_3$, CO) and chain lengths (n = 0–3) have established they possess a common $^3[d_{xy} \leftarrow \pi^*]$ emissive state, while electrochemical studies indicate that the most reducing excited states among this class should possess potentials not less than –2.5 V vs. $FeCp_2^{0/+}$. The excited-state structures of these compounds are linear, as deduced by time-resolved XAS studies for $\mathbf{1}_{n=0}$ (in collaboration with Dr. Lin Chen at Argonne) and time-resolved resonance Raman spectroscopy for $\mathbf{1}_{n=1}$ and $\mathbf{1}_{n=2}$. These findings suggest the presence of a π-conjugated pathway for photochemical delivery of electrons through the phenylene-ethynylene chain to a terminal catalyst or electron reservoir.

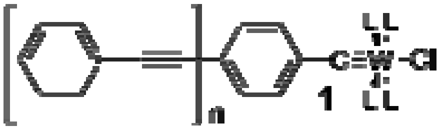

1

We have also discovered that the tungsten center in compounds of type **1** can be protonated to form seven-coordinate alkylidyne hydride ions, as established by NMR spectroscopy and X-ray crystallography. This observation is significant because it opens the way to regenerate the resting d^2 configuration of **1** (following excited-state oxidation) via an H-atom-transfer/deprotonation cycle, rather than through the use of conventional sacrificial donors. We have now demonstrated all forward and reverse steps of this cycle, and begun to characterize the thermodynamic relationships among these compounds.

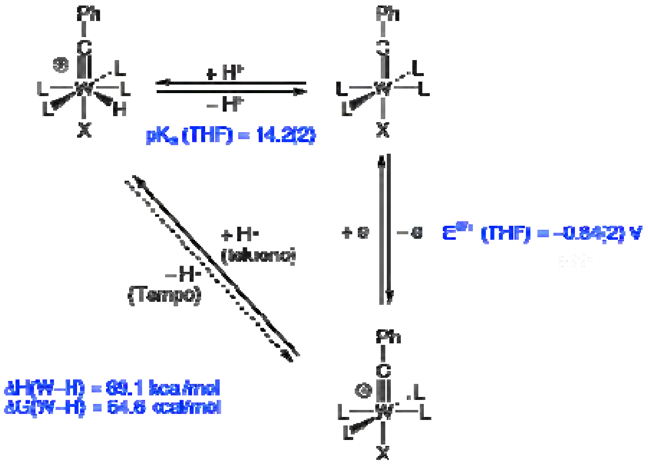

Porphyrin–alkylidyne dyads: Charge separation and lifetime reservoir effects. We have synthesized and characterized dyads comprised of a Zn(TPP) antenna, a tungsten–alkylidyne luminophore/reductant, and a variable-length spacer for the control of energy- and electron-transfer kinetics, for use as platforms for the reductive photosensitization of electrocatalysts. In THF the n = 1 compound undergoes fast charge separation upon photoexcitation to form the strongly reducing $[ZnP]^{-}$—$[W]^{+}$ state. Preliminary experiments indicate that dative attachment to the Zn center of simple organic electron acceptors (PDI, NDI), which serve as redox proxies for to-be-studied electrocatalysts, harvests the electron to produce $[A]^{-}$—ZnP—$[W]^{+}$.

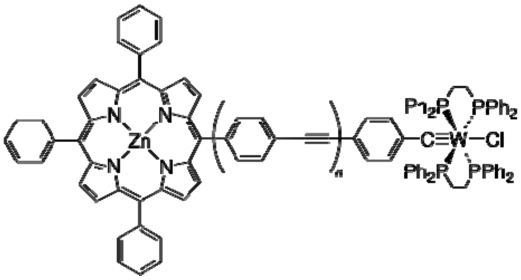

In toluene solution the n = 1 dyad exhibits remarkable photophysical properties. Phosphorescence is observed from the $^{3}[d_{xy} \leftarrow \pi^{*}]$ state of the tungsten center, but with a lifetime that is 20× longer than parent **1**. Spectroscopic data and kinetic modeling suggest this enhancement arises from the thermal equilibrium of the emissive state with the dark T_1 state of the Zn(TPP) center. This lifetime reservoir effect can be tuned significantly via ligation to the Zn center, which pushes the enhancement to > 1000×.

Future studies. The $[ZnP]^{-}$—$[W]^{+}$ state of these dyads is sufficiently reducing to active several known CO_2 reduction catalysts, and we are currently working out the synthetic chemistry needed to append these catalysts to this platform. The photophysical properties and excited-state reactions of the resulting triads will be a major focus of our studies over the next few months. In addition, we are studying the excited-state processes that underlie the extraordinary lifetime reservoir effects manifested by the dyads, with the aim of determining whether Zn(TPP) could be a generally useful adjunct chromophore for improving the photophysical properties of compounds with lifetimes too short for energy-storage or other applications.

DOE Sponsored Publications 2007-2009

1. Dramatically enhanced photoluminescence lifetimes via equilibration with the T_1 excited state of Zn(TPP). B. W. Cohen, B. M. Lovaasen, C. K. Simpson, S. D. Cummings, R. F. Dallinger, M. D. Hopkins. J. Am. Chem. Soc., submitted.

2. Excited-State Structure and Bond Energy of the MoO Bond of d^2 Molybdenum–Oxo Complexes. R. E. Da Re, M. D. Hopkins, Inorg. Chem., submitted.

3. Molecular Structure of the Excited State of d^2 Tungsten–Benzylidyne Complexes. B. W. Cohen, C. K. Simpson, L. X. Chen, M. D. Hopkins, in preparation.

4. Molecular Structures and Acid–Base Chemistry of Fluxional Tungsten–Alkylidyne Hydride Complexes. M. I Newsom, M. D. Hopkins, in preparation.

Session III

Theory of Electron Transfer In Donor-Acceptor Pairs

REDUCED ELECTRONIC SPACES FOR MODELLING DONOR/ACCEPTOR INTERACTIONS

Marshall D. Newton
Chemistry Department, Brookhaven National Laboratory
Upton, New York 11973-5000

Electronic overlap between localized donor (D) and acceptor (A) sites is a crucial factor controlling electronic transfer and transport processes, including those central to schemes for the capture and transformation of solar energy. In conjunction with other factors such as polaron trapping, the strength of the electronic overlap dictates the dynamical transport mechanism in condensed phases: *e.g.*, coherent electron or hole tunneling *vs.* sequential hopping. In modelling electronic transport, a fundamental issue is the nature of the (reduced) electronic state space adopted, and the states constructed within this space. For compactness and computational efficiency, it is desirable to keep the reduced space as small as possible, but with adequate flexibility to accommodate the D/A coupling for the process of interest, including the role of covalently linked bridges or solvent in mediating the coupling. A 2-state space may be suitable, especially for bimolecular cases, if such a space is dominated by orbitals on the D and A sites, and isolated energetically from other states (when a bridge is present, the validity of the 2-state model requires weak coupling of D and A to the bridge, relative to the energy gap between the bridge and the D and A levels). However, in many cases, *e.g.*, where low-lying excited states associated with the D,A, or unsaturated bridge sites are present, larger state spaces should be considered. Once a space is defined, then one can choose the states within this reduced space: *eg*, fully or partially delocalized eigenstates (adiabatic) or localized diabatic states corresponding to the initial and final states in a particular transport process.

Here, we focus on electron transfer (ET) processes and, after defining diabatic states based on an appropriate physical criterion, explore the dependence on state space size of diabatic properties important for mechanistic analysis of ET: effective D/A coupling (H_{DA}), effective D/A separation distance (r_{DA}), and solvent reorganization energy (λ). Results are illustrated for some mixed-valence binuclear ruthenium complexes (with RJ Cave). For bimolecular ET, it may be possible to define diabatic states in terms of the separated (non-interacting) D and A moieties. However, such an approach is usually not well-defined for intramolecular (bridged) systems. Thus we adopt the Generalized Mulliken Hush model (GMH), applicable to an arbitrary state space and arbitrary nuclear configuration, and encompassing both class II and class III situations. Once the electronic state space is selected (a set of $n \geq 2$ adiabatic states), the charge-localized GMH diabatic states are defined as the eigenstates of the dipole moment operator. Addressing questions as to whether the estimate of H_{DA} 'improves' as one increases n, and in what sense the GMH approach ‘converges’ with n, we conclude from the calculations for the mixed-valence Ru systems, that the 2-state model gives the most appropriate estimate of the *effective* coupling, finding that similar magnitudes (within 10%) are obtained by superexchange (se) correction of H_{DA} values based on larger spaces (n=3-5): *ie*, to within 10%, the GMH approach, supplemented by se corrections for n>2, yields an invariant value for H_{DA} over the range explored in the calculations (n=2-5). These results help to reconcile contradictory assertions in the recent literature regarding the proper role of multi-state frameworks in the formulation of coupling for both intra- and intermolecular ET systems. It is important to recognize that the effective H_{DA}

values, while dominated by D and A contributions, nevertheless also contain essential 'tails' from any intervening spacer moiety. When the 2-state model is valid for a given system, these different factors will be suitably balanced, while increasingly larger state spaces for the same system will yield increasingly more localized D and A states, and the corresponding uncorrected (ie, 'bare') coupling element (H_{DA}) will tend to approach the limiting value pertinent to direct (through space) coupling.

DOE Sponsored Publications 2006-2008

1. Mulliken-Hush Elucidation of the Encounter (Precursor) Complex in Intermolecular Electron Transfer via Self–Exchange of Tetracyanoethylene Anion-Radical, S.V. Rosokha, M.D. Newton, M. Head-Gordon, and J.K. Kochi, *Chem. Phys.* **324**, 117 (2006)

2. A parameter free quantum mechanical approach to the calculation of electron transfer rates for large systems in solution, Roberto Improta, Vincenzo Barone , and Marshall D. Newton, *Chem. Phys Chem.* **7**, 1211 (2006)

3. Activation Entropy of Electron Transfer Reactions, A. Milischuk, D. V. Matyushov, and M. D. Newton, *Chem. Phys*. **324**, 172 (2006)

4. A Simple Comparison of Interfacial Electron-Transfer Rates for Surface-Attached and Bulk Solution-Dissolved Redox Moieties, John F. Smalley, Marshall D. Newton, and Stephen W. Feldberg, *J. Electroanal. Chem.* **589**, 1 (2006)

5. Dissociative electron transfer in D-peptide-A systems: results for kinetic parameters from a density functional/polarizable continuum model, Vincenzo Barone, Marshall D. Newton, and Roberto Improta, *J. Phys. Chem. B* **110**, 12632 (2006)

6. Closed form expressions of quantum electron transfer rates based on the stationary phase approximation, Seogjoo Jang and Marshall D. Newton, *J. Phys. Chem. B* **110**, 18996 (2006)

7. The role of dielectric continuum models in electron transfer: theoretical and computational aspects, Marshall Newton, In *"Continuum Solvation Models in Chemical Physics: From Theory to Applications"*, Eds., B. Mennucci and R. Cammi, John Wiley & Sons, Ltd., New York (2007), p389.

8. First-principles Studies on the Structural and Electronic Properties of (Ga1-xZnx)(N1-xOx) Solid Solution Photocatalyst, Linlin Zhao, James T. Muckerman, and Marshall D. Newton,
J. Phys. Chem. C **112**, 3439 (2008)

9. Structure, energetics and electronic coupling in the TCNE/TCNE^{-} encounter complex in solution: a polarizable continuum study, Qian Wang and M.D. Newton,
J. Phys. Chem. B **112**, 586 (2008)

10. The Spectral Elucidation *versus* the X-ray Structure of the Critical Precursor Complex in Bimolecular Electron Transfers. Application of Theoretical/Experimental Solvent Probes to Ion-Radical (Redox) Dyads, Sergiy V. Rosokha, Marshall D. Newton, Almaz S. Jalilov and Jay K. Kochi, *J. Am. Chem. Soc.* **130**, 1944 (2008).

ELECTRON TRANSFER UNDER DYNAMICAL ARREST

Brandon Deason, Naoki Ito, Ranko Richert, Dmitry V. Matyushov, Ian R. Gould
Department of Chemistry and Biochemistry, and, Department of Physics
Arizona State University
Tempe, AZ 85281

All applications of photoinduced electron transfer take place in rigid or heterogeneous systems, where the medium is at least partially frozen on the electron transfer timescale, i.e. under conditions of *dynamical arrest*. Freezing the medium changes the reaction energetics, however, in addition to asking "by how much?", one must also ask "on what timescale?"

This is *different* from the solvent dynamical effects embodied in Kramers theory. The key assumption in Kramers, and conventional transition state theories, is a Boltzmann description of the transition state energy that arises as a consequence of equilibration with the medium. Kramers theory also includes energy dissipation to the medium in transition state, yielding a rate constant with an inverse relation to solvent viscosity, where *all rate constants are influenced equally by the medium*. Under dynamical arrest, however, the equilibrium energy assumption is invalid. Some nuclear modes of the system do not contribute to the barrier, the activation energy depends upon the reaction rate constant, and *different rate constants are influenced by the medium to different extents*. The goal of this project is to understand such nonergodic effects. We describe experimental studies in organic glasses, and theoretical studies in photosynthetic systems.

$k_{et} = A^T \exp[-E_a/kT]$	*Transition State Theory*
$k_{et} = A^K \tau^{-1} \exp[-E_a/kT]$	*Kramers Theory*
$k_{et} = A^D \exp[-\boldsymbol{E_a(k_{et})}/kT]$	*Dynamical Arrest*

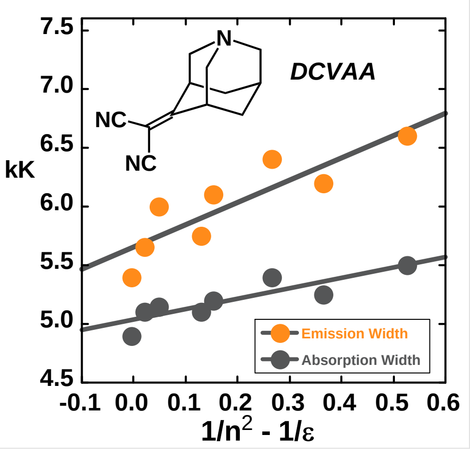

Our experimental work uses a spectroscopic approach. Dicyanovinylazaadamantane (DCVAA) has well-separated CT-transitions, has internal reorganization energies that have been previously characterized using resonance Raman spectroscopy and has a short excited state lifetime, which makes it an ideal probe for non-ergodic effects. The dependence of the absorption and emission maxima on the Pekar factor in homogeneous liquid solutions at room temperature is consistent with large excited state and small ground dipole moments. The spectral widths of the energy-corrected spectra, however, differ both in magnitude and in their dependence on the Pekar factor, as a consequence of dipole induced solvent polarization.

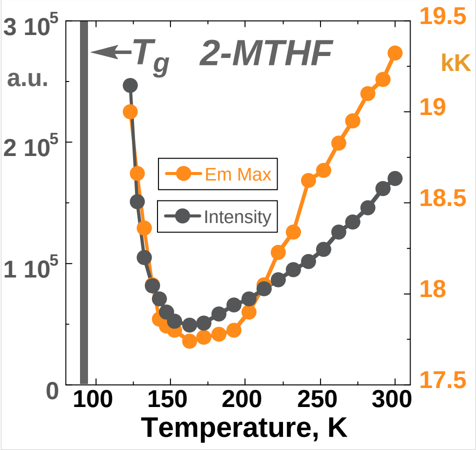

Non-ergodic effects are readily observed in glasses. In PMMA at room temperature, the emission spectrum is excitation wavelength dependent. Quantitative analysis of the CT emission spectra yields an effective frozen energetic distribution of CT states of 0.08 eV due to non-relaxing medium effects. Emission measurements in 2-methylTHF, from 300 - 90K, reveal dramatic shifts in the emission maximum and intensity significantly above the conventional glass transition temperature of 90K. Excited DCVAA essentially ignores the conventional Tg, due to partial freezing of the solvent modes on the electron transfer timescale.

The bulk of our theoretical program has concentrated on electron transfer in the natural photosynthetic center. We have performed the most extensive numerical MD simulations of the bacterial reaction center reported so far. Our first study was directed towards learning about the energetics of primary charge separation [1]. We showed that the equilibrium reorganization energy for this reaction, ca. 1.5 eV, far exceeds the values required to fit the measured reaction rate. The inclusion of a nonergodic cutoff of the nuclear fluctuations reduced this reorganization energy to about 0.35 eV, in very good agreement with the current fits of experimental time-dependent data. We carefully studied contributions of different interaction potentials to the reaction kinetics and observed a significant splitting between the reorganization energy from the energy gap fluctuations (free energy curvature) and the half Stokes shift. This effect, though not very significant for ultrafast charge separation, should gain importance for slower transfer steps in the bacterial charge-transfer chain.

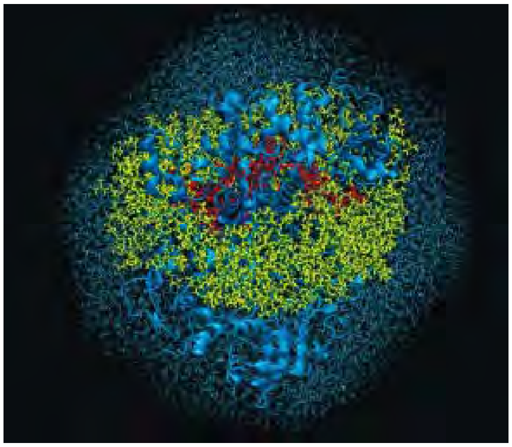

To test the universality of the splitting between the free energy curvature and the Stokes shift, more extensive simulations of the bacterial reaction center were performed [2] with the goal of studying slower recombination rates and obtaining a first glimpse at the energetics of the inactive branch of the bacterial reaction center. Our initial observation was confirmed and we found a significant splitting between the Stokes shift and the curvature for all electronic transitions in the reaction center. The experimentally reported free energies for the reactions simply cannot be rationalized without taking this splitting into account. The astonishing conclusion is that bacterial photosynthesis operates by combining non-linear solvation with substantial non-ergodicity in the first step of the reaction. A full analysis of the data required a more well-developed theoretical procedure, described in Ref [3].

We want to extend our observations in natural photosynthetic systems to reactants used in artificial photosynthesis schemes. We have initiated studies of charge-transfer kinetics in colloidal particles with sizes comparable to proteins. We first want to know how the non-linear effects observed in simulations can be experimentally detected. Electrochemical measurements of redox proteins represent suitable subjects since nonlinear effects seen in simulations should be reflected in the electrochemical transfer coefficients [4]. In search for non-linear effects observed for proteins we have started to study electrostatics of cavities in water [5]. The first simulation of C-60 in water gave results consistent with the standard Marcus energetics, and we are currently study how this will change when the size of the impurity is increased [5].

DOE Sponsored Publications 2006-2008

1. D. N. LeBard, V. Kapko, D. V. Matyushov, Energetics and Kinetics of Primary Charge Separation in Bacterial Photosynthesis, J. Phys. Chem. B ***112*** (2008) 10322.

2. D. N. LeBard and D. V. Matyushov, Energetics of bacterial photosynthesis, J. Phys. Chem. B, to be submitted.

3. D. V. Matyushov, Nonergodic activated kinetics in polar media, J. Chem. Phys. 2009, in press.

4. D. V. Matyushov, Standard potential, Tafel equation, and the solvation thermodynamics, J. Chem. Phys., submitted.

5. A. Friesen and D. V. Matyushov, Electrostatic potential fluctuations inside large cavities in water, in preparation.

Session IV

Photosynthetic Photoconversion

MAPPING STRUCTURE WITH FUNCTION IN BIOMIMETIC AND NATURAL PHOTOSYNTHETIC ARCHITECTURES

David M. Tiede,[1] Karen L. Mulfort,[1] Jenny V. Lockard,[1] Lisa M. Utschig,[1] Oleg Poluektov,[1] Lin X. Chen,[1]
and
Libai Huang,[3] Shana Bender,[1] Iltai Kim,[2] Gary Wiederrecht[2]
[1]Chemical Sciences and Engineering Division and [2]Center for Nanoscale Materials, Argonne National Laboratory, Argonne, IL 60439
[3]Radiation Laboratory, University of Notre Dame
Notre Dame, IN 46556

Natural photosynthesis provides a paradigm for solar energy conversion based on molecular materials composed of sustainable atomic compositions, featuring catalysts using naturally abundant 1st row transition metals, and syntheses using self-assembly and repair. Key features of natural photosynthesis are the hierarchal, modular designs and module-specific protein host-cofactor guest chemistries. This partitioning of photochemical function allows the individual tasks of solar energy conversion such as light-harvesting, charge separation, water-splitting and reductive fuels chemistries to be optimized within individual functional modules, which can then be integrated, regulated, and repaired for optimized overall solar energy conversion throughput. As a result, the resolution of fundamental mechanisms for photosynthesis requires mapping function on to structure across multiple length scales. Accordingly, in this program we are investigating correlations between structure and photosynthetic function in biomimetic and natural photosynthetic architectures in both molecular and hierarchical nanoscale assemblies.

In-situ Supramolecular Structure Determination. Advances in supramolecular chemistry are allowing synthetic molecular architectures to be designed that mimic the hierarchal, modular designs in biology. We have developed x-ray scattering combined with coordinate-based analysis as an approach for correlating supramolecular structure with function in liquids. New developments include the use of molecular dynamics for analysis of wide-angle x-ray scattering and a molecule "fragments" approach for the analysis of dynamic modular supramolecular assemblies. We have extended these approaches for the analysis of the photosensitizer-linker-cobaloxime catalyst architectures recently introduced by Fontecave and coworkers (*Angew. Chem. Int. Ed.* **2008,** *47,* 564). These supramolecular assemblies are of interest as minimalist

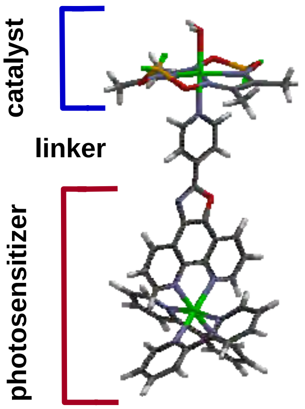

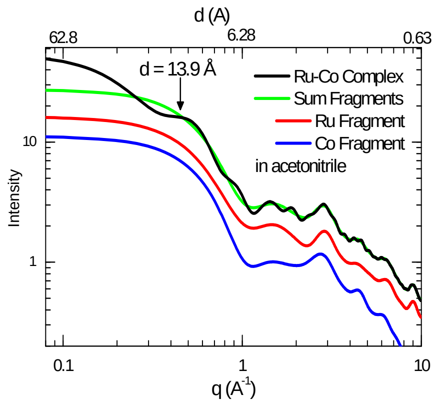

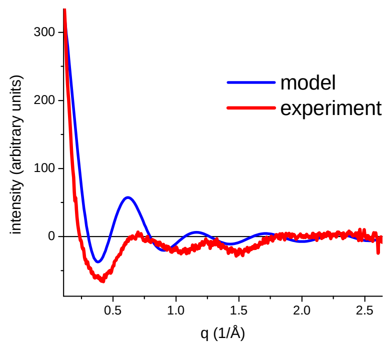

architectures for solar hydrogen production. We have compared of x-ray scattering, electron paramagnetic resonance (EPR), and transient optical spectroscopy for supramolecular assemblies composed of cobaloximes axially coordinated to pyridyl functionalized photosensitizers including a perylene-3,4:9,10-bis(dicarboximide), Ru(II) tris(bipyridyl), and Ru(II) bis(terpyridiyl). The results show that the assembly of the supramolecular complex varies with the photosensitizer and can be correlated with photochemical function.

Ultrafast imaging of photosynthetic solar energy flow at the molecular scale. In a second approach for correlating structure with function in photosynthesis, we are applying ultrafast time-resolved transient absorbance spectroscopy to study the primary electron transfer processes in reaction center (RC) and in collaboration with Neil Hunter (Sheffield) on RC-light harvesting I (RC-LHI) core complex single crystals. These experiments allow us directly correlate energy and electron transfer pathways with atomic scale structure determined by x-ray crystallography. Work on single RC crystals from *Rhodobacter (Rb) sphaeroides* shows that at room temperature the charge separation between the bacteriochlorophyll dimer, P, and the primary electron acceptor bacteriopheophytin, H_L, is approximately two-fold slower in crystals than in solution and displays multiphasic kinetics, indicating that the complex kinetics seen in solution persists in the crystalline state. At low temperature electron the electron transfer kinetics become monophasic. The strong optical dichroism in single crystals allows contributions of normally optically degenerate individual cofactors to be more completely distinguished. Transient absorption measurements show simultaneous contributions of both H_L and B_L anion transitions, possibly more indicative of a shared "I^-" electron acceptor involving both H_L-B_L rather than a sequential electron transfer. Further, polarization-selective cofactor excitation shows distinguishable excited-state reaction pathways and final states are created depending which cofactor optical transition is excited. This work is resolving asymmetry in the electronic structure of the reaction cofactor manifold

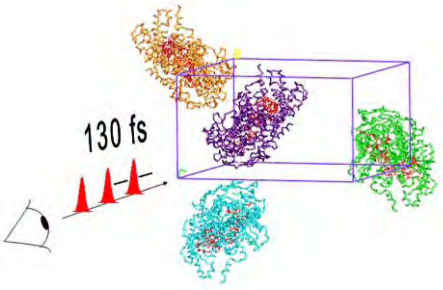

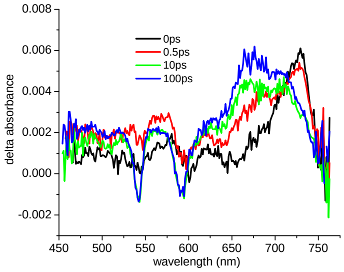

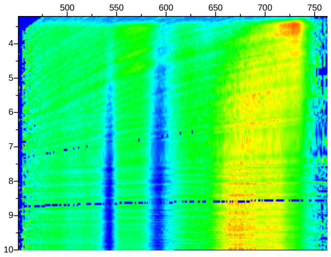

Ultrafast imaging of photosynthetic solar energy flow at the nanometer scale. Techniques for spatially resolving ultrafast solar energy flow in photosynthesis are being developed by exploiting localized, nanoparticle surface plasmons as nanoscale point sources for spatially localized light injection into natural and artificial photosynthetic molecular 2D arrays. We have carried out initial optical characterization of electron beam lithographically patterned arrays of Au and Ag nanoparticles on silicon supports as localized excitation sources for solar imaging.

DOE Sponsored Publications 2006-2009

1. X-ray Scattering Combined with Coordinate-Based Analyses for Applications in Natural and Artificial Photosynthesis, D. M. Tiede, K.L. Mardis, and X. Zuo, invited review, *Photosyn. Research,* (2009) *submitted*.

2. Hydrophobic Dimerization and Thermal Dissociation of Perylenediimide-Linked DNA Hairpins, M. Hariharan, Y. Zheng, H. Long, T. A. Zeidan, G. C. Schatz, J. Vura-Weis, M. R. Wasielewski, X. Zuo, D. M. Tiede, and F. D. Lewis, J. Am. Chem. Soc. (2009) *J. Amer. Chem. Soc.* **131**(16): 5920-5929.

3. The Conformational Ensemble of a Hexameric Porphyrin Array Characterized Using Molecular Dynamics and Wide-Angle X-ray Scattering, K. L. Mardis, H. M. Sutton, X. Zuo, J.S. Lindsey, and D. M. Tiede, *J. Phys. Chem. A* (2009) **113**: 2516-2523.

4. *In Situ* Measurement of the Preyssler Polyoxometalate Morphology upon Electrochemical Reduction, M. R. Antonio, M.-H. Chiang, S. Seifert, D. M. Tiede, and P. Thiyagarajan, *J. Electroanal. Chem.* (2009) **626**:103-110.

5. Attenkofer, K.; Kodituwakku, N.; Goerlich, M.; Adams, B.; Ross, S. K.; Nielsen, T.; Nielsen, M. M.; Tiede, D. M. In *Using coplanar wave guides to excite molecular motions in the frequency range of 10-1000GHz*, 33rd International Conference on Infrared, Millimeter and Terahertz Waves, Pasadena, CA, Sep 15-19, 2008; IEEE: Pasadena, CA, 2008; pp 742-743.

6. Cavity-tailored, Self-sorting Supramolecular Catalytic Boxes for Selective Oxidation, S. J. Lee, S.-H. Cho, K.L. Mulfort, D.M. Tiede, J.T. Hupp, and S.T. Nguyen, *J. Am. Chem. Soc.* (2008) **130**: 16828-16829.

7. Correlating Ultrafast Function with Structure in Single Crystals of the Photosynthetic Reaction Center, L. Huang, G.P. Wiederrecht, S. Schlesselman, C. Xydis, P.D. Laible, D.K. Hanson, D.M. Tiede, *Biochemistry* (2008) **47**: 11387-11389.

8. Electron Paramagnetic Resonance Study of Radiation Damage in Photosynthetic Reaction Center Crystals, L. M. Utschig, S. D. Chemerisov, D. M. Tiede, and O. G. Poluektov, *Biochemistry* (2008) **47**: 9251-9257**.**

9. Fast energy transfer within a self-assembled cyclic porphyrin tetramer, R.A. Jensen, R.F. Kelley, S. J. Lee, M.R. Wasielewski, J.T. Hupp, D. M. Tiede, *Chem. Comm.* (2008) **16**: 1886-1888.

10. Intramolecular Energy Transfer within Butadiyne-Linked Chlorophyll and Porphyrin Dimer-Faced, Self-assembled Prisms, R. F. Kelley, S. J. Lee, T. M. Wilson, Y. Nakamura, D. M. Tiede, A. Osuka, J. T. Hupp, and M. R. Wasielewski, *J. Am. Chem. Soc.* (2008) **130**, 4277-4284.

11. Global Architecture and Interface: Refining a RNA:RNA Complex Structure Using Solution X-ray Scattering Data, X. Zuo, J. Wang, T. R. Foster, C. D. Schwieters, D. M. Tiede, S. E. Butcher, and Y.-X. Wang, *J. Am. Chem. Soc.* (2008) **130**, 3292-3293.

12. X-ray Scattering for Bio-Molecule Structure Characterization, D. M. Tiede and X. Zuo, in *"Biophysical Methods in Photosynthesis"* Volume II, (Thijs J. Aartsma and Jörg Matysik, eds.), Series Advances in Photosynthesis and Respiration, Vol. 26, Springer, Dordrecht, pp 151-165 (2008)

13. Coordinative Self-Assembly and Solution-phase X-ray Structural Characterization of Cavity-Tailored Porphyrin Boxes, S. J. Lee, K. L. Mulfort, X. Zuo, A. J. Goshe, P. J. Wesson, J. T. Hupp, and D. M. Tiede, *J. Am. Chem. Soc.* **130**, 836-838 (2008)

14. Time-Resolved High-Field EPR Spectroscopy Of Natural Photosynthesis: Photoinduced Electron Transfer Pathways In Photosystem I, O. Poluektov, L. Utschig, S. Paschenko, K. Lakshmi, D. Tiede, *Photosyn. Res*. 91 (2-3), 150-151 (2007)

15. Photocatalytic probing of DNA sequence by using TiO2/dopamine-DNA triads, J.L. Liu, X. Zuo, L. de la Garza, Nada M. Dimitrijevic, X. Zuo, D. M. Tiede, T. Rajh, *Chem. Phys.,* **339**, 154-163 (2007)

16. Solution-phase structural characterization of supramolecular assemblies by high-angle molecular diffraction, J.L. O'Donnell, X. Zuo, A.J. Goshe, L. Sarkisov, R. Q. Snurr, J. T. Hupp, D. M. Tiede, *J. Am. Chem. Soc.*, **129**, 1578-1585 (2007)

17. Charge Separation and Surface Reconstruction : A Mn2+ Doping Study, Saponjic, Z.V.; Dimitrijevic, N.M.; Poluektov O.G.; Chen, L.X.; Wasinger, E.; Welp, U.; Tiede, D.M.; Zuo, X. and Rajh, T. *J. Phys. Chem. B,* **110** (50), 25441-25450 (2006)

18. Supramolecular Porphyrinic Prisms: Coordinative Assembly and Preliminary Solution-phase X-ray Structural Characterization , S.J. Lee, K. L. Mulfort, J. L. O'Donnell, X. Zuo, A. J. Goshe, S. T. Nguyen, J. T. Hupp, and D. M. Tiede, *Chem. Comm.,* **44**, 4581 - 4583 (2006)

19. Linearly Polarized Emission of an Organic Semiconductor Nanobelt, Datar, A.; Balakrishnan, K.; Yang, X.; Zuo, X.; Huang, J.; Oitker, R.; Yen, M.; Zhao, J.; Tiede, D. M.; Zang, L., *J. Phys. Chem. B,* **110**, 12327-12332 (2006)

20. X-ray Diffraction "Fingerprinting" of DNA Structure in Solution for Quantitative Evaluation of Molecular Dynamics Simulation, X. Zuo, G. Gui, K.M. Merz, L. Zhang, F.D. Lewis, and D.M. Tiede, *Proceed. Natl. Acad. Sci. USA*, **103** (10), 3534-3539 (2006)

PHOTOSYNTHETIC INTERPROTEIN ELECTRON TRANSFER

Lisa M. Utschig, Oleg G. Poluektov, Lin X. Chen, Jenny V. Lockard, Sergey Milikisiyants and David M. Tiede
Chemical Science and Engineering Division
Argonne National Laboratory
Argonne, IL 60439

Photosynthetic reaction center (RC) proteins are finely tuned molecular systems optimized for solar energy conversion. In natural photosynthesis, the photon energy, efficiently captured as a stabilized charge-separation across the RC, is utilized to drive a series of reactions that ultimately result in the chemical transformation of CO_2 into carbohydrates. Our group has undertaken studies to develop approaches to exploit the initial light-induced RC reactions to drive non-native chemical reactions for solar fuels production. Recent work is focused on understanding structure-function relationships in natural photosynthetic systems with the intent of applying this knowledge to the design and optimization of novel biohybrid systems. Specifically, we are developing experimental methods to interrogate native protein docking and electron transfer events that take place subsequent to photo-induced charge-separation in the Photosystem I (PSI) RC. The large membrane PSI protein catalyzes light-driven electron transfer across the thylakoid membrane from plastocyanin located in the lumen to one of two small electron carrier proteins, ferredoxin or flavodoxin, in the stroma. These small proteins then shuttle the reducing equivalents from PSI to several metabolic pathways. Our discovery of native transition metal ion sites on the acceptor docking side of PSI enables us to capitalize on the spectroscopic properties of metal ions and directly probe the stromal region of PSI, PSI-charge carrier protein docking mechanisms, and interprotein electron transfer reactions. Our experimental approach utilizes both specialized "spin-edited" (i.e. samples that involve isotopic labeling and/or native paramagnetic metal ion replacement) samples and multifrequency pulsed electron paramagnetic resonance (EPR) techniques as well as X-ray absorption fine structure (XAFS) spectroscopy.

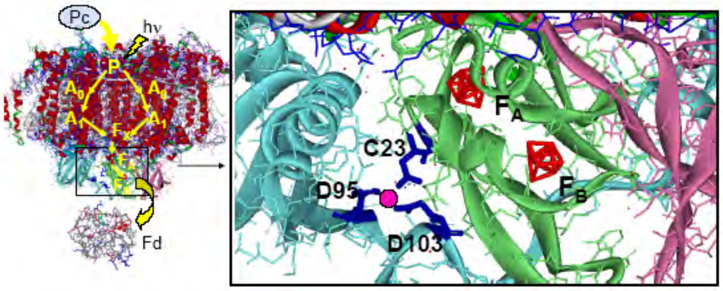

Figure 1 Left: Photosystem I reaction center (PDB 1JB0) showing the photo-initiated sequential electron transfer pathway from the primary donor P to the terminal electron acceptors, F_A and F_B. Ferredoxin (Fd) (PDB 1A70) accepts the light-generated electron from PSI; plastocyanin (Pc) reduces the oxidized donor, P^+. Right: Enlargement of the stromal subunits showing proposed Cu binding site ligands in PSI. A putative Cu atom is illustrated.

Discovery of Native Metal ion Sites in Photosystem I. Using a combination of bioinorganic and spectroscopic techniques, we have examined the intrinsic surface Zn^{2+} and Cu^{2+} sites of PSI. Two-dimensional hyperfine sublevel correlation (HYSCORE) spectroscopy shows coupling to the so-called remote nitrogen of a single histidine coordinated to one of the Cu^{2+} centers. EPR and X-ray absorption fine structure (XAFS) studies of 2Cu-PSI complexes prove the direct interaction of ferredoxin with the Cu^{2+} centers on PSI, establishing the location of native metal sites on the ferredoxin docking side of PSI. Based on these spectroscopic results and previously reported site-directed mutagenesis studies, inspection of the PSI crystal structure reveals a cluster of three highly conserved residues, His(D95), Glu(D103), and Asp(C23), as a likely Cu^{2+} binding site.(Figure 1) In collaboration with John Golbeck (Penn State University), we are measuring optical kinetics of Cu-PSI and Zn-PSI complexes to look for any metal-dependent changes in PSI electron transfer rates. We directly probe dynamic features of the peptide environment surrounding the metal Cu^{2+} ($3d^9$, $S = ½$) site, (i.e. response to protein binding and electron transfer) using pulsed EPR experiments of specifically-prepared isotopically labeled samples. Furthermore, XAFS experiments provide a means to directly examine the Cu^{1+} state of the metal site that occurs in the presence of reductants that are necessary to facilitate successive turnovers of PSI. Future work will take advantage of these metal sites in innovative bioinorganic approaches to modify photosynthetic proteins for solar fuels production.

Coupling PSI ET to Soluble Electron Carriers. PSI (~300 kDa) performs light-induced electron transfer across the thylakoid membrane in plants, algae and cyanobacteria, resulting in the reduction of low-potential (~ -400 mV) electron carriers; either [2Fe-2S] ferredoxin or flavodoxin in the case of iron deficiency. Although both proteins are of different size (~11 kDa for ferredoxins, ~20 kDa for flavodoxins) both types of proteins are strongly acidic, whereas the stromal surface of PSI is positively charged. Thus, electrostatic forces are of major importance for the interactions between PSI and these electron carrier proteins. We are designing experimental setups to look in detail at PSI interprotein interactions. Whereas ferredoxin and flavodoxin reduction by PSI has been extensively studied and reported in the literature, only a few EPR studies of PSI-Ferredoxin or PSI-Flavodoxin complexes have been reported. In each case, the complexes were either co-crystals or chemically crosslinked to PSI and the ferredoxin or flavodoxin were chemically reduced with dithionite. We are interested in looking at the native PSI reduction of ferredoxin and flavodoxin in solution using freeze-trap methods and EPR spectroscopy. Importantly, fully deuterated flavodoxin is available in our laboratory. Deuteration effectively narrows the line width of the flavin mononucleotide radical such that the EPR signals of reduced flavodoxin and PSI can be resolved at both low (X-band, 9 GHz) and high (D-band, 130 GHz) field EPR, enabling us to examine interprotein electron transfer reactions and protein interactions with advanced time-resolved pulsed EPR methodologies. Initial experiments show some surprising results with regards to both bidirectional and low temperature interprotein electron transfer.

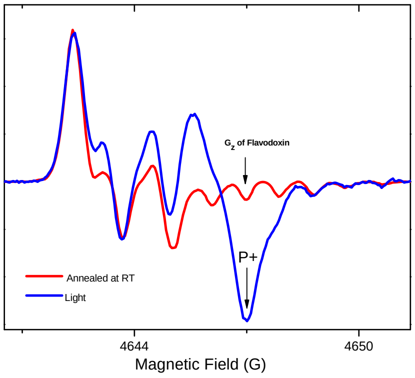

Figure 2 HF EPR spectrum of PSI-^{2}H Flavodoxin complex . The light-induced signal from the primary donor, P^+, is resolved from the reduced flavodoxin acceptor.

DOE Sponsored Publications 2006-2009

1. A. A. Dubinskij, L. M. Utschig, and O. G. Poluektov "Spin-Correlated Radical Pairs: Differential Effects in High-Field ENDOR Spectra" *Appl. Magn. Reson.*, **2006**, *30,* 269-286.

2. O. G. Poluektov, L. M. Utschig, M. C. Thurnauer, and G. Kothe "Exploring Hyperfine Interactions in Spin-Correlated Radical Pairs from Photosynthetic Proteins: High-Frequency ENDOR and Quantum Beat Oscillations" *Appl. Magn. Reson.*, **2007**, *31* (1-2), 123-143.

3. U. Heinen, L. M. Utschig, O. G. Poluektov, G. Link, E. Ohmes, and G. Kothe "Structure of the Charge Separated State $P^+_{865}Q^-_A$ in the Photosynthetic Reaction Centers of *Rhodobacter sphaeroides* by Quantum Beat Oscillations and High-Field Electron Paramagnetic Resonance: Evidence for Light-Induced Q^-_A Reorientation" *J. Am. Chem. Soc.*, **2007**, *129,* 15935-15946.

4. L. Huang, G. P., Wiederrecht, L. M. Utschig, S. L. Schlesselman, C. Xydis, P. D. Laible, D. K. Hanson, D. M. Tiede, "Correlating Ultrafast Function with Structure in Single Crystals of the Photosynthetic Reaction Center" *Biochemistry,* **2008**, *47,* 11387-11389.

5. L. M. Utschig, S. D. Chemerisov, D. M. Tiede, and O. G. Poluektov "Electron Paramagnetic Resonance Study of Radiation Damage in Photosynthetic Reaction Center Crystals" *Biochemistry,* **2008**, *47*, 9251-9257.

6. L. M. Utschig, L. X. Chen, and O. G. Poluektov "Discovery of Native Metal Ion Sites Located on the Ferredoxin Docking Side of Photosystem I" *Biochemistry*, **2008**, *47,* 3671-3676.

7. O. G. Poluektov and L. M. Utschig "Protein Environments and Electron Transfer Processes Probed with High-Frequency ENDOR" In *The Purple Phototrophic Bacteria. Advances in Photosynthesis and Respiration*, C. N. Hunter, F. Daldal, M. C. Thurnauer, and J. T. Beatty, Eds., **2009**, Vol 28, pp. 155-179, Springer, Dordrecht, The Netherlands.

8. L. M. Utschig, S. D. Dalosto, M. C. Thurnauer, and O. G. Poluektov, "The Surface Metal Site in *Blc. Viridis* Photosynthetic Bacterial Reaction Centers: Cu^{2+} as a Probe of Structure, Location, and Flexibility" *Appl. Magn. Reson.* **2009**, submitted

9. O. G. Poluektov, S. V. Paschenko, and L. M. Utschig, "Spin-Dynamics of the Spin-Correlated Radical Pair in Photosystem I. Pulsed Time-Resolved EPR at High Magnetic Field." *Phys. Chem. Chem. Phys.* **2009**, submitted.

Session V

Heterogeneous Systems for Solar Photoconversion

CHEMICAL CONTROL OVER THE ELECTRICAL PROPERTIES OF GaAs AND Zn_3P_2 SEMICONDUCTOR SURFACES AND PHOTOELECTRODES

Gregory M. Kimball, Matthew C. Traub, and Nathan S. Lewis
Division of Chemistry and Chemical Engineering
California Institute of Technology
Pasadena, CA 91125

Our work has focused on the fundamental interfacial chemistry and surface chemistry of two potentially very important semiconductor-based systems for solar energy capture, conversion and storage: GaAs and Zn_3P_2. GaAs is a well-established semiconductor but relatively little is known about its surface chemistry, passivation and functionalization. Chemically synthesized GaAs nanocrystals provide several opportunities for improved performance and cost-efficiency relative to single crystal based devices. However, exploitation of these advantages requires passivation of the dramatically larger surface area of these nanocrystals relative to devices made from conventional, planar junction systems. Zn_3P_2 is a potentially very attractive material for solar energy capture and conversion due to its near-optimal band gap (1.5 eV), long minority carrier diffusion lengths (~10 um), and the abundance of its composing elements. Only a handful of papers have been published on the surface properties of Zn_3P_2, and we have explored the surface chemistry and photoelectrochemistry of this material as a key portion of this work.

We have demonstrated an effective protocol to synthesize crystalline GaAs nanocrystals and to chemically passivate native surface states. Treatment of HCl-etched GaAs nanocrystals with hydrazine or sodium hydrosulfide resulted in a functionalized semiconductor surface. After annealing, the N 1s peak of N_2H_2-exposed GaAs nanocrystals shifted by 3.2 eV to a lower binding energy as determined by XPS. The band-gap photoluminescence was weak from the Cl^- and $N_2H_2^-$ or sulfide-terminated nanocrystals, but the annealed nanocrystals displayed strongly enhanced band-edge PL, indicating that the surface states of GaAs nanocrystals were effectively passivated by this two-step, wet chemical treatment (Fig 1). Functionalization with PEt_3 and PCl_3 has been attempted using the Cl-terminated GaAs surface as a starting point. PEt_3 has been found to react with 30-50% of surface sites, leaving Cl atoms bound to the remaining surface Ga atoms. The ability to prepare phosphine-terminated surfaces that are initially free of oxide and As^0 contaminants provides a useful platform for further functionalization chemistry.

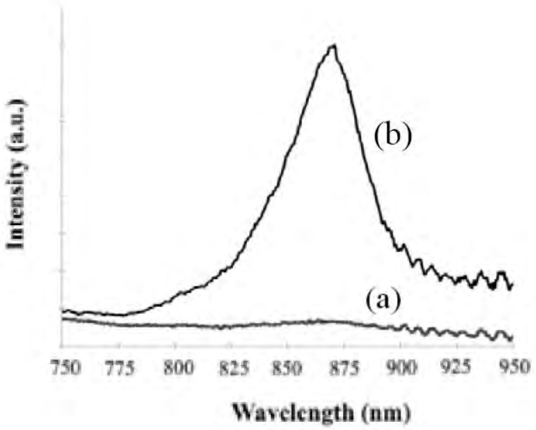

Fig. 1. Steady-state photoluminescence intensity of N_2H_2-functionalized samples (a) before and (b) after annealing.

The Zn_3P_2 wafers used in this study were grown by physical vapor transport starting from elemental zinc and phosphorus. After etching with Br_2 in methanol, we observe a large photoluminescence enhancement in comparison to the as-polished wafers as well as the first demonstration of photoluminescence from large grain Zn_3P_2 in the temperature range 150-310K. Zn_3P_2 wafers fabricated in our laboratory show good performance in Mg Schottky diodes with open-circuit voltages (V_{OC})'s of 0.5-0.6 V at 1 sun illumination (Fig. 2), demonstrating the high purity and low recombination of the bulk semiconductor. Preliminary work with nonaqueous photoelectrochemical cells shows evidence of Fermi-level pinning in the Zn_3P_2 surface. With an ideal semiconductor liquid junction, Zn_3P_2 cells could give V_{OC}'s of 0.8-1.0 V, but in experiments conducted using the cobaltocene or decamethylcobaltocene redox couples, V_{OC}'s have been limited to about 0.2 V at 1 sun illumination.

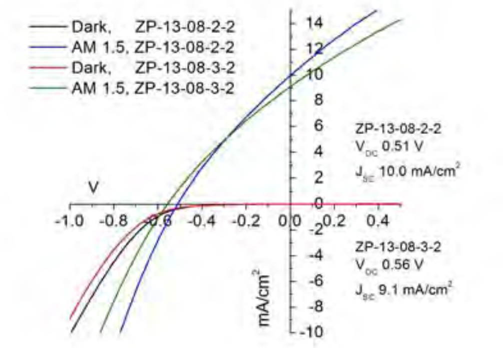

Fig. 2. Dark and light J-V traces of two Mg/Zn3P2 Schottky diodes.

We plan to continue the GaAs functionalization using molecules that could be useful bridges for electron transfer reactions. Thiol-on-Au chemistry is a well-studied system, and α,ω-alkanedithiols should bind GaAs nanocrystals to Au substrates. SAMs of 6-sulfanyl-1-hexanol on GaAs have been used as precursors for polymer growth,[64] and OH-terminated thiol molecules provide an opportunity for utilization of organic synthetic methods to further functionalize the particles. Should N-based surface chemistry provide superior electronic passivation, asymmetric hydrazines such as 4-hydrazinobenzoic acid can be used as linkers. Because the binding of these species to GaAs surfaces has not previously been demonstrated, we will first test the binding of a similar molecule, 2-hydrazino-4-(trifluoromethyl)pyrimidine. The $-CF_3$ moiety is easily observable by XPS, and will provide clear evidence of its presence on the surface.

The record Zn_3P_2 solar energy conversion device employs a Mg Schottky junction (~6% efficiency) but to date the source of the high performance in the Mg/Zn_3P_2 system is not known. We plan to study the Mg/Zn_3P_2 interface by etching the Mg metal and probing the interfacial layer with nonaqueous semiconductor-liquid junctions. Previous authors working on solid-state Zn_3P_2 heterojunctions also observed Fermi-level pinning at V_{OC}'s of about 0.2 V in ZnO/Zn_3P_2 and ITO/Zn_3P_2 devices and found extremely high densities of surface states at the interface ($>10^{13}$ $ev^{-1}cm^{-2}$). As Zn_3P_2 and ZnSe are lattice matched, we plan to use thin layers of epitaxially electrodeposited ZnSe layers to reduce the high surface state density.

DOE Sponsored Publications 2006-2008

Matthew C. Traub, Julie S. Biteen, David J. Michalak, Lauren J. Webb, Bruce S. Brunschwig, and **Nathan S. Lewis**, “High-Resolution X-ray Photoelectron Spectroscopy of Chlorine-Terminated GaAs(111)A Surfaces”, *J. Phys. Chem. B*, **2006**, *110*, 15641.

George W. Crabtree and **Nathan S. Lewis**, “Solar Energy Conversion”, *Phys. Today*, **2007**, *60(3)*, 37.

Nathan S. Lewis, “Toward Cost-Effective Solar Energy Use”, *Science*, **2007**, *315(5813)*, 798.

Nathan S. Lewis “The World Energy Book (contributed chapter)”, **2007**.

Stephen Maldonado, Anthony G. Fitch, and **Nathan S. Lewis**, “Semiconductor/Liquid Junction Photoelectric Chemical Solar Cells”, in *Series on Photoconversion of Solar Energy Volume III - Nanostructured and Photoelectric Chemical Systems for Solar Photon Conversion*, Mary D Archer; and Arthur J Nozik; Eds., Imperial College Press: London, **2008**, 537.

Nathan S. Lewis, “Legal and Policy Issues Related to a Global Carbon Emissions-Control Regime”, *Stanford Law and Policy Review*, **2007**, *Submitted for publication*.

Nathan S. Lewis, “Powering the Planet”, *MRS Bulletin*, **2007**, *32*, 808.

Gregory M. Kimball, **Nathan S. Lewis**, and Harry A. Atwater, “Synthesis and Surface Chemistry of Zn_3P_2”, *Conference Record of the Thirty-third IEEE Photovoltaic Specialists Conference*, **2008**.

George W. Crabtree, **Nathan S. Lewis**, David Hafemeister, B. Levi, M. Levine, and P. Schwartz, "Solar Energy Conversion" *AIP Conf. Proc. (Physics of Sustainable Energy)*, **2008,** *1044*, 309-321.

Nathan S. Lewis, “Powering the Planet: Where in the World Will Our Energy Come From?”, *Energeia*, **2008**, *19(4)*, 1.

Nathan S. Lewis, “Powering the Planet”, *Eng. Science*, **2007**, *LXX(2)*, 12.

Amanda L. Smeigh, Jordan E. Katz, Bruce S. Brunschwig, **Nathan S. Lewis**, and James K. McCusker, "Effect of the Presence of Iodide on the Electron Injection Dynamics of Dye-Sensitized TiO_2-Based Solar Cells" *J. Phys. Chem. C*, **2008**, 112(32), 12065.

Irene E. Paulauskas, Jordan E. Katz, Gerald E. Jellison Jr., **Nathan S. Lewis**, Lynn A. Boatner, Gilbert M. Brown, “Growth, Characterization, and Electrochemical Properties of Doped n-type $KTaO_3$ Photoanodes”, *J. Electrochem. Soc*., **2008**, 156, B580-587

Irene E. Paulauskas, Jordan E. Katz, Gerald E. Jellison Jr., **Nathan S. Lewis**, Lynn A. Boatner, *Thin Solid Films*, **2008**, Photoelectrochemical studies of semiconducting photoanodes for hydrogen production via water dissociation

Matthew C. Traub, Julie S. Biteen, Bruce S. Brunschwig, and **Nathan S. Lewis**, "Passivation of GaAs Nanocrystals By Chemical Functionalization", *J. Am. Chem. Soc.*, **2007**, *130*, 955.

Matthew C. Traub, Julie S. Biteen, David J. Michalak, Lauren J. Webb, Bruce S. Brunschwig, and **Nathan S. Lewis**, "Phosphine Functionalization of GaAs(111)A Surfaces", *J. Phys. Chem., C*, **2008**, 112, 18467-18473.

Kimberly M. Papadantonakis, Bruce S. Brunschwig, and **Nathan S. Lewis**, "Use of Alkane Monolayer Templates to Modify the Structure of Alkylether Monolayers on Highly Ordered Pyrolytic Graphite", Langmuir, **2008**, 24, 857.

CONTROLLED NITROGEN DOPING OF TiO_2 FOR VISIBLE LIGHT PHOTOACTIVITY

MA Henderson, SA Chambers, T Ohsawa, I Lyubinetsky and Y Du
Chemical and Materials Sciences Division
Pacific Northwest National Laboratory
Richland, WA 99352

The ambition of supplementing the nation's energy needs through solar photocatalytic water splitting is far from being realized with current photocatalytic materials. TiO_2-based materials (anatase, rutile and various titanates) are promising photocatalysts that show activity in the UV and stability over a wide range of conditions. However, one of the problems with TiO_2 as a stand-alone photocatalyst is that it absorbs little of the solar spectrum. Doping offers the possibility of incorporating donor and/or acceptor states into the TiO_2 band gap that lower the threshold energy for photon absorption without significantly compromising photoactivity. While much applied work exists involving doping of TiO_2, there has been little effort aimed at understanding the fundamental properties of doped TiO_2. In this project, we examine the controlled doping of single crystal films of anatase and rutile TiO_2 with both anion and cation dopants using oxygen plasma-assisted molecular beam epitaxy (OPAMBE). We have recently explored the properties of N-doped rutile and anatase single crystal surfaces, and show that the absorption thresholds of these are shifted into the visible, that a transition exists in dopant concentration between pure substitutional anion doping (N for O) and phase separation (new Ti oxynitride phase), and that the former shows signs of trapping holes during photon irradiation of rutile but not anatase.

Fig. 1 illustrates that in anion-doped TiO_2 electrons are excited by visible light from low lying anion-dopant levels in the TiO_2 band gap (right side of cartoon) to the CB. These have the same reductive power (i.e., same potential energy) as electrons excited in band-to-band transitions (left side of cartoon). In both cases, excited electrons settle to the bottom of the CB. (It should be noted that little is known about how anion-doping affects the conduction band states of TiO_2.) In contrast, holes generated by excitation of dopant states should have less oxidative power (i.e., be located higher on the potential energy diagram) than those formed in the TiO_2 VB from band-to-band excitations. In concept, holes located in the mid-gap states have been viewed as 'trapped', but little is know about their mobility or extent of localization. It is also likely that holes generated in the TiO_2 VB trap at dopant levels, as illustrated in the middle portion of the figure.

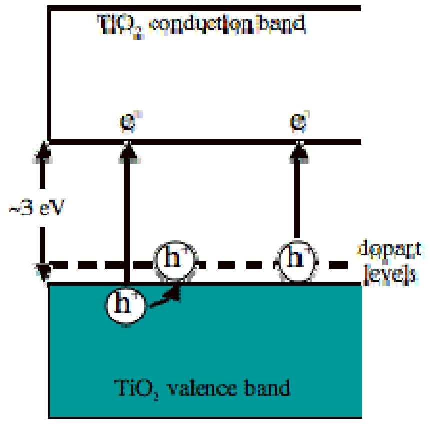

Fig. 1 Schematic illustration of band-to-band (left) and dopant-to-CB excitations in doped TiO_2.

Using OPAMBE, N-doping was achieved by mixing N_2 and O_2 in an ECR source and impinging the mixed beam of N, O, N_2, O_2 and nitrogen oxides onto the substrate, along with a

Ti atom beam from a high-temperature effusion cell. Rutile was selectively grown by using $TiO_2(110)$ whereas anatase preferentially nucleated on $LaAlO_3(001)$ and $SrTiO_3(001)$ substrates.

Fig. 2 shows CO_2 photodesorption rates for UV induced photodecomposition of adsorbed trimethyl acetate (TMA) on pure rutile TiO_2, on $TiO_{1.99}N_{0.01}$, and on $TiO_{1.98}N_{0.02}$, all grown on $TiO_2(110)$. All films thicknesses were ~ 50 nm. Full UV-vis emission from a 100 W Hg arc lamp for 300 sec while at the focal point of a QMS. The instantaneous rise at $t = 0$ is accompanied by a rapid drop in rate as photogenerated holes migrate to the surface and decompose the TMA. After some time (~200 sec), the reaction rate decays to near zero before all TMA has been consumed due to the absence of O_2 in the chamber to scavenge electrons from the surface. The associated charge buildup shuts down the photodesorption process and prevents photodissociation of all the TMA. The integrated area under each trace is proportional to the number of TMA anions photodissociated in 300 sec. As N is added to the lattice, the total amount of TMA decomposed in the specified time interval drops with increasing N concentration, so much so that by 1% N there was very little photodecomposition of TMA. Our interpretation of this result is that the localized N 2p states at the top of the valence band act as hole traps, preventing the photogenerated holes in the bulk of the film from reaching the surface and decomposing the TMA. These traps are not irreversible filled as the rate does not increase with time. No surface photochemistry is observed when visible light is used, despite the fact that the N-doped $TiO_2(110)$ films are shown to absorb visible light. These photodesorption results are consistent with complimentary STM images.

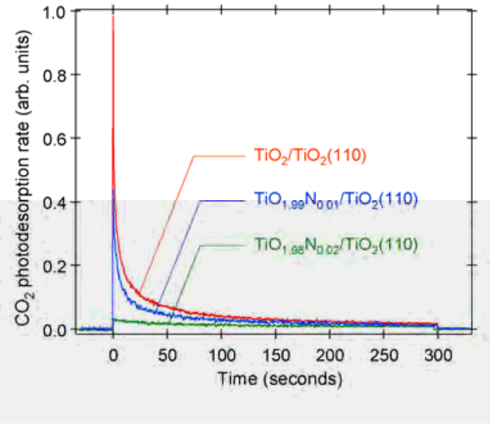

Fig. 2 CO_2 photodesorption spectra for TMA on pure and N-doped TiO_2 rutile.

In contrast, Fig. 3 shows results from analysis of STM images during the photodecomposition of TMA on anatase $TiO_2(001)$. TMA photochemistry on the N-doped anatase (001) surface is not significantly inhibited in the UV, and visible light is shown to promote TMA photodecomposition on this N-doped surface. (Photodesorption studies yield similar results.) These results indicate that holes generated at N-dopant sites are able to migrate via the O 2p-dominated valence band to the anatase $TiO_2(001)$ surface. Similar studies on the rutile (110) surface (see above), as well as other rutile ((100) and (001)) and anatase (101) surfaces do not show visible activity, indicating that strong anisotropic factors favors hole diffusion in anatase along the <001> direction.

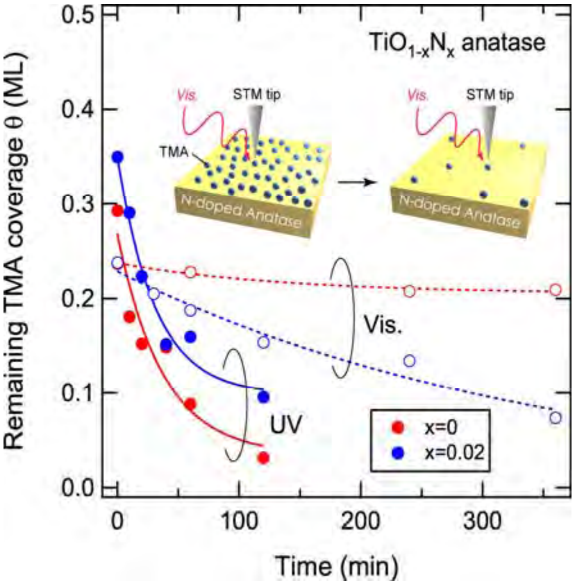

Fig. 3 STM results on the photodecomposition of TMA on pure and N-doped anatase (001) using UV and visible light.

Publications supported by this program, 2006-2008

O. Bondarchuk and I. Lyubinetsky, “Preparation of TiO_2(110)-(1 x 1) Surface Via UHV Cleavage: An STM Studies,” **Reviews of Scientific Instrumentation** 78 (2007) 113907.

S.A. Chambers, S.H. Cheung, V. Shutthanandan, S. Thevuthasan, M.K. Bowman and A.G. Joly, “Properties of Structurally Excellent N-doped TiO_2 Rutile,” special issue of Chemical Physics entitled *Doping and Functionalization of Photoactive Semiconducting Metal Oxides*, ed. C. DiValentin, U. Diebold, A. Selloni, **Chemical Physics** 339 (2007) 27. (*invited review article)*

S.A. Chambers, “Advances in the Surface Science of TiO_2 - A Global Perspective,” **Journal of Surface Science, Japan** 28 (2007) 561. (*invited review article*)

S.A. Chambers, “Molecular Beam Epitaxial Growth of Doped Transition Metal Oxide Semiconductors,” **Journal of Physics: Condensed Matter** 20 (2008) 264004. (*invited review article)*

S.H. Cheung, P. Nachimuthu, A.G. Joly, M.H. Engelhard, M.K. Bowman and S.A. Chambers, “N Incorporation and Electronic Structure in N-doped TiO_2(110) Rutile,” **Surface Science** 601 (2007) 1754.

S.H. Cheung, P. Nachimuthu, M.H. Engelhard, C.M. Wang and S.A. Chambers, “N Incorporation, Composition and Electronic Structure in N-doped TiO_2(001) Anatase Epitaxial Films Grown on $LaAlO_3$(001),” **Surface Science** 602 (2008) 133.

Y. Du, Z. Dohnálek and I. Lyubinetsky, “Transient Mobility of Oxygen Adatoms upon O_2 Dissociation on Reduced TiO_2(110),” **Journal of Physical Chemistry C** 112 (2008) 2649. *(Featured on journal cover.)*

C.D. Lane, N.G. Petrik, T.M. Orlando and G.A. Kimmel, “Electron-Stimulated Oxidation of Thin Water Films Adsorbed on TiO_2(110),” **Journal of Physical Chemistry C** 111 (2007) 16319.

C.D. Lane, N.G. Petrik, T.M. Orlando and G.A. Kimmel, “Site-Dependent Electron-Stimulated Reactions in Water Films on TiO_2(110),” **Journal of Chemical Physics** 127 (2007) 224706.

S.-C. Li, Z. Zhang, D. Sheppard, B.D. Kay, J.M. White, Y. Du, I. Lyubinetsky, G. Henkelman and Z. Dohnálek, “Intrinsic Diffusion of Hydrogen on Rutile TiO_2(110),” **Journal of The American Chemical Society** 130 (2008) 9080.

T. Ohsawa, I.V. Lyubinetsky, M.A. Henderson and S.A. Chambers, “Hole-mediated Photodecomposition of Trimethylacetate on a TiO_2(001) Anatase Epitaxial Thin Film Surface,” **Journal of Physical Chemistry C** 20050 (2008) 112.

N.G. Petrik and G.A. Kimmel, “Hydrogen Bonding, H/D Exchange and Molecular Mobility In Thin Water Films on TiO_2(110),” **Physical Review Letters** 99 (2007) 196103.

Z.Q. Yu, C.M. Wang, Y. Du, S. Thevuthasan and I. Lyubinetsky, “Reproducible Tip Fabrication and Cleaning for UHV STM,” **Ultramicroscopy** 108 (2008) 873.

FROM MOLECULAR TO MICROSTRUCTURAL DESIGN OF HETEROMETALLIC OXIDE/ORGANIC SOLIDS FOR VISIBLE-LIGHT PHOTOCATALYSIS

Paul A. Maggard
Department of Chemistry
North Carolina State University
Raleigh, NC 27695

The synthetic preparation of metal oxides as visible-light photocatalysts for water splitting has for several decades been limited to conventional high-temperature ceramic methods. New synthetic routes for the manipulation of the molecular to the microstructural level features of metal oxides are required to enable the design of more efficient solar photocatalysts, and in our research includes: a) the incorporation of organic ligands into metal oxides to enable a finer molecular-level structural control and b) molten-salt flux reactions for the controlled growth of metal-oxide particle sizes from nanometers to micrometers. These investigated new classes of photocatalytic metal oxides feature specific combinations of d^0 (e.g., Ta^{5+}) with d^{10} (e.g., Ag^+) electron configurations to create an optimal band-energy profile for visible-light absorption and for the photocatalytic splitting of water.

Understanding the effects of ligand coordination geometries and sizes on the internal structures of metal oxides is essential for optimizing their optical and photocatalytic properties at the molecular level. Our hydrothermal synthetic efforts utilize a number of selected types of coordinating ligands, and which have resulted in a growing new class of heterometallic-oxide/organic solids (i.e., MM'OL; M/M' = transition metals with d^0 and d^{10} electron configurations; L = coordinating ligand) in the Cu/Re, Ag/Re, Ag/V, Ag/Nb, and Cu/Nb systems. In the vanadate systems, a series of new hybrid solids were prepared that are comprised of silver-vanadate layers pillared by organic ligands (i.e., bpy, dpa, or pzc). These have led to a new understanding of the effect of ligand length on the amount and reversibility of water absorption into their structures (e.g., $[Ag(bpy)]_4V_4O_{12}\cdot 2H_2O$ versus $[Ag(dpa)]_4V_4O_{12}\cdot 4H_2O$). The coordination geometry of the ligand was also found to impact the network dimensionality and which resulted in a significant variability of the optical bandgap sizes from ~2.45 – 2.95 eV, with the smallest bandgap size of

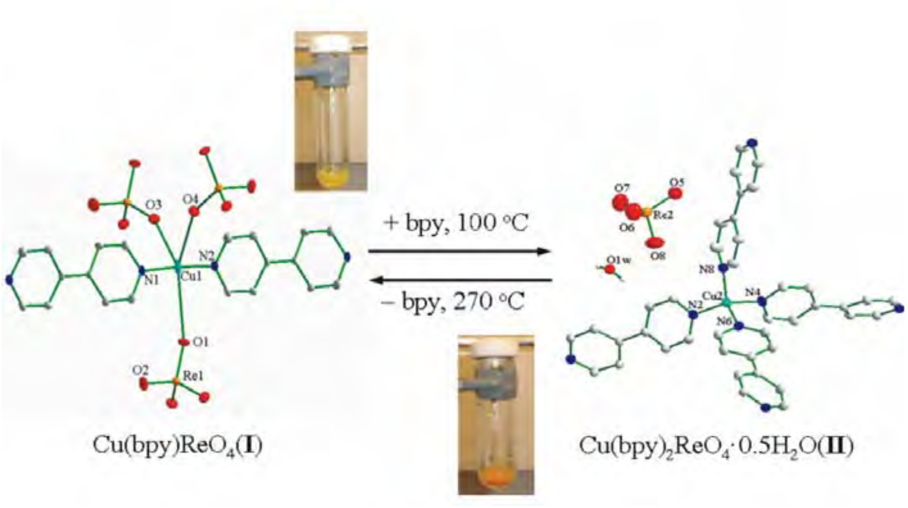

Figure 1. Two new Cu^I/Re^{VII} hybrids and their crystal-to-crystal interconversion with a change in bandgap size (2.5 eV to 2.2 eV) via a modification of the local Cu coordination environment that is a function of the ligand stoichiometry.

2.45 eV achieved for $Ag_4(pzc)_2V_2O_6$. Further, the latter material is the first known hybrid-oxide/organic that has been found to exhibit photocatalytic activity under visible-light irradiation. In the rhenate hybrid systems, significant diversity in the dimensionality of the organic/inorganic components has been found, such as from isolated trimeric and tetrameric cluster units in $Ag_3(pdc)_3(ReO_4)_3 \cdot 1.5H_2O$ and $Cu_2(pda)_3(ReO_4)_2 \cdot H_2O$ to layered structures in $M(bpy)ReO_4$ (A = Cu, Ag), and network types of structures in $Cu(bpy)_2ReO_4 \cdot \frac{1}{2}H_2O$, $Ag(id)_2ReO_4$, and $Ag(dpa)_2ReO_4$, for example. Their optical and photocatalytic property measurements are currently continuing and are enabling new investigations into the effects of coordination environments and framework dimensionalities on the measured bandgap sizes and types, and the optical absorption coefficients.

At a larger size-scale regime, the molten-salt flux growth of heterometallic-oxide particles (e.g., MM'O) in the Ag/Nb and Cu/Nb systems has been investigated towards achieving a finer control over particle sizes and morphologies, as well as for improved product homogeneity. In an initial feasibility study, the (110) layered perovskite $La_2Ti_2O_7$ was first selected to study the effects of flux synthetic conditions on the underlying particle features and surfaces that govern its high photocatalytic activity. Platelet-shaped particles with size dimensions of ~500 – 6,000 nm in width and <100nm in thickness could be prepared in a Na_2SO_4/K_2SO_4 flux at 1100 ^oC in short reaction times of 1 – 10h. The particle sizes can be controlled within these ranges by adjusting the reaction time and flux amounts, and exhibited high photocatalytic rates for hydrogen formation in both aqueous methanol (~55-140 μmol H_2 $h^{-1}g^{-1}$) and in deionized water solutions (~31 μmol H_2 $h^{-1}g^{-1}$). Using flux conditions to control the particle growth, our studies have been able to reveal that the crystallite edges and (010) and (001) crystal faces play a key role in its photocatalytic reactivity. We also expanded these investigations to the $AgNbO_3$, $CuNbO_3$, and $CuNb_3O_8$ solids, to investigate whether flux preparations can similarly act to generate active surfaces for these solids that have visible-light bandgap absorption. In ongoing work, the rapid single-step synthesis of $AgNbO_3$ particles with sizes of ~500 – 5,000 nm can be obtained in a Na_2SO_4 flux at 900 ^oC in only 1 – 10 h. Smaller particle-size distributions are found for increasing amounts of flux and longer reaction times. Their photocatalytic activity in visible light has been correlated with the formation of ~20 – 50 nm 'nano-terraced' surface features, and which are absent in the non-active $AbNbO_3$ samples prepared by solid-state methods. The highest observed photocatalytic rates for $AgNbO_3$ particles of ~60 μmol H_2 $h^{-1}g^{-1}$ are obtained in an aqueous methanol solution for the largest particle sizes, but which have a larger amount of the 'nano-terraced' surfaces features. Currently, our studies on $AgNbO_3$ have shown that while particle size can generally impact the amount of total surface area of a metal oxide, it is even more critical to be able to closely assess the relative amounts of active surfaces on the particles.

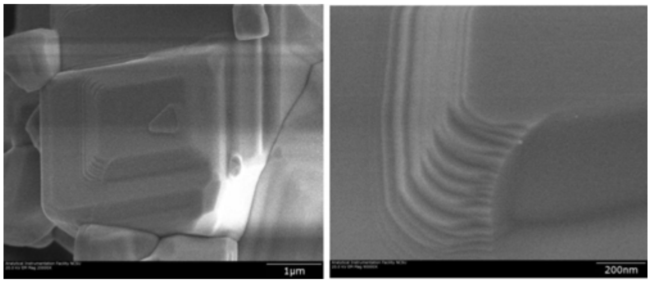

Figure 2. SEM Images of $AgNbO_3$ particle surfaces exhibiting nano-stepped features.

DOE Sponsored Publications 2007-2009

1. "Syntheses and Structures of a New Series of Silver-Vanadate Hybrid Solids and Their Optical and Photocatalytic Properties" Lin, H.; Maggard, P.A.* *Inorg. Chem.* **2008**, 47, 8044-8052.

2. "New Molten-Salt Synthesis and Photocatalytic Properties of $La_2Ti_2O_7$ Particles" Arney, D.; Greve, B.; Porter, B.; Greve, B.; Maggard, P.A.* *J. Photochem. Photobio. A: Chem.* **2008**, 199 230-235.

3. "Ligand-Mediated Interconversion of Multiply-Interprating Frameworks in Cu^{I}/Re^{VII}-Oxide Hybrids" Lin, H.; Maggard, P.A.* **2009**, submitted for publication.

4. "Syntheses, Crystal Structures and Optical Properties of a Series of Ten New Silver(I)-Rhenate(VII) Hybrids" Lin, H.; Maggard, P.A.* **2009**, revised for publication.

5. "Hydrothermal Synthesis of Microporous Cu^{I}/Nb^{V} Oxyfluoride Hybrids and Their Optical Properties" Lin, H.; Maggard, P.A.* **2009**, revised for publication.

Session VI

Molecular Photocatalysis at Surfaces

OXOMANGANESE CATALYSTS FOR SOLAR FUEL PRODUCTION

Gary W. Brudvig, Victor S. Batista, Robert H. Crabtree and Charles A. Schmuttenmaer
Department of Chemistry
Yale University
New Haven, CT 06520-8107

The design principles for efficient heterogeneous photocatalysis remain unclear and are the focus of this project. High-valent oxomanganese (oxo-Mn) complexes have been studied in great detail to understand how Nature makes O_2 from water during photosynthesis. Sensitized TiO_2 nanoparticles (NPs) are robust materials for efficient light harvesting by photoexcitation of surface complexes and interfacial electron transfer (IET). The goal of this project is to integrate these two systems to construct solar-driven photocatalytic cells, based on our own water-oxidation catalysts, and to investigate how to achieve the efficiency breakthroughs necessary to make photocatalytic water oxidation an economically viable solar fuel resource.

Four research groups in the Chemistry Department at Yale University are working together to synthesize TiO_2 NPs and anchor-linker-ligand conjugates, develop new methods for surface attachment of catalysts using oxidation-resistant anchors and linkers that are stable in water, develop and apply computational methods to analyze IET and characterize catalytic water-oxidation complexes, and use spectroscopic methods to characterize the photochemistry. See also posters by Robert Crabtree and Charles Schmuttenmaer.

Molecular Assemblies. The well-established, rigid aromatic catecholate moiety was our initial choice as an anchor to attach an oxo-Mn catalyst to TiO_2 NPs.[1] Our computational studies predicted favorable electronic couplings and suitable positioning of the electronic energy levels to allow for photoinduced Mn(II)→Mn(III) oxidation concomitant with ultrafast electron injection. This was borne out by THz and EPR spectroscopic measurements. However, catecholate proved to be suboptimal as an anchor because the oxidizing power of the resulting Mn(III) complex and the possibility of advancing the oxidation state of the complex to higher valent states were limited by the relatively high electronic states of catechol and the detrimental oxidation pathway of catechol to the ortho-quinone. Therefore, we have explored derivatized acetylacetonate (acac), siloxane and hydroxamate molecules as anchors.[2,3,5] All have proven to be oxidation resistant and stable under aqueous conditions.

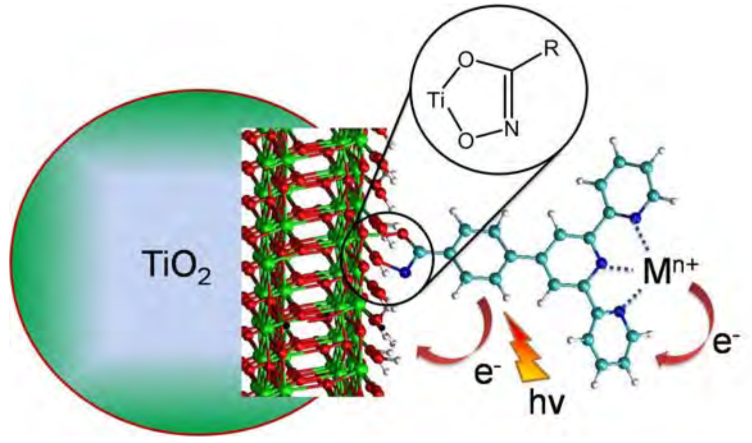

Figure 1. Hydroxamate anchor for robust functionalization of TiO_2 nanoparticles under aqueous conditions.

We have synthesized molecules with acac or hydroxamate anchors linked to 2,2’:6,2’’-terpyridine (terpy), where a phenylterpyridine ligand bound to a Mn catalyst is attached to the derivatized anchor. When attached to TiO_2 NPs (Figure 1), these anchors sensitize the system for visible light-induced IET on a sub-picosecond time scale, as monitored by optical pump–THz probe transient measurements and computer simulations. An advantage of probing charge injection with THz spectroscopy over measuring cell efficiencies is that it focuses solely on charge injection. Interfacial electron injection induces Mn(II)→Mn(III) photooxidation, as determined by EPR spectroscopy. These systems are promising for further study, both as applied to photocatalytic oxidation chemistry and for the development of dye-sensitized solar cells based on these anchors that are more stable to humidity than the classic carboxylate anchors.

Catalysis. We previously reported a dinuclear Mn(III,IV)-terpy complex that catalytically produces oxygen from water in the presence of a chemical oxidant such as oxone. We have linked this catalyst to the surface of TiO_2 NPs (Figure 2)[4] and are investigating visible light-induced oxidation catalysis. In parallel with this effort, we have been exploring other water-oxidation catalysts with improved stability and/or catalytic activity.

Plans. In the future, we aim to continue with the development of photocatalytic systems. We plan to attach oxo-Mn catalysts to TiO_2 NPs by using our new acac or hydroxamate anchors and investigate the visible-light photocatalytic activity of these surface-attached complexes. In parallel with these measurements, IET will be investigated by time-resolved THz spectroscopy and modeled by computational methods. We also aim to investigate methods to extract electrons from TiO_2 NPs in fuel-forming reactions. A longer-term goal of this project is to implement first-generation photoelectrochemical cells that would connect the photochemical oxidation of water to a fuel-forming reaction. Towards this goal, we have set up the equipment to make solar cells and characterize their efficiency. One immediate objective of our work on the development of robust anchors is to implement our new acac and hydroxamate anchors for dye-sensitized solar cells that are stable under aqueous or high humidity conditions.

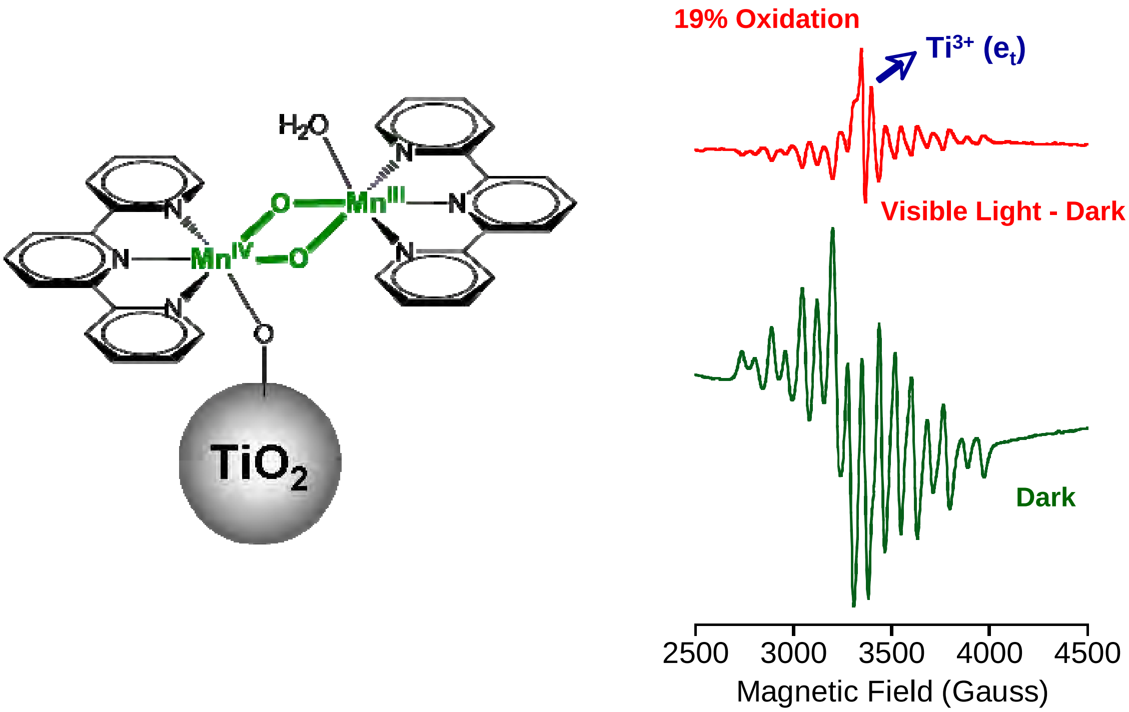

Figure 2. An oxomanganese water oxidation catalyst, bound toTiO_2 NPs through oxo bridges, exhibits visible-light photooxidation from Mn(III,IV) to Mn(IV,IV).

DOE Sponsored Publications 2007-2009

1. "Ultrafast Photooxidation of a Mn(II)-terpyridine Complex Attached to TiO_2 Nanoparticles", Sabas G. Abuabara, Clyde W. Cady, Jason B. Baxter, Charles A. Schmuttenmaer, Robert H. Crabtree, Gary W. Brudvig and Victor S. Batista (2007) *J. Phys. Chem. C 111*, 11982-11990.
2. "Acetylacetonate Anchors for Robust Functionalizaion of TiO_2 Nanoparticles with Mn(II)-terpyridine Complexes", William R. McNamara, Robert C. Snoeberger III, Gonghu Li, James M. Schleicher, Clyde W. Cady, Macarena Poyatos, Charles A. Schmuttenmaer, Robert H. Crabtree, Gary W. Brudvig and Victor S. Batista (2008) *J. Am. Chem. Soc. 130*, 14329–14338.
3. "Characterization of Siloxane Adsorbates Covalently Attached to TiO_2", Nobuhito Iguchi, Clyde Cady, Robert C. Snoeberger III, Bryan M. Hunter, Eduardo M. Sproviero, Charles A. Schmuttenmaer, Robert H. Crabtree, Gary W. Brudvig and Victor S. Batista (2008) *Proc. of SPIE 7034*, 70340C1-8.
4. "Deposition of an Oxomanganese Water Oxidation Catalyst on TiO_2 Nanoparticles: Computational Modeling, Assembly and Characterization", Gonghu Li, Eduardo M. Sproviero, Robert C. Snoeberger III, Nobuhito Iguchi, James D. Blakemore, Robert H. Crabtree, Gary W. Brudvig and Victor S. Batista (2009) *Energy & Environ. Sci. 2*, 230-238.
5. "Coherent Control of Quantum Dynamics with Sequences of Unitary Phase-Kick Pulses", Luis G.C. Rego, Lea F. Santos and Victor S. Batista (2009) *Annu. Rev. Phys. Chem. 60*, 293-320.
6. "Hydroxamate Anchors for Functionalization of Semiconductor Surfaces", William R. McNamara, Robert C. Snoeberger III, Gonghu Li, Christiaan Richter, Laura J. Allen, Rebecca L. Milot, Charles A. Schmuttenmaer, Robert H. Crabtree, Gary W. Brudvig and Victor S. Batista (2009) *J. Am. Chem. Soc.*, submitted.
7. "Synergistic Effect between Anatase and Rutile TiO_2 Nanoparticles in Dye-senstized Solar Cells", Gonghu Li, Christiaan Richter, Rebecca L. Milot, Charles Schmuttenmaer, Robert H. Crabtree, Gary W. Brudvig and Victor S. Batista (2009) *J. Chem. Soc., Dalton Trans.*, submitted.
8. "Single Molecule Electron Transfer Dynamics in Interfacial Donor-bridge-nanoparticle Acceptor Complexes", Shengye Jin, Robert C. Snoeberger III, Abey Issac, Victor S. Batista and Tianquan Lian (2009) *J. Am. Chem. Soc.*, submitted.
9. "Interfacial Electron Transfer in TiO_2 Surfaces Sensitized with Ru(II)-polypyridine Complexes", Elena Jakubikova, Robert C. Snoeberger III, Victor S. Batista and Enrique R. Batista (2009) *J. Phys. Chem. A*, submitted.
10. "Visible Light Sensitization of TiO_2 Based on Surface Functionalization with Tris(8-hydroxyquinoline)Aluminum(III)", Luis G.C. Rego, Robson da Silva, Jose A. O. Freire, Robert C. Snoeberger III and Victor S. Batista (2009) *J. Am. Chem. Soc.*, submitted.

HETEROBINUCLEAR UNITS FOR DRIVING H_2O OXIDATION OR CO_2 REDUCTION CATALYSTS ON SILICA NANOPORE SURFACES

Heinz Frei
Physical Biosciences Division, Lawrence Berkeley National Laboratory
Berkeley, CA 94720

Conversion of CO_2 to methanol or another low alcohol using H_2O as electron source is an attractive goal for sunlight to fuel conversion. To take advantage of the flexibility and precision by which light absorption, charge transport and catalytic properties can be controlled by discrete molecular structures, we are exploring an inorganic 'molecular' approach for assembling artificial photosynthetic systems. Photocatalytic units anchored on silica nanopore surfaces consist of an oxo-bridged binuclear metal-to-metal charge-transfer chromophore (MMCT) which is coupled to a multi-electron transfer catalyst. We have developed mild, selective synthetic methods for assembling a variety of hetero-binuclear chromophores featuring first row metals. The selectivity is based on acidity differences between metal-OH groups and surface silanols (e.g. synthesis of TiOCo^{II}, TiOCe^{III}, ZrOCu^{I}, TiOMn^{II}) or on selective redox reactivity (e.g. TiOCr^{III}). The chromophores serve as visible light electron pumps with selectable redox potential that depends on the choice of donor and acceptor metal and its oxidation state. Precise matching of redox potentials is essential for attaining thermodynamic efficiency and directional charge flow. Photocatalytic units for CO_2 splitting to CO and for the H_2O oxidation half reaction have been demonstrated. Recent effort has focused on the detailed structural characterization of these units by vibrational, EPR and X-ray spectroscopy, and on time-resolved optical and FT-infrared studies for gaining a quantitative understanding of these robust all-inorganic photocatalysts.

Photocatalytic unit for visible light water oxidation

Using selective redox coupling of Ti and Ir precursors with Cr centers anchored on silica nanopore surfaces of MCM-41 material, we have assembled photocatalytic units consisting of a $\text{TiOCr}^{III} \rightarrow \text{Ti}^{III}\text{OCr}^{IV}$ metal-to-metal charge transfer chromophore coupled to an Ir oxide nanocluster (2 nm). The unit evolves O_2 from water (pH 7) with visible light with a quantum yield of $\geq$ 14 percent (Clark electrode). The remarkable efficiency indicates that electron transfer from the Ir oxide cluster to transient Cr^{IV} donor is competitive with back reaction of the excited TiOCr chromophore. In-situ FT-Raman spectroscopy revealed the formation of O_2^- (superoxide) (994 cm^{-1} in H_2O, 961 ($^{18}O^{16}O^-$) and 930 cm^{-1} ($^{18}O_2^-$) in $H_2{}^{18}O$). EPR measurements showed that the superoxide formed as a $\text{Ti}^{IV}\text{--}O_2^-$ complex whose formation indicates trapping of the evolving O_2 by transient Ti^{III} centers. If the half reaction is performed in the absence of persulfate acceptor, a steady-state buildup of Ti^{III} is observed. This confirms that the Ir oxide nanocluster catalyst couples efficiently with the Cr donor center. This MMCT unit constitutes the first example of an all-inorganic visible charge-transfer chromophore with selectable donor redox potential for driving water oxidation. The synthetic flexibility of assembling such charge-transfer sites and coupling them to catalysts opens up the development of robust photocatalysts on nanoporous supports with tailored light absorption properties and matched redox potentials.

Cr K-edge EXAFS measurement of the TiOCr^{III} unit revealed a second-shell peak originating from backscattering by the Ti center at a distance of 3.0 Angstrom. Curve fitting indicates two CrO bond distances, namely 2.0 A for CrOSi linkages and 1.8 A for the CrO bond that is part of the CrOTi bridge. The shorter CrO bond length of the heterobinuclear bridge is consistent with a 0.4 eV blue shift of the Cr K-edge of the TiOCr unit compared to isolated Cr^{III} centers, indicating a small charge transfer contribution to the ground state.

Time-resolved optical absorption study of electron transfer of MMCT units

In order to establish the lifetime and back electron transfer kinetics of excited metal-to-metal charge-transfer states of hetero-binuclear heterobinuclear chromophores in silica nanopores, we have conducted a nanosecond transient absorption study of $TiOMn^{II}$ units anchored on SBA-15 silica nanopores. The $TiOMn^{II}$ unit was selected because the $TiOMn^{II} \rightarrow Ti^{III}OMn^{III}$ charge-transfer absorption is the most prominent transition across the visible spectrum. When conducting spectroscopy in transmission mode using index-matching liquids, a transient bleach of several microseconds duration was observed whose amplitude mirrored the MMCT absorption profile. Hence, the recovery of the signal is attributed to back electron transfer $Ti^{III}OCr^{IV} \rightarrow Ti^{IV}OCr^{III}$ (Figure). The decay kinetics is best described as a superposition of first order decays with a spread of rate constants (Albery model: mean time constant 1.6 μsec, γ = 1). The dispersive first order kinetics is indicative of structural heterogeneity of the silica surface environment of the MMCT chromophore, consistent with the amorphous nature of the mesoporous silica material. We speculate that the unusually long lifetime of the excited charge-transfer unit is due to reorganization of the interaction of the Cr and Ti metal centers with neighboring O centers (siloxane, silanol, siloxy groups in the silica nanopore surface) as the systems responds to the photo-induced oxidation state changes, resulting in a substantial barrier for back electron transfer. The slow back electron transfer explains the observed photochemical activity of these heterobinuclear charge-transfer chromophores.

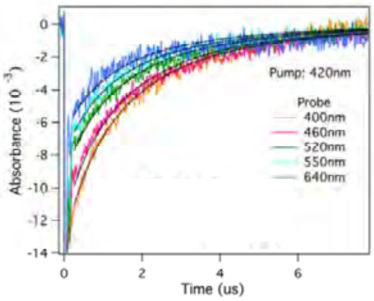

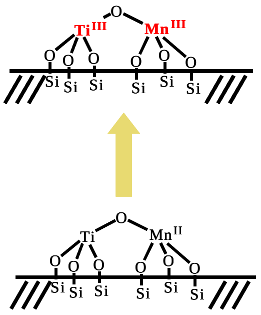

Time-resolved ATR-FT-IR spectroscopy of water oxidation at metal oxide nanoparticle catalysts

Elucidation of elementary steps of the 4-electron process of H_2O oxidation to O_2 at metal oxide nanoparticles is critical for designing more efficient multi-electron catalyst for oxygen evolution. To determine the feasibility and optimize the spectroscopic sensitivity for time-resolved studies on photocatalytic units using the attenuated total reflection (ATR) method, we have begun experiments with aqueous colloidal solutions of Ir oxide catalyst particles driven by a visible light sensitizer. With the rapid-scan method, transient intermediates on the millisecond time scale are observed that exhibit isotope shifts upon use of $H_2{}^{18}O$ (e.g. at 1125 and 868 cm^{-1}). The goal of these studies is to gain a step-by-step understanding of the reaction mechanism for oxygen evolution on catalytically active metal oxide nanoparticle surfaces.

Taking advantage of the selective synthetic methods for the assembly of inorganic photocatalytic units on nanoporous supports developed in the past few years, future effort will focus on optical, vibrational, EPR and X-ray steady state and time-resolved spectroscopic studies for developing a detailed understanding of the dynamical and mechanistic aspects of these systems. Insights into the physical and chemical properties that limit photochemical efficiency will form the basis for developing more efficient photocatalytic units.

DOE Sponsored Publications 2006-2008 (Field Work Proposal "Chemistry with Near Infrared Photons")

R. Nakamura and H. Frei. Visible Light-Driven Water Oxidation by Ir oxide Clusters Coupled to Single Cr Centers in Mesoporous Silica. *J. Am. Chem. Soc.* **128**, 10668-10669 (2006).

L.K. Andersen and H. Frei. Dynamics of CO in Mesoporous Silica Monitored by Time-Resolved Step-Scan and Rapid-Scan FT-IR Spectroscopy. *J. Phys. Chem. B* **110**, 22601-22607 (2006).

H. Frei. Selective Hydrocarbon Oxidation in Zeolites (Perspective Article). *Science* **313**, 309-310 (2006).

J.F. Cahoon, M.F. Kling, K.R. Sawyer, H. Frei, and C.B. Harris. 19-Electron Intermediates in the Ligand Substitution of $CpW(CO)_3^{\cdot}$ with a Lewis Base. *J. Am. Chem. Soc.* **128**, 3152-3153 (2006).

W. Lin and H. Frei. Bimetallic Redox Sites for Photochemical CO_2 Splitting in Mesoporous Silicate Sieve. *Cont. Rend. Sci.* **9**, 207 (2006).

H. Han and H. Frei. Visible Light Absorbing Ti-Co Metal-to-Metal Charge-Transfer Sites on Mesoporous Silica Surface. *Microporous Mesoporous Mater*. **103**, 265-272 (2007).

G. Mul, W.A. Wasylenko, and H. Frei. Cyclohexene Photooxidation over Vanadia Catalyst Analyzed by Time-Resolved ATR-FT-IR Spectroscopy. *Phys. Chem. Chem. Phys.* **10**, 3131-3137 (2008).

H. Han and H. Frei. Controlled Assembly of Hetero-binuclear Sites on Mesoporous Silica: Visible Light Charge-Transfer Units with Selectable Redox Properties. *J. Phys. Chem. C* **112**, 8391-8399 (2008).

H. Han and H. Frei. In-Situ Spectroscopy of Water Oxidation at Ir Oxide Nanocluster Driven by Visible TiOCr Charge-Transfer Chromophore in Mesoporous Silica. *J. Phys. Chem. C* **112**, 16156-16159 (2008)

W. Weare and H. Frei. Artificial Photosynthesis, In: *Yearbook of Science and Technology;* Weil, J., Ed.; McGraw Hill: New York (2009); p.28-31.

H. Han, W. Weare, and H. Frei. Artificial Photosynthesis in Nanoporous Solids. *J. Chem. Soc. Dalton Trans.,* submitted.

W. Weare, F. Jiao, and H. Frei. Polynuclear Units in Nanoporous Silica for Sunlight to Fuel Conversion. *Chimia,* submitted.

T. Cuk, W.W. Weare, and H. Frei. Long Lifetime of Excited Metal-to-Metal Charge-Transfer State of $TiOMn^{II}$ Binuclear Unit Anchored on Silica Nanopore Surface. To be submitted.

TOWARD PHOTOCHEMICAL WATER SPLITTING
USING BAND-GAP-NARROWED SEMICONDUCTORS
AND TRANSITION-METAL BASED MOLECULAR CATALYSTS

James T. Muckerman,[†‡] José A. Rodriguez,[†] and Etsuko Fujita[†]
[†]Chemistry Department and [‡]Center for Functional Nanomaterials
Brookhaven National Laboratory
Upton, NY 11973-5000

We are carrying out coordinated theoretical and experimental studies of toward photochemical water splitting using band-gap-narrowed semiconductors (BGNSCs) with attached multi-electron molecular water oxidation and hydrogen production catalysts. We focus on the coupling between the materials properties and the H_2O redox chemistry, with an emphasis on attaining a fundamental understanding of the individual elementary steps in the following four processes:

(1) Light-harvesting and charge-separation of stable oxide or oxide-derived semiconductors for solar-driven water splitting, including the discovery and characterization of the behavior of such materials at the aqueous interface;
(2) The catalysis of the four-electron water oxidation by dinuclear hydroxo transition-metal complexes with quinonoid ligands, and the rational search for improved catalysts;
(3) Transfer of the design principles learned from the elucidation of the DuBois-type hydrogenase model catalysts in acetonitrile to the rational design of two-electron hydrogen production catalysts for aqueous solution;
(4) Combining these three elements to examine the function of oxidation catalysts on BGNSC photoanode surfaces and hydrogen production catalysts on cathode surfaces at the aqueous interface to understand the challenges to the efficient coupling of the materials functions.

1. Elucidation and Characterization of the Structure, Band Gap and Interfacial Properties of the GaN/ZnO Solid-Solution Photocatalyst. Domen *et al*. reported encouraging photocatalytic performance for the solid-solution photocatalyst $(Ga_{1-x}Zn_x)(N_{1-x}O_x)$ loaded with mixed oxides of rhodium and chromium in overall water splitting. Perhaps most impressive was that if silver nitrate was used as a sacrificial electron acceptor, the quantum efficiency for oxygen evolution rose to 51% at 420–440 nm, which is 20 times higher than that for overall water splitting. We have carried out a systematic study of the structural and electronic properties of the $(Ga_{1-x}Zn_x)(N_{1-x}O_x)$ solid solution as a function of zinc (oxygen) concentration, x, using density-functional theory (DFT). The DFT+U approach has been adopted, and two different periodic supercells, the 16-atom $(Ga_{8-n}Zn_n)(N_{8-n}O_n)$ and 32-atom $(Ga_{16-n}Zn_n)(N_{16-n}O_n)$, have been used to model this solid solution.

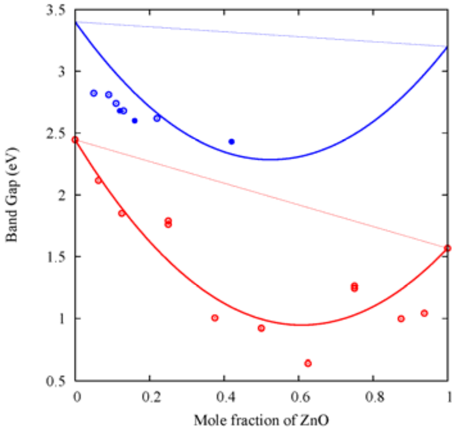

Variation of band gap as a function of Zn (O) concentration, x. Red: calculated BGs and smoothed $E_g(x)$ curve using the estimated bowing parameter b. Blue: experimental data for $(Ga_{1-x}Zn_x)(N_{1-x}O_x)$ solid solution and predicted experimental $E_g(x)$ behavior using the estimated b and the limiting GaN and ZnO band gaps.

The calculated band gap as a function of ZnO content, x, is shown in the figure above as red points along with the red curve showing the best fit a quadratic equation with a bowing parameter *b* indicating the leading term from ideal behavior. The blue curve shows the interpolation of the experimental band gaps for GaN and ZnO with the calculated value of *b*, and the blue points indicate experimental band gap measurements from Domen's group. Our prediction is that a minimum band gap of ca. 2.4 eV should occur at roughly $x = 0.5$. More recent theoretical work has shown that an H_2O monolayer on the GaN(10$\underline{1}$0) surface dissociates completely, and that additional overlayers or MD simulations of the bulk H_2O interface cause the structure of the surface monolayer to change. Future work will pursue H_2O oxidation pathways at surfaces of GaN/ZnO with different compositon and exposed faces using DFT, first-principles MD and kinetic Monte Carlo techniques. Recent experimental work has elucidated the mechanism of GaN/ZnO synthesis from Ga_2O_3/ZnO mixtures and NH_3 using time-dependent powder XRD, and current work is exploring synthesis routes for producing GaN/ZnO solid solutions of arbitrary composition.

2. Characterization of the electrochemistry of $Ru^{II}(OH_2)(Q)(tpy)$, the Tanaka catalyst and its monomer through construction of experimental and theoretical Pourbaix diagrams. We have investigated the redox states of $Ru(OH_2)(Q)(tpy)^{2+}$ (Q = 3,5-di-*tert*-butyl-1,2-benzoquinone, tpy = 2,2´:6´,2″-terpyridine), the monomer of the Tanaka catalyst, $[Ru_2(OH)_2(Q)_2(btpyan)]^{2+}$ (Q = 3,6-di-*tert*-butyl-1,2-benzoquinone, btpyan = 1,8-bis(2,2´:6´,2″-terpyrid-4´-yl)-anthracene), containing non-innocent quinone ligands, through experimental and theoretical UV-vis spectra and Pourbaix diagrams. The electrochemical properties were determined for the species resulting from deprotonation and redox processes in aqueous solution. The formal oxidation states of the redox couples in the various intermediate complexes were systematically assigned using electronic structure theory. The various pK_a values and reduction potentials, including the consideration of proton-coupled electron-transfer (PCET) processes, were calculated, and the theoretical version of the Pourbaix diagram was constructed in order to elucidate and assign several previously ambiguous regions in the experimental diagram (see figure above). Guided by the redox behavior of the monomer, we are constructing the Pourbaix of the dimer catalyst to aid the design of improved catalysts, and have tentatively proposed its water oxidation mechanism to be that shown in the figure at the right in which the oxidation state of the metal centers remains predominantly 2+ throughout the catalytic cycle. The O–O bond is formed by the reaction of two oxyl radicals to form a superoxide species.

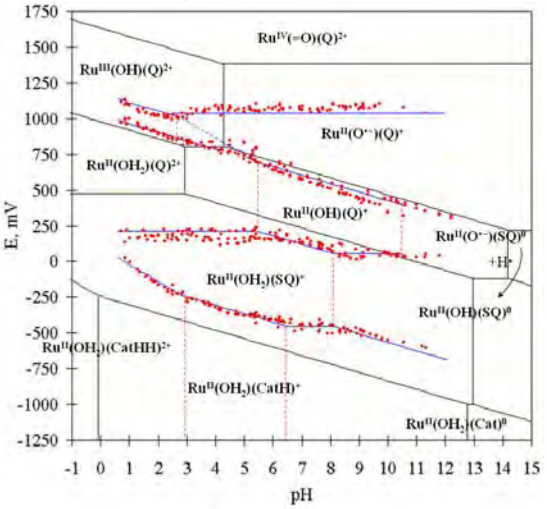

An experimental and theoretical Pourbaix diagram of $Ru(OH_2)(Q)(tpy)^{2+}$. $E_{1/2}$ is relative to the SCE. The red dashed and solid blue lines correspond to the experimental pK_a and redox potentials. The black lines are the theoretical predictions.

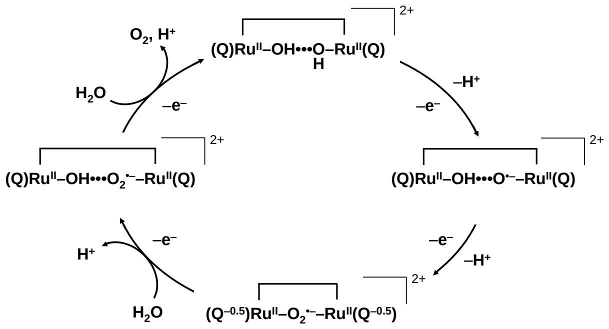
(Q)Ru^II–OH•••O–Ru^II(Q)
H
2+
–H+
–e–
(Q)Ru^II–OH•••O^•–Ru^II(Q)
2+
–e–
–H+
(Q^−0.5)Ru^II–O2^•−–Ru^II(Q^−0.5)
2+
H2O
H+
–e–
(Q)Ru^II–OH•••O2^•−–Ru^II(Q)
2+
H2O
O2, H+
–e–

Proposed mechanism for water oxidation by the Tanaka catalyst in aqueous solution at pH 4.

DOE Sponsored Publications: Hydrogen Fuel Initiative 2006-2008

1. Nambu, A.; Graciani, J.; Rodriguez, J. A.; Wu, Q.; Fujita, E.; Fernandez-Sanz, J. “N-doping of TiO_2(110): Photoemission and Density Functional Studies” *J. Chem. Phys.* **2006**, *125*, 094706-1,8.
2. Wilson, A. D.; Newell, R. H.; McNevin, M. J.; Muckerman, J. T.; DuBois, M. R.; DuBois, D. L. “Hydrogen oxidation and production using nickel-based molecular catalysts with positioned proton relays” *J. Am. Chem. Soc.* **2006**, *128*, 358-366.
3. Chen, H.; Nambu, A.; Wen, W.; Graciani, J.; Zhong, Z.; Hanson, J. C.; Fujita, E.; Rodríguez, J. A. “Reaction of NH_3 with Titania: N-doping of the Oxide and TiN formation” *J. Phys. Chem. C* **2007**, *111*, 1366-1372.
4. Fernández-García, M.; Wang, X.; Belver, C.; Hanson, J. C.; Rodriguez, J. A. “Anatase-TiO_2 Nanomaterials: Morphological/Size Dependence of the Crystallization and Phase Behavior Phenomena” *J. Phys. Chem. C* **2007**, *111*, 674-682.
5. Fernández-García, M.; Belver, C.; Hanson, J. C.; X. Wang; Rodriguez, J. A. “Anatase-TiO_2 Nanomaterials: Analysis of Key Parameters Controlling Crystallization” *J. Am. Chem. Soc.* **2007**, *129*, 13604-13612.
6. Graciani, J.; Fernandez-Sanz, J.; Asaki, T.; Nakamura, K.; Rodriguez, J. A. “Interaction of oxygen with TiN(001): $\mathrm{N}\leftrightarrow\mathrm{O}$ exchange and oxidation process” *J. Chem. Phys.* **2007**, *126*, 244713-1,8.
7. Wilson, A. D.; Shoemaker, R. K.; Miedaner, A.; Muckerman, J. T.; DuBois, D. L.; DuBois, M. R. “Nature of hydrogen interactions with Ni(II) complexes containing cyclic phosphine ligands with pendant nitrogen bases” *PNAS* **2007**, *104*, 6951-6956.
8. Jensen, L.; Muckerman, J. T.; Newton, M. D. “First-Principles Studies of the Structural and Electronic Properties of the $(Ga_{1-x}Zn_x)(N_{1-x}O_x)$ Solid Solution Photocatalyst” J. Phys. Chem. C **2008**, *112*, 3439-3446.
9. Muckerman, J. T.; Polyansky, D. E.; Wada, T.; Tanaka, K.; Fujita, E. “Water Oxidation by a Ruthenium Complex with Non-Innocent Quinone Ligands: Possible Formation of an O–O Bond at a Low Oxidation State of the Metal. Forum ‘on Making Oxygen’” *Inorg. Chem.* **2008**, *47*, 1787-1802.
10. Tseng, H.-W.; Zong, R.; Muckerman, J. T.; Thummel, R. “Mononuclear Ru(II) Complexes That Catalyze Water Oxidation” *Inorg. Chem.* **2008**, *47*, 11763-11773.
11. Chen, H.; Wen, W.; Wang, Q.; Hanson, J. C.; Muckerman, J. T.; Fujita, E.; Frenkel, A.; Rodriguez, J. A. “Preparation of $(Ga_{1-x}Zn_x)(N_{1-x}O_x)$ Photocatalysts from the Reaction of NH_3 with Ga_2O_3/ZnO and $ZnGa_2O_4$: In situ Time-Resolved XRD and XAFS Studies” *J. Phys. Chem. C* **2009**, *113*, 3650-3659.
12. Shen, X.; Allen, P. B.; Hybertsen, M. S.; Muckerman, J. T. “Water Adsorption on the GaN (1010) Non-polar Surface.” (Letter) *J. Phys. Chem. C* **2009,** *113*, 3365–3368.
13. Graciani, J.; Alvarez, L. J.; Rodriguez, J. A.; Fernandez-Sanz, J. “N Doping of Rutile TiO_2(110) Surface. A Theoretical DFT Study” *J. Phys. Chem. C* **2008**, *112,* 2624-2631.
14. Tsai, M.-K.; Rochford, J.; Polyansky, D. E.; Wada, T.; Tanaka, K.; Fujita, E.; Muckerman, J. T. “Characterization of Redox States of $Ru(OH_2)(Q)(terpy)^{2+}$ (Q = 3,5-di-tert-butyl-1,2-benzoquinone, terpy = 2,2′:6′,2″-terpyridine) and Related Species through Experimental and Theoretical Studies” *Inorg. Chem.* **2009**, ASAP, DOI: 10.1021/ic900057y.

DOE Sponsored Publications: Solar Energy Utilization Initiative 2006-2008

1. Fujita, E.; Muckerman, J. T.; Tanaka, K. "Photochemical CO_2 Reduction by Rhenium and Ruthenium Complexes" *Am. Chem. Soc. Div. Fuel Chem.* **2008**, *53(1).*
2. Polyansky, D. E.; Cabelli, D.; Muckerman, J. T.; Fukushima, T.; Tanaka, K.; Fujita, E. "Mechanism of Hydride Donor Generation using a Ru(II) Complex Containing an NAD^+ Model Ligand: Pulse and Steady-State Radiolysis Studies" *Inorg. Chem.* **2008**, *47*, 3958-3968 (Featured as a cover article).
3. Muckerman, J. T.; Fujita, E. "Artificial Photosynthesis" In *Chemical Evolution II: From Origins of Life to Modern Society. ACS Symposium Series*; Zaikowski, L.; Friedrich, J. M., Eds.; American Chemical Society: Washington, D.C., **2009**, in press.
4. Achord, P.; Fujita, E.; Muckerman, J. T. "Theoretical Investigation of Tuning the Hydricity of Photogenerated Hydrides for Catalytic CO Reduction" in preparation.
5. Fukushima, T.; Fujita, E.; Muckerman, J. T.; Polyansky, D. E.; Tanaka, K. "Stereospecific Photogeneration of a Renewable Hydride Donor" in preparation

DOE Sponsored Publications: Core Program 2006-2008

1. Fujita, E.; Brunschwig, B. S.; Creutz, C.; Muckerman, J. T.; Sutin, N.; Szalda, D. J.; van Eldik, R. "Transition State Characterization for the Reversible Binding of Dihydrogen to Bis(2,2'-bipyridine)rhodium(I) from Temperature- and Pressure-Dependent Experimental and Theoretical Studies" *Inorg. Chem.* **2006**, *45*, 1595-1603.
2. Grills, D. C.; Huang, K.-W.; Muckerman, J. T.; Fujita, E. "Kinetic Studies of the Photoinduced Formation of Transition Metal-Dinitrogen Complexes Using Time-Resolved Infrared and UV-vis Spectroscopy" *Coord. Chem. Rev.* **2006**, *250*, 1681-1695.
3. Grills, D. C.; van Eldik, R.; Muckerman, J. T.; Fujita, E. "Direct Measurements of Rate Constants and Activation Volumes for the Binding of H_2, D_2, N_2, C_2H_4 and CH_3CN to $W(CO)_3(PCy_3)_2$: Theoretical and Experimental Studies with Time-Resolved Step-Scan FTIR and UV-vis Spectroscopy" *J. Am. Chem. Soc.* **2006**, *128*, 15728-15741.
4. Huang, K.-W.; Han, J. H.; Musgrave, C. B.; Fujita, E. "Carbon Dioxide Reduction by Pincer Rhodium η^2-Dihydrogen Complexes: Hydrogen Binding Modes and Mechanistic Studies by Density Functional Theory Calculations" *Organometallics* **2007**, *26*, 508-513.
5. Miyasato, Y.; Wada, T.; Muckerman, J. T.; E. Fujita; Tanaka, K. "Generation of Ru(II)-Semiquinone-Anilino Radical through Deprotonation of Ru(III)-Semiquinone-Anilido Complex" *Angew. Chem. Int. Ed.* **2007**, *46*, 5728-5730.
6. Muckerman, J. T.; Fujita, E.; Hoff, C. D.; Kubas, G. J. "Theoretical Investigation of the Binding of Small Molecules and the Intramolecular Agostic Interaction at Tungsten Centers with Carbonyl and Phosphine Ligands" *J. Phys. Chem. B* **2007**, *111*, 6815-6821.
7. Polyansky, D.; Cabelli, D.; Muckerman, J. T.; Fujita, E.; Koizumi, T.-A.; Fukushima, T.; Wada, T.; Tanaka, K. "Photochemical and Radiolytic Production of Organic Hydride Donor with Ru(II) Complex Containing an NAD^+ Model Ligand" *Angew. Chem. Int. Ed.* **2007**, *46*, 4169-4172.

8. Shinozaki, K.; Hayashi, Y.; Brunschwig, B. S.; Fujita, E. "Characterization of transient species and products in photochemical reactions of Re(dmb)$(CO)_3$ Et with and without CO_2" *Res. Chem. Intermed.* **2007**, *33*, 27-36.
9. Fujita, E.; Muckerman, J. T. "Catalytic Reactions Using Transition-Metal-Complexes toward Solar Fuel Generation" (Invited Review Article) *Bull. Jpn. Soc. Coord. Chem.* **2008**, *51*, 41-54.
10. Huang, K.-W.; Grills, D. C.; Han, J. H.; Szalda, D. J.; Fujita, E. "Selective Decarbonylation by a Pincer PCP-Rhodium(I) Complex" *Inorg. Chim. Acta* **2008**, *361*, 3327-3331.
11. Doherty, M. D.; Grills, D. C.; Fujita, E. "Synthesis and Photophysical Characterization of Fluorinated Re(4,4′-X_2-2,2′-bipyridine)$(CO)_3Cl$ Complexes in CH_3CN and $scCO_2$" *Inorg. Chem.* **2009**, *48*, 1796-1798.
12. Achord, P.; Fujita, E.; Muckerman, J. T.; Scott, B.; Fortman, G. C.; Temprado, M.; Xiaochen, C.; Captain, B.; Isrow, D.; Weir, J. J.; McDonough, J. E.; Hoff, C. D. "Experimental and Computational Studies of Binding of Dinitrogen, Nitriles, Azides, Diazoalkanes, Pyridine and Pyrazines to $M(PR_3)_2(CO)_3$ (M = Mo,W; R = Me, ^{i}Pr)" *Inorg. Chem.*, submitted.
13. Doherty, M. D.; Grills, D. C.; Huang, K.-W.; Polyansky, D.; Fujita, E. "Kinetics and Thermodynamics of Small Molecule Binding to a PCP-Pincer Rhodium(I) Complex: Direct Addition to a Three-Coordinate Intermediate" *J. Am. Chem. Soc.*, submitted.

Session VII

Dye Sensitized Semiconductors

MONODISPERSED ZINC OXIDE NANOPARTICLE-DYE DYADS AND TRIADS: CHARACTERIZATION OF THE EARLY EVENTS IN DYE-SENSITIZED SEMICONDUCTOR ELECTRODES

David A. Blank, Wayne L. Gladfelter and Kent R. Mann
Department of Chemistry
University of Minnesota
Minneapolis, MN 55455

The overarching goal of this research is to study the relationship between structure, energetics, and dynamics in a set of synthetically controlled donor-acceptor dyads and triads. These studies will provide an understanding of the light absorption and charge transfer steps at the heart of dye sensitized solar cells that use ZnO, thus enabling significant future advances in cell efficiencies. Understanding the surface chemistry of zinc oxide nanocrystals (NCs) is a vital step towards understanding the electronic coupling between the dye and NC. Unlike nanocrystalline ZnO films that have been heat treated prior to dye adsorption, we have discovered that the excited state of $\{Ru[bpy]_2[dcbpy]\}[PF_6]_2$, [bpy = 2,2'-bipyridine; dcbpy = 4,4'-diacid-2,2'-bipyridine] which has found extensive use with TiO_2 is not quenched by the NC dispersions despite being entirely quenched by thin films of ZnO. In contrast, we have shown that a new terthiophene carboxylate dye similar to one that is quenched on TiO_2 is also quenched by zinc oxide NCs. Our studies showed that the Ru dye prefers coordination to Zn(II) solution species, either left over from the NC synthesis or generated from reactions with the ZnO surface. In the terthiophene case, we have found efficient quenching of the terthiophene fluorescence by the ZnO that suggests carboxylate binding depends on the nature of the dye.

The observation of these nuances in surface chemistry that affect dye binding have focused much of our NC synthesis effort on understanding the nature of the NC surface and the surfactant to understand this difference in quenching behavior. Monodispersed, spherical ZnO NCs were synthesized from the reaction of an amide precursor, $[Zn(N^iBu_2)_2]_2$, with hexylamine followed by reactions of the as-formed solution in a moist air flow. Room temperature reactions led to 2.8-5.3 nm NCs with the sizes increasing in direct proportion to the relative humidity. Purification afforded multigram quantities of stable, NCs that were dispersible in nonpolar solvents. The NCs were characterized using elemental analysis, X-ray diffraction, transmission electron microscopy, thermal gravimetric analysis (TGA), X-ray photoelectron spectroscopy (XPS), solution and solid-state NMR, IR, UV-Vis absorption and photoluminescence spectroscopies. In addition to providing H_2O to serve as the source of oxygen in the ZnO, the airflow adds CO_2 that converts the alkylamine into an alkylammonium alkylcarbamate, which serves as the surfactant. Elemental analysis, TGA and XPS results established that the total number of N-hexyl fragments on a 3.7 nm NC was 200, where they exist as an equal number of anionic carbamates and cationic ammonium ions. The addition of pure hexylammonium hexylcarbamate to ZnO NCs prepared by literature methods resulted in the formation of a product that was similar to, but not identical with, the ZnO formed using $[Zn(N^iBu_2)_2]_2$. Larger NCs up to 7.3 nm were also obtained by heating smaller NCs in a mixture of hexylamine and toluene at 119 °C. We have subsequently synthesized several Ru and Ir complexes with uncomplexed amine and carbamate substituents and are currently studying the incorporation of these dyes into the carbamate-coated NCs.

We have observed charge injection from the Ru-based dye, N719, and Coumarin 343 (C343) into colloidal ZnO NCs. The top figure shows pump-probe spectra for N719 alone and bound to ZnO NCs in solution. The highlighted region around 810 nm of N719 alone shows little change so this region was used to measure a charge injection rate of ~30 ps with no evidence for charge recombination in the first 900 ps. Charge injection from C343 was measured via both pump-probe and time resolved fluorescence (the middle figure shows fluorescence). There is multi-faceted charge injection on sub-ps, ps, and 100 ps time scales. Fluorescence is nearly completely quenched by 100 ps, demonstrating that in our C343/ZnO NC solutions virtually all dye molecules are bound to the ZnO surface. The charge injection dynamics show evidence for acceleration of the injection at higher excitation energies.

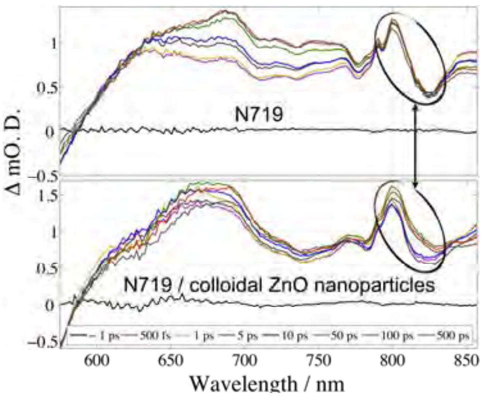

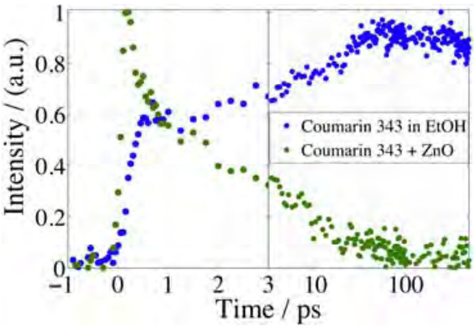

We have also investigated how electronic substituents influence the excited state properties of a series of substituted terthiophenes to be used as potential direct sensitizers or dye substituents. Substitution offers synthetic control over the absorption frequencies and redox potentials. Absorption, fluorescence, Stokes shifts, fluorescence quantum yields, excited state lifetimes, and ultrafast pump-probe and fluorescence were measured in a range of solvents. The lowest figure shows the pump-probe spectrum for a dinitro-substituted terthiophene. Excited state absorption from the initially excited singlet state appears immediately and then transforms into triplet absorption in 300 ps (see the trace at 7 ns probe delay). The excited single and triplet absorptions are completely overlapped, but ISC and the spectral assignments are confirmed by contrast with time resolved fluorescence (inset, fluorescence is the blue trace). Absorption was tunable across 12,000 cm^{-1} in the visible.

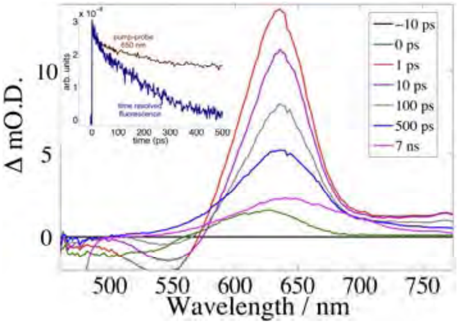

The future experiments will quantify the ZnO-dye binding constants as a function of the dye structure, binding chemistry, surfactant and NC diameter. The synthesis of additional dye molecules containing oxygen donor atoms that will produce Zn surface complexes with six membered rings (e. g. β-diketonates) for attachment is in progress. These dyes include metal complexes and oligothiophenes with β-diketonates groups either as remote substituents or with π-systems directly coupled into the chromophore. The ultrafast spectroscopic and kinetic measurements will explore charge injection as a function of the excited state potentials as well as the above chemical variations. In addition, we will explore the impact on charge injection of the number of dyes bound to each NC and search for evidence of hot electron injection.

DOE Sponsored Publications

1. Bing Luo, Julia Rossini and Wayne L. Gladfelter*, "Zinc Oxide Nanocrystals Stabilized by Alkylammonium Alkylcarbamates", submitted for publication.

2. Bing Luo and Wayne L. Gladfelter*, "On The Way to Monodispersed ZnO Nanocrystals. Structure of a Zinc Dimer Bearing Primary Amido Ligands", submitted for publication.

3. Adam S. Huss, Ted Pappenfus, Jon Bohnsack, Michael Burand, Kent R. Mann, and David A. Blank, "The Influence of Internal Charge Transfer on Non-radiative Decay in Substituted Terthiophenes", submitted for publication.

FIRST-ROW TRANSITION METAL-BASED CHROMOPHORES FOR DYE-SENSITIZED SEMICONDUCTORS: FUNDAMENTAL ISSUES AND APPLICATIONS

Amanda Smeigh, Allison Brown, Lindsey Jamula, Dong Guo, and James K. McCusker*
Department of Chemistry
Michigan State University
East Lansing, MI 48824

The goal of our research program is to develop chromophores based on first-row transition metal ions for use in dye-sensitized, nanoparticle-based solar cells (DSSCs). The underlying motivation for this research is two-fold. First, since the report by Ferrere and Gregg in 1998 of a functional (albeit low efficiency) device based on a FeII polypyridyl sensitizer there has been little in the way of a concerted effort to further explore the use of first-row transition metal complexes in these devices; such compounds represent a large class of redox-active, synthetically tunable chromophores that have yet to be adequately examined for possible applications in this technology. Second, in order to achieve cost/efficiency ratios in DSSCs necessary for them to compete effectively with fossil fuel-based technologies, it is our belief that multicomponent assemblies will ultimately be required. This (among other reasons) necessitates the use of extremely inexpensive materials for all components of the device. This presentation will summarize the first phase of what we expect will be an expansive effort to examine all aspects of DSSC performance with the notion of using earth-abundant materials as a cornerstone of cell design.

One of the key concepts driving our research effort is understanding (and ultimately controlling) the intramolecular electronic surface crossings that compete with interfacial electron transfer in DSSCs; we believe this is a critical parameter for the eventual implementation of first-row transition metal chromophores in this technology. Our level of understanding of the factors that govern ultrafast dynamics in molecules lags far behind what we know concerning ground-state recovery dynamics. As such, we have been exploiting a range of spectroscopic tools in order to examine various aspects of excited-state evolution in transition metal-based systems. Our initial efforts along these lines resulted in the first determination of the time scale of formation of the 5T2 ligand-field state, which corresponds to the end-point of excited-state evolution in FeII compounds. The system we examined was [Fe(tren(py)3)]2+, a compound that serves as a convenient prototype for ultrafast spectroscopic studies of FeII chromophores. As shown by Drago and co-workers, this compound sits very close to the so-called spin-crossover point wherein the energies of the low-spin (1A1) and high-spin (5T2) forms are in close proximity. Compound **1** possesses a low-spin ground state whereas the steric constraints imposed by the introduction of the CH3 group in compound **2** requires an

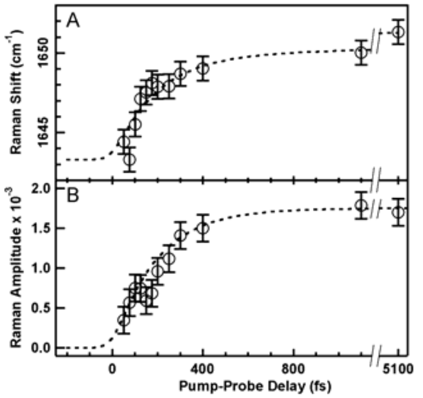

Figure 1. Time-dependence of the change in energy (A) and spectral amplitude (B) of the C=N stretching vibration of $[Fe(tren-(py)_3)](PF_6)_2$ (**1**) derived from femtosecond stimulated Raman scattering data. The dashed lines correspond to fits to expo-nential kinetic models. Both the spectral shift and amplitude can be modeled with the same initial time constant of τ = 190 ± 50 fs which is assigned to the formation of the $^5T_2$ excited state of the

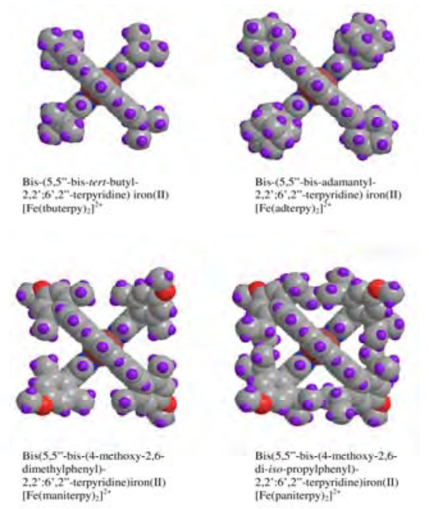
Bis-(5,5"-bis-*tert*-butyl-
2,2':6',2"-terpyridine) iron(II)
[Fe(tbuterpy)$_2$]$^{2+}$
Bis-(5,5"-bis-adamantyl-
2,2':6',2"-terpyridine) iron(II)
[Fe(adterpy)$_2$]$^{2+}$
Bis(5,5"-bis-(4-methoxy-2,6-
dimethylphenyl)-
2,2':6',2"-terpyridine)iron(II)
[Fe(maniterpy)$_2$]$^{2+}$
Bis(5,5"-bis-(4-methoxy-2,6-
di-*iso*-propylphenyl)-
2,2':6',2"-terpyridine)iron(II)
[Fe(paniterpy)$_2$]$^{2+}$

Drawing 1. Drawings of four members of a series of Fe^{II} terpyridyl complexes that have been prepared in order to explore steric effects on the rate of charge transfer-to-ligand field-state conversion.

elongation of the Fe-N bond, resulting in stabilization of the high-spin 5T2 term as its ground state. This system thus has the unique characteristic of having reciprocal ground- and lowest-energy excited states, thereby provide the opportunity for definitive spectro-scopic assignments associated with excited-state evolution (Figure 1). These data thus provide us with a mechanistic blueprint for the excited-state dynamics of this class of chromophores.

A more critical process as it pertains to applications in DSSCs is conversion from the (redox-active) charge-transfer manifold to the ligand-field excited states of the system. We are exploring spectroscopic as well as synthetic approaches for elucidating the nature of the reaction coordinate coupled to charge transfer-state relaxation. Toward this end, we have prepared a series of substituted bis-terpyridyl FeII complexes (Drawing 1); time-resolved absorption data on several members of this series are shown in Figure 2. It is obvious from this plot that the dynamics associated with charge transfer-state relaxation are *significantly* different in [Fe(maniterpy)2]2+ and [Fe(paniterpy)2]2+ as compared to the *t*-butyl-derivatized analog. Contrary to our initial expectations, the increase in steric bulk appears to be *accelerating* the rate of charge transfer-to-ligand-field conversion. To be sure, this is not the direction in which we had hoped the dynamics would evolve, but the fact that the dynamics are changing at all in response to compositional changes in the chromophore indicates that tuning of the ultrafast dynamics of this system through synthetic means is, in fact, feasible. Additional data suggesting that the CT and LF relaxation coordinates may be coupled has also recently been obtained.

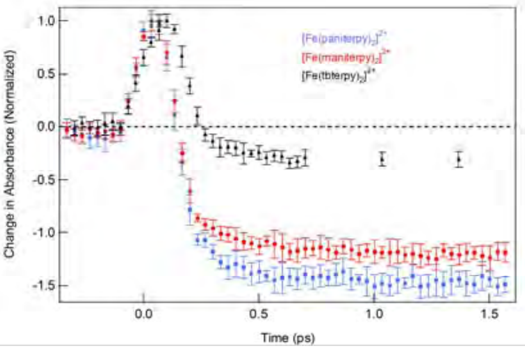

Figure 2. Femtosecond time-resolved absorption data for the three compounds indicated following ca. 100 fs excitation at 560 nm in CH_3CN solution. The data clearly indicate much shorter MLCT lifetimes for both the [Fe(maniterpy)$_2$]$^{2+}$ and [Fe(paniterpy)$_2$]$^{2+}$ complexes relative to the *tert*-butyl analog.

Iron-based chromophores were selected for study first primarily due to our familiarity with their ultrafast photophysics, the logical extension they represent from Ru^{II}-based sensitizers, and the fact that there had been some DSSC work done on Fe^{II}-based systems by other groups. Nevertheless, it has never been our position that Fe^{II}-based compounds constitute "the answer" as a first-row alternative to Ru^{II}-based chromophores. Cu^{I} polypyridyl complexes represent an intriguing option for DSSCs for a number of reasons including the presence of MLCT absorptions and, more importantly, the absence of low-lying ligand-field states. We have therefore initiated a program to explore the possible use of Cu^{I}-based chromophores in TiO_2-based photovoltaic devices. Some of our preliminary results along these lines will be discussed.

DOE Sponsored Publications 2006-2008

1. "Picosecond X-Ray Absorption Spectroscopy of a Photo-induced Iron(II) Spin-Crossover Reaction in Solution", Munira Khalil, Matthew A. Marcus, Amanda L. Smeigh, James K. McCusker, Henry H.W. Chong, and Robert W. Schoenlein, *J. Phys. Chem. A* **2006**, *110*, 38-44.
2. "Ultrafast Dynamics of Ligand-Field Excited States", Eric A. Juban, Amanda L. Smeigh, Jeremy E. Monat, and James K. McCusker, *Coord. Chem. Rev.* **2006**, *250*, 1783-1791.
3. "Ultrafast Dynamics of Fe(II) Polypyridyl Chromophores: Design Implications for Dye-Sensitized TiO2-Based Photovoltaics", Amanda L. Smeigh and James K. McCusker, in *Ultrafast Phenomena XV*, Springer Series in Chemical Physics 88, P. Corkum, D. Jonas, D. Miller, and A.M. Weiner, eds., Springer-Verlag, Berlin, 2007, pp. 273-275.
4. "Picosecond X-ray Absorption Spectroscopy of Photochemical Transient Species in Solution", Munira Khalil, Matthew A. Marcus, Amanda L. Smeigh, James K. McCusker, Henry H.W. Chong, and Robert W. Schoenlein, in *Ultrafast Phenomena XV*, Springer Series in Chemical Physics 88, P. Corkum, D. Jonas, D. Miller, and A.M. Weiner, eds., Springer-Verlag, Berlin, 2007, pp. 722-724.
5. "Effect of the Presence of Iodide on the Electron Injection Dynamics of Dye-Sensitized TiO2-Based Solar Cells", Amanda L. Smeigh, Jordan E. Katz, Bruce S. Brunschwig, Nathan S. Lewis, and James K. McCusker, *J. Phys. Chem. C.* **2008**, *112*, 12065-12068.
6. "Femtosecond Time-Resolved Optical and Raman Spectroscopy of Photo-induced Spin-Crossover: Temporal Resolution of Low Spin-to-High Spin Optical Switching", Amanda L. Smeigh, Marc Creelman, Richard A. Mathies, and James K. McCusker, *J. Am. Chem. Soc.* **2008**, *130*, 14105-14107.
7. "Probing Reaction Dynamics of Transition-Metal Complexes *in Solution* via Time-Resolved Soft X-ray Spectroscopy", Nils Huse, Tae Kyu Kim, Munira Khalil, Lindsey Jamula, James K. McCusker, and Robert W. Schoenlein, in *Ultrafast Phenomena XVI*, Springer Series in Chemical Physics, P. Corkum, S, de Silvestri, and K. Nelson, eds., Springer-Verlag, Berlin, in press.
8. "Charge Transfer-State Formation and Deactivation in d6 Metal Polypyridyl Complexes: Fundamental Issues and Applications in Solar Energy Conversion", Amanda L. Smeigh, Allison Brown, and James K. McCusker, manuscript in preparation as an invited Feature Article in *J. Phys. Chem. A.*
9. "Dependence of Interfacial Electron-Transfer Kinetics on Electrolyte Ions in Dye-Sensitized Solar Cells", Jordan E. Katz, Amanda L. Smeigh, Bruce S. Brunschwig, James K. McCusker, and Nathan S. Lewis, manuscript in preparation for submission to *J. Phys. Chem. C.*
10. "Ultrafast Excited-State Processes in Transition Metal Complexes", James K. McCusker, manuscript in preparation as an invited contribution to *Chem. Rev.*

Session VIII

Photophysics of Quantum Dots

CARRIER MULTIPLICATION IN SEMICONDUCTOR NANOCRYSTALS: CURRENT STATUS AND CHALLENGES

Victor I. Klimov
Chemistry Division and Center for Integrated Nanotechnologies
Los Alamos National Laboratory
Los Alamos, New Mexico, 87545

Conventionally, absorption of a photon by a semiconductor results in a single electron-hole pair (exciton), while energy in excess of the energy gap is dissipated as heat by exciting phonons (Figure 1, left). Strong carrier-carrier Coulomb interactions can open a competing relaxation channel in which the excess energy of the conduction-band electron is instead transferred to a valence-band electron, exciting it across the energy gap (Figure 1, right). As a result, absorption of a single photon produces two excitons, a process known as carrier multiplication (CM) or multiexciton generation (MEG). This effect can potentially increase the power output of photovoltaic cells via increased photocurrent [1].

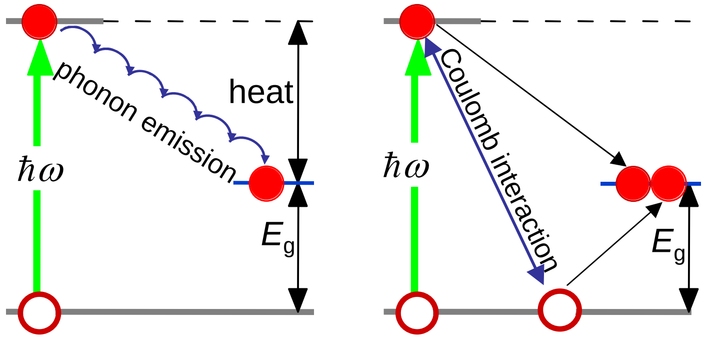

Figure 1. Traditional photoexcitation (left) versus carrier multiplication (right). E_g is the energy gap, which separates the valence from the conduction band.

In bulk semiconductors, CM is inefficient due to relatively weak Coulomb interactions, the constraints imposed by translational momentum conservation, and fast phonon emission. Enhanced CM efficiency has been anticipated in nanoscale semiconductor particles, nanocrystals (NCs), because of a wide separation between discrete electronic states, which inhibits phonon emission (the "phonon bottleneck") [2]. In addition, strong Coulomb interactions and relaxation of translational momentum conservation can further enhance CM in nanocrystalline materials.

The first experimental observation of efficient CM in quantum-confined PbSe particles was reported in ref. [3], where this effect was detected on the basis of a distinct decay component due to Auger recombination of multiexcitons. Later, spectroscopic signatures of CM were observed in NCs of other compositions including PbS, PbTe, CdSe, InAs, and Si. Several groups also reported observations of CM-enhanced photocurrent in NC-based devices. Lately, the situation in CM research has become more complicated as several studies measured low or negligible CM efficiencies [4] at odds with prior reports while some other recent publications presented record-high values of multiexciton yields [5]. In addition to conflicting experimental reports, the mechanism by which CM operates in NCs has also become a subject of intense debate in theoretical literature [6-8].

In my presentation, I will discuss both experimental and theoretical aspects of the CM process. Specifically, I will describe our most recent experimental work on PbSe NCs, in which we analyze potential reasons for observed discrepancies in the reported multiexciton yields, including sample-to-sample variations, differences in detection techniques, and the influence of extraneous "CM–like" effects. In our studies, we apply two complementary spectroscopic techniques - time-resolved photoluminescence and transient absorption [9]. Both techniques show clear signatures of CM with efficiencies that are in good mutual agreement. We observe that NCs of the same energy gap show moderate batch-to-batch variations (within ~30%) in apparent multiexciton yields and larger variations (more than a factor of 3) due to differences in sample conditions (stirred vs. static solutions). These results indicate that NC surface properties may affect the CM process. They also point toward potential interference from extraneous effects such as NC photoionization that can distort the results of CM studies and lead to discrepancies in reported apparent multiexciton yields.

We re-evaluate CM yields under conditions when extraneous effects are suppressed via intense sample stirring and the use of extremely low pump levels (0.02 - 0.03 photons absorbed per NC per pulse). These measurements indicate that both the electron-hole creation energy (the energy required to generate an extra exciton) and the CM threshold in NCs are reduced by roughly a factor of two compared to those in bulk solids (Figure 2). These results are consistent with an expected confinement-induced enhancement of the CM process in NC materials.

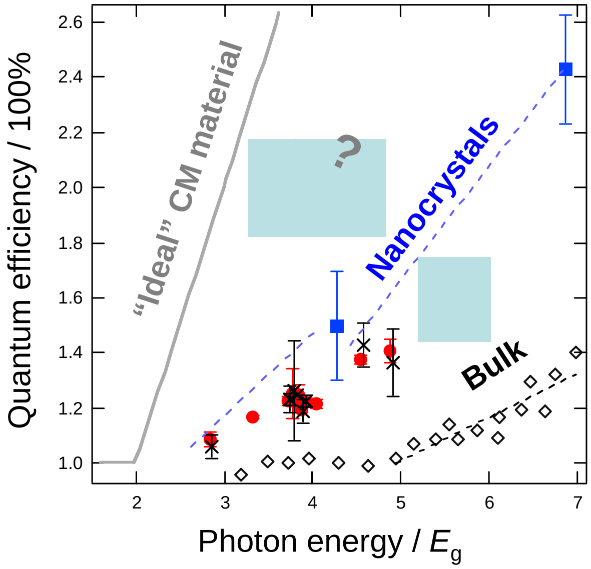

Figure 2. Photon-to-exciton conversion efficiencies in PbSe nanocrystals compared to bulk PbS. The grey line is the "ideal" efficiency line defined by energy conservation.

We further analyze CM pathways within a "unified" theoretical model, which takes into account both a traditional CM mechanism of impact ionization [6] as well as NC-specific "direct-photogeneration" processes [7,8]. This analysis indicates an enhanced role of "direct photogeneration" pathways in quantum-confined particles, which is a result of relaxation of momentum conservation leading to strong Coulomb coupling between states of various exciton multiplicities. These findings point toward potential approaches for increasing CM yields by manipulating both electron-photon coupling and Coulomb interactions in all-semiconductor heterostructures and hybrid semiconductor-metal systems.

References

[1] Werner, J. H.; Kolodinski, S.; Queisser, H. J. *Phys Rev. Lett.* **1994**, *72*, 3851.
[2] Nozik, A. J. *Physica E* **2002**, *14*, 115.
[3] Schaller, R. D.; Klimov, V. I. *Phys. Rev. Lett.* **2004**, *92*, 186601.
[4] Nair, G.; Geyer, S. M.; Chang, L.-Y.; Bawendi, M. G. *Phys. Rev. B* **2008**, *78*, 125325.
[5] Ji, M.; Park, S.; Connor, S. T.; Mokari, T.; Cui, Y.; Gaffney, K. J. *Nano Letters* **2009**, *9*, 1217.
[6] Franceschetti, A.; An, J. M.; Zunger, A. *Nano Lett.* **2006**, *6*, 2191
[7] Shabaev, A.; Efros, A. L.; Nozik, A. J. *Nano Lett.* **2006**, *6*, 2856
[8] Schaller, R. D.; Agranovich, V. M.; Klimov, V. I. *Nature Phys.* **2005**, *1*, 189.
[9] McGuire, J. A.; Joo, J.; Pietryga, J. M.; Schaller, R. D.; Klimov, V. I. *Acc. Chem. Res.* **2008**, *41*, 1810.

HOT ELECTRON DYNAMICS IN QUANTUM DOTS

Byungmoon Cho, William K. Peters, Robert J. Hill, and David M. Jonas
Department of Chemistry and Biochemistry
University of Colorado
Boulder, CO 80309-0215

Following the initial report by Klimov and co-workers, there has been controversy over the possibility of efficient multiple exciton generation in quantum dots. Using the same transient absorption technique (high pump photon energy, bandgap probe photon energy), Nozik and co-workers reported multiple exciton generation for several quantum dot materials. Key assumptions underlying the interpretation of these experiments are that transient absorption at the bandgap is proportional to the number of excitons and that the multiple exciton generation yield can be determined from the ratio of maximum signal amplitude to the amplitude for radiative recombination. Interpreting time-resolved spontaneous emission at the bandgap with the same assumptions, Bawendi and co-workers reported lower multiple exciton generation yields consistent with those found in the bulk materials. It is not yet clear whether the different yields arise from the probe method or sample preparation and handling. Within the experimental time resolution of about 100 fs, the multiple exciton generation timescale is apparently instantaneous.

Proposed multiple exciton generation mechanisms invoke “instantaneous” preparation of multi-exciton states through virtual excitation of hot single exciton states (Klimov), optical preparation of a coherent superposition state that evolves from initial hot single exciton character to multi-exciton character (Efros), and impact ionization by hot carriers into an increased density of multi-exciton states (Zunger). With sufficiently short pulses, the virtual excitation of the first model will become the superposition state evolution invoked in the second model. Beyond the magnitude of the coupling, the first two mechanisms are distinguished by whether the dephasing that stabilizes the multi-exciton state is dominated by electronic inter-band coupling (Klimov) or electron-phonon interactions (Efros).

The experiments described here were designed to probe the optically excited hot single exciton state that is the pre-cursor to multiple exciton generation in all three mechanisms. Two identical pulses of less than 25 fs duration were used to both pump hot single exciton states and probe their subsequent decay. Because single quantum dot spectroscopy shows that off states can persist for seconds (Krauss), a vacuum tight sample cell with a 250 micron path was spun at 1800-3000 rpm so that the sample was rotated out of the beam between laser shots (centrifugal forces cause up to 2x reduction in dot concentration at the probed radius.) Except when studying Auger recombination and the pump fluence dependence of the signal, pump pulses with 1 nJ energy in a 100 micron diameter spot excited PbS quantum dots dispersed in toluene for measurements of hot electron dynamics. Such fluences excite 10% of the dots.

The pump-probe signal for PbS quantum dots at 610 nm (3x the band gap) is compared to the signal for a solution of the saturable absorber DQOCI at the same absorbance in Figure 1. A positive signal indicates increased transmission through the sample (bleaching). If the excited state does not absorb (as for saturable absorbers), the pump-probe signal is proportional to the product of the absorbance and the molar extinction coefficient. The extinction coefficient of the quantum dots is 20x that of the saturable absorber; so dots absorbing as a unit without excited state absorption should give 20x more signal than DQOCI, or 500x more than observed. Excited state absorption reduces the pump-probe signal from the quantum dots by about 500.

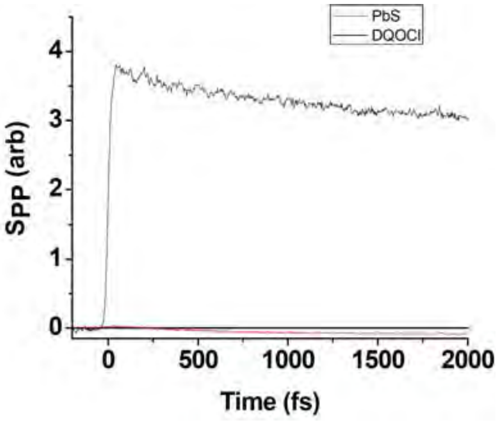

Figure 1 (left) strength of the PbS quantum dot pump-probe signal vs. DQOCI.

Figure 2 (right) wavelength dependence of the PbS pump-probe signal.

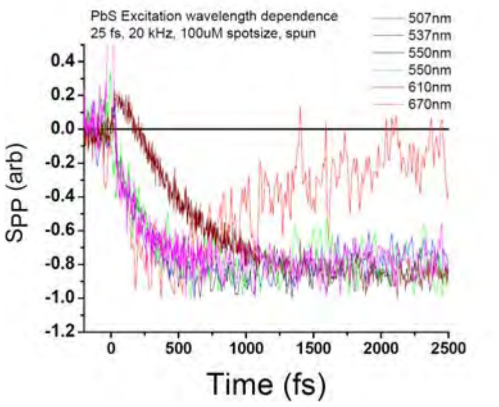

The signal from the PbS quantum dots in Figure 1 shows a small positive bleach near T=0, with negative signal (indicating induced absorption dominates) from T=200 fs onward. At a series of nearby wavelengths, Figure 2 shows zero signal at T=0 (the signals in Fig. 2 have been scaled to show similarities). Subsequent growth of a negative signal can be fit with a 220 fs exponential rise. The absence of any initial bleach in these signals indicates near-perfect cancellation between depleted ground state absorption, excited state emission, and excited state absorption. In 2D spectroscopy, such cancellation would indicate a lack of coupling – the rest of the electrons in a dot keep absorbing because they do not yet feel the excitation. The initial bleach at 610 nm is attributed to excitation of the E1 transition; as in the bulk, the upper state of the E1 transition decays by inter-valley scattering (a solid state analog of internal conversion). Except for the 507 nm transient, which rapidly decays to zero, the induced absorptions have similar decays – fits yield a 150 ps decay on top of a constant background of equal amplitude. Measurements of Auger recombination indicate a bi-exciton lifetime of about 150 fs.

Although it is possible that the small signals observed on the picosecond timescale arise from a small minority of quantum dots in the sample, the near-zero signal at T=0 must be explained for the entire sample. The bulk band structure indicates that the electron wavepacket has a group velocity of about 0.9 nm/fs and a width of 2 nm. The hole wavepacket velocity is 0.6 nm/fs. Until the electron and hole wavepackets separate, in about 6 fs, short wavelength carriers probed in the rest of the dot may not feel the excitation. Because the electron velocity exceeds the limiting velocity in hot electron semiconductor devices by an order of magnitude, the mean free path could be much shorter than that for thermal electrons (13 nm). This suggests significant cooling of the hot electron by the time it separates from the hot hole. This cooling can involve both impact ionization (multiple exciton generation) and electron-phonon coupling. The rest of the electrons in the dot start to feel the photo-excitation as the carriers cool, which takes about 500 fs. In 1983, Brus suggested that quantum confinement might require scattering lengths much larger than the dot; we suggest hot electrons with shorter scattering lengths will not feel confined even when band gap transitions show strong confinement. Such fast dephasing of hot electrons is unfavorable to the virtual excitation and coherent superposition mechanisms.

IMAGING OF ENERGY AND CHARGE TRANSPORT IN NANOSCALE SYSTEMS

Jao van de Lagemaat[†] and Manuel Romero[‡]
[†]Chemical Sciences and Biosciences Center
[‡]National Center for Photovoltaics
National Renewable Energy Laboratory
Golden, Colorado, 80401

New applications and increased scientific insight into the fundamental interaction of matter and energy at small scales have been made possible by recent developments in the manipulation and scientific study of nanoscale matter by new spectroscopic and microscopic techniques. These applications depend on the extraordinary properties of electrons and excitons when confined to small spaces and on energy flow phenomena between such nanoscale features. Generally, the techniques that address these phenomena either have a good energy resolution (e.g. optical spectroscopy), a good spatial resolution (e.g. atomic force microscopy AFM), or a good temporal resolution (e.g. THz spectroscopy). Few of them exhibit all of the desired characteristics at the same time. For a comprehensive understanding, all three factors are needed. This project attempts to provide new imaging techniques and approaches that address this gap.

Our imaging approach is based around a method that enables imaging of photophysical and photochemical properties of a surface called scanning tunneling luminescence (STL). In this method, tunneling current from a tip excites luminescence from a sample. Several mechanisms for this luminescence have been identified such as the excitation of (surface) plasmons in the substrate or substrate/tip ensemble by tunneling electrons after which the plasmons radiatively decay. Also, electroluminescence can be directly generated by injection of charge carriers from both the substrate and the tip. STL allows for a variable spatial resolution depending on the emission process or the transport of energy to the emitting center as well as energy resolution embedded in the emission spectrum and using the dependence on the applied bias between tip and substrate. The goal of the current work is to further develop this technique and to add time resolution using several approaches. First we'll describe a small subset of recent results and then we'll briefly discuss future research.

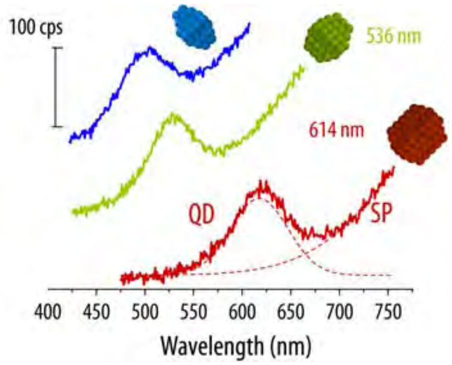

Fig 1. Electroluminescence from CdSe quantum dots of different sizes labeled with their PL maximum.

We showed that emission patterns of the plasmon-mediated luminescence on gold substrates exhibit distinct spatial features that can be assigned to the localized modes of the surface plasmon confined to the tunneling gap and propagating modes that are not as localized.[1] Tunneling luminescence spectroscopy reveals that the plasmon localization at the tip increases when modes of higher energy are excited.

We observed tunneling luminescence from individual CdSe:ZnS core-shell quantum dots on gold when absorbed on a gold substrate (see Fig. 1).[3] The luminescence appears to be due to strong coupling to a surface plasmon present in the tip-substrate gap as evident from the fact that the dots only luminescence when the plasmon emission is of high enough energy to directly excite the dots. We also observe tantalizing evidence for strong coupling between the excitonic states on the quantum dots and the surface plasmons by the observation of a second luminescence peak between the two energies in some measurements. The emission from the quantum dots appears shifted and broadened by Stark effects. Also, it is possible that the surface plasmon carries the excitation to more distant dots before reemission.

Using scanning tunneling spectroscopy (STS) we have studied several different quantum dot energy-funnel structures, wherein successive multilayers of quantum dots of different HOMO-LUMO separation are used to "funnel" excitation. These multilayers show complex behavior that we do not yet fully understand (see Fig. 2). Future research will focus on the dynamics of this luminescence behavior.

Future extensions of the techniques will allow for time resolution. Several approaches are contemplated. In the first approach, current pulses are used to provide short excitation timespans of milliseconds to microseconds. Secondly, excitation by using a tapping-mode conducting AFM tip will lead to even shorter excitation pulses of 10's of nanoseconds. Lastly, exciting the tunneling current using fast laser pulses, can lead to ultrafast tunneling current pulses that excite luminescence from the substrate. We can thus spatially and temporally control the excitation. We have already shown that it is possible to excite short current pulses by using a vibrating tip that makes intermittent contact to the substrate and observe the luminescence as a function of time. Pico-second time-resolved STL from the decay of tip-induced surface plasmons has been observed before by using fast laser excitation by others on plain gold substrates (Uehara *et al. Appl. Phys. Lett.* **2000**, *76*, 2487) We will extend this technique to more relevant nanoscale systems such as quantum dot nanotube composites, individual nanotubes, quantum dot arrays, plasmon-active nanostructures and semiconducting organics.

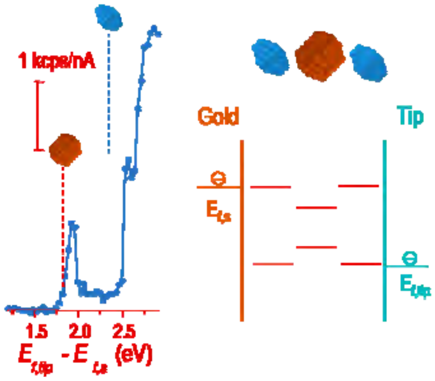

Fig. 2. Tunneling luminescence spectroscopy of a quantum dot multilayer structure.

DOE Sponsored Publications 2006-2008

1. M. J. Romero, J. van de Lagemaat, G. Rumbles, M. Al-Jassim, "Plasmon excitations in scanning tunneling microscopy: simultaneous imaging of modes with different localization coupled at the tip," Appl. Phys. Lett. **90**, 193109 (2007) (partial support by BES)

2. J. C. Johnson, T. H. Reilly, A. C. Kanarr, J. van de Lagemaat "The ultrafast photophysics of pentacene coupled to surface plasmon active nanohole films" *J. Phys. Chem. C* **113**, 6971 (2009). (partial support)

3. M. J. Romero, J. van de Lagemaat, "On the energy coupling between quantum dots and STM–induced nanocavity plasmons" **2009**, submitted for publication.

Session IX

Photocatalysis in Nanostructures

NANOSTRUCTURED PHOTOCATALYTIC WATER SPLITTING SYSTEMS

W. Justin Youngblood, Kazuhiko Maeda, Seung-Hyun Anna Lee, Renzhi Ma, Hideo Hata,
Paul G. Hoertz, Yoji Kobayashi, Miharu Eguchi, Lucas Jellison, and Thomas E. Mallouk
Department of Chemistry, The Pennsylvania State University, University Park, PA 16802
Thomas A. Moore. Ana L. Moore, and Devens Gust
Department of Chemistry and Biochemistry, Arizona State University, Tempe, AZ 85287

Our DOE-supported work develops hydrogen- and oxygen-evolving photosystems based on molecular sensitizers, oxide semiconductors, and catalyst nanoparticles, and couples them to study visible light-driven water photolysis and photoelectrolysis. The goals of the project are to achieve (1) a quantitative mechanistic understanding of the oxygen and hydrogen evolving half cycles, (2) sensitizer/ligand designs for controlling forward and back electron transfer, and (3) new techniques for achieving nanoscale structural control.

Bidentate dicarboxylate capping ligands for stabilizing $IrO_2{\cdot}nH_2O$ *nanoparticles.* Hydrated iridium oxide ($IrO_2{\cdot}nH_2O$) was first characterized as an effective water oxidation catalyst by Harriman et al. Water oxidation can be driven with this catalyst using photochemically generated Ru (III) tris(bipyridine). Our previous studies established that surface Ir atoms generate O_2 at turnover rates of ~ 50 s^{-1} and that the reaction rate is limited by outer sphere electron transfer between Ru(III) and Ir(IV). In order to incorporate $IrO_2{\cdot}nH_2O$ into overall water splitting systems, suitable capping ligands are needed to stabilize molecule-size particles and couple them to photosensitizers. We surveyed various mono- and bidentate ligands and found that malonate and succinate derivatives stabilized 1-2 nm $IrO_2{\cdot}nH_2O$ colloids made by hydrolysis of aqueous $IrCl_6^{2-}$. These ligands are not easily exchanged at the nanoparticle surface. Analogous monodentate (acetate) and tridentate (citrate) carboxylate ligands, as well as phosphonate and di-phosphonate ligands, are less effective as stabilizers and lead to different degrees of nanoparticle aggregation. Ruthenium tris(2,2'-bipyridyl) sensitizers containing malonate and succinate groups in the 4,4-positions are also good stabilizers of $IrO_2{\cdot}nH_2O$ colloids. Electron transfer from Ir(IV) to Ru(III) occurs with a first-order rate constant of 8×10^2 s^{-1}, and oxygen is evolved. The sensitizer-$IrO_2{\cdot}nH_2O$ diad is thus a functional catalyst for photo-oxidation of water, and is a useful building block for overall visible light water splitting systems.

Visible light water splitting in a dye-sensitized photoelectrochemical cell. Sensitizer-$IrO_2{\cdot}nH_2O$ colloid diads were incorporated into dye-sensitized solar cells and studied photoelectrochemically. Overall water splitting in this system is illustrated schematically in Fig. 1. We designed a heteroleptic ruthenium dye (Fig. 1) to serve as both the sensitizer and a molecular bridge to connect $IrO_2{\cdot}nH_2O$ particles to the porous TiO_2 electrode surface. Phosphonates are chemically selective for TiO_2 and the malonate group is selective for $IrO_2{\cdot}nH_2O$. The bpy ligands in this complex minimize the distance between the ruthenium center and the surfaces of the respective oxides. At pH 5.75, in a three-electrode cell containing Ag/AgCl reference and Pt counter electrodes, photoelectrochemical oxygen and hydrogen evolution are observed at potentials positive of of -325 mV vs. Ag/AgCl,

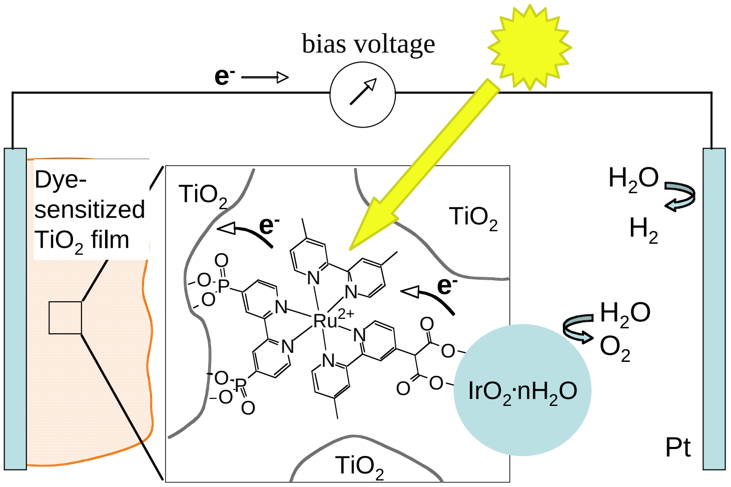
bias voltage
e⁻
Dye-sensitized TiO₂ film
TiO₂
TiO₂
TiO₂
e⁻
e⁻
Ru²⁺
N
IrO₂·nH₂O
H₂O
H₂
H₂O
O₂
Pt

Fig. 1. Schematic of water splitting in an aqueous dye sensitized solar cell.

corresponding to an open circuit photovoltage of 980 mV. The quantum yield for photocurrent generation with 450 nm light is 0.9%. Recently, we found that coating the TiO_2 film with ~ 5 nm of ZrO_2 or Nb_2O_5 increases the photocurrent by about a factor of two. Flash photolysis experiments show that back electron transfer from TiO_2 to the oxidized dye occurs on a 370 μs timescale in this system, and the low quantum yield can be attributed to slow electron transfer (~ 2.2 ms) between the $IrO_2 \cdot nH_2O$ particle and oxidized sensitizer.

Photosensitized nanoscrolls and nanosheets. We have also studied photochemical hydrogen generation using a sacrificial electron donor (EDTA) and ruthenium polypyridyl sensitizers adsorbed to niobate nanoscrolls and nanosheets. The goal of these studies is to make an efficient hydrogen-evolving photosystem that can be coupled to water oxidation catalysts for overall water splitting. The exfoliation of $K_4Nb_6O_{17}$ produces scrolled single-crystalline niobate sheets that are very good media for transferring photoinjected electrons to Rh or Pt nanoparticles. Fig. 2 shows an electron micrograph of the scrolls and a cartoon of photochemical hydrogen evolution. With adsorbed $Ru(bpy)_2(4,4'-(PO_3H_2)_2bpy)^{2+}$, the external quantum yield for hydrogen evolution is 20-25%, implying that the internal quantum yield from electrons that are photoinjected into the scrolls is nearly unity. The dependence of H_2 yield on Pt loading is consistent with very fast electron transfer from the sensitizer to Pt, followed by much slower electron transfer between the EDTA electron donor and Ru(III).

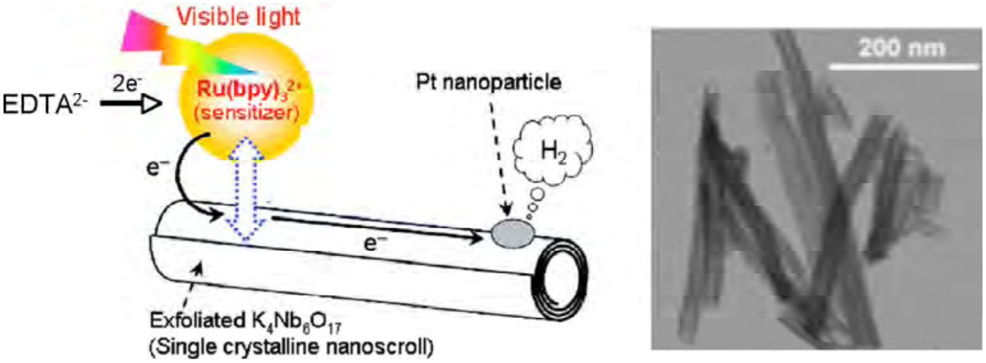
Visible light
EDTA²⁻
2e⁻
Ru(bpy)₃²⁺ (sensitizer)
Pt nanoparticle
H₂
e⁻
e⁻
Exfoliated K₄Nb₆O₁₇ (Single crystalline nanoscroll)
200 nm

Fig. 2. Left: scheme for photochemical H_2 evolution. Right: TEM image of single crystalline nano-scrolls derived from $K_4Nb_6O_{17}$.

DOE Sponsored Publications 2007-2009

1. K. Maeda, M. Eguchi, W. J. Youngblood, and T. E. Mallouk, "Calcium Niobate Nanosheets Prepared by the Polymerized Complex Method as Catalytic Materials for Photochemical Hydrogen Evolution," submitted to *Chem. Mater.*
2. K. Maeda and T. E. Mallouk, "Comparison of two- and three-layer restacked Dion-Jacobson niobate nanosheets as catalysts for photochemical hydrogen evolution," *J. Mater. Chem.,* in press.
3. K. Maeda, M. Eguchi, S.-H. A. Lee, W. J. Youngblood, H. Hata, and T. E. Mallouk, "Photocatalytic Hydrogen Evolution from Hexaniobate Nanoscrolls and Calcium Niobate Nanosheets Sensitized by Ruthenium(II) Bipyridyl Complexes," *J. Phys. Chem. C,* in press.
4. W. J. Youngblood, S.-H. A. Lee, Y. Kobayashi, E. A. Hernandez-Pagan, P. G. Hoertz, T. A. Moore, A. L. Moore, D. Gust, and T. E. Mallouk "Photoassisted Overall Water Splitting in a Visible Light-Absorbing Dye Sensitized Photoelectrochemical Cell," *J. Am. Chem. Soc.* 131, 926-927 (2009).
5. R. Ma, Y. Wang, and T. E. Mallouk, "Patterned Nanowires of Se and Corresponding Metal Chalcogenides from Patterned Amorphous Se Nanoparticles," *Small,* 5, 356-360 (2009).
6. R. Ma, Y. Kobayashi, W. J. Youngblood, and T. E. Mallouk, "Potassium Niobate Nanoscrolls Incorporating Rhodium Hydroxide Nanoparticles for Photocatalytic Hydrogen Evolution," *J. Mater. Chem.*, 18, 5982-5985 (2008).
7. K. Maeda, M. Eguchi, W. J. Youngblood, and T. E. Mallouk, "Niobium Oxide Nanoscrolls as Building Blocks for Dye-Senitized Hydrogen Prodution from Water under Visible Light Irradiation," *Chem. Mater.*, 20, 6770-6778 (2008).
8. H. Hata, Y. Kobayashi, V. Bojan, W. J. Youngblood, and T. E. Mallouk, "Direct deposition of trivalent rhodium hydroxide nanoparticles onto a semiconducing layered calcium niobate for photocatalytic hydrogen evolution," *Nano Letters,* 8, 794-799 (2008).
9. P. G. Hoertz, Y. I. Kim, W. J. Youngblood, and T. E. Mallouk, "Bidentate Dicarboxylate Capping Groups and Photosensitizers Control the Size of IrO_2 Nanoparticle Catalysts for Water Oxidation," *J. Phys. Chem. B.* 111, 6945-56 (2007).

"ELECTROCHEMICALLY WIRED" SEMICONDUCTOR NANOPARTICLES: TOWARD VECTORAL ELECTRON TRANSPORT IN HYBRID SYSTEMS

Neal R. Armstrong, Jeffery Pyun, S. Scott Saavedra
Department of Chemistry
University of Arizona
Tucson, Arizona 85721
(nra@email.arizona.edu)

Recent DOE-support research efforts have focused on: a) examination of the mechanisms for electrochemically tethering semiconductor nanoparticles, such as ligand-capped 2-7 nm diameter CdSe NPs (Fig. 1, upper); b) characterization of rates of SC-NP sensitized photoelectrochemical electron transfer to solution acceptors (including H^+), as a function of polymer host, the nature of SC-NP incorporation into the polymer host, NP diameter, and redox potential of the solution electron acceptor. Results confirm Marcus-like relationships in both the polymer and NP frontier orbital energies in controlling k_{ET} (Fig. 2, lower); c) potential-modulated attenuated total reflectance spectroscopy (PM-ATR) for spectroelectrochemical characterization of frontier orbital energies and k_{ET} for monolayer-tethered CdSe SC-NPs on ITO/waveguide substrates; d) exploration of the frontier orbital energies for monolayer-tethered SC-NPs, before and after ligand capping, using photoemission spectroscopies; e) development of new earth-abundant nanoparticle materials for photoelectrochemical hydrogen production and water splitting.

New approaches have been developed for electrochemical capture of SC-NPs into polymer hosts. Pulsed potential step deposition protocols, with variable duty cycle, provide for "refilling" of the diffusion layer with slow diffusing nanoparticles, and significant improvement in efficiency of NP capture, at the polymer film/solution interface. These studies have been extrapolated to a wider variety of thiophene-based polymer hosts, and significant improvements in photoelectrochemical efficiency of ET to a solution acceptor (e.g. methyl viologen, Fig. 1) are seen for

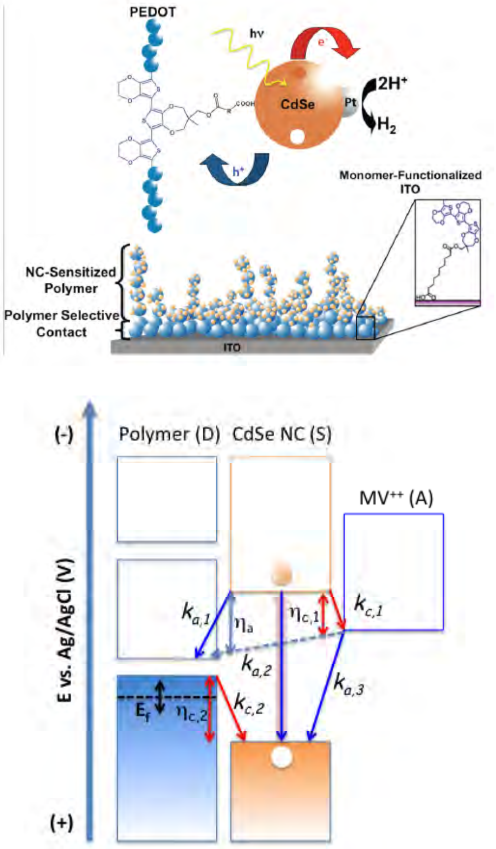

Fig. 1 – (upper) Schematic views of electrochemically tethered semiconductor nanoparticles; (lower) frontier orbital energy levels which control rates of ET to/from the photoexcited SC-NP.

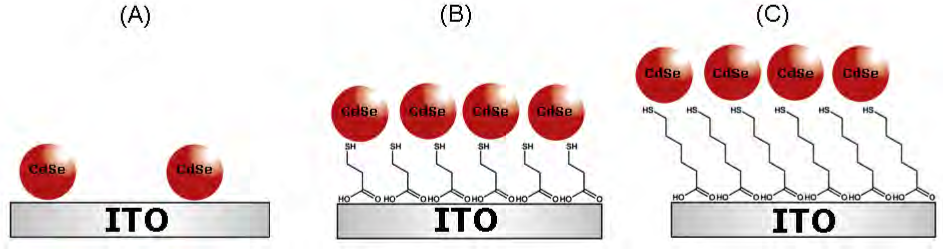

Fig. 2 – Schematic view of monolayer-tethered CdSe NPs on an ITO/waveguide substrate. Our recent studies have focused on determination of rates of electron injection into the tethered NP, as a function of tether length, type of ligand, and NP diameter, using PM-ATR. The sensitivity of this technique allows characterization of single monolayers of NPs, using the modulated optical response (changes in absorbance of the lowest energy exciton band in the NP as reduction/oxidation occurs).

electron rich ProDOT-based polymers with facile oxidation/reduction doping. Clear increases are seen in photoelectrochemical efficiency as the HOMO energy of the polymer, and the LUMO energy of the NP are tuned to maximize rates of hole capture and electron capture respectively.

To facilitate the characterization of the LUMO energies of bare and ligand-capped CdSe NPs we have adapted potential-modulated attenuated total internal reflectance (PM-ATR) spectroelectrochemical methods to characterize the first reduction potentials of NPs tethered at monolayer coverages on an ITO/waveguide substrate. On these waveguides we have sufficient sensitivity to uniquely monitor changes in absorbance at the first exciton band as a function of applied potential and modulation frequency, as a function of NP diameter and (in upcoming studies) type of capping ligand. The results confirm the significant shifts in HOMO/LUMO energies which occur upon moving from vacuum to solution/electrolyte environments, and are complementary to our UV-photoemission studies of frontier orbital energies for bare and ligand-capped SC-NPs.

Recent publications arising from full or partial DOE support:

"Electrodeposited, "Textured" poly(3-hexyl-thiophene) (e-P3HT) Films for Photovoltaic Applications," Erin L. Ratcliff, Judith L. Jenkins, Ken Nebesny and Neal R. Armstrong, Chemistry of Materials 20, 5796-5806 (2008).

"Poly-(3, 4-ethylenedioxythiophene)-Semiconductor Nanoparticle Composite Thin Films Tethered to Indium Tin Oxide Substrates via Electropolymerization," R. Clayton Shallcross, Gemma D. D'Ambruoso, Bryan D. Korth, H.K. Hall Jr., Zhiping Zheng, Jeffrey Pyun, Neal R. Armstrong, J. Amer. Chem. Soc., 129, 11310-11311, (2007 and JACS Select 2008).

"Oxide Contacts in Organic Photovoltaics: Characterization and Control of Near-Surface Composition in Indium-Tin Oxide (ITO) Electrodes," Neal R. Armstrong, P. Alex Veneman, Diogenes Placencia, Erin Ratcliff, Michael Brumbach, Accounts Chemical Research (invited), submitted.

"Organic/Organic' Heterojunctions: Organic Light Emitting Diodes and Organic Photovoltaic Devices," Neal R. Armstrong, Weining Wang, Dana M. Alloway, Diogenes Placencia, Erin Ratcliff, Michael Brumbach, Macomol. Rapid Comm., Invited Review, in press.

"Charge Injection Kinetics in Submonolayers of CdSe Nanoparticles Tethered to a Spectroelectrochemical Planar Waveguide," Zeynep Ozkan, R. Clayton Shallcross, Neal R. Armstrong, S. Scott Saavedra, J. Amer. Chem. Soc., submitted.

"Polymer-Tethered Semiconductor Nanoparticles: Photoelectrochemical Energy Conversion," R. Clayton Shallcross, Jeff Pyun, Neal R. Armstrong, manuscript in preparation.

"Type-II CdSe/CdTe Solar Cells Displaying Retention of Quantum Confinement," R. Clayton Shallcross, Avery Lindemann, Neal R. Armstrong, in preparation.

"Colloidal Polymerization of Polymer Coated Ferromagnetic Nanoparticles into Cobalt Oxide Nanowires," Pei Yuin Keng, Bo Yun Kim, Inbo Shim, Rabindra Sahoo, P. Alex Veneman, Neal R. Armstrong, HeeMin Yoo, Jeanne A. Pemberton, Mathew M. Bull, Jared J. Griebel, Erin L. Ratcliff, Kenneth G. Nebesny, Jeffrey Pyun, ACS Nano, submitted.

"Ferrocene Functional Polymer Brushes on Indium Tin Oxide via Surface Initiated Atom Transfer Radical Polymerization," Bo Yun Kim, Erin L. Ratcliff, Neal. R. Armstrong, Tomasz Kowalewski and Jeffrey Pyun, Macromolecules, submitted.

"Shifting the effective work function and frontier orbital energies of monolayer-tethered CdSe nanocrystals with capping ligands," Andrea Munro, Amy Graham, Neal R. Armstrong, manuscript in preparation.

INSIGHTS INTO REDOX CATALYSIS ON METALLIC PARTICLES

Dan Meisel
Radiation Laboratory and Department of Chemistry & Biochemistry
University of Notre Dame,
Notre Dame, Indiana 46556

We investigate two aspects of photo-induced water splitting processes: a) Detailed understanding of the mechanisms of redox catalysis, currently on metallic particles, and b) Design and building a system to maximize separation of the water splitting redox products. In the present report we focus on the first issue.

The use of metallic or metal-oxide particles in the catalytic evolution of hydrogen and oxygen is commonly accepted as an indispensible step in photo-induced water splitting. This step required in order to transform the inherently single-electron process of photo-induced redox reactions to multi-electron transfer molecular products. Whereas this requirement has been realized for some time, the detailed mechanism for the catalytic process is still unknown. Clearly, for the hydrogen evolution cycle an electron is transferred from an excited state, or more commonly from an intermediate radical to the metallic particle followed by proton transfer but beyond these generalization the details are not clear. Does the electron donor adsorb on the particle and for how long? At what stage does the proton from water neutralize the excess electron on the particle, how fast and how long does it stay as an adsorbed hydrogen atom? To address these questions we initiated the present effort. We combine radiolytic and photolytic techniques to obtain detailed information on the particles during the catalysis. Below we describe the use of the ultra sensitive highly specific surface enhanced Raman spectroscopy (SERS) in these studies.

To avoid complication by the commonly utilized stabilizers present at the surface of the metallic particles we utilizing a recently developed synthesis for the production of silver and gold particles obtained by reduction of the corresponding oxide by H_2. Suspensions of these particles contain only the metal, water, and their ions. We follow H_2 evolution and in parallel the SERS spectra of a well-studied, adsorbed probe molecule, p-aminothiopheneol (*p*-ATP) present a low concentrations, 1-10 µM, well below saturation of the surface. We find that the particles in the suspension are stabilized by hydroxide ions or silver ions at pHs above and below the point of zero charge, respectively. The particles in these suspensions are extremely stable to coagulation even at very high particle concentrations (mol L^{-1} levels). The concentration of each species in the solution can be determined using a combination of conductivity, pH and inductively coupled plasma measurements. The sizes of particles in the suspension can be predetermined by controlling the rate of the reactions that lead to their production in the range of ~15-250 nm, with relatively narrow size distributions.

The particles of both metals, Ag and Au, were used as catalysts in the reduction of water by radiolytically generated strongly reducing radicals. We show that the probe is not destroyed as a result of the irradiation. Nonetheless, the intensity of the SERS spectra during the production of H_2 was change in response to experimental conditions. We identify two stages, preconditioning of the particles and their active stage. The spectra diminish and relative intensities of charge-transfer sensitive lines change upon injection of electrons into the particles but are recovered on adding the corresponding metal ions. We attribute these effects to changes in the Fermi level of the particle. Coupling of the particles' Fermi level to the ground state vibrational levels of the probe molecule is altered in response to the position of the Fermi level, affecting the charge -transfer component of the SERS enhancement (Scheme I). From literature correlations with electrochemical potential one can estimate the overpotential for the particles during the hydrogen evolution reaction. Effects of pH on the SERS intensity are similar. Preliminary computations of model prototypes of the probe on silver suggest changes in the Fermi levels alter the ground state charge distribution between the probe and the particle, leading to further different enhancements of different modes.

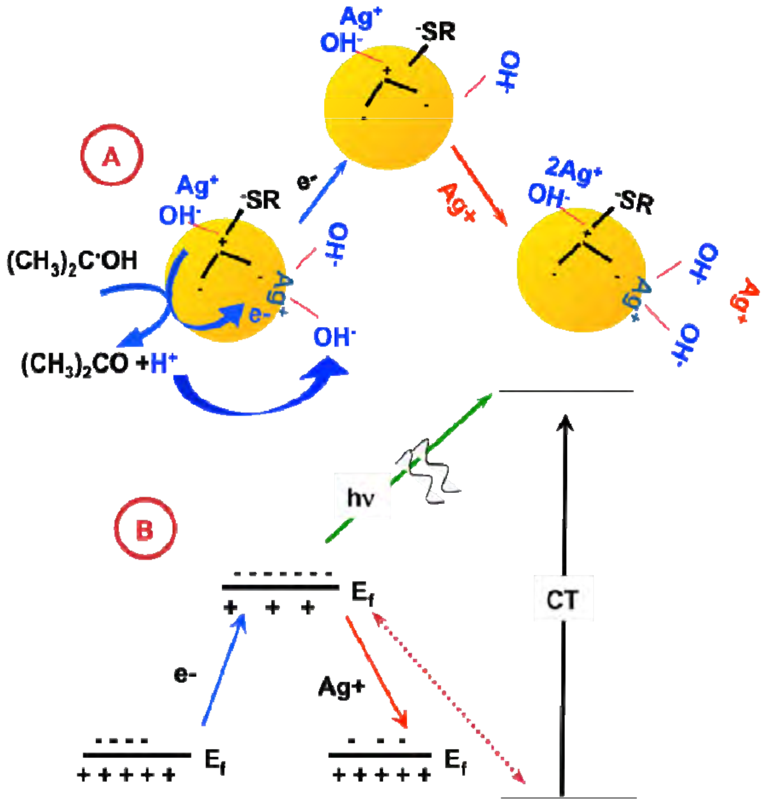

Scheme 1: (A) Changes in a particle in response to external chemical reactions. Left-hand side – electron transfer reduces Ag^+ but is accompanied by proton transfer. Right-hand side - addition of Ag^+. (B) Changes in Fermi-level energy in response to the chemical processes shown in (A). The dashed red double-arrow indicates the energy-dependent vibronic coupling of the Fermi level to the ground state.

We suggest that the use of SERS in this context can shed light on the details of the particles state as well as on species at the surface. To obtain more direct information, in-situ initially and time-domain later experiments are proposed for future experiments. Furthermore, recent literature reports show that it is possible to obtain similar information from metallic seeds deposited on wide-band oxides, e.g. TiO_2. If verifiable, these would open up a window into studies of the oxidation cycle, albeit with added complexity.

DOE Sponsored Publications 2006-2008

Published:

1. “Radiolytic Yields in Aqueous Suspensions of Gold Particles,” G. Merga, B. H. Milosavljevic, D. Meisel, J. Phys. Chem. B 110, 5403-8 (2006).

2. “Monitoring the Synthesis and Composition of Microsilica Encapsulated Rhodium Catalyst,” Dai, Q.; Menzies, D.; Wang, Q.; Ostafin, A. E.; Brown, S. N.; Meisel, D.; Maginn, E. J., IEEE Trans. Nanotech. 5, 677-82 (2006).

3. “Effect Of Silica-Supported Silver Nanoparticles On Dihydrogen Yields From Irradiated Aqueous Solutions,” Tomer Zidki, Haim Cohen, Dan Meyerstein and Dan Meisel, J. Phys. Chem. C 111, 10461-6 (2007).

4. “Reactions of Radicals With Hydrolyzed Bismuth (III) Ions: A Pulse Radiolysis Study,” R. Benoit, M-L. Saboungi, M. Tréguer-Delapierre, B. H. Milosavlljevic, D. Meisel, J. Phys. Chem. A 111, 10640-5 (2007).

5. “Redox Catalysis On “Naked” Silver Nanoparticles,” Getahun Merga, Robert Wilson, Geoffrey Lynn, Bratoljub H. Milosavljevic, and Dan Meisel, J. Phys. Chem. C 111, 12220-6 (2007).

6. “Probing Silver Nanoparticles During Catalytic H_2 Evolution,” Getahun Merga, Laura C. Cass, Daniel M. Chipman, and Dan Meisel, J. Am. Chem. Soc. 130, 7067-76 (2008).

7. “Layer-By-Layer Self-Assembly Of Colloidal Gold-Silica Multilayers,” Zhenyuan Zhang, Dan Meisel, Prashant Kamat and Masaru Kuno, Chem. Ed. 13, 153-7 (2008).

8. “Laterally Controlled Template Electrodeposition of Polyaniline,” Tali Sehayek, Dan Meisel, Alexander Vaskevich, and Israel Rubinstein, Israel J. Chem. 48, 359-66 (2008).

Submitted:

9. “Naked Gold Nanoparticles: Synthesis, Characterization, Catalytic Hydrogen Evolution, and SERS,” Getahun Merga, Nuvia Saucedo, Laura C. Cass, James Puthussery, and Dan Meisel.

10. “Reactions of Reducing Radicals with Nitro-Aromatic Molecules in Metallic Nanoparticle Suspensions,” Laura C. Cass Getahun Merga, and Dan Meisel.

Session X

Charge Separation in Structural Organic Molecular Systems

DEFECTS, DOPING AND TRANSPORT IN EXCITONIC SEMICONDUCTORS

Brian A. Gregg, Ziqi Liang, Dong Wang and Michael Woodhouse
Chemical and Biosciences Center
National Renewable Energy Laboratory
Golden, CO 80401

A major goal or our research in recent years has been the development of a unified, self-consistent model that semiquantitatively describes all aspects of photoconversion in excitonic semiconductors, XSCs, and is compatible with our understanding of DSSCs, inorganic PV cells and natural photosynthesis. A recent focus is on morphological and chemical defects. Charged defects, whether purposely added as dopants or not, often control the electrical behavior of XSCs yet their influence is rarely included in existing theoretical models. Much of our recent work attempts to elucidate the number, influence and, ideally, the chemical identity of defects while also developing chemical methods to modify or eliminate them. Simple thermodynamic considerations show that entropy, which favors defect formation, will be most important when the enthalpy of crystal formation is low. Thus even “perfect” crystals of van der Waals-bonded organic semiconductors may have 6 – 12 orders of magnitude more defects than crystalline silicon; and most XSC films of interest for photoconversion are far from perfect crystals.

Most models of transport in thin film XSCs are based on Bässler’s Gaussian Disorder model, GDM. We have argued that this model is valid for the amorphous insulators it was designed for, but not for materials with a high density of charged defects. Charged defects act like dopants, thus our model based on doped liquid crystal perylene diimides should be valid also for these adventitiously doped materials, although they are expected to be more complex. Because of the low dielectric constant and localized carrier wavefunctions, most dopant electrons (for n-type dopants) remain electrostatically bound near dopant cations. This results in an activation energy, $E_{a,n}$ (often 100 – 300 meV), for free carrier production (Fig. 1). The bound carriers and their counterions create strong dipoles that perturb the conduction and valence bands, thus forcing mobile carriers to traverse a fluctuating electrostatic potential. These fluctuations of CB and VB result in an activation energy for the mobility, $E_{a,\mu}$ (Fig. 1)

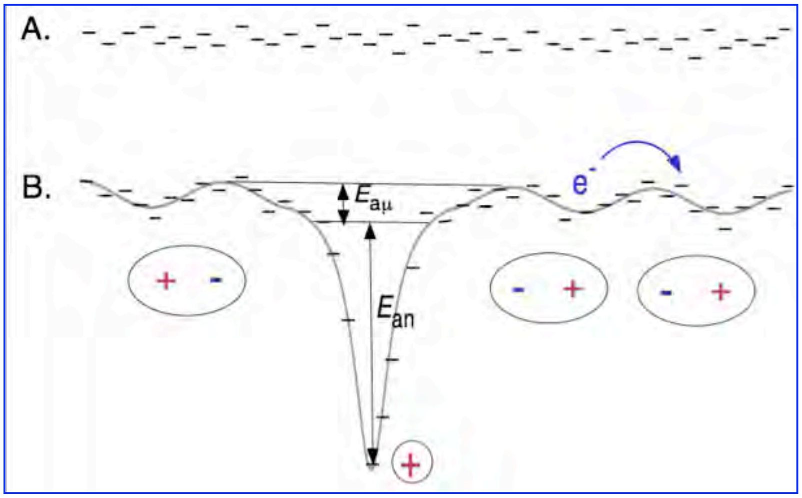

Figure 1. A. Schematic of an XSC conduction band showing uncorrelated gaussian disorder. **B.** Same with an ionized n-type dopant showing the (correlated) fluctuations caused by the majority of charges which remain bound. Activation energies for carrier generation and for mobility are shown.

An unscreened charge

in a material of dielectric constant 4 will have a Debye radius of ~140 Å, perturbing the energy levels of all molecules within this radius. Thus, above a charged defect density of N_{cd} ~10^{17} cm^{-3}, there will be practically no electrostatically unperturbed pathways through the semiconductor. Transport will be governed by the electrostatic fluctuations. In ostensibly pure, regioregular poly(3-hexylthiophene), P3HT, for example, N_{cd} ~10^{18} cm^{-3}. We employed such considerations to propose an alternative (and much simpler) explanation for the otherwise puzzling occurrence of "correlated" energetic disorder and low-field Poole-Frenkel mobilities in π-conjugated polymers (Figure 1). The several competing transport models, mostly based on the GDM, do not consider N_{cd} and must make a number of mechanistic assumptions to explain the data.

Amorphous silicon when first produced had such a high density of defects, ~10^{20} cm^{-3}, that it was useless as a semiconductor. Growing it in a hydrogen atmosphere, however, reduced the defect density by orders of magnitude. Similar to the hydrogenation of a-Si, we reasoned that treatment of π-conjugated polymers with strong electrophiles such as dimethyl sulfate, Me_2SO_4, and/or strong nucleophiles such as lithium aluminum hydride, LAH, might passivate some of the charged defects and thus improve the semiconductor properties. These reactions would also clarify the influence of defects and might provide a method of improving π-conjugated polymers to suit a particular application. Neither Me_2SO_4 nor LAH can react with unstrained (defect-free) P3HT. However, the sp^2-hybridized carbon backbone of P3HT is subject to strong shear forces in solution (where our reactions are performed) and even stronger forces during film deposition. An sp^2-carbon that is deformed from its equilibrium planar and trigonal configuration creates an electronic state in the bandgap of the solid, and becomes more reactive to either electrophiles or nucleophiles (or both) when in solution. The addition reactions with Me_2SO_4 and/or LAH should convert a strained, electroactive sp^2 carbon into an electroinactive sp^3 carbon (Figure 2). The degree of reaction is apparently less than one thiophene unit in 10^4, thus common chemical analysis is not applicable. Although there are no changes in absorption or emission spectra, there are substantial changes in the electrical properties of the solid films. The reaction of P3HT with Me_2SO_4 triples the hole mobility, almost doubles the exciton diffusion length, substantially stabilizes the polymer against photo-oxidation and shifts the Fermi energy ~200 meV positive. Treatment with LAH has similar effects except that it increases the mobility by ten fold and it shifts the Fermi energy ~500 meV negative. The preliminary conclusion is that removing charged defects—whether anionic, cationic or both—improves many of the electrical properties and the chemical stability of P3HT. This introduces the first chemical method to beneficially modify existing π-conjugated polymers.

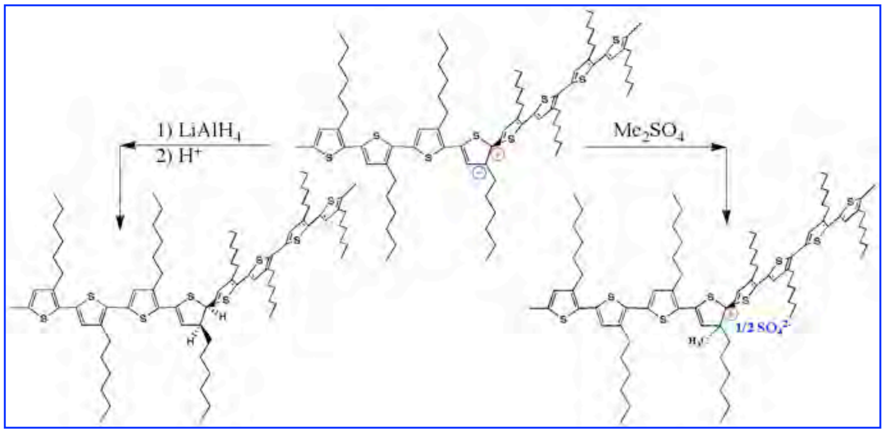

Figure 2. Cartoon of a charged defect in P3HT and its possible reaction with LAH or Me_2SO_4. No particular stereochemistry is implied.

DOE Sponsored Publications 2006-2008

1. Gregg, B. A., Gledhill, S. E. and Scott, B. "Can True Space-Charge-Limited Currents Be Observed in π-conjugated Polymers?", *J. Appl. Phys.* **2006**, *99*, 116104.

2. Gregg, B. A., "Organic Photovoltaic Cells with an Electric Field Integrally-Formed at the Heterojunction Interface", US Patent No. US 7,157,641 B2, Jan. 2, 2007.

3. Gregg, B. A., Kose, M. E., "Reversible Switching Between Molecular and Charge Transfer Phases in a Liquid Crystalline Organic Semiconductor", *Chem. Mater.*, **2008**, *20*, 5235-5239.

4. Wang, D., Reese, M. O., Kopidakis, N., Gregg, B. A., "Do the Defects Make it Work? Defect Engineering in π-Conjugated Polymer Films and Their Solar Cells", *Proc. 33rd IEEE Photovoltaic Specialists Conference*, 2008.

5. Wang, D., Kopidakis, N., Reese, M. O., Gregg, B. A., "Treating Poly(3-hexylthiophene) with Dimethylsulfate Improves Its Photoelectrical Properties", *Chem. Mater.,* **2008**, *20*, 6307-6309.

6. Gregg, B. A., "Transport in Charged Defect-Rich π-Conjugated Polymers", *J. Phys. Chem. C.,* **2009**, *113*, 5899-5901.

CONJUGATED IONOMERS FOR PHOTOVOLTAIC STRUCTURES

Mark C. Lonergan
Department of Chemistry
University of Oregon
Eugene, OR 97403

Most widely studied organic photovoltaics are based on junctions between materials with offsets between their HOMO/LUMO energy levels (valence/conduction band edges). Unlike in inorganic photovoltaics, the terms n- and p are often used to refer to the electron donor or acceptor rather than intentional doping. As stated in a recent Department of Energy report on solar energy utilization: "the interfacial junction between the n- and p-type regions does not produce an electric field and serves a different purpose than the inorganic p-n junction." Unlike common photovoltaic architectures, such as the silicon pn junction, discontinuities in the sign and density of charge carriers are not typically engineered into organic device structures.

A primary limitation that has prevented the wide study of interfaces between dissimilarly doped conjugated polymers is the mobility of dopant ions. In the case of a pn homojunction, for instance, any diffusible dopant ions will support a bulk redox reaction between the n- and p-type regions that destroys the junction. We have developed ionically functionalized polyacetylenes (polyacetylene ionomers or polyacetylene polyelectrolytes) to overcome instabilities due to dopant ion diffusion. Doping of these materials can be achieved with the formation of internally compensated (IC) states where the dopant ions are covalently attached to the polymer backbone and hence immobile. We have demonstrated that IC states can indeed be used to stabilize interfaces between dissimilarly doped materials. An important aspect of this work is developing methods to fabricating well-defined pn junctions. As with most conjugated polymers, direct casting of p- and n-type films is not possible because the doped states are insoluble.

As schematically illustrated in Figure 1, we have developed polyelectrolyte-mediated electrochemistry (PMEC) as a tool for the fabrication of conjugated ionomer pn junctions. In PMEC, a supporting electrolyte based on a large polymeric ion is used to control the electrochemistry of solid films. In the limit that the polymeric ion is too large to permeate the film, any redox process that requires its incorporation will not be possible. Developing PMEC along with polyacetylene ionomers of varying ionic functional group density now allows us to fabricate pn junctions with controlled dopant density. Fig. 2 shows the current-voltage behavior of a pn junction where the anionic and cationic ionomers have an ionic functional group density

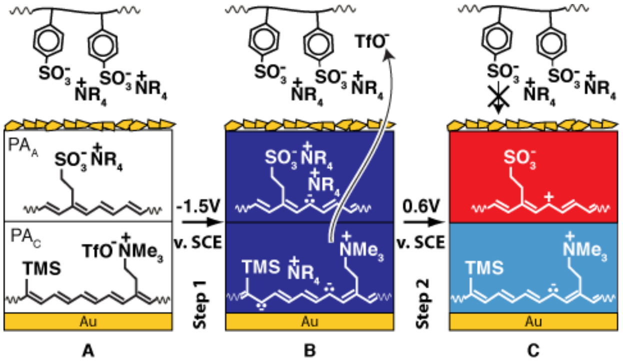

Figure 1 - PMEC fabrication of a polyacetylene-based pn junction using a Bu_4NPSS / CH_3CN supporting electrolyte. (A) Initial undoped bilayer of solid films of a polyacetylene anionomer and a polyacetylene cationomer sandwiched between gold electrodes. (B) Structure following the application of -1.5 V vs. SCE to n-dope the films. (C) Structure following the application of 0.6 V to p-dope the PA_A layer while preserving the PA_C layer in an IC n-type form. Complete reoxidation and p-doping of the PA_C layer is not possible because the OTf^- ions were previously lost to the solution and the PSS^- is too large to permeate the polymer film.

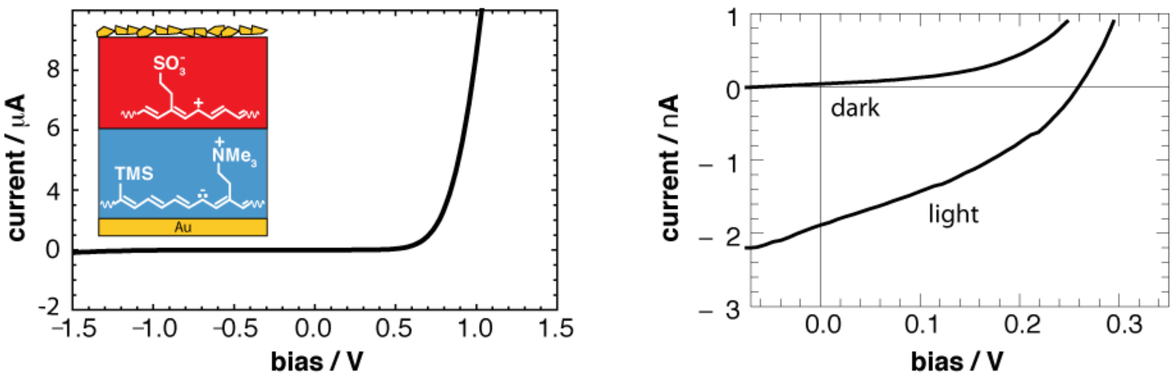

Figure 2 - (left) Current-voltage behavior of the polyacetyelene ionomer pn junction schematically shown inset. (right) Expanded current voltage curve including under illumination (50mW white light, tungsten-halogen)

of 1 per 4 and 30 double bonds, respectively. Diode behavior is observed with the sign of forward bias consistent with classic pn junction theory. The ratio of the forward to the reverse current at 1V is over 500. The structure, in particular the film thicknesses, are not optimized for a photovoltaic response. Nevertheless a small photovoltaic effect is observed. The polyacetylene ionomers making up this junction nominally have a near zero band offset. The observed photovoltaic effect is suggestive of charge separation being driven by a built-in field.

In addition to junctions between polymers with different signs of electronic carriers, we have also been exploring junctions between conjugated ionomers where there is a change in the sign of ionic carriers, for instance, that shown in Figure 3B. The exchange of ions at the junction can potentially lead to a built-in field. To explore this possibility, the response of these so-called heteroionic junctions is being explored. Figure 3 shows the photovoltage as a function of time for a heteroionic junction as compared to a single layer film. Unlike with single layer films, the sign of the photovoltage does not change depending on the side of the structure illuminated consistent with the effect arising from the ionic junction rather than a light-induced asymmetry.

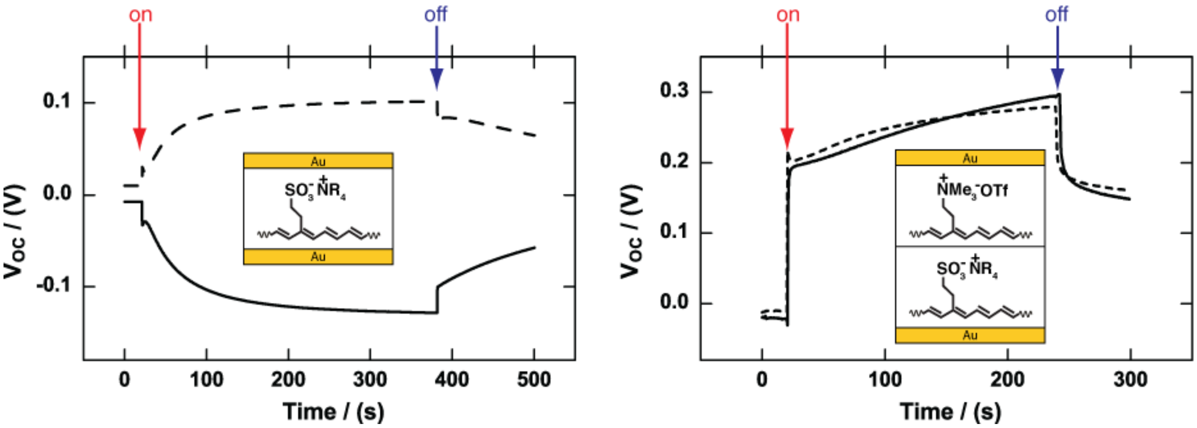

Figure 3 - Time dependence of the photovoltage for a single layer ionomer structure and a bilayer heteroionic junction with illumination (100mW @ 532nm) on either side (solid vs. dashed line)

DOE Sponsored Publications 2006-2008

1. S.G. Robinson, D.H. Johnston, C. Weber, M.C. Lonergan, "Polyelectrolyte mediated electrochemical fabrication of a polyacetylene ionomer pn junction", *J. Am.. Chem. Soc.*, submitted April 2009.

2. F. Lin, E. Walker, M.C. Lonergan, "Photovoltaic effect at polyacetylene ionomer heteroionic junctions", *manuscript in preparation.*

3. S.G. Robinson, D. Stay, and M.C. Lonergan, " Development and applications of ion-functionalized conjugated polymers", book chapter in preparation for *Iontronics: Ionic carriers in organic electronic materials and devices.*

CHARGE TRANSFER AT CONJUGATED POLYMER:FULLERENE INTERFACES

Garry Rumbles, Nikos Kopidakis, Andrew Ferguson, David Coffey, Jeffrey Blackburn, and
Michael Heben

Chemical and Biosciences Center
National Renewable Energy Laboratory
Golden, Colorado 80401-3393

Flash photolysis, transient microwave conductivity (fp-TRMC) studies of poly(3-alkylthiophene) with the soluble derivative of C_{60}, PCBM, and with single-walled carbon nanotubes (SWNTs) will be reported. Investigations of blends of PCBM with poly(3-hexylthiophene), P3HT, have enabled us to determine the efficiency of exciton dissociation and charge production, followed by the subsequent trapping and recombination of these carriers on timescales from nanoseconds to milliseconds (see Figure 1). New studies of SWNTs dispersed in P3HT verify that some nanotubes are capable of effectively replacing the PCBM in the dissociation process, but the direct excitation of the nanotubes themselves does not result in transfer of a hole back to the polymer. The presentation will discuss these two studies in detail, providing a picture of the fate of excitons and carriers in these two important donor-acceptor systems that are to be found in bulk heterojunction photovoltaic solar cells.

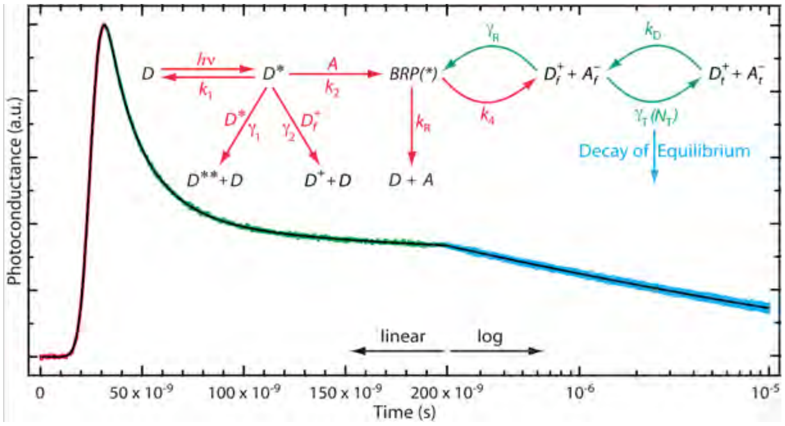

Figure 1 - TRMC signal from a 1% blend of PCBM dispersed in P3HT recorded at moderately high laser powers to accentuate the second-order recombination process. The fit through the data arises from analysis of the kinetic scheme shown in the inset.

We have examined a series of blends of PCBM in P3HT at weight ratios from 1% up to the device ratio of 50%. Figure 1 shows a typical transient recorded for the 1% blend, and recorded at a high laser power, where higher-order kinetic processes can be readily identified. The kinetic scheme shown as an inset in Figure 1, arises from the global analysis of these data, with the associated rate constants for the fate of the holes over this 10 microsecond time window given in table 1. Based on previous work[6], the quantum yield of holes resulting from exciton dissociation at low light levels is 0.7 with 1% PCBM, and is close to unity at 5%. These holes are mobile carriers and are readily detected by the microwave detection system. The decay of the signal in the first 200 ns arises from a combination of hole trapping, and recombination with the electrons in the PCBM, although at low light levels the effect of recombination is at a minimum. At times longer than 200 ns, the trapped and mobile carriers are in equilibrium, with the mobile carriers susceptible to recombination, which is why the signal decays slowly at long times. The kinetic processes are consistent with the proposed model that the mobile carriers are produced directly from the dissociating exciton and the process proceeds via a hot (non-thermalized) bound radical pair

(BRP*) state, while recombination proceeds via a thermalized BRP state.

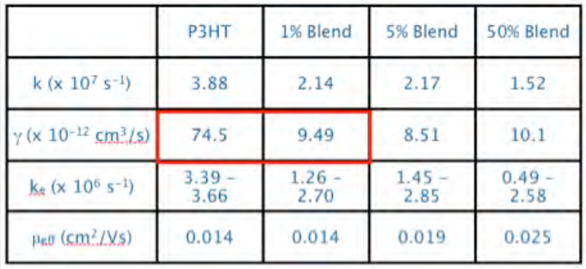

	P3HT	1% Blend	5% Blend	50% Blend
k (x 10^7 s^{-1})	3.88	2.14	2.17	1.52
γ (x 10^{-12} cm^3/s)	74.5	9.49	8.51	10.1
k_e (x 10^6 s^{-1})	3.39 – 3.66	1.26 – 2.70	1.45 – 2.85	0.49 – 2.58
μ_{eff} (cm^2/Vs)	0.014	0.014	0.019	0.025

Table 1 – Rate constants (see inset Figure 1) for the 1%, 5% and 50% blend of PCBM in P3HT. Note the large second-order recombination rate constant for carriers produced directly in the polymer with no PCBM.

SWNTs dispersed with P3HT were successfully prepared in organic solvents, where spectroscopic evidence suggests that the polymer serves to both isolate and solvate the SWNTs; an isolation that remains when thin films are prepared from these solutions. Fp-TRMC studies of these films were carried out exciting the polymer at 532 nm. The transients displayed profiles very similar to those of a 1% blend of PCBM in P3HT, revealing the presence of long-lived separated charge carriers, assumed to be holes in the polymer and electrons in the SWNTs. Thus the SWNTs have been shown to mimic the important property of PCBM (C_{60}) of inhibiting carrier recombination. Excitation of the SWNTs at longer wavelengths, revealed a very fast signal that showed no evidence for the dissociation of an exciton in the SWNT via the transfer of a hole back to the polymer. Further studies of isolated SWNTs in an inert polymer host, carboxymethyl cellulose (CMC), reveal the formation of short-lived carriers (lifetime ~3.5 ps measured by transient terahertz spectroscopy, TRTS) that show little evidence of the excitonic character of excitations that are expected in isolated SWNTs. This result is consistent with TRTS studies on the same samples, and it remains unclear what the efficiency of the exciton dissociation is, and why it is independent of the excitation wavelength.

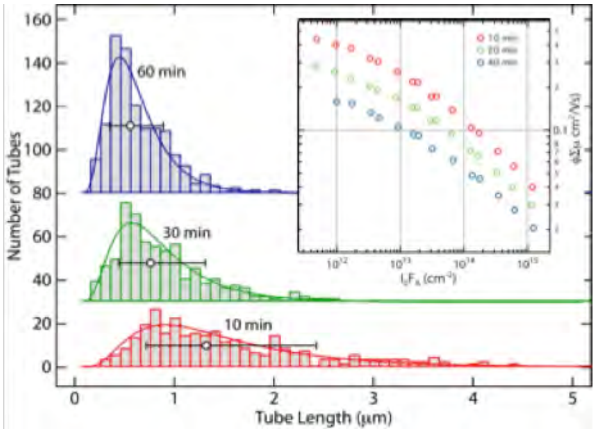

Figure 2 – SWNT nanotube length distributions after 10, 30 and 60 minutes sonication. Inset shows how the peak TRMC signal is reduced as the nanotube length is decreased.

The magnitude of the TRMC signal when exciting the SWNTs directly is due to both electrons and holes, and while the signal is large, it is not as large as would be predicted for carriers with mobilities expected to be in excess of 10^5 cm^2/Vs. While this can be partly attributed to the short, 3.5 ps carrier lifetime leading to signal loss during the 5 ns laser pulse, the signal remains smaller than would be expected. By sonicating SWNT samples for varying times and producing SWNTs of different length (see Figure 2), we have now shown that the carrier mobility measured by TRMC (or TRTS) is reduced by the effective mean free path for the carriers being longer than the lengths of the nanotubes, and it is therefore reduced from its optimum value.

In this presentation, the importance of these results will be discussed and how they relate to the performance of the prototypical bulk heterojunction photovoltaic solar cells that are based on P3HT:PCBM blends, and how this might be modified by replacing the PCBM with SWNTs. An examination of the long-term strategy for the much-needed improvements in the power conversion efficiencies of these devices will be included.

DOE Sponsored Publications 2006-2008[1-23]

1. Xu, Q.; Tucker, M. P.; Arenkiel, P.; Ai, X.; **Rumbles**, G.; Sugiyama, J.; Himmel, M. E.; Ding, S. Y., Labeling the planar face of crystalline cellulose using quantum dots directed by type-I carbohydrate-binding modules. *Cellulose* **2009,** *16* (1), 19-26.

2. Xu, Q.; Song, Q.; Ai, X.; McDonald, T. J.; Long, H.; Ding, S. Y.; Himmel, M. E.; **Rumbles**, G., Engineered carbohydrate-binding module (CBM) protein-suspended single-walled carbon nanotubes in water. *Chemical Communications* **2009,** (3), 337-339.

3. Mitchell, W. J.; Ferguson, A. J.; Kose, M. E.; Rupert, B. L.; Ginley, D. S.; **Rumbles**, G.; Shaheen, S. E.; Kopidakis, N., Structure-Dependent Photophysics of First-Generation Phenyl-Cored Thiophene Dendrimers. *Chemistry of Materials* **2009,** *21* (2), 287-297.

4. Scholes, G. D.; **Rumbles**, G., Excitons in Nanoscale Systems: Fundamentals and Applications. . In *Annual Review of Nano Research 2*, Cao, G.; Brinker, C. J., Eds. World Scientific: Hackensack, NJ, 2008; Vol. 2, pp 103-157.

5. Piris, J.; Ferguson, A. J.; Blackburn, J. L.; Norman, A. G.; **Rumbles**, G.; Selmarten, D. C.; Kopidakis, N., Efficient photoinduced charge injection from chemical bath deposited CdS into mesoporous TiO2 probed with time-resolved microwave conductivity. *Journal of Physical Chemistry C* **2008,** *112* (20), 7742-7749.

6. Ferguson, A. J.; Kopidakis, N.; Shaheen, S. E.; **Rumbles**, G., Quenching of excitons by holes in poly(3-hexylthiophene) films. *Journal of Physical Chemistry C* **2008,** *112* (26), 9865-9871.

7. Blackburn, J. L.; McDonald, T. J.; Metzger, W. K.; Engtrakul, C.; **Rumbles**, G.; Heben, M. J., Protonation effects on the branching ratio in photoexcited single-walled carbon nanotube dispersions. *Nano Letters* 2008, *8* (4), 1047-1054.

8. Scholes, G. D.; Tretiak, S.; McDonald, T. J.; Metzger, W. K.; Engtrakul, C.; **Rumbles**, G.; Heben, M. J., Low-lying exciton states determine the photophysics of semiconducting single wall carbon nanotubes. *Journal of Physical Chemistry C* **2007,** *111* (30), 11139-11149.

9. Piris, J.; Kopidakis, N.; Olson, D. C.; Shaheen, S. E.; Ginley, D. S.; **Rumbles**, G., The Locus of Free Charge-Carrier Generation in Solution-Cast Zn(1-x)Mg(x) Poly(3-hexylthiophene) Bilayers for Photovoltaic Applications. *Advanced Functional Materials* **2007,** *17* (18), 3849-3857.

10. Metzger, W. K.; McDonald, T. J.; Engtrakul, C.; Blackburn, J. L.; Scholes, G. D.; **Rumbles**, G.; Heben, M. J., Temperature-dependent excitonic decay and multiple states in single-wall carbon nanotubes. *Journal of Physical Chemistry C* **2007,** *111* (9), 3601-3606.

11. McDonald, T. J.; Blackburn, J. L.; Metzger, W. K.; **Rumbles**, G.; Heben, M. J., Chiral-selective protection of single-walled carbon nanotube photoluminescence by surfactant selection. *Journal of Physical Chemistry C* **2007,** *111* (48), 17894-17900.

12. Kose, M. E.; Mitchell, W. J.; Kopidakis, N.; Chang, C. H.; Shaheen, S. E.; Kim, K.; **Rumbles**, G., Theoretical Studies on Conjugated Phenyl-Cored Thiophene Dendrimers for Photovoltaic Applications. *J. Am. Chem. Soc.* **2007,** *129* (46), 14257-14270.

13. Jones, M.; Metzger, W. K.; McDonald, T. J.; Engtrakul, C.; Ellingson, R. J.; **Rumbles**, G.; Heben, M. J., Extrinsic and intrinsic effects on the excited-state kinetics of single-walled carbon nanotubes. *Nano Letters* **2007,** *7* (2), 300-306.

14. Ai, X.; Xu, Q.; Jones, M.; Song, Q.; Ding, S. Y.; Ellingson, R. J.; Himmel, M.; **Rumbles**, G., Photophysics of (CdSe) ZnS colloidal quantum dots in an aqueous environment stabilized with amino acids and genetically-modified proteins. *Photochemical & Photobiological Sciences* **2007,** *6,* 1027-1033.

15. Scholes, G. D.; **Rumbles**, G., Excitons in nanoscale systems. *Nature Materials* **2006,** *5* (9), 683-696.

16. Rumbles, G.; Lian, T.; Murakoshi, K., *Electron transfer in nanomaterials*. The Electrochemical Society: Pennington, 2006; Vol. PV 2004-22, p 458.

17. McDonald, T. J.; Jones, M.; Engtrakul, C.; Ellingson, R. J.; **Rumbles**, G.; Heben, M. J., Near-infrared Fourier transform photoluminescence spectrometer with tunable excitation for the study of single-walled carbon nanotubes. *Review of Scientific Instruments* **2006,** *77* (5), 053104.

18. McDonald, T. J.; Engtrakul, C.; Jones, M.; **Rumbles**, G.; Heben, M. J., Kinetics of PL quenching during single-walled carbon nanotube rebundling and diameter-dependent surfactant interactions. *Journal of Physical Chemistry B* **2006,** *110* (50), 25339-25346.

19. Jones, M.; Ding, S. Y.; Tucker, M. P.; Kim, Y. H.; Zhang, S. B.; Himmel, M. E.; **Rumbles**, G. In *Stabilization of (CdSe)ZnS Quantum Dots in Water Using Amino Acid Capping Groups*, 205th Meeting of the Electrochemical Society, San Antonio, 9-14 May 2004; Rumbles, G.; Lian, T.; Murakoshi, K., Eds. The Electrochemical Society: San Antonio, 2006; pp 340-349.

20. Ellingson, R. J.; Engtrakul, C.; Jones, M.; **Rumbles**, G.; Heben, M. J.; Nozik, A. J. In *Excitation Energy Dependence of the Ultrafast Transient Absorption Response of Single-Wall Carbon Nanotubes*, 205th Meeting of the Electrochemical Society, San Antonio, 9-14 May 2004; Rumbles, G.; Lian, T.; Murakoshi, K., Eds. The Electrochemical Society: San Antonio, 2006; pp 415-420.

21. Ding, S. Y.; Xu, Q.; Bayer, E. A.; Qian, X.; **Rumbles**, G.; Himmel, M. E., Bacterial Protein Complexes with Potential Applications in Nanotechnology. In *Microbial Bionanotechnology: Biological Self-Assembly Systems and Biopolymer-Based Nanostructures*, Rehm, B., Ed. Horizon Bioscience: U.K., 2006; pp 269-305.

22. Ding, S. Y.; Xu, Q.; Ali, M. K.; Baker, J. O.; Bayer, E. A.; Barak, Y.; Lamed, R.; Sugiyama, J.; **Rumbles**, G.; Himmel, M. E., Versatile derivatives of carbohydrate-binding modules for imaging of complex carbohydrates approaching the molecular level of resolution. *Biotechniques* **2006,** *41* (4), 435-443.

23. Ai, X.; Beard, M. C.; Knutsen, K. P.; Shaheen, S. E.; **Rumbles**, G.; Ellingson, R. J., Photoinduced charge carrier generation in a poly(3-hexylthiophene) and methanofullerene bulk heterojunction investigated by time-resolved terahertz spectroscopy. *Journal of Physical Chemistry B* **2006,** *110* (50), 25462-25471.

Posters

ORGANIC SOLAR MATERIALS: PHOTOCONVERSION AND CONCENTRATORS

Carlijn Mulder, Philip Reusswig, Tim Heidel, Marc Baldo, Seth Difley,* Troy Van Voorhis*
Electrical Engineering and Computer Science, * Department of Chemistry
Massachusetts Institute of Technology
Cambridge, MA 02139

1. *Organic Solar Cells.* The most important process in an organic solar cell is the dissociation of a localized exciton into separated charges. There are two competing models for this process: the hot carrier model, which assumes that the dissociated charge travels over the Coulombic binding potential before relaxing, and a thermionic emission model that assumes that slow recombination rates allow a relaxed carrier trapped within the Coulombic binding potential the opportunity to eventually hop over the barrier. We have been investigating this process in planar heterojunctions comprised of small molecular weight materials. We observe no difference in charge collection efficiency when the spin of the charge transfer state is altered, and hence our data is consistent with the hot carrier model. We have also found a weak dependence of the dissociation process on the excess energy of the exciton and a much stronger dependence on the charge carrier mobility. Drawing upon this model of exciton dissociation, we have constructed organic solar cells with thin (1-2nm) interfacial layers inserted at the donor-acceptor interface. This design is characteristic of exciton dissociation in photosynthesis and we find that it also improves external quantum efficiency and the open circuit voltage in organic solar cells. We will present both our fundamental studies of exciton dissociation and device results.[1]

2. *Luminescent solar concentrators* (LSCs) are planar waveguides with a thin film organic coating on the face of inorganic solar cells attached to the edges. Light is absorbed by the coating and reemitted into waveguide modes for collection by the solar cells. In the past year we have developed single and tandem waveguide organic solar concentrators with quantum efficiencies exceeding 50% and projected power conversion efficiencies as high as 6.8%.[2] The exploitation of near-field energy transfer, solid-state solvation, and phosphorescence enables tenfold increases in the power obtained from photovoltaic cells without the need for solar tracking. We also report: (i) cast LSCs constructed from phycobilisomes, model antenna systems from photosynthesis, (ii) linearly polarized LSCs employing polymerizable liquid crystals, and (iii) hybrid organic/inorganic LSCs based on neodymium glass. The cast LSCs avoid the requirement for a potentially expensive, high index glass substrate. Linearly-polarized LSCs can be used to replace polarizers in video displays thereby converting liquid crystal and organic LED displays into solar cells. Finally, the neodymium-based LSC is a stable and efficient technology that appears compatible with float glass manufacturing. Its expected low costs and compatibility with silicon solar cells make it a potentially revolutionary solar cell technology.

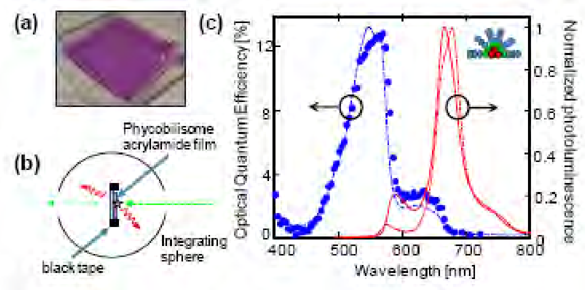

Fig. 1. Luminescent solar concentrators employing phycobilisomes.

---

1. Jiye Lee, *et al*; Tim Heidel, *et al*. papers in preparation.
2. Currie, *et al*. Science **321** 226 (2008)
3. Mulder, *et al*. Advanced Materials, in press
4. Mulder, *et al*.; Reusswig, *et al*. papers in preparation.

SINGLE MOLECULE SPECTROSCOPIC STUDIES OF CHARGE SEPARATION AND CHARGE TRANSFER

Rodrigo E. Palacios, Joshua C. Bolinger, Kwang Jik Lee, William M. Lackowski, and Paul F. Barbara
Center for Nano and Molecular Science and Technology
The University of Texas at Austin
Austin, TX and 78712

The present pace of development of OPV nanomaterials is still far below what is required for most solar energy applications in the next few decades. The tremendous complexity of OPV materials has severely limited the molecular-level understanding of these materials. This in turn, has been a barrier to the rational design and engineering of these materials. In this poster present, a new single molecule (particle) spectroscopy (SMS) method for OPV device prototypes toward the goal of obtaining new molecular level information on the PV mechanism is presented. This SMS approach should lead to a much better understanding of what molecular-level factors determine the photon to electrical power energy conversion efficiency of a given material.

The basic idea behind this experiment is summarized in the figure, along with preliminary data on the yield and dynamics of charge separation between donor/acceptor F8BT and TFB. Different prototype capacitor-like device geometries with for measuring the quantum charge separation hole transfer, and electron transfer for the various interfaces. In these experiments the quantum efficiency for charge separation is indirectly probed by monitoring the quenching of the single-molecule fluorescence spectroscopy intensity in device geometry with external electrodes**.** Single molecule electron transfer rate constants k_{et} and other aspects of the kinetics and dynamics have been studied using **coordinated and simultaneous single molecule spectroscopy and device modulation** (E-field, excitation intensity, etc).

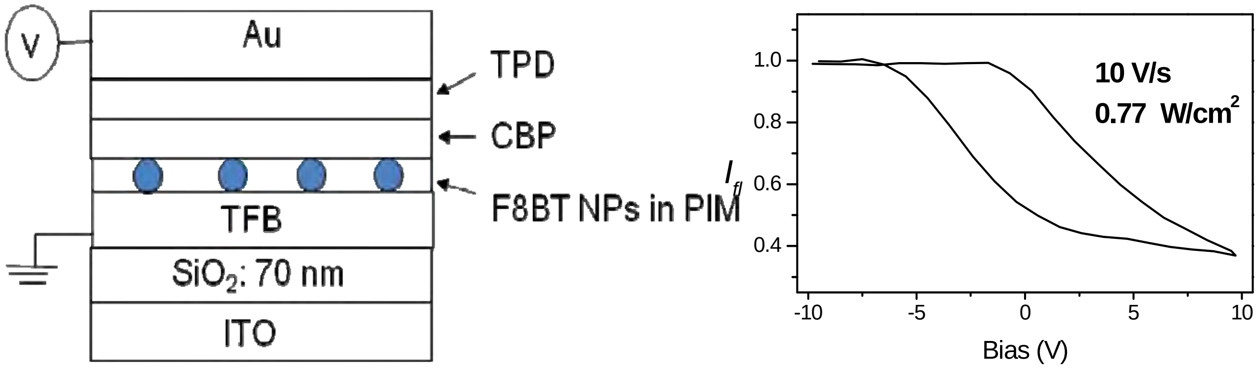

.

VARIATIONS IN THE QUANTUM EFFICIENCY OF MULTIPLE EXCITON GENERATION FOR A SERIES OF CHEMICALLY-TREATED PBSE NANOCRYSTAL FILMS

Matthew C. Beard, Aaron Midgett, Matt Law, Octavi Semonin, Randy J. Ellingson and Arthur J. Nozik
Chemical and Biosciences Center
National Renewable Energy Laboratory
Golden, Co and 83401

We study multiple exciton generation (MEG) in two series of chemically-treated PbSe nanocrystal (NC) films. We find that the average number of excitons produced per absorbed photon varies between 1.0 and 2.4 (± 0.2) at a photon energy of ~4E_g for films consisting of 3.7 nm NCs, and between 1.1 and 1.6 (± 0.1) at hν ~5E_g for films consisting of 7.4 nm NCs. The variations in MEG depend upon the size of the NCs and the chemical treatment used to electronically couple the NCs in each film. The single and multi-exciton lifetimes also change with the chemical treatment: biexciton lifetimes increase with stronger inter-NC electronic coupling and exciton delocalization, while single exciton lifetimes decrease after most treatments relative to the same NCs in solution. Single exciton lifetimes are particularly affected by surface treatments that dope the films *n*-type, which we tentatively attribute to an Auger recombination process between a single exciton and an electron produced by ionization of the dopant donor. These results imply that a better understanding of the effects of surface chemistry on film doping, NC carrier dynamics, and inter-NC interactions is necessary to build solar energy conversion devices that can harvest the multiple carriers produced by MEG. Our results show that the MEG efficiency is very sensitive to the condition of the NC surface as well as to NC size, and suggest that the wide range of MEG efficiencies reported in the recent literature may be a result of uncontrolled differences in NC surface chemistry. We discuss recent results of MEG in isolated NCs for flowing and static conditions and show that the MEG efficiency is only ~5-10% lower in the flowing samples for photon energies less 4 E_g and is sensitive to the surface conditions.

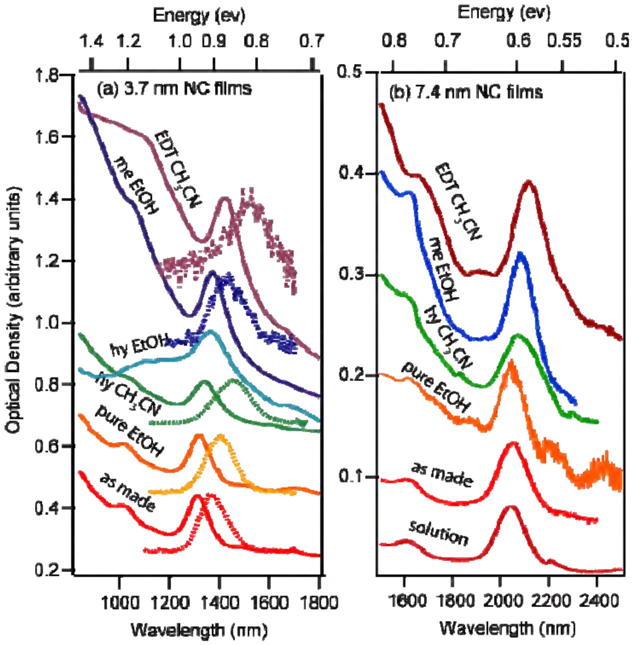

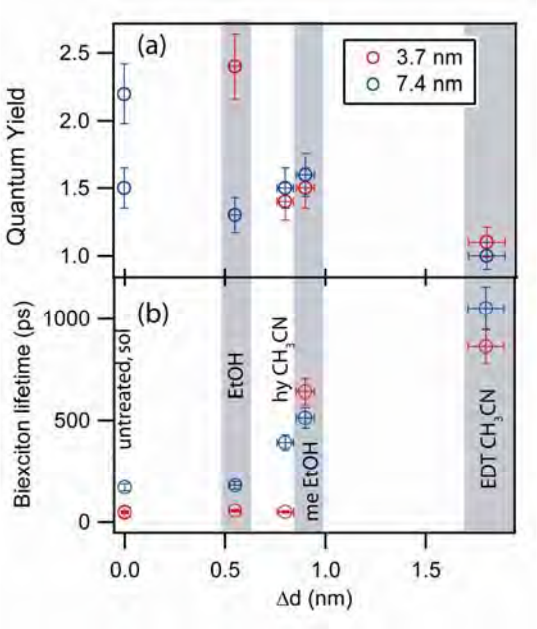

THEORY OF ONE- AND TWO-ELECTRON TRANSFER BETWEEN QUANTUM DOTS

D. Balamurugan[a], S.S. Skourtis[b], and D.N. Beratan[a]
[a]Department of Chemistry, Duke University, Durham, North Carolina 27708
[b]Department of Physics, University of Cyprus, Nicosia 1678, Cyprus

We are developing theoretical methods to describe photoinduced charge separation between chemically linked quantum dots. The initially prepared state is an excitonic or biexcitonic state of a semiconductor quantum dot assembly. Our aims are three-fold: 1) to understand the dependence of one-electron and two-electron charge separation rates on the structure and connectivity of the linked dots, 2) to explore how rates scaling with bridge connectivity may differ for one and two-electron transfer reactions, and 3) to develop schemes to optimize photo-induced charge transfer in specific coupled quantum dots under study in the laboratories of our collaborators. Our model approach uses electronic structure methods (model Hamiltonians, semi-empirical Hamiltonians, and density functional theory) to analyze the charge transfer interactions in specific donor-bridge-acceptor (D-B-A) systems. Explorations are underway on CdS and CdSe diads linked by alkene dithiols. In these studies, we compute the electronic coupling interactions in a many-electron Green's function framework in order to determine the nature of the one- and two-electron interactions, their dependence on assembly architecture, and the quantum interferences for single- and multi-electron events.

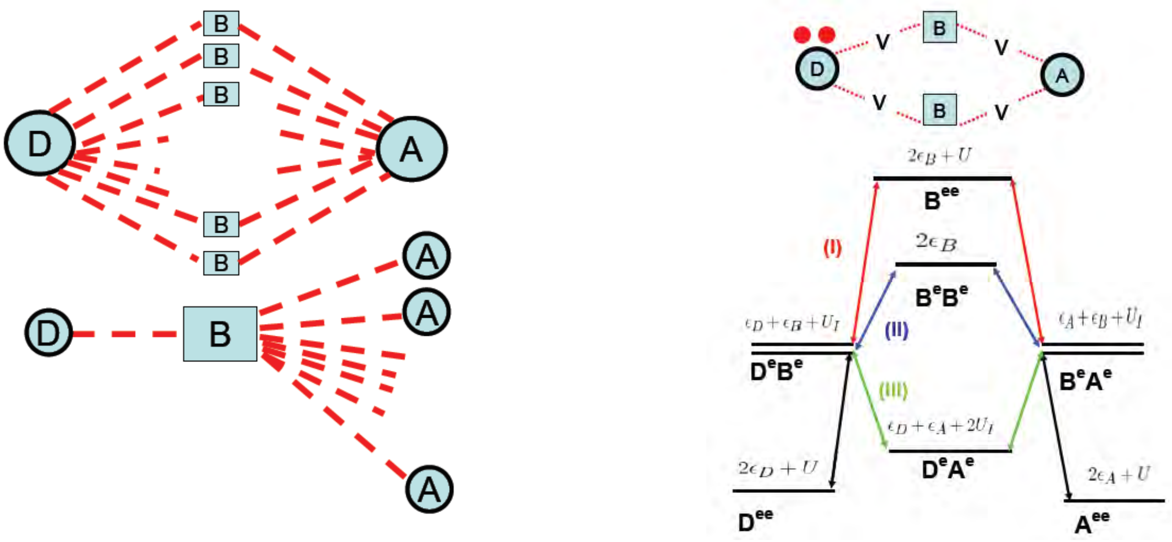

Figure 1. (**left**) The influence of donor-bridge-acceptor architectures are being examined for one- and two-electron transfer couplings. Architectures with multiple parallel bridges (top left) and one bridge with many acceptors (bottom left) are being analyzed and scaling laws developed. (**right**) The initial, intermediate and final states for two-electron transfer are shown schematically for a bridge with two parallel paths. The contributions of the many consequent coupling pathways are computed using a Hubbard Hamiltonian.

INTERACTIONS OF SINGLE-WALLED CARBON NANOTUBES WITH POLYMERS: IMPLICATIONS FOR SEPARATIONS AND PHOTOCHEMISTRY

Jeff Blackburn,^ John-David Rocha,^ Andrew Ferguson,^ Brian Larsen,^ Pravas Deria,#
Michael Therien,# Garry Rumbles,^ Michael Heben^*
^National Renewable Energy Laboratory, Golden, CO
#Duke University, Durham, NC
*The University of Toledo, Toledo, OH

Single-walled carbon nanotubes (SWNTs) are two-dimensionally confined quantum wires that have the potential to impact a variety of solar photochemical applications. SWNTs have many properties that are well suited to solar conversion, including strong, size-tunable light absorption and excellent charge carrier mobilities. One major obstacle to observing the intrinsic properties of SWNTs *and* incorporating SWNTs into solar applications is the high degree of polydispersity obtained from typical SWNT syntheses. A major breakthrough occurred in 2002 with the use of micelle-forming surfactants to disperse SWNTs as individual SWNTs that could be probed by spectroscopic methods to elucidate some of the intrinsic SWNT properties.[1] Furthermore, selective interactions of these surfactants with SWNTs have paved the way for separation of SWNTs by electronic structure, diameter, and chirality.[2, 3] These major breakthroughs have allowed for a much deeper understanding of fundamental SWNT physical and chemical properties, and are opening up the potential to rationally consider which types (specific chiralities, diameters, electronic structures) of SWNTs are best suited for particular solar applications.

While much attention has been given to surfactants for isolation and separation of SWNTs, less work has been done on high molecular weight polymers. Polymers confer a large degree of flexibility for SWNT isolation and separation, including: very strong (and potentially chirality-dependent) interactions with the SWNT sidewall; the potential to change the polymer molecular weight and length to tune separations; the potential to isolate and separate SWNTs in a variety of different media by slightly altering the polymer structure. This poster focuses on the interactions of SWNTs with various polymers, both inert and photo-active, as studied by several different spectroscopic techniques. Raman and photoluminescence excitation spectroscopies yield information on how the relative dielectric environment changes as a function of polymer and solvent. We also monitor electronic structure-dependent charge transfer reactions that depend critically on the relative binding energy of the polymer to m-SWNTs and s-SWNTs. These observations are used to guide and understand separations of a bulk mixture by electronic structure. Finally, we discuss spectroscopic studies of SWNTs with the photo-active polymer, poly 3-hexylthiophene (P3HT), and their implication for exciton dissociation within this hybrid system.

1. O'Connell, M. J.; Bachilo, S. M.; Huffman, C. B.; Moore, C. M.; Strano, M. S.; Haroz, E. H.; Rialon, K.; Boul, P. J.; Noon, W. H.; Kittrell, C.; Ma, J. P.; Hauge, R. H.; Weisman, R. B.; Smalley, R. E., *Science* **2002,** 297, 593.
2. McDonald, T. J.; Blackburn, J. L.; Metzger, W. K.; Rumbles, G.; Heben, M. J., *J. Phys. Chem. C* **2007,** 111, 17894.
3. Blackburn, J. L.; Barnes, T. M.; Beard, M. C.; Kim, Y.-H.; Tenent, R. C.; McDonald, T. J.; To, B.; Coutts, T. J.; Heben, M. J., *ACS Nano* **2008,** 2, (6), 1266-1274.

HOLE TRANSFER DYNAMICS IN TETRAPYRROLIC DYADS

James R. Diers,[a] Masahiko Taniguchi,[b]
Dewey Holten,[c] Jonathan S. Lindsey,[b] and David F. Bocian[a]

[a]Department of Chemistry University of California, Riverside CA 92521-0403
[b]Department of Chemistry, North Carolina State University, Raleigh, NC 27695-8204
[c]Department of Chemistry, Washington University, St. Louis, MO 63130-4889

Efficient solar-energy conversion requires that holes generated after excited-state electron-injection can move efficiently away from the anode, thereby preventing charge-recombination. Thus, understanding hole mobility in prototypical light-harvesting and charge-separation systems is of fundamental interest. Towards this goal, the ground-state hole-transfer dynamics of the monocations of a variety of tetrapyrrolic dyads have been investigated using EPR spectroscopy. In our previous studies, the dyads have been zinc chelates in which the atoms of the macrocycle are of natural isotopic composition or contain ^{13}C labels at the meso or α-pyrrole carbons. The ^{14}N and/or ^{13}C nuclei provide provide hyperfine clocks that provide information on hole transfer in the 50-200 ns range. Regardless, it would be highly desirable to have a still faster hyperfine clock. Inspection of the characteristics of the nuclei across the periodic table shows that there are relatively few options for attaining a faster hyperfine clock. By far the best choice of a nucleus is thallium. Thallium is readily inserted into tetrapyrroles. ^{203}Tl and ^{205}Tl occur naturally in a 30/70 isotope ratio; both are S=1/2 nuclei with near equal magnetogyric ratios. Most importantly, the magnetogyric ratio(s) is extremely large, ~60% of that of ^{1}H. Accordingly, only very small spin density on the Tl metal center should yield significant hyperfine splitting. This hypothesis has been tested by examining several benchmark $\mathrm{Tl^{III}TMP}$ (TMP = tetramesitylporphyrin) monomers prepared by the Lindsey laboratory. The room temperature EPR spectra of two monomeric monocations, which differ in the nature of the axial ligand to the $\mathrm{Tl^{III}}$ ion ($\mathrm{Cl^-}$ versus $\mathrm{CN^-}$) are shown in Figure 1. The spectrum of the $\mathrm{Cl^-}$ ligated species is characterized by a doublet due to interactions of the electron with the S=1/2 Tl nucleus; the hyperfine splitting is much larger, ~27 G (~76 MHz), than that of either ^{13}C or ^{14}N. The spectrum of the $\mathrm{CN^-}$ ligated species exhibits an even larger hyperfine splitting, ~58 G (~160 MHz). Thus, the $^{203/205}$Tl hyperfine interaction reduces the lower limit on the timescale for monitoring hole transfer to less than 10 ns. The $^{203/205}$Tl interaction is also sufficiently large that good quality simulations of thermally activated hole transfer in dyads can be obtained. The simulations provide a direct measure of the hole-transfer rates as well as the activation energies and electronic coupling matrix elements governing the dynamics of hole transfer.

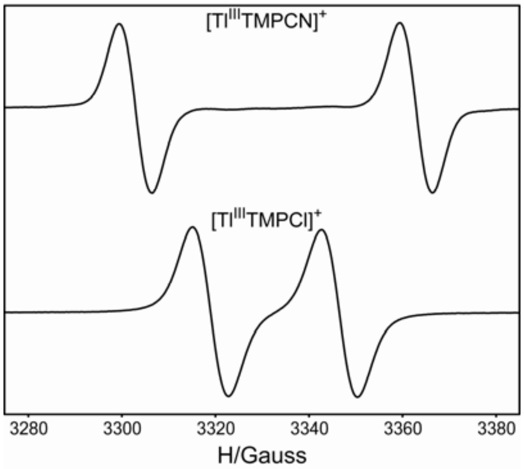

Figure 1. Room-temperature EPR spectra of **$\mathrm{Tl^{III}TMPCl}$**$]^+$ and [**$\mathrm{Tl^{III}TMPCN}$**$]^+$.

PHOTOINITIATED ELECTRON COLLECTION IN MIXED-METAL SUPRAMOLECULAR COMPLEXES: DEVELOPMENT OF PHOTOCATALYSTS FOR HYDROGEN PRODUCTION

Karen J. Brewer, Travis White, Shamindri Arachchige, David Zigler, Krishnan Rangan
Department of Chemistry
Virginia Tech, Blacksburg, VA 24061-0212 (kbrewer@vt.edu)

This project is aimed at developing and studying a class of mixed-metal supramolecular complexes with promising redox and excited state properties. These systems couple charge transfer light absorbing metals to reactive metals such as rhodium(III) that will allow these complexes to undergo photoinitiated electron collection while possessing reactive metal sites capable of delivering these electrons to a substrate to facilitate the production of H_2. This project period has focused on the factors that impact the photocatalysis reaction aimed at understanding more clearly the mechanism of function of these systems.

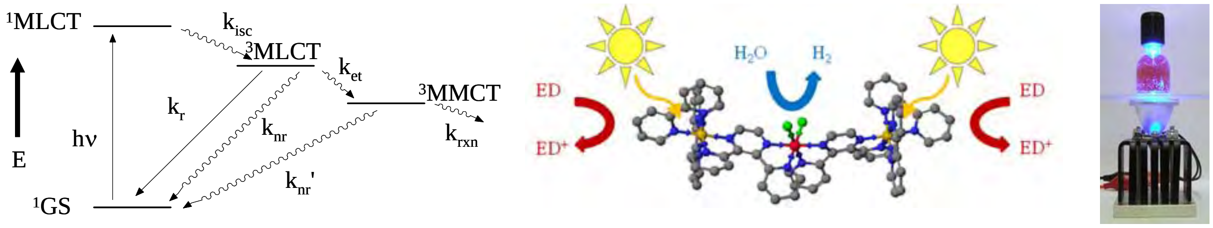

Figure 1. State diagram and structure of one photocatalyst for the production of H_2 from H_2O.

Series of mixed-metal Ru(II) and Rh(III) complexes of the general forms $[\{(TL)_2Ru(BL)\}_2RhX_2](PF_6)_5$ and $[(TL)_2Ru(BL)RhCl_2(TL')](PF_6)_3$ have been prepared and studied with TL = terminal ligand, BL = bridging ligand and X = Cl^- or Br^-. These supramolecular architectures are unusual in their coupling of reactive cis-$Rh^{III}X_2$ sub-units to light absorbing Ru sites. They represent the first photoinitiated electron collectors shown to reduce H_2O to H_2. Through the variation of TL, BL and X we have been able to modulate the energetics of the excited states and the driving force for excited state electron transfer. The new series of Ru,Rh bimetallic complexes are structurally analogous to the trimetallic complexes, possess similar excited state energetic but display very different photochemistry providing significant insight into the role of the two Ru light absorbing units in the desired photoreduction of water.

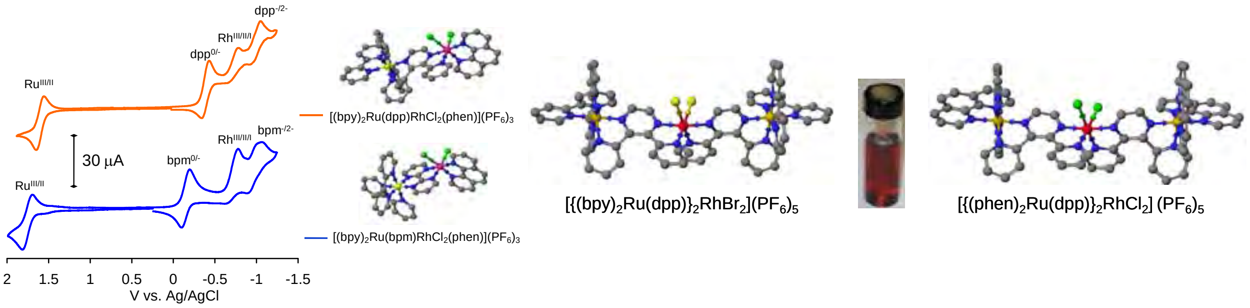

Figure 2. Structures of representative examples of mixed-metal Ru(II), Rh(III) complexes.

BASAL PLANE CHEMISTRY OF GRAPHENE

Louis Brus
Chemistry Department
Columbia University
New York, NY, 10027

Single layer graphene is a transparent semimetal; it promises to become a useful inexpensive replacement for ITO windows in solar devices. It has the added advantage that the Fermi level can be significantly shifted by chemical doping, due to a low density of states in comparison with normal 3 dimensional metals. Thus the work function can be adjusted to facilitate charge injection into organic and nanocrystal conductive layers. Raman scattering is a valuable non-contact optical probe for graphene doping level and Crystallinity. In addition to chemical doping by adsorbed species, we explore basal plane reactions that break the pi conjugation, converting sp2 Carbon to sp3 Carbon. Such chemically reacted regions become insulating. If reactions are initiated by electron beam or light irradiation, then one can lithographically pattern the conductivity in a large sheet. We describe reversible H atom bonding to graphene; H atoms are created by electron beam cross linking of an HSQ layer on the graphene. We also describe photochemical bonding of organic radicals, initiated by visible light irradiation of graphene with adsorbed benzoyl peroxide in toluene.

HOT VIBRATIONAL STATE STRUCTURES OF PHOTOEXCITED STATE METAL COMPLEXES REVEALED BY LASER-INITIATED TIME-RESOLVED X-RAY ABSORPTION SPECTROSCOPY

Lin X. Chen,[1,2] Jenny V. Lockard,[1] Andrew B. Stickrath,[1] Xiaoyi Zhang,[3] Klaus Attenkofer,[3] Guy Jennings,[3] in collaboration with the Castellano Group[4]

[1]Chemical Sciences and Engineering Division, [2]X-ray Science Division, Argonne National Laboratory, Argonne, Illinois 60439; [3]Department of Chemistry, Northwestern University, Evanston, Illinois 60208; [4]Department of Chemistry, Bowling Green State University, Bowling Green, Ohio 43403

The excited state structural dynamics of a Pt-Pt dimer [Pt(ppy)(m-R_2pz)]$_2$, which is an excellent candidate for photocatalysis and organic light emitting diode (OLED) is investigated by the laser-initiated time-resolved X-ray absorption spectroscopy (LITR-XAS). Using an improved beamline configuration at the Advanced Photon Source (APS), the X-ray absorption spectra of the metal-to-metal-to-ligand-charge-transfer (MMLCT) state as a function of the delay time after the photoexcitation (527 nm) are collected. The observed difference spectra (Laser-on – laser-off) show a series of oscillations whose relaxation time corresponds well with the excited state lifetime of the compound (Figure 1). However, we have found that the spectral differences cannot be modeled well by the static structure of the excited state. Instead, the spectra revealed the hot vibrational state structures of the ground electronic state generated by internal conversion, which cause the oscillatory spectral differences. A model of the excited state dynamics is established which includes the initial excited state manifold population redistribution within 300 fs, the internal conversion to the hot vibrational states in the ground electronic state, and radiative decay of the excited state in 700 – 900 ns. The results established the experimental requirements for the signal to noise ratio for resolving the excited state structures in the presence of hot vibrational states of the ground electronic state. The results can be applied in other studies of excited state metal complexes that undergo energy and electron transfer reactions in solar energy conversion.

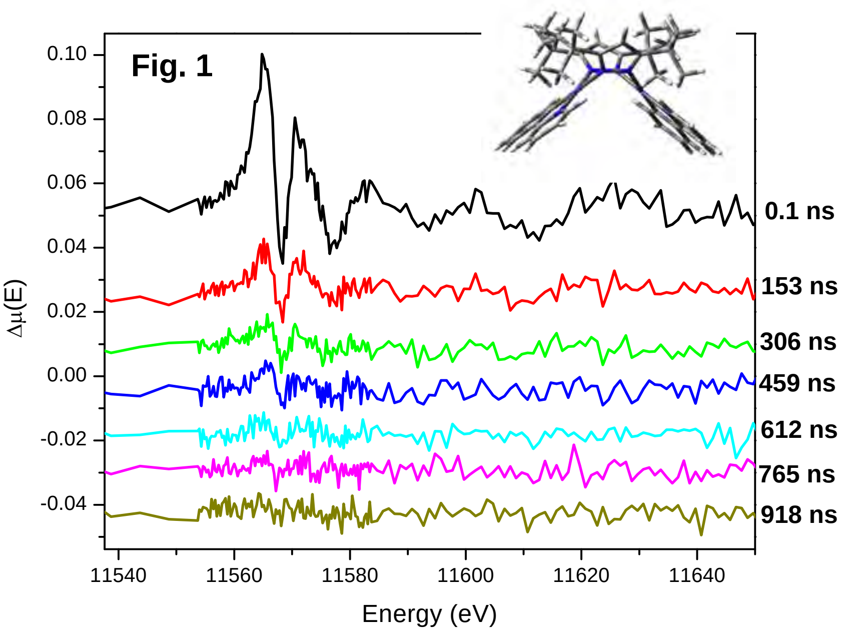

ELECTROCHEMICAL ROUTES TO CONSTRUCT α–Fe_2O_3 PHOTOELECTRODES

Ryan L. Spray, Kenneth J. McDonald and Kyoung-Shin Choi
Department of Chemistry
Purdue University
West Lafayette, IN 47907

Ferric oxide (α-Fe_2O_3, hematite) is an n-type semiconductor highly desirable for use in solar energy conversion because its bandgap (E_g = ~2.2 eV) allows for utilizing a significant portion of the solar energy spectrum. The low cost and environmentally benign nature of iron makes developing α-Fe_2O_3-based photoelectrochemical cells even more attractive. α-Fe_2O_3 is also one of the few materials that is resistant to photocorrosion and has a good chemical stability in neutral and basic aqueous media, making it a viable candidate to photoelectrolyze water to generate oxygen and hydrogen. Its conduction band, however, is located slightly below the level needed for hydrogen production while its valence band is well suited for oxygen production. Therefore, forming tandem cells, photoelectrochemical diodes, or bi-photoelectrodes with other materials of suitable band positions is necessary to use α-Fe_2O_3 for photoelectrolysis of water without using an external bias. In this context, producing α-Fe_2O_3 as a thin-film type electrode is highly desirable as this form allows for facile construction of photoelectrochemical cells with multi-component and multi-junction photoelectrode architectures.

In this presentation, we present various electrochemical synthesis routes (cathodic vs. anodic, acidic vs. basic, aqueous vs. nonaqueous) to prepare α-Fe_2O_3 photoelectrodes. The effect of deposition conditions on the electrode morphologies and photoelectrochemical properties will be discussed in detail (Figure 1). Establishing various deposition conditions for α-Fe_2O_3 films will enable us to deposit α-Fe_2O_3 on a broad range of semiconducting layers that are stable only for a limited range of deposition potentials and pH when preparing multi-junction electrodes.

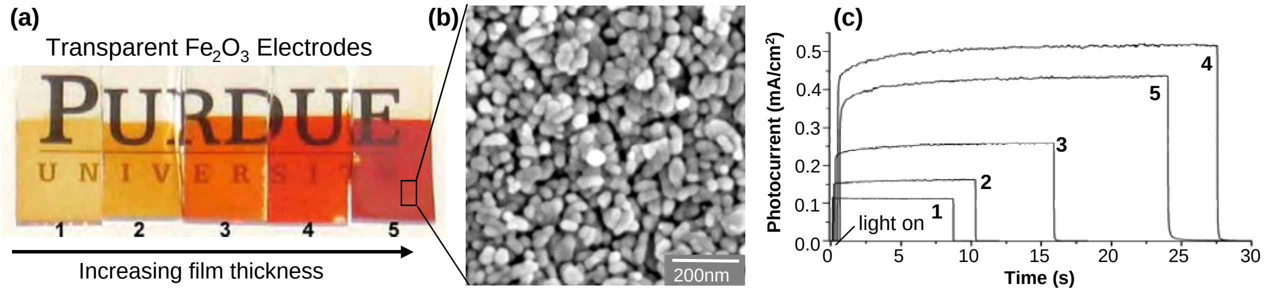

Figure 1. (a) Photograph, (b) SEM and (c) short-circuit photocurrents of anodically prepared α-Fe_2O_3 films in an acidic aqueous medium with varying deposition times; **1** (1 min), **2** (2 min), **3** (4 min), **4** (8 min), and **5** (16 min).

THE CRYSTALLINE-NANOCLUSTER Ti-O PHASE: STUDYING NANOPARTICLES WITH ADSORBED MOLECULES IN PERIODIC ARRAYS

Philip Coppens and Jason Benedict
Department of Chemistry
University at Buffalo, State University of New York
Buffalo, NY 14260-3000

Although TiO_2 surfaces have been studied extensively given their importance in photovoltaic cells, atomic resolution information is generally lacking. The accuracy of diffraction measurements of surface structure and molecules adsorbed on surfaces is limited and inadequate when instantaneous changes in geometry on molecular excitation are to be measured. Crystalline solids composed of nano-clusters have been studied because of their catalytic properties but seem to have been overlooked as models for photovoltaic cell surfaces. Experimental structures of clusters with 3, 5, 11, 12, 17 and 18 Ti atoms have been described in the literature. To explore the synthetic methods and examine the relation between cluster structure and known phases of TiO_2, we have prepared a number of small clusters with adsorbed biphenol and isonicotinic acid. Two of the results are shown in Figure 1. Synthesis of larger clusters is in progress. Unlike the rutile structure in which the 6-fold coordination of the Ti atoms is highly regular, the octahedral coordination of Ti in anatase is strongly distorted.

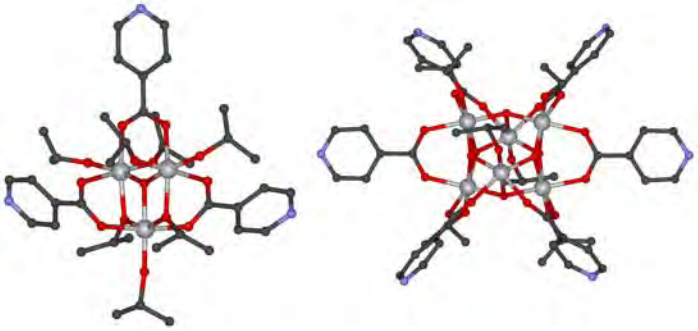

Figure 1: Newly synthesized n=3 (left) and n=6 (right) titanium oxide nanoclusters containing the bridging isonicotinate adsorbate. Hydrogen's omitted for clarity.

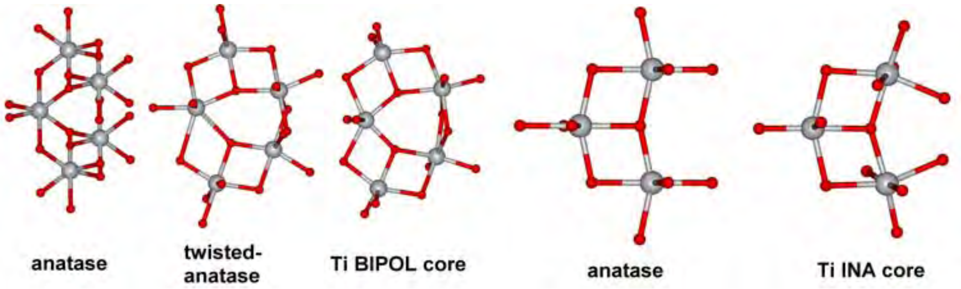

Figure 2: Cores of two newly synthesized Ti-O nanoclusters strongly resemble fragments of bulk anatase and exhibit the under-coordination found on anatase surfaces. INA=isonicotinic acid, BIPOL.=2,2′-biphenol. The two diagrams of anatase are different views.

While the cluster cores bear a striking resemblance to the anatase fragments (Figure 2), lower Ti coordination found in surface structures is present. The structures indicate that ligands with relevance to photovoltaics can be readily anchored to clusters of a variety of sizes which can be obtained in single crystalline form.

DESIGN AND SYNTHESIS OF ROBUST ANCHORS FOR SOLAR FUEL PRODUCTION

Bill McNamara, Laura Allen, Victor Batista, Gary Brudvig, Charles Schmuttenmaer, Robert Crabtree
Chemistry Department
Yale University
New Haven CT, 06520-8107

Current anchors based on carboxylates are labile in aqueous solution or even with simple humidity. Since our goal is a water splitting solar cell, we need a robust anchor. Not only does the anchor have to be water-stable but it must also permit charge injection. We have, therefore, examined a series of alternate binding groups. Last year, we reported data for acetylacetonate groups.[1] This year, we report hydroxamate anchors that are stable in water and show good injection characteristics – indeed our data suggest that hydroxamate shows better injection than the standard carboxylate.

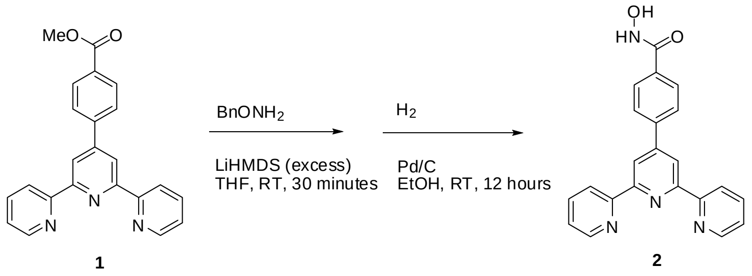

Figure 1. Synthesis of hydroxamate-terpyridine anchor.

Because nature employs hydroxamates in siderophores, we have looked at this group. One factor that may well endow it with enhanced binding properties for metal ions is the ability of hydroxamate to act as a doubly deprotonated ligand. Figure 1 shows the synthesis of the terpyridine version of this anchor.[2] Deposition onto TiO_2 NPs occurs easily. The attachment is robust to water and binding in the doubly deprotonated mode is suggested by IR data and computational modeling.

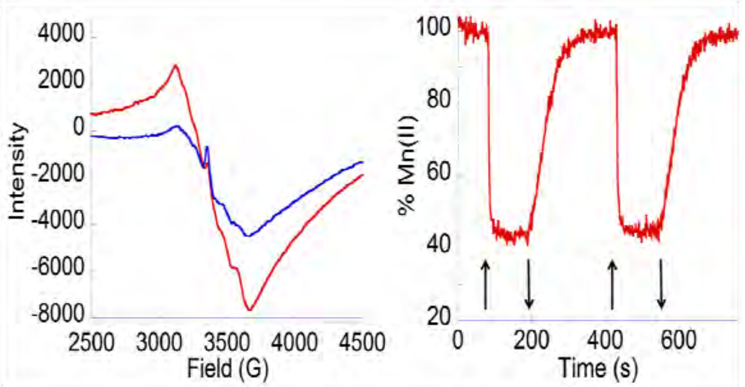

Figure 2. EPR measurement of Mn(II) photooxidation.

Functionalization of the terpyridine with $Mn(OAc)_2$ was also easily achieved and the resulting construct gave charge injection with visible light as monitored by the change in the EPR spectrum of the Mn(II) center when oxidized to Mn(III) (Figure 2). THz experiments show that the injection is more effective for the hydroxamate than the carboxylate with 400 nm excitation (see Schmuttenmaer poster).

1. McNamara W, Snoeberger R, Li G, Schleicher J, Cady C, Poyatos M, Schmuttenmaer CA, Crabtree RH, Brudvig GW, Batista VS, Acetylacetonate Anchors for Robust Functionalization of TiO_2 Nanoparticles with Mn(II)-Terpyridine Complexes J. Am. Chem Soc, 2008, 130, 14329–14338.
2. McNamara W, Snoeberger R, Li G, Richter C, Allen LC, Milot RL, Schmuttenmaer CA, Crabtree RH, Brudvig GW, Batista VS, Hydroxamate Anchors for Functionalization of Semiconductor Surfaces, J. Am. Chem Soc, 2009, submitted.

COUPLED ELECTRON AND PROTON TRANSFER? A PULSE RADIOLYSIS STUDY

Diane Cabelli, Brian W. Cohen, and Carol Creutz
Chemistry Department
Brookhaven National Laboratory
Upton, NY 11973

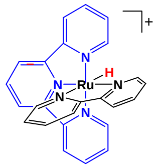

Ru(tpy)(bpy)H$^+$

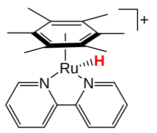

Ru(η^6-$(CH_3)_6C_6$)(bpy)H$^+$

We are seeking the production of metal hydride complexes reactive in water and CO_2 reduction by a sequence one-electron and proton-transfer steps. The Ru(II) hydride complexes Ru(tpy)(bpy)H$^+$ and Ru(η^6-$(CH_3)_6C_6$)(bpy)H$^+$ reduce CO_2 to formate in water.[1-3] Pulse and continuous radiolysis experiments on aqueous solutions provide a particularly useful approach to studying how these hydride complexes may be generated. Previous BNL pulse-radiolysis studies established (among others) the generation and protonation of Co(III) hydrides starting from aqua Co(II) complexes[4] and the generation of an organic hydride donor with a Ru(II) complex containing an NAD$^+$ model ligand.[5]

Reduction of Ru(tpy)(bpy)(OH)$^+$ at pH 12 yields a ligand-centered radical (stage A, Fig. 1) which is consumed by a process second-order in the species. "X", the product of stage B (red dots in Fig. 2) is slowly transformed to Ru(tpy)(bpy)(H)$^+$ (black dots in Fig.2).

$$\mathrm{Ru^{II}\,(tpy)(bpy)(OH)^+ + e\text{-}aq \longrightarrow Ru^{II}(tpy\bullet^-)(bpy)(OH)} \qquad \text{(A)}$$

$$\mathrm{2\,Ru^{II}(tpy\bullet^-)(bpy)(OH) \longrightarrow X} \qquad \text{(B)}$$

$$\mathrm{X \longrightarrow \longrightarrow Ru^{II}\,(tpy)(bpy)(H)^+} \qquad \text{(C)}$$

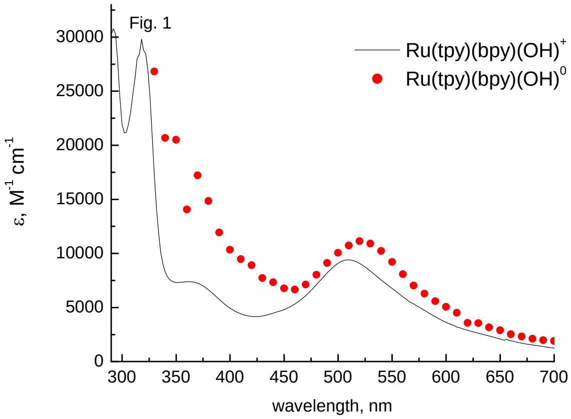

Fig. 1

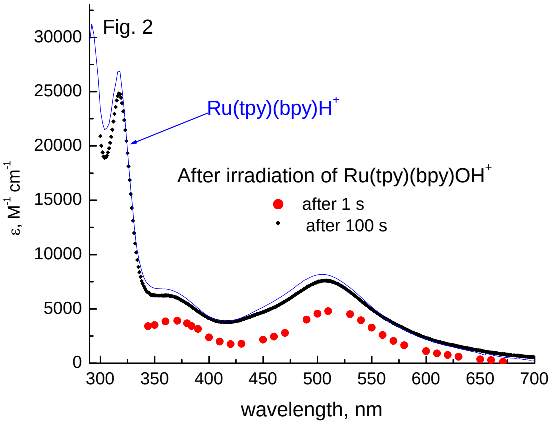

Fig. 2

References: (1)Hayashi, H.; Ogo, S.; Fukuzumi, S. Aqueous hydrogenation of carbon dioxide catalysed by water-soluble ruthenium aqua complexes under acidic conditions, *Chem. Comm.* **2004**, 2714-2715. (2)Creutz, C.; Chou, M. H. Rapid Transfer of Hydride Ion from a Ruthenium Complex to C_1 Species in Water, *J. Am Chem. Soc.* **2007**, *129*, 10108 - 10109. (3)Creutz, C.; Chou, M. H. Hydricities of d^6 Metal Hydride Complexes in Water*J. Am. Chem. Soc.* **2009**, *131*, 2794-2795. (4)Creutz, C.; Schwarz, H. A.; Wishart, J. F.; Fujita, E.; Sutin, N. Thermodynamics and Kinetics of Carbon dioxide binding to two stereoisomers of a cobalt(I) macrocycle in aqueous solutions, *J. Am. Chem. Soc.* **1991**, *113*, 3361-3371. (5) Polyansky, D.; Cabelli, D.; Muckerman, J. T.; Fujita, E.; Koizumi, T.; Fukushima, T.; Wada, T.; Tanaka, K. Photochemical and radiolytic production of an organic hydride donor with a RuII complex containing an NAD$^+$ model ligand, *Angew. Chem.-Intl. Ed.* **2007**, *46*, 4169-4172.

NEW OPEN-LOOP CONTROL METHODOLOGIES TO IDENTIFY PHASE SENSITIVITY IN THE PREPARATION OF EXCITED STATE POPULATIONS:

EXPERIMENTS AND SIMULATIONS TO EXPLORE COHERENT CONTROLLABILITY OF MEG IN LEAD-SELENIDE QUANTUM DOTS

Niels H. Damrauer, Erik M. Grumstrup, Matthew A. Montgomery
Department of Chemistry and Biochemistry
University of Colorado at Boulder
Boulder, CO 80309

The control of electronically and reactively complex systems is a reality using closed-loop adaptive learning procedures in vast parameters spaces made possible by broad-band ultrashort laser pulses. Experimental successes in the control community suggest that adaptive methods are likely to play a significant role ushering in a “control age” in science. In 2008 (Wintergreen, VA) we presented preliminary evidence that multiple exciton generation yield in PbSe quantum dot systems is controllable using closed-loop heuristic learning. However, such experiments face challenges. In the control spaces of most interesting problems the success of adaptive learning is highly dependent on signal-to-noise levels of photoproduct observables. This situation, coupled with the fact that low laser fluences must be employed to minimize the risk of trivial multiple exciton signals due to sequential multiple-photon absorption, means that successful adaptive experiments are hard to achieve correctly, difficult to repeat, and challenging to interpret.

In this presentation we discuss efforts to develop new open-loop control methodologies capable of identifying, with high fidelity, instances of phase sensitivity of photoproduct yields; i.e., quantum control. These methods which we call phase switching stem from recent efforts in our laboratory to develop 2D-electronic spectroscopy using Fourier-domain pulse shaping tools. At its root, phase switching systematically explores two-color interferences and is capable of revealing spectroscopic underpinnings of control problems involving multiphoton interactions. Its utility goes further; theoretical and experimental work are underway that exhibit how phase switching exposes cases where electronic and/or vibronic interference phenomena in the Franck-Condon region alter product yields elsewhere in the excited-state manifold.

Fig. 1 shows initial experimental results for phase switching experiments on ~ 8 nm PbSe quantum dots in solution using a pump field (λ_{pump}=522 nm) that is more than 3 times the band gap energy. The modulation of population suggests coherent quantum mechanical interference effects on MEG yield during excitation since fluence is kept constant. However, challenges we have faced simulating the interaction of these fields with the material system has lead us to consider a simpler phase-switching methodology. This poster discusses these experimental and simulation efforts and motivates the need for shorter laser pulses capable of modulating interference pathways in competition with dephasing.

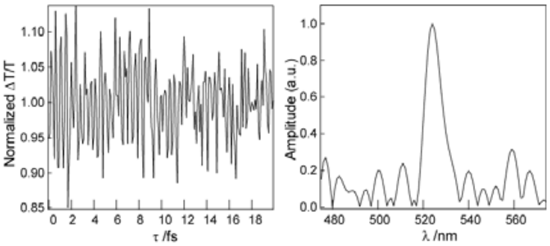

Fig 1: (left) Normalized transient absorption signal (λ_{pump}=522 nm, λ_{probe}=1712 nm; Δt = 27 ps) during phase switching. (right) Fourier transform of signal.

ULTRAFAST SPECTROSCOPIC STUDIES OF CHARGE INJECTION INTO ZEOLITES

Prabir Dutta, Bern Kohler
Departments of Chemistry
The Ohio State University
Columbus, Ohio 43210

Using ultrafast transient absorption spectroscopy we have studied the photophysics of the photosensitizer $[(bpy)_2RuL_{DQ}]^{4+}$ (where bpy = bipyridine, LDQ = 1-[4-(4'-methyl)-2,2'-bipyridyl)]-2-[4-(4'-N,N'-tetramethylene-2,2'-bipyridinium]). Excitation with a femtosecond laser pulse of either a ligand-based or an MLCT transition produces a charge-separated state, which corresponds to transfer of an electron from the metal center to the diquat end of the functionalized ligand. This intramolecular charge transfer takes place via a state that is initially delocalized across the entire LDQ ligand (Fig 1, red curve) within 1 ps leading to a vibrationally excited reduced ligand state (Fig 1 blue curve). The same final charge separated state is reached regardless of excitation wavelength, but vibrational cooling is dependent on excitation wavelength. The charge-separated state decays via back electron transfer with a time constant of 1.45 ns (Fig 1, black curve).

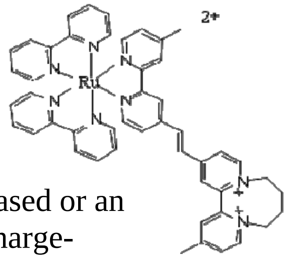

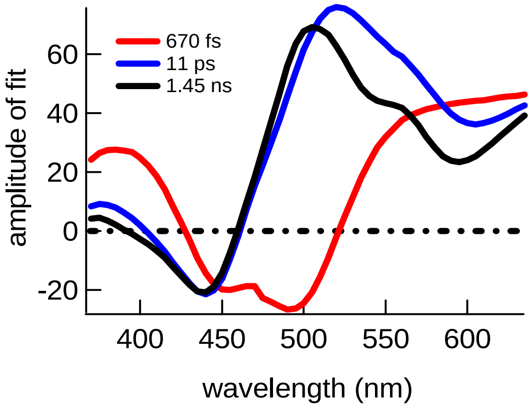

Figure 1. Species Associated Difference Spectra for $[(bpy)_2RuL_{DQ}]^{4+}$

Photoinduced electron transfer from $[(bpy)_2RuL_{DQ}]^{4+}$ and $[(bpy)_2RuL]^{2+}$ (L = 1, 2-bis[4- (4'-methyl)-2,2'-bipyridyl] ethene) attached to the surface of zeolite Y particles was investigated to methyl viologen inside the zeolite supercages. The zeolite-bound $[(bpy)_2RuL_{DQ}]^{4+}$ species was found to be emissive at 695 nm with a lifetime of 796 ns. About 40% of the one-electron-reduced methyl viologen generated via photoinduced electron transfer from surface-bound $[(bpy)_2RuL_{LQ}]^{4+}$ survived for the duration of the experiment (milliseconds). Femtosecond transient absorption experiments have shown that there is still a fast component to the 450 nm dynamics, which is reminiscent of the spectral dynamics measured for L_{DQ} in homogeneous solution (Figure 2). This suggests that charge injection to the LDQ ligand proceeds on an ultrafast time scale even when bound to the zeolite.

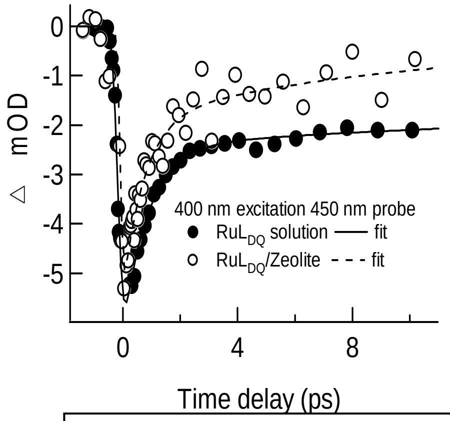

Figure 2. Kinetic traces of RuLDQ in solution and anchored to zeolite

LIGHT DRIVEN GENERATION OF HYDROGEN FROM WATER: NEW DEVELOPMENTS, NEW STRATEGIES AND NEW RESULTS

Pingwu Du, Theodore Lazarides, Theresa McCormick, Genggeng Luo, Jacob Schneider, Paul Jarosz, William Brennessel, and Richard Eisenberg
Department of Chemistry
University of Rochester
Rochester, New York 14627

The conversion of light to stored chemical energy in a molecularly-based system for artificial photosynthesis relies on light absorption, photoinduced charge separation (PICS), the accumulation of redox equivalents, and catalysis. Recent efforts are described that focus on the reductive side of water splitting and the visible light-driven generation of hydrogen from aqueous protons and a sacrificial electron source. Systems able to carry out this reaction contain a chromophore, an electron relay and a catalyst. To date the chromophores examined in these efforts have been mainly Pt(II) bi- and terpyridyl acetylide complexes with a triplet charge transfer (CT) excited state. To shift the chromophore absorption to lower energies, different complexes have been studied. While Pt(II) diimine dithiolate complexes sensitize H_2 formation with light of $\lambda > 500$ nm and are photostable, they are not strongly absorbing. To increase sensitizer absorptivity, organic dyes have been examined, either as sensitizers of Pt bpy or tpy charge transfer excited states, or as chromophores themselves. While halogenated derivatives of BODIPY and fluorescein dyes do serve to promote the photogeneration of H_2, they exhibit substantial photo-instability. Ongoing strategies to address this specific issue involve derivatizing these dyes so that other heavy atoms can be incorporated into them to promote intersystem crossing for electron transfer chemistry while removing the photo-sensitive carbon-halogen bonds from the active dyes.

While colloidal Pt has been most frequently and successfully employed as the catalyst, recent efforts have focused on the development of molecular catalysts. While purported Pt(II) molecular catalysts only serve as precursors to colloids, we find that cobaloxime complexes actually do function as catalysts for the photogeneration of H_2. The activity of systems having these Co catalysts compare well to those containing colloidal Pt, and mechanistic studies support the notion of catalyst reduction to Co(I), protonation to Co(III)-H, a second reduction and a second protonation to liberate H_2. The cobaloxime catalysts (**1-3**) that promote hydrogen generation with Pt sensitizers are also found to be effective with the brominated fluorescein dye Eosin Y (**EY**) as the sensitizer. More than 2000 turnovers of H_2 are obtained from this "non-platinum" system using triethanolamine as the sacrificial donor. New efforts to improve this system and build better integrated systems in which the molecular catalyst is attached to the electron relay or the chromophore directly will be described.

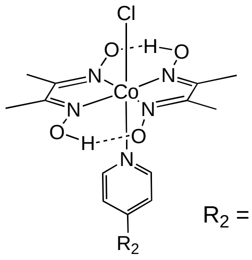

R_2 = H **1**
COOMe **2**
NMe_2 **3**

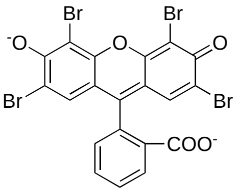

EY^{2-}

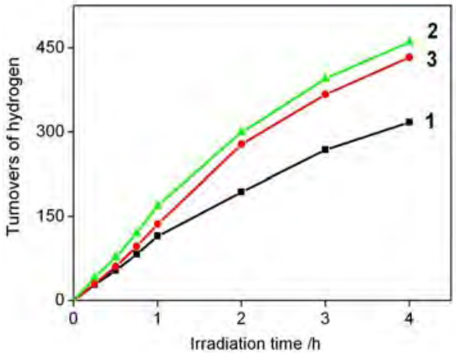

H_2 yield using Eosin Y (1.1×10^{-5} M) and different cobalt complexes (2.0×10^{-5} M), 1.6×10^{-2} M TEOA at pH=8.5.

LIGHT-MATTER INTERACTIONS
IN SEMICONDUCTOR NANOCRYSTALLINE ABSORBERS

Randy J. Ellingson
Department of Physics and Astronomy, and
Wright Center for Photovoltaics Innovation and Commercialization (PVIC)
The University of Toledo
Toledo, OH 43606

Colloidal semiconductor nanocrystals (NCs) continue to generate significant interest for solar energy conversion studies owing to their size-dependent optoelectronic properties and potential for low-cost, solution-based processing. In addition, they offer unique avenues to study elemental photoconversion processes, including interfacial charge- and energy-transfer, photochemistry (and photostability), inter-particle electronic coupling, array assembly mechanisms, and quantum confinement effects. Although several compelling fundamental effects in colloidal NCs have been reported over the past ~5 years, including demonstrations of slowed carrier cooling,[1-3] single-exciton optical gain,[4] and multiple exciton generation (MEG),[5-7] significant opportunities exist to advance our understanding of fundamental interactions in NCs. While in general these effects have been engineered and controlled at least on a basic level, MEG has largely eluded conclusive control. Experiments are planned to study new interactions in both isolated NCs and NC assemblies. As one example, optical studies are planned to investigate the influence of the NC surface capping layer on the efficiency of both cooling and MEG. In particular, interactions between interband (photo)-excited NCs and vibrationally-excited NC capping molecular ligands will be investigated for a dependence of ultrafast charge carrier processes on the effective temperature of the local nanoscale "bath". Colloidal nanocrystal and related synthetic capabilities are in development at UT; during this development stage, the proposed research will proceed as a collaboration with the NREL group (M. Beard and A. Nozik). These studies may reveal mechanisms for utilizing the significant but elusive infrared solar spectral region, in support of enhanced overall conversion efficiencies.

(1) Blackburn, J. L., Ellingson, R. J., Micic, O. I., Nozik, A. J. *J. Phys. Chem. B* **2003**, *107*, 102-109.
(2) Pandey, A.; Guyot-Sionnest, P. *Science* **2008**, *322*, 929-932.
(3) Guyot-Sionnest, P.; Wehrenberg, B.; Yu, D. *The Journal of Chemical Physics* **2005**, *123*, 074709.
(4) Klimov, V. I.; Ivanov, S. A.; Nanda, J.; Achermann, M.; Bezel, I.; McGuire, J. A.; Piryatinski, A. *Nature* **2007**, *447*, 441-446.
(5) Schaller, R.; Klimov, V. *Phys. Rev. Lett.* **2004**, *92*, 186601.
(6) Ellingson, R. J.; Beard, M. C.; Johnson, J. C.; Yu, P.; Micic, O. I.; Nozik, A. J.; Shabaev, A.; Efros, A. L. *Nano Lett.* **2005**, *5*, 865.
(7) Beard, M. C.; Knutsen, K. P.; Yu, P.; Luther, J. M.; Song, Q.; Metzger, W. K.; Ellingson, R. J.; Nozik, A. J. *Nano Lett.* **2007**, *7*, 2506-2512.

LIGHT INDUCED CHARGE SEPARATION
EMPLOYING COPPER PHENANTHROLINE COMPLEX CHROMOPHORES

C. Michael Elliott, Megan Lazorski and Lance Ashbrook
Department of Chemistry
Colorado State University
Fort Collins, CO 80523

Ruthenium(II) polypyridyl complexes have served as one of the primary types of chromophores employed in synthetic systems designed to undergo light-induced charge separation. The reasons are manifold but include a strong visible MLCT optical transition, a long-lived triplet excited state and favorable excited state redox potentials. Heteroleptic ruthenium complexes incorporating potential electron-transfer moieties (i.e., electron acceptors and donors) are straightforward to prepare, isolate and purify due their inertness to ligand substitution. Moreover, we have demonstrated that certain Donor-Chromophore-Acceptor (DCA) triads based on trisbipyridineruthenium(II) form photoinduced charge-separated states (CSS) with uniformly high quantum efficiency (Φ_{CSS}). The origin of this large Φ_{CSS} lies in the existence of a ground-state association between the phenothiazine-type donor and chromophore's π-system. As a consequence of the enhanced D/C coupling, the CSS forms with nearly unity Φ_{CSS} and its formation is essentially independent of driving force for formation. Moreover, a large fraction of the incident photon energy (>50%) can be stored in the CSS for > 1μs.

Bisphenanthrolinecopper(I) complexes possess some of the same photophysical attributes as trisbipyridineruthenium(II): an intense MLCT transition in the visible spectral region and a relatively long-lived triplet state which is capable of electron-transfer quenching (particularly oxidative quenching). There are, however, important differences between these two chromophores as well. First, these Cu(I) complexes are generally quite labile. Also, the photoexcited state and the formally oxidized Cu(II) species each undergo large structural changes relative to the ground state copper(I) complex. Nonetheless, it might prove possible, with proper molecular design, to replace trisbipyridineruthenium(II) as the chromophore in DCA triads with bisphenanthrolinecopper(I). Additionally, the same D/C association responsible for the high Φ_{CSS} in the ruthenium–based systems is anticipated to occur in Cu(I)-based systems.

We are currently conducting preliminary studies on heteroleptic bisphenanthrolinecopper(I) DCA complexes. In these complexes, one ligand contains a covalently attached viologen acceptor appended to the phenanthroline through the 5,6- positions and two relatively small methyl-substituents in the 2- and 9-positions. The second ligand contains two N-methylphenoxazine donors located at the 2- and 9-positions. The significantly different steric requirements of the two types of 2,9-substituents enables the formation the heteroleptic complex shown at the left. We are presently isolating and characterizing this Cu(I) based DCA triad. Again, we anticipate the same kind of intramolecular interactions between the donors and the phenanthroline π-system as exists in the ruthenium DCA analogs (and is responsible for the large quantum efficiency for CSS formation in the latter system).

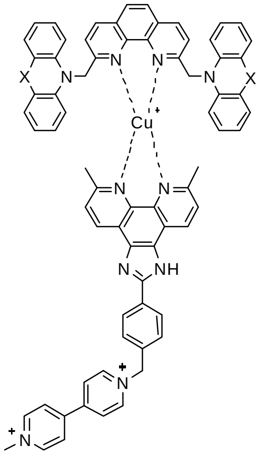

QUANTUM DYNAMICS, PHOTOSYNTHESIS AND ITS REGULATION

Graham R Fleming, Akihito Ishizaki, Yuan-Chung Cheng, Tae Ahn, Tessa
Calhoun and Gabriela Schlau-Cohen
Department of Chemistry, University of California Berkeley
Physical Biosciences Division, Lawrence Berkeley National Laboratory
Berkeley, CA 94720 USA

Progress is multi-dimensional electronic spectroscopy has enabled the clear observation of quantum electronic coherence in light harvesting complexes. By utilizing the non-rephasing pulse sequence, it has proved possible to map the energy location of the exciton states onto the excitation spectrum [1]. Modeling the quantum dynamics of such a system is very challenging as there is no large (or small) parameter in this system. We have developed a formally exact reduced hierarchy approach to accurate calculation of the quantum dynamics [2,3]. This allows us to explore (a) the temperature dependence and find that quantum coherence is significant even at 300K [4], (b) study how the combined quantum system facilitates the connection of the chlorosome with the reaction center via the FMO complex in green sulfur bacteria and (c) address questions of more subtle quantum phenomena such as entanglement.

Two dimensional spectroscopy enables the dissection of relaxation pathways in great detail, and again the use of the non-rephasing sequence has proved very valuable. The results of our analysis of energy flow in LHCII will be presented (see figures). Finally the four independent light pulses (three excitation and one-signal) allow the setting of four independent polarizations. Use of this degree of freedom enables arithmetic to be performed on spectra obtained with differing polarization sequences to highlight or suppress selected peaks in the 2D spectrum and to assign transition to specific chromophore. Application of this method to the minor light harvesting complex CP29 which is implicated in the regulation of light harvesting will be described.

REFERENCES

1. T.R. Cahoun, N.S. Ginsberg, G.S. Schlau-Cohen, Y-C Cheng, M. Ballottari, R. Bassi & G.R. Fleming. Quantum Coherence Enabled Determination of the Energy Landscape in LHCII. (Submitted)
2. A. Ishizaki and G.R. Fleming, On the Adequacy of the Redfield Equation and Related Approaches to the study of Quantum Dynamics in Electronic Transfer. (J.Chem.Phys. In Press)
3. A. Ishizaki and G.R. Fleming, Unified Treatment of Quantum Coherent and Incoherent Hopping Dynamics in Electronic Energy Transfer. (J. Chem.Phys. In Press)
4. A. Ishizaki and G.R. Fleming. (In preparation)

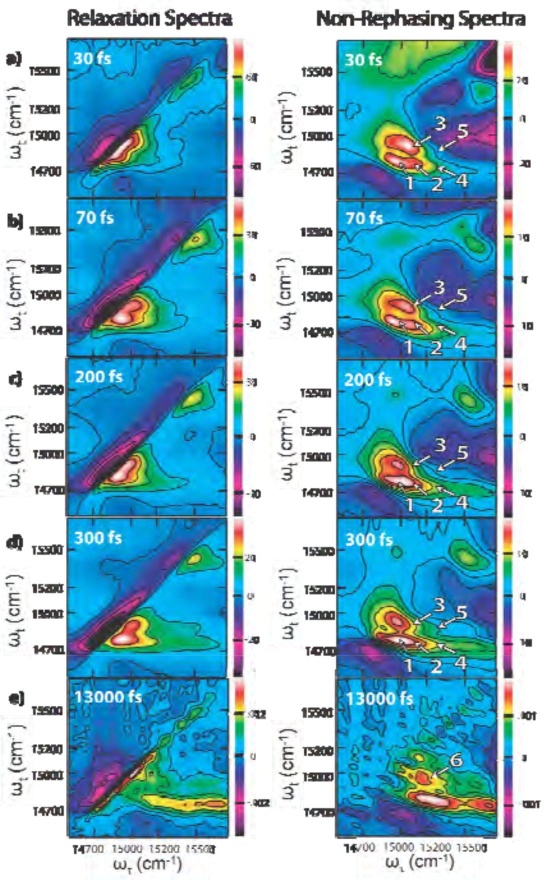

Figure 1. Experimental real 2D relaxation (left) and non-rephasing (right) spectra of LHCII at 77K. Arrows point to cross-peaks on the non-rephasing spectra to highlight energy transfer dynamics.

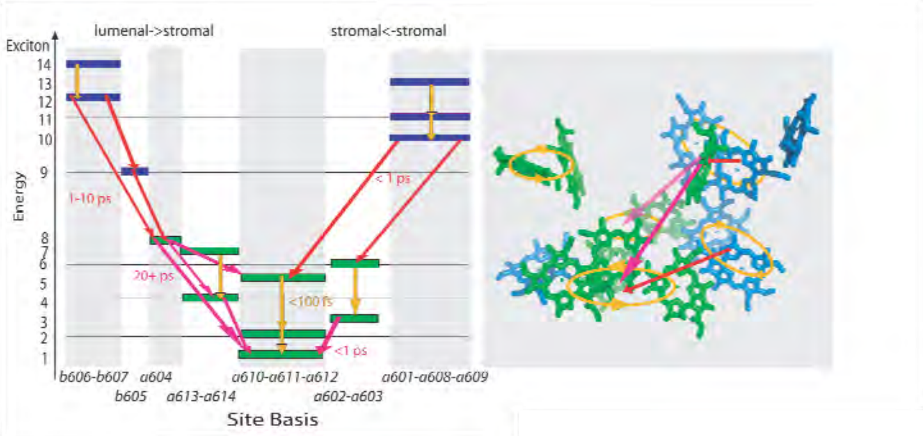
lumenal->stromal
stromal<-stromal
Exciton
14
13
12
11
10
9
8
7
6
5
4
3
2
1
Energy
1-10 ps
20+ ps
<100 fs
<1 ps
<1 ps
b606-b607
b605
a604
a613-a614
a610-a611-a612
a602-a603
a601-a608-a609
Site Basis

Figure 2. The pathways of energy flow in LHCII and their spatial locations as mapped onto the crystal structure. The timescales indicate the approximate time at which the cross-peak signal corresponding to that pathway reaches its maximum.

ORDERED SENSITIZED HETEROJUNCTIONS:
BOTTOM-UP ELECTROCHEMICAL SYNTHESIS OF COPPER INDIUM DISULFIDE IN ORIENTED N-TITANIA NANOTUBE ARRAYS

Qing Wang, Kai Zhu, Nathan R. Neale, and Arthur J. Frank
Chemical and Biosciences Center
National Renewable Energy Laboratory
Golden, CO 80401

Traditional dye-sensitized TiO_2 solar cells are relatively easy to fabricate because most of the commonly used liquid electrolytes fill the entire pore network of the nanoporous films and form intimate electronic contact with the TiO_2 surface. Replacing the liquid electrolyte with an inorganic p-type semiconductor material is much more challenging synthetically. It is difficult to attain complete pore filling between two charge-conducting networks. Electrochemical deposition is a facile technique for depositing semiconducting and conducting materials in nanoscaled pores of *electrically insulating* films. However, for an electrically conducting host n-type semiconductor film, such as TiO_2, the p-type semiconductor is deposited preferentially at the outermost surface as a pore blocking overlayer, which precludes complete pore filling.

We describe (Nano Lett. **2009**, *9*, 806) a synthetic scheme for electrochemically controlling the spatial growth profile of p-type semiconductors in the nanopores of *electrically conducting* n-type metal oxide materials. As an example of this approach, we discuss the results of our study of the electrochemical deposition of p-$CuInSe_2$ in nanoporous n-TiO_2 NT arrays and nanoparticle films. We demonstrate that the average distance electrons travel before they react with precursor ions at the semiconductor/electrolyte interface can be tuned, via the ambipolar diffusion effect,[33] by varying the composition of the deposition solution. Changing the solution composition is found to alter the ion/electron diffusion coefficients and the interfacial electron transfer kinetics, which determine the ambipolar diffusion length. By controlling the ambipolar diffusion length, the p-type semiconductor can be deposited preferentially either as a pore-blocking overlayer (Figure 1a) or from the bottom-up (Figure 1b), filling the entire pore network.

(a) Overlayer deposition

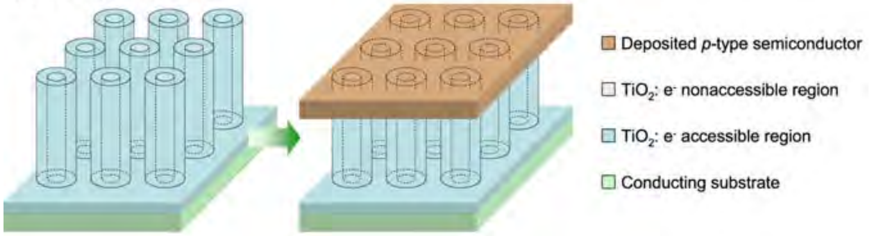
▨ Deposited *p*-type semiconductor
☐ TiO_2: e⁻ nonaccessible region
▨ TiO_2: e⁻ accessible region
▨ Conducting substrate

(b) Bottom-up deposition

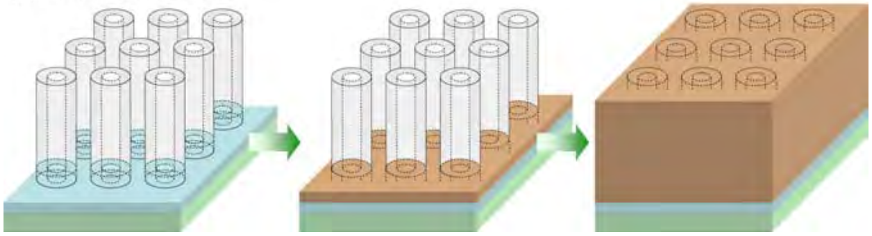

ELECTRONIC STRUCTURE CALCULATIONS ON NANOSTRUCTURES: THEORY AND APPLICATIONS

Ting Wang, Louis Brus, Mike Steigerwald, Art Bovachevarov, and Richard A. Friesner
Department of Chemistry
Columbia University
NY NY 10027

We have studied the electronic structure of oligothiophenes, materials which are of significant interest in efforts to develop organic solar cells. Density functional theory has been employed to investigate the singlet-triplet splitting, redox properties, and behavior of monocations and dications as a function of chain length and substituents. In several cases contact can be made with experiment and reasonable agreement is achieved. We find that there are significant effects of substituents on conjugation length and that these effects are manifested in the electronic structure of doubly charged species, as well as the behavior of the singlet-triplet gap as a function of chain length. A typical dicationic oligothiophene structure that we have studied is shown below in Fig. 1.

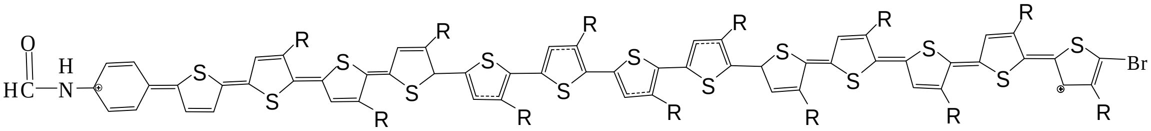

Figure 1. The possible dicationic structure of series 1,2,3. R=H, $-CH_3$, $-CH_2CH(CH_3)_2$

We have also investigated the electronic structure of TiO_2 clusters using DFT methods. In contrast to other efforts, we have carried out these studies using a solvated environment for the TiO_2; capping hydroxyl groups are appended to dangling bonds at the surface, and continuum solvation methods are used to embed the cluster in aqueous solvent. We focus attention in a number of areas, including the differences between rutile and anatase based structures, and the ionization potential and electron affinity of various clusters in the gas phase and in solution. One major objective was to search for localized trapping states, as are involved in electron transport in the Gratzel cell. We find that, in our current model, states containing an excess electron are delocalized. This suggests that counterions or defects are needed to explain localized trapping. Counterions provide an attractive explanation of both trapping and transport, and we intend to carry out electronic structure calculations including counterions in future work.

Finally, we have made significant progress in our efforts to develop an improved version of density functional theory based on localized orbital corrections. Encouraging results have been obtained for transition metals and more recently for transition states. The average error for transition metal bond energies is reduced from 5 kcal/mole to 1.5 kcal/mole, while the average error in transition state barrier heights is reduced from 3.3 kcal/mole to 1.2 kcal/mole for 105 diverse reactions. These recent results will be described and a path towards a complete theory in which the energy is corrected for arbitrary nuclear geometries will be outlined.

MODEL DYES FOR STUDY OF MOLECULE/METAL OXIDE SEMICONDUCTOR INTERFACES AND ELECTRON TRANSFER PROCESSES

Chi Hang Lee, Artem Khvorostov, Piotr Piotrowiak, Elena Galoppini
Chemistry Department
Rutgers University, Newark, NJ 07102

The study at the molecular level of electron transfer processes between a dye and a metal oxide semiconductor surface is an essential part for understanding and designing solar energy conversion systems. The poster will describe our most recent results in one of the research areas investigated in the past year: Anchoring group dependence in Mid-IR measurements of the injected electrons in the conduction band of TiO_2 semiconductor nanoparticles sensitized by Ru(II)-based chromophores.

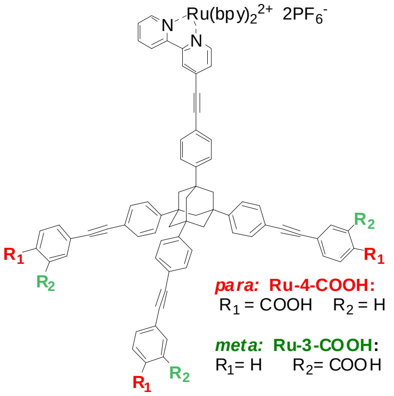

Two model dyes were synthesized for the experiments by an improved procedure: *meta* (Ru-3-COOH) and *para* (Ru-3-COOH) designed to compare the effect of a) different anchoring groups on surface binding modes and b) footprints size on injection and recombination dynamics. Binding was done on TiO_2 nanoparticle films, but sensitization of other semiconductor morphologies will be studied in the future.

The interpretation of ultrafast electron transfer experiments of model Ru(II)-bpy complexes/TiO_2 is complicated by the overlapping absorption bands of the excited state and the oxidized form of the sensitizer. With a tunable mid-IR OPA, with sub-100 fs pulses in range 2600-4200 nm, we are studying the absorption of the conduction band electron in a region that is far from the triplet state of the Ru-dyes (700-1500 nm) and from surface trap states (700-1200 nm), in addition to injection and recombination kinetics (For recombination See Fig at left).

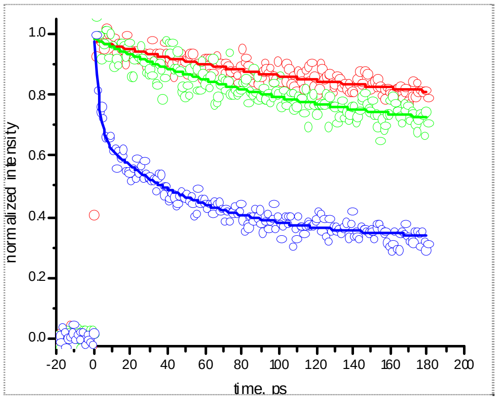

Reference compound Ru(bpy)$_2$(dcbpy)
530 nm pump, 1000 nm probe

We will also discuss data obtained with Ru-3-COOH and Ru-4-COOH on planar single crystal TiO_2 surfaces (in collaboration with B. Parkinson) to address the influence of the anchoring group in matching binding sites on different crystal surfaces.

1. Thyagarajan, S., Galoppini, E.; Persson, P.; Giaimuccio, J.; Meyer, G.J. Langmuir, Articles **2009** ASAP
2. Kopecky, A.; Galoppini, E. *SPR: Photochemistry* **2009**, *37*, 1-31
3. Tacconi, N.; Chanmanee, W.; Rajeshwar, K., Rochford, R.; Galoppini, E. *J. Phys. Chem. C* **2009**, *113*, 2996.
4. M. Abrahamsson, G.J. Meyer, O.Taratula, E. Galoppini, P. Persson, *J. Photochem. Photobiol.* **2009** submitted
5. Y. Zhang, ; E. Galoppini, invited review, *CheSusChem* **2009**, submitted
6. S. Pal, V. Sundström, E. Galoppini, P. Persson, special issue *Dalton Transactions* **2009**, submitted
7. Rochford, J. ; Galoppini, E. *Langmuir* **2008**, *24*, 5366

THE PHOTOCATALYTIC REDUCTION OF CO_2 IN SUPERCRITICAL CO_2 AND IONIC LIQUIDS

David C. Grills, Mark D. Doherty, Etsuko Fujita
Chemistry Department
Brookhaven National Laboratory
Upton, NY 11973

Our research focuses on gaining a fundamental understanding of the processes involved in the chemical conversion of solar energy, with a goal of developing systems that are capable of efficiently storing solar energy in the form of useful fuels and chemicals. To this end, we have been developing new CO_2-soluble homogeneous catalysts based on the general formula, $[Re(L)(4,4'-(C_nF_{2n+1}CH_2CH_2CH_2)_2-2,2'\text{-bipyridine})(CO)_3]^{m+}$ (n = 6 (dnb-F_{26}) or 8 (dub-F_{34}); L = Cl^- (m=0) or $P(OR)_3$ (m=1); R = alkyl or fluorinated alkyl) for the photocatalytic reduction of CO_2 to CO in supercritical CO_2 ($scCO_2$).[1] These compounds have been designed to exhibit a high solubility in $scCO_2$. Thus, they allow us to investigate the photoinduced reduction of CO_2 in (i) the absence of conventional solvents, which have previously been shown to bind to metal radical centers, inhibiting their reactivity,[2] and (ii) the presence of very high concentrations of CO_2 (up to 22 M), which will increase the rates of dark reaction steps.

In this poster, the results of photophysical and photochemical investigations on some of these catalysts, in both $scCO_2$ and conventional solvents are presented, including the characterization of the excited states and the one-electron reduced species using nanosecond transient spectroscopy. The photocatalytic activities of the catalysts in $scCO_2$ are also compared to their activities in conventional solvents, leading to a set of criteria for optimum catalytic performance in $scCO_2$. The possible advantages of performing these reactions in high-pressure biphasic ionic liquid-$scCO_2$ solvent systems are also discussed, together with the results of our preliminary experiments in such systems.

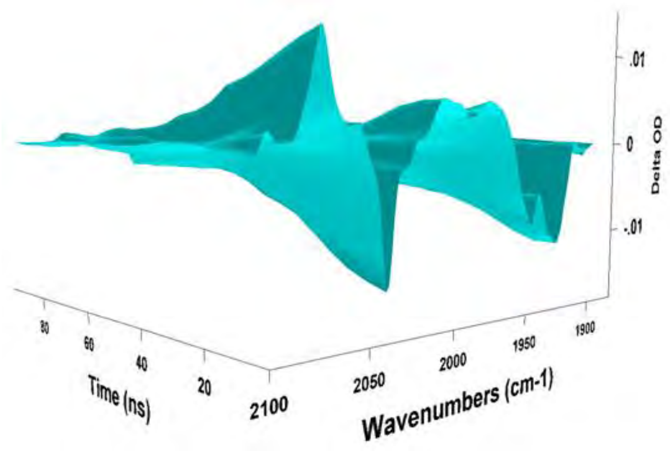

Time-resolved step-scan FTIR spectra of the MLCT excited state of $ReCl(dnb-F_{26})(CO)_3$ in $scCO_2$ (35 °C, 13.8 MPa), recorded after 410 nm excitation.

References

(1) Doherty, M. D.; Grills, D. C.; Fujita, E. *Inorg. Chem.* **2009**, *48*, 1796-1798.
(2) Fujita, E.; Muckerman, J. T. *Inorg. Chem.* **2004**, *43*, 7636-7647.

Si-DOPED A–Fe_2O_3 NANOTUBE ARRAYS FOR EFFICIENT WATER-PHOTOELECTROLYSIS

Thomas J. LaTempa, Xinjian Feng, Maggie Paulose, and Craig A. Grimes

Department of Electrical Engineering and The Materials Research Institute
The Pennsylvania State University
University Park, Pennsylvania 16802
Email: cgrimes@engr.psu.edu

Abstract

Vertically oriented nanotube arrays provide a highly ordered material architecture which is nearly ideal for efficient charge generation and separation in photo-devices. We report on the fabrication and photoelectrochemical properties of silicon doped α-Fe_2O_3 (hematite) nanotube arrays up to 4.5 μm in length, prepared by potentiostatic anodization of iron foil [1]. An electrolyte containing ethylene glycol + 0.3 wt. % NH_4F is used with the addition of 2 - 4% water; anodization is carried out at room temperature with an applied bias of 40 to 60 V. Nanotube formation occurs after ~ 180 s with an average pore diameter of 80 nm and wall thickness of 20 nm. Crystallization and Si doping of the resulting arrays is achieved through post-annealing in argon atmosphere at 450°C with a tetraethyl orthosilicate (TEOS) precursor. We have found a maximum photocurrent density of ≈ 1.27 mA/cm^2 at a potential of 0.34 V vs. Ag/AgCl, under AM 1.5 illumination in a 1 M NaOH solution, corresponding to a maximum photoconversion efficiency of 0.87 %. We discuss performance as a function of nanotube array wall thickness, length, and crystallization. Our current efforts are focused on reducing the nanotube wall thickness to that comparable to the minority carrier length, which we believe will result in a significant increase in the measured photocurrents.

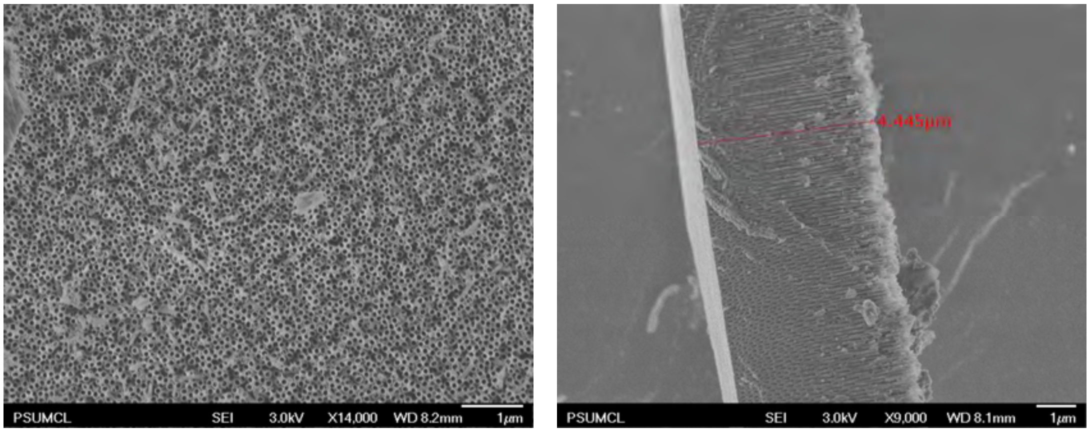
PSUMCL SEI 3.0kV X14,000 WD 8.2mm 1μm
4.445μm
PSUMCL SEI 3.0kV X9,000 WD 8.1mm 1μm

Fig. 1: Hematite nanotube arrays formed by anodization of Fe foil.

[1] K. Shankar, J. I. Basham, N. K. Allam, O. K. Varghese, G. K. Mor, X. Feng, M. Paulose, J. A. Seabold, K. S. Choi, C. A. Grimes. A Review of Recent Advances in the Use of TiO_2 Nanotube and Nanowire arrays for Oxidative Photoelectrochemistry. In press, J. Phys. Chem C (2009)

PORPHYRIN-FULLERENE ELECTROPOLYMERS FOR SOLAR ENERGY CONVERSION

Devens Gust, Thomas A. Moore, Ana L. Moore, Paul A. Liddell, Miguel Gervaldo, Gerdenis Kodis, Bradley Brennan and James Bridgewater
Center for Bioenergy and Photosynthesis, Department of Chemistry and Biochemistry
Arizona State University
Tempe, AZ 85287

Organic photovoltaics, which are based on conducting polymers that absorb visible light, are potentially very inexpensive and easy to manufacture, and they can have other advantages such as flexibility and partial transparency. However, the efficiency of organic photovoltaics is currently only ~5%. This is due in part to the fact that the conducting polymers used were in general developed for other purposes, and have not been optimized for solar energy applications.

We are using the basic chemical and physical principles underlying natural photosynthetic energy conversion to design new conducting polymers that overcome some of the problems inherent in the present generation of materials, and may ultimately be useful as components of efficient, inexpensive organic solar cells. An example is the polymer shown in Fig. 1. The polymer is readily formed as a film on a transparent electrode by electropolymerization of a porphyrin-fullerene dyad. Film thicknesses >100 nm can be easily achieved. In cyclic voltammetry, the film shows reversible waves at 0.95 and -0.63 V vs. SCE, corresponding to oxidation of the porphyrin and reduction of the fullerene moities, respectively. The absorption spectrum of the film, (Fig. 2) shows that the porphyrin Soret and Q-bands are still present, but broadened and red-shifted, compared to the monomer. Absorbance is seen throughout the visible spectral region.

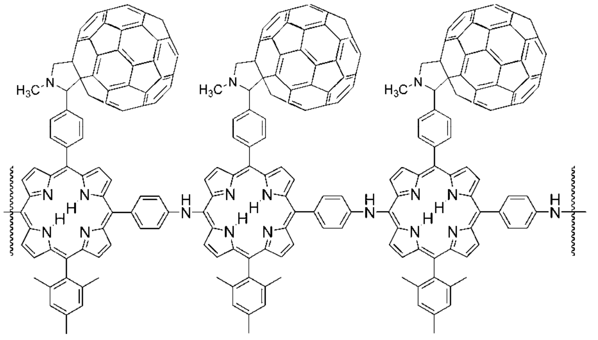

Fig. 1

The film is virtually non-fluorescent; the porphyrin excited singlet state lifetime is quenched to a few ps due to photoinduced electron transfer to the fullerene. Similar behavior is observed in a model monomeric porphyrin-fullerene dyad. Thus, the polymer acts at a "molecular heterojunction" wherein light absorption is followed by immediate charge separation, without the need for exciton migration. This is in contrast to the "bulk heterojunctions" used in conventional organic photovoltaic systems, in which excitation must migrate through a material until it encounters a phase junction where photoinduced electron transfer can occur, leading to energy conversion losses due to decay of excited states. In preliminary experiments, the new polymer has been found to produce photocurrents upon illumination.

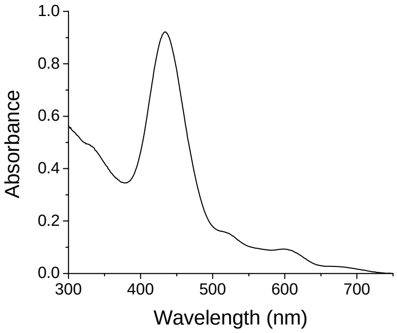

Fig. 2

TYPE-SEPARATED NANOTUBE ELECTRODES IN THZ, ELECTROCHEMICAL, AND PHOTOELECTROCHEMICAL INVESTIGATIONS

Jeffrey L. Blackburn,[#] Drazenka Svedruzic,[#] Matthew C. Beard,[#] Chaiwat Engtrakul,[#] Robert C. Tenent,[#] Paul W. King,[#] and Michael J. Heben[*]
[#]National Renewable Energy Laboratory
Golden, CO 80401
[*]The University of Toledo
Toledo, OH 43606

Single-walled carbon nanotubes (SWNTs) are one-dimensional wires that are produced as either semiconductors or metals, depending on the structure. Consequently, SWNTs have the potential to impact a variety of solar photochemical applications. Recently, methods have been developed to separate nanotubes according to electronic structure to enable the preparation of nearly pure semiconducting (s-SWNT) and metallic (m-SWNT) samples. With these samples in hand, the electrical transport, electrochemistry, and photoelectrochemistry of type-pure films could be investigated.

In addition to adapting the membrane-transfer technique[1a] for type-separated samples,[1b] we also developed a spray processing route[2] that enabled the preparation of a variety of films for study. The poster will present and discuss results on the electrochemistry of neat films as well as films containing nanotubes complexed with [Fe-Fe] hydrogenase.[3] Consistent with expectations, films having the same SWNT areal density show improved current densities when m-SWNTs are the predominant species.

In THz spectroscopy studies, we showed that free-carriers are generated with unexpectedly high yields (> 60%) in both s- and m-SWNT films at low light intensities. The exciton dissociation process occurs within <1 ps and is independent of excitation wavelength or tube type.

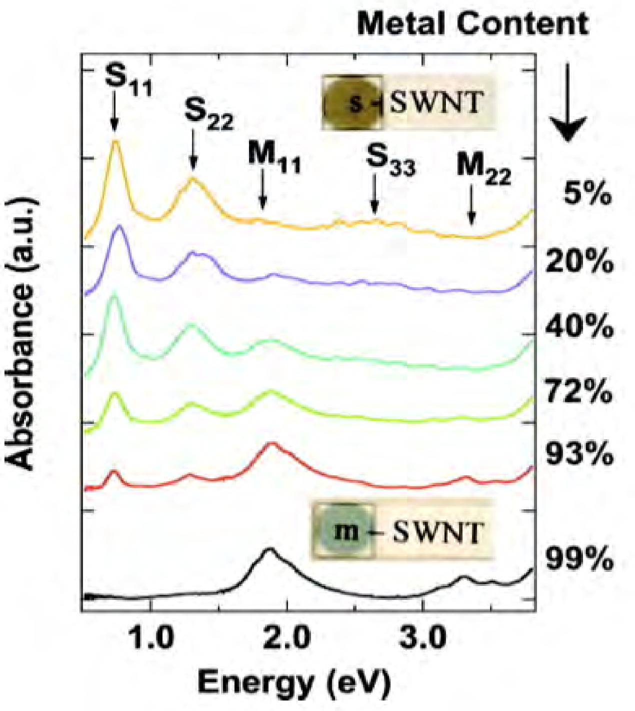

Figure: Absorption spectra of films formed from m- and s-SWNT samples.

Results from photoelectrochemistry experiments, conducted with 1-electron redox couples and both s- and m-SWNT electrodes, will also be presented.

1. Wu, et al., *Science* **2004**, *305*, 1273–1276; Arnold, et al., *Nat. Nanotechnol.* **2006**, *1*, 60–65
2. Tenent, et al., *Advanced Mat.* **2009,** in press
3. Blackburn, et al., *Dalton Trans.* **2008**, *40*, 5454-5461; McDonald, et al., *Nano Lett.* **2007**, *7*, 3528-3534
4. Beard, et al., *Nano Lett*. **2008**, *8*, 4238-4242

EXCITED-STATE ENERGY TRANSFER BETWEEN NONADJACENT SITES IN MULTIPORPHYRIN ARRAYS

Hee-eun Song,[a] Masahiko Taniguchi,[b] Markus Speckbacher,[b] Lianhe Yu,[b]
Jonathan S. Lindsey,[b] David F. Bocian,[c] and Dewey Holten[a]

[a]Department of Chemistry, Washington University, St. Louis, MO 63130-4889
[b]Department of Chemistry, North Carolina State University, Raleigh, NC 27695-8204
[c]Department of Chemistry University of California, Riverside CA 92521-0403

Understanding the rates and mechanisms of energy flow in multichromophore arrays is essential for the rational design of molecular architectures with superior light-harvesting performance, as required for implementation of a variety of solar-energy collection and conversion strategies. Our prior studies of various diarylethyne-linked multiporphyrin arrays have revealed that energy transfer is through bond (as opposed to through space) in nature and that energy flow between nearest neighbor porphyrins is the dominant pathway (as expected). However, energy transfer between second-neighbor (nonadjacent) porphyrins, which is also through bond in nature and utilizes the intervening porphyrin as a superexchange mediator, is significant and makes an important contribution to the overall energy-transfer dynamics and efficiency. Such results were obtained on arrays comprised of up to 21 diphenylethyne-linked porphyrins and are illustrated below for triad **ZnZnFbU**. It is desirable to extend these studies and elucidate the relationship between the rates of energy transfer involving nonadjacent versus adjacent sites in arrays containing other linkers. This prompted us to investigate a series of phenylene-linked dyads and triads containing zinc, magnesium and free base porphyrins. The results are illustrated below for phenylene-linked triad **ZnZnFbΦ**. The observation that energy transfer between nonadjacent sites in both the phenylene- and diphenylethyne-linked porphyrin arrays is only 5-10-fold slower than between adjacent sites further suggests that this magnitude of scaling between the rates of the two types of processes is a relatively general characteristic of these architectures. This knowledge can be utilized to evaluate the efficacy of initial designs of large multicomponent architectures prior to a substantial investment of time in the synthesis of the arrays. Furthermore, this knowledge is useful in the modeling of the energy-transfer dynamics and efficiency of complex multicomponent porphyrinic arrays wherein the rates of nonadjacent energy transfer are not readily measurable.

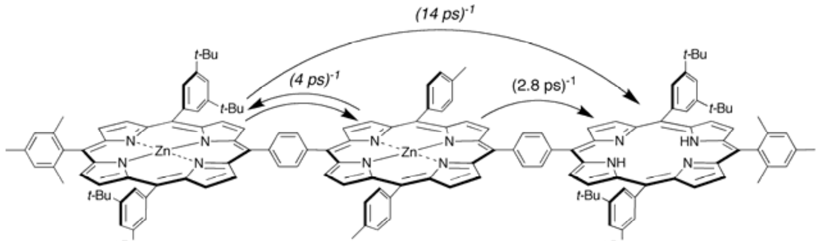

ZnZnFbΦ

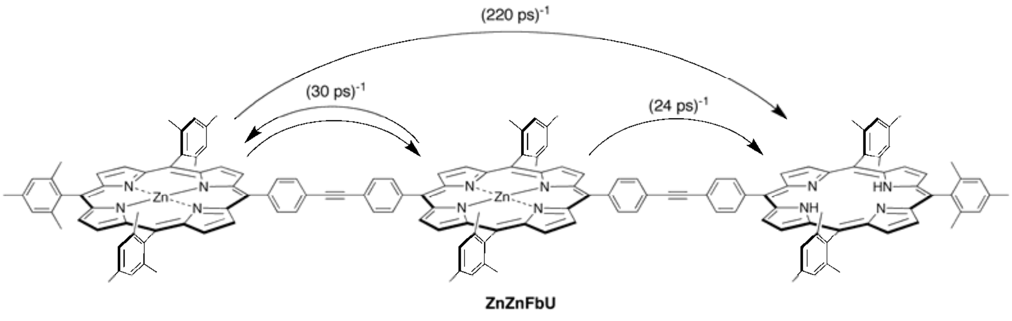

ZnZnFbU

SURFACE PLASMON ENHANCEMENT EFFECT ON CHARGE SEPARATION IN PHOTOSYNTHETIC REACTION CENTERS

Cameron Postnikoff and Libai Huang
Notre Dame Radiation Laboratory
University of Notre Dame, Notre Dame, IN 46556

Photosynthetic reaction centers (RCs) are pigment-protein complexes that are responsible for the primary processes of photo-induced charge separation in photosynthesis. RCs contain molecular optical and electronic circuitry organized by a protein scaffold. The hierarchical structures of photosynthetic protein complexes ensure high efficiency in energy harvesting and conversion. Thus these protein complexes are attractive candidates for active media in solar energy conversion if they can be integrated into solid-state devices. By using bimolecular linkers, one can assemble photosynthetic proteins with nanoparticles into hybrid superstructures that potentially can function as building blocks in solid-state devices. Theoretical calculations have shown that chemical production rate in photosynthetic protein complexes can be further enhanced by surface plasmon resonance (SPR) of metallic nanoparticles [1]. Here I will present our recent experimental efforts on synthesizing and characterizing such hybrid photosynthetic nanostructures. We have successfully synthesized hybrid structures that incorporate silver nanoparticles with RCs. Our initial results provide strong experimental evidence for SPR enhanced chemical production rate in such hybrid nanostructures compared to natural state of RCs.

RCs were purified from R26 strains of *Rhodobacter sphaeroides*. Citrate-capped silver nanoparticles (NPs) were used in our studies, with a plasmon resonance at 405 nm that has significant spectral overlap with the soret band of RCs. 11-amino-1-undecanethiol was used to covalently link RCs with NPs. Hybrid structures formed with RCs and silver NPs exhibited a Raman enhancement factor as high as 30, which proved that RCs were in close proximity (< 5nm) to the NPs (Figure 1). Photo-induced charge separation processes in these hybrid structures were characterized by femtosecond transient absorption spectroscopy. We observed a 2-3 fold~~s~~ increase in photo-induced charge production in the hybrid structures compared to pure RCs (Figure 2). SPR and resulting optical near-field are strongly modified by nanoparticle shape, size, composition, and environment. Experimental efforts are currently underway to optimize the coupling between SPR and protein complexes by tuning the physical parameters of metallic nanoparticles.

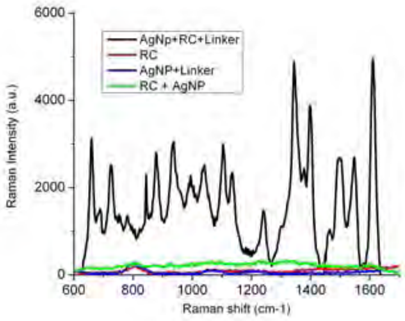

Figure 1: Raman spectra of RCs linked with Ag NPs compared with pure RCs, Ag NPs with linkers and unlinked RCs and Ag NPs.

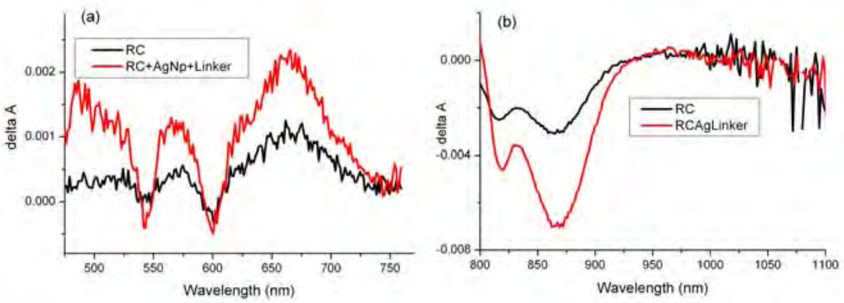

Figure 2: Transient Absorption spectra taken at pump-probe delay time of 80 ps for linked RC -Ag NP complexes compared with pure RCs for (a) visible and (b) near IR wavelength regions.

ADVENTURES WITH POPHYRINIC SUPER-CHROMOPHORES

Joseph T. Hupp
Department of Chemistry
Northwestern University
Evanston, IL 60208

Highly conjugated porphyrin oligomers are attractive chromophores for sensitizing solar cells. From the work of Anderson and co-workers and Therien and co-workers, chromophores of this kind are known to exhibit highly broadened electronic absorption spectra and strongly allowed red or far-red transitions. See figure (below left) for examples. We have tailored these chromophores so that they are: a) non-aggregating and b) strongly adsorbing on metal-oxide semiconductor surfaces; see figure (below right). The figure on the bottom left illustrates the light harvesting efficiency for the tetrameric chromophore on an electrode with 400X geometric surface area. The figure on the bottom right illustrates the LHE with 1,600X geometric area.

We find that these chromophores are capable of sensitizing TiO_2, but better suited to sensitizing SnO_2 – behavior that can be understood by considering relative energetics of the semiconductor band edges and the molecular excited states. Rather complex behavior is observed with redox shuttles. Triiodide appears to associate strongly with the tetramer, resulting in large dark currents and low photovoltages. In contrast, with large-diameter cobalt complexes as redox shuttles, the tetramer displays blocking behavior that inhibits dark currents and enhances photovoltages. These findings along with fundamental photophysics will be presented.

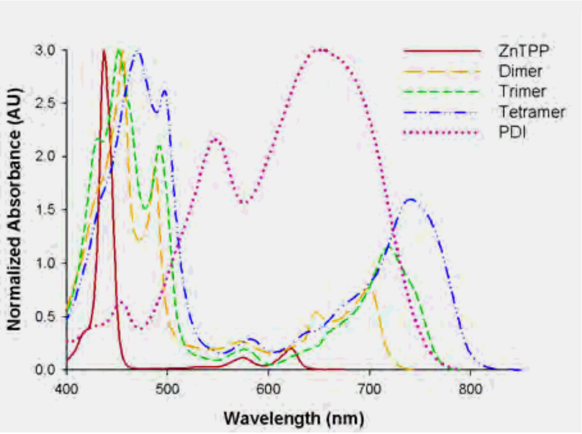

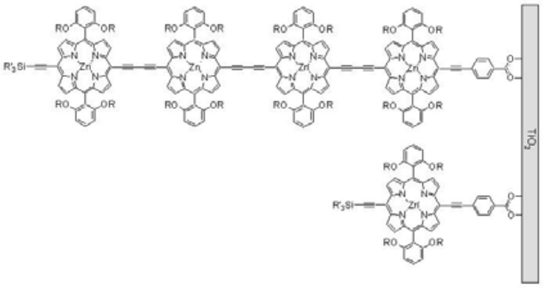

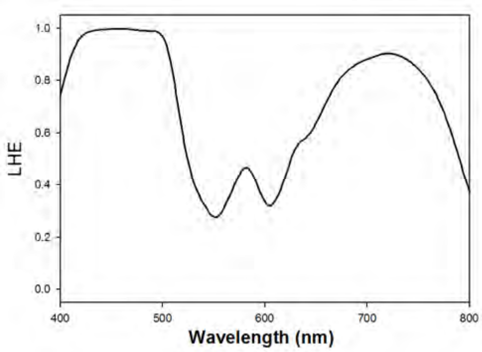

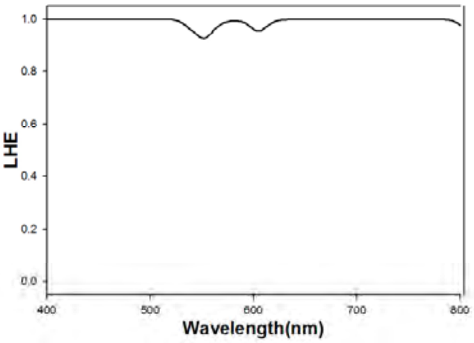

PHOTOINITIATED WATER OXIDATION BY THE “BLUE DIMER”

Jonathan L. Cape and James K. Hurst
Chemistry Department
Washington State University
Pullman, WA 99164-4630

Metal ion-catalyzed water oxidation is most frequently studied in highly acidic media containing strong oxidants (notably Ce^{4+}). These conditions can introduce numerous complications in mechanistic analyses, among the most serious being oxidative degradation of organic ligands that is exacerbated by the presence of excess oxidant and rate-retarding anation of the complexes in the necessarily high salt reaction environments. One means of avoiding these complications is to generate the oxidant photochemically, thereby allowing systematic investigation of the reactions under a wider range of concentrations while minimizing inactivating side reactions. We have investigated O_2 evolution from the reaction, $2S_2O_8^{2-} + 2H_2O \rightarrow O_2 + 4H^+ + 4SO_4^{2-}$, which can be photocatalyzed when both RuL_3^{2+} and $[RuL_2(OH_2)]_2O^{n+}$ ions are present (L = 2,2’-bipyridine or a structural analog). One pathway for this reaction is illustrated stylistically below:

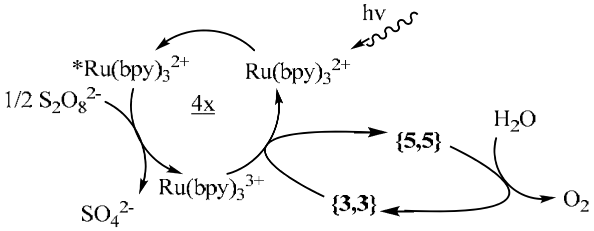

Major findings from these studies are listed below:

i) Oxidation of the dimer to its catalytically active **{5,5}** state, as determined by kinetic and resonance Raman analyses, could be achieved only with very high potential photosensitizers (e.g., $Ru(dcb)_2bpy^{2+}$ (dcb = 4,4-dicarbethoxybipyridine, E^o = 1.5 V (NHE)). O_2 evolution observed when lower potential analogs were used probably involved oxidation of **{4,5}** by intermediary $SO_4^{\bullet -}$ ions.

ii) Apparent rate constants for O_2 evolution (k_{cat}) increased with increasing alkalinity over the range pH 2-10 for several $[RuL_2(OH_2)]_2O^{n+}$ complexes whose bpy ligands had electron-donating and withdrawing substituents. Maximal turnover rate achievable by these catalysts are k_{cat} = 0.1-1.0 s^{-1}.

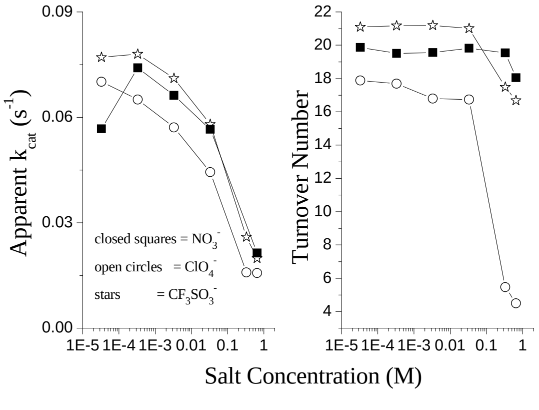

iii) Rate-retarding salt effects, presumably arising from anation of the catalyst, were clearly demonstrated by adding potassium salts of NO_3^-, ClO_4^-, and $CF_3SO_3^-$ to pH 7 photocatalytic systems; k_{cat} was unaffected by high concentrations of $B(OH)_4^-$ and $H_2PO_4^-$ /HPO_4^{2-}, however.

THE KINETICS OF TRIPLET FORMATION AND DECAY IN DIMERS AND SOLIDS DESIGNED FOR SINGLET FISSION

Justin C. Johnson,[1] Arthur J. Nozik,[1,2] Akin Akdag,[2] Josef Michl[2]
[1]National Renewable Energy Laboratory
Golden, CO 80401
[2]Dept. of Chemistry and Biochemistry, University of Colorado-Boulder

Triplet excitations in organic chromophores play a role in a variety of photoconversion schemes. Recent investigations in designed molecular systems have been aimed at generating two triplet excitons per absorbed photon via a process called singlet fission (SF). Demonstration of efficient SF has the potential to lead to ultraefficient photovoltaic and photoelectrochemical devices. Studies of covalently bound dimers and non-covalent solids of chromophores with optimal singlet and triplet energy level alignment have led to considerable insight into the mechanism of SF in systems that exhibit different degrees of intermolecular coupling. In addition, the role of the environment surrounding the excited state in the promotion or inhibition of SF and its reverse, triplet-triplet annihilation, is being explored. Comparison is also made between mechanistic models of SF and the analogue in quantum dots, multiple exciton generation (MEG).

The figure below demonstrates the different degrees of coupling present in the series of 1,3-diphenylisobenzofuran (DPIBF) derivatives explored in one set of investigations. Values of the triplet quantum yield (Φ_T) and the inferred triplet formation (τ_T) time are shown. Studies of thin crystalline films of polyacenes have revealed further mechanistic details about the SF process.

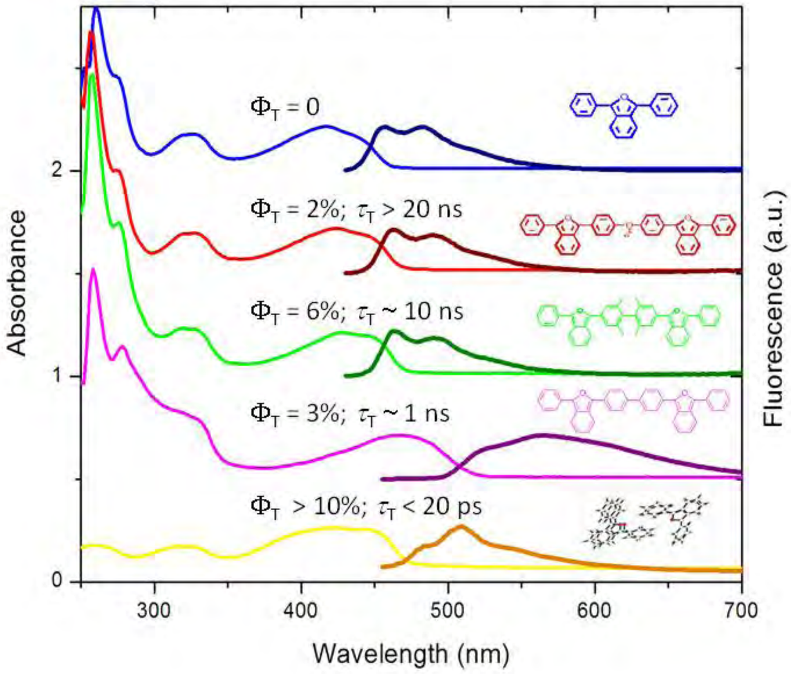

QUANTUM DOT SENSITIZED SYSTEMS FOR SOLAR PHOTOCONVERSION.
A TALE OF TWO SEMICONDUCTOR NANOCRYSTALS: CdSe AND CdTe.

Jin Ho Bang, Kevin Tvrdy, David Baker and Prashant V. Kamat
Radiation Laboratory, University of Notre Dame
Notre Dame IN 46556

TiO_2 nanotube arrays and particulate films are modified with CdSe and CdTe quantum dots with an aim to tune the response of the photoelectrochemical cell in the visible region.[1-5] The interfacial charge transfer processes between semiconducting nanoparticles and the oxide substrate to which they are anchored, have been probed by depositing 4.2 nm diameter CdSe quantum dots on both TiO_2 and SiO_2 substrates and subjecting them to steady state and pulsed laser irradiation. Spectroscopic measurements under both atmospheric and vacuum conditions highlight the role of the substrate in dictating the photochemistry of CdSe quantum dots.

CdSe and CdTe semiconductor nanocrystals exhibit markedly different external quantum efficiencies (~70% for CdSe and ~0.1% CdTe at 555 nm) when employed as sensitizers in quantum dot solar cells. Although CdTe having a favorable conduction band energy (E_{CB} = -1.0 V vs. NHE) is capable of injecting electrons into TiO_2 faster than CdSe (E_{CB} = -0.6 V vs. NHE), hole scavenging by a sulfide redox couple remains a major bottleneck. The sulfide ions dissolved in aqueous solutions are capable of scavenging photogenerated holes in photoirradiated CdSe system but not in CdTe. The anodic corrosion and exchange of Te with S dominate the charge transfer at the CdTe interface. The factors that dictate the efficiency and photostability of CdSe and CdTe quantum dots will be discussed.

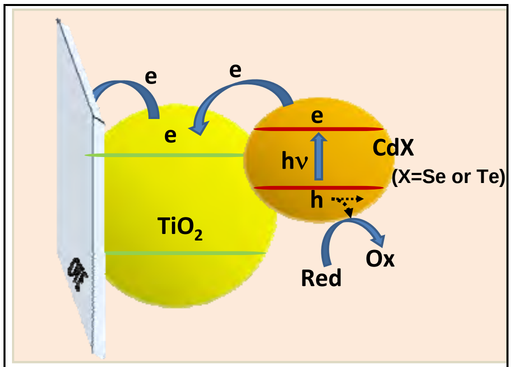

Scheme 1. Charge injection from excited semiconductor nanocrystal, CdX (X= Se or Te) into TiO_2 nanoparticle and scavenging of holes by a Red-Ox couple.

References

1. Kamat, P. V., *Quantum Dot Solar Cells. Semiconductor Nanocrystals as Light Harvesters. J. Phys. Chem. C*, **2008**, *112*, 18737-18753 (*Centennial Feature article*).
2. Baker, D. R.; Kamat, P. V., *Photosensitization of TiO_2 Nanostructures with CdS Quantum Dots. Particulate versus Tubular Support Architectures. Adv. Funct. Mater.*, **2009**, *19*, 805-811.
3. Tvrdy, K.; Kamat, P., *Substrate driven photochemistry of CdSe Quantum Dot Films: Charge Injection and Irreversible Transformation on Oxide Surfaces, . J. Phys. Chem. C*, **2009**, *113*, DOI: in press.
4. Harris, C. T.; Kamat, P. V., *Photocatalysis with CdSe Nanoparticles in Confined Media: Mapping Charge Transfer Events in the Subpicosecond to Second Timescales. ACS Nano*, **2009**, *3*, in press.
5. Bang, J. H.; Kamat, P. V., *Quantum Dot Sensitized Solar Cells. CdTe versus CdSe Nanocrystals J. Phys. Chem.*, **2009**, submitted.

SPIN STATE DYNAMICS IN GaSe NANOPARTICLES

Hoda Mirafzal, Deborah Lair and David F. Kelley
University of California, Merced
Merced, CA 95340

Two aspects of the singlet/triplet dynamics of GaSe nanoparticles are studied: relaxation to thermal equilibrium at low temperatures and the reversal of the singlet and triplet states in strongly-interacting nanoparticle aggregates. Quantum confinement effects result in a larger singlet-triplet gap in GaSe nanoparticles, compared to the bulk material. Time-resolved, temperature-dependent luminescence polarization measurements indicate the nanoparticle singlet-triplet splitting is about 3 time that in bulk GaSe and that spin relaxation times vary from being fast at room temperature (<100 fs) to relatively slow (30 – 50 ps) at 20 K. These energetics and dynamics are depicted in the figure below.

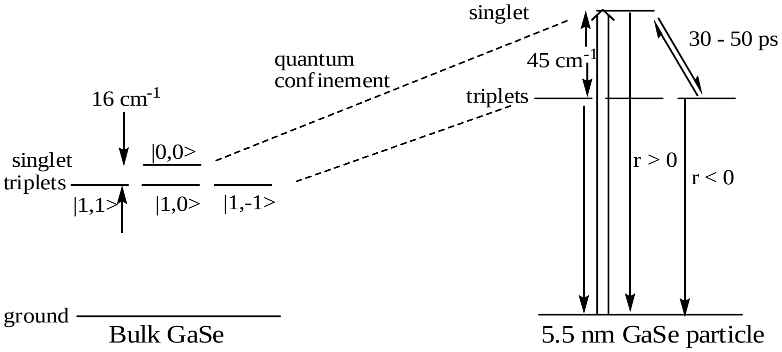
singlet
30 - 50 ps
quantum
confinement
45 cm-1
16 cm-1
triplets
|0,0>
singlet
triplets
r > 0
r < 0
|1,1>
|1,0>
|1,-1>
ground
Bulk GaSe
5.5 nm GaSe particle

GaSe nanoparticles ligated with relatively non-bulky alkyl aldehydes form strongly-coupled aggregates. The strong coupling of the singlet states results in a reversal of the singlet and triplet states which has two dramatic effects. Upon aggregation, the fluorescence quantum yield increases from 4.7% to 61% (due to a decrease in the radiative lifetime) and there is a change in the polarization spectroscopy which reflects luminescence from a purely linear oscillator. The reversal of the spin states is depicted for the case of a dimer in the figure below.

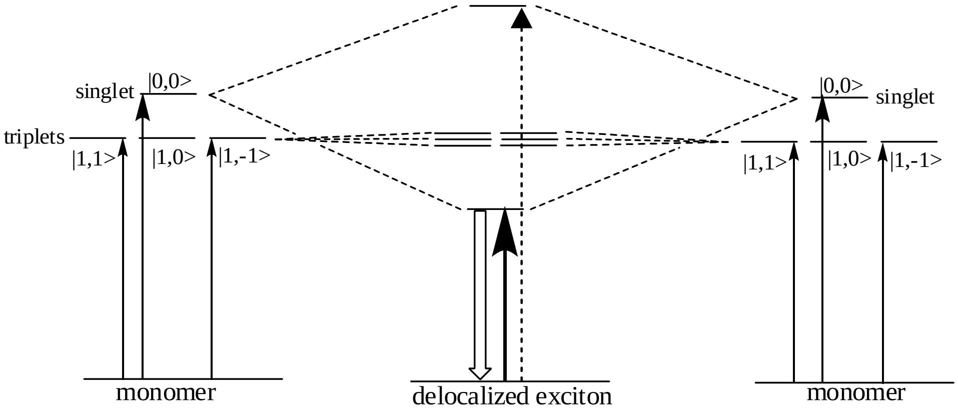
singlet
|0,0>
triplets
|1,1>
|1,0>
|1,-1>
|0,0>
singlet
|1,1>
|1,0>
|1,-1>
monomer
delocalized exciton
monomer

DO CAROTENOID NEUTRAL RADICALS HAVE A ROLE IN LHC II?

Lowell D. Kispert, A. Ligia Focsan, Tatiana A. Konovalova, Péter Molnár, Nikolay E. Polyakov

Department of Chemistry, The University of Alabama, Tuscaloosa, AL 35487 US, Department of Pharmacognosy, University of Pécs, H-7624 Pécs, Rókus u. 2, Pécs, Hungary, Institute of Chemical Kinetics & Combustion, Institutskaya Str. 3, 630090, Novosibirsk, Russia

Carotenoids (Car) serving as quenching agents are indispensable to plants for protection against photooxidative damage by excessive light. Recently it has been shown that carotenoid radical cations ($\mathrm{Car}^{\bullet+}$) are involved in quenching chlorophyll’s excess energy in minor light harvesting complexes. We proposed that carotenoid neutral radicals ($\#\mathrm{Car}^{\bullet}$) formed by proton loss (indicated by #) from $\mathrm{Car}^{\bullet+}$ could also participate in quenching. In order to examine their properties, we trapped the carotenoid radicals on silica derivatives such as silica-alumina, MCM-41 or metal-substituted MCM-41. ENDOR studies in combination with density functional theory (DFT) calculations have revealed that photo-oxidation of carotenoids in these artificial matrices produces a mixture of Car radicals, namely $\mathrm{Car}^{\bullet+}$ and $\#\mathrm{Car}^{\bullet}$ listed in the table below.

Our ENDOR results in artificial matrices supported by DFT calculations show that only $\#\mathrm{Zea}^{\bullet}$ and $\#\mathrm{Lut}^{\bullet}$ can be formed by proton loss at the **methylene** and **methyl** groups of the terminal rings of the radical cation as summarized in the table below. In light harvesting complex LHC II, proton loss from the methyl groups along the polyene chain of all carotenoid radical cations would be prevented because of their location in the hydrophobic region. However, $\#\mathrm{Zea}^{\bullet}$ and $\#\mathrm{Lut}^{\bullet}$ could be formed due to the arrangement of the carotenoids with the terminal rings oriented towards the hydrophilic lumen and stroma regions where the proton loss would be efficient. In contrast, $\mathrm{Vio}^{\bullet+}$ and 9′-*cis* $\mathrm{Neo}^{\bullet+}$ do not form neutral radicals because the **epoxide** groups and the **allene** bond prevent the proton loss, consistent with the fact that they are not involved in quenching. We found that the expected ability to form neutral radicals in LHC II environment matches their proposed role in that protein complex. This work was supported by U.S. Dept. of Energy Grant No. DE-FG02-86ER 13465.

Car	$\mathrm{Car}^{\bullet+}$ in minor LHC II	Lose protons from terminal rings of $\mathrm{Car}^{\bullet+}$?	Quenching role in LHC II	Formation of neutral radicals in artificial matrix *terminal rings
Zea	Yes	Yes	Yes	**#Zea$^{\bullet}$(4)***, **#Zea$^{\bullet}$(4′)***, **#Zea$^{\bullet}$(5)***, **#Zea$^{\bullet}$(5′)***, #Zea$^{\bullet}$(9), #Zea$^{\bullet}$(9′) ,#Zea$^{\bullet}$(13), #Zea$^{\bullet}$(13′)
Lut	Yes	Yes	Yes	**#Lut$^{\bullet}$(6′)***, **#Lut$^{\bullet}$(4)***, #Lut$^{\bullet}$(4′)* , **#Lut$^{\bullet}$(5)***, #Lut$^{\bullet}$(5′)*, #Lut$^{\bullet}$(9), #Lut$^{\bullet}$(9′), #Lut$^{\bullet}$(13), #Lut$^{\bullet}$(13′)
Vio	not obs.	No	No	#Vio$^{\bullet}$(9), #Vio$^{\bullet}$(9′), #Vio$^{\bullet}$(13), #Vio$^{\bullet}$(13′)
9′-*cis* Neo	not obs.	No	No	#Neo$^{\bullet}$(9), #Neo$^{\bullet}$(9′), #Neo$^{\bullet}$(13), #Neo$^{\bullet}$(13′)

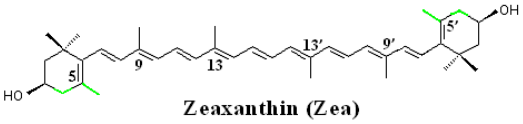

Zeaxanthin (Zea)

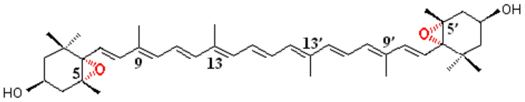

Violaxanthin (Vio)

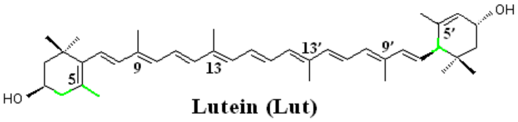

Lutein (Lut)

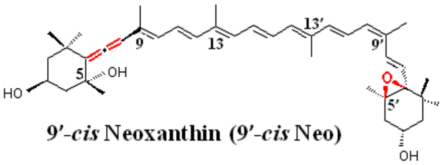

9′-*cis* Neoxanthin (9′-*cis* Neo)

UNUSUALLY BRIGHT FLUORESCENCE FROM SINGLE-WALLED CARBON NANOTUBES

Andrea J. Lee, Xiaoyong Wang, Lisa J. Carlson, and Todd D. Krauss
Department of Chemistry
University of Rochester
Rochester, NY 14627-0216

Single-walled carbon nanotubes (SWNTs) are tubular graphitic molecules with exceptional and unusual mechanical, electrical, and optical characteristics. Regarding their potential as novel materials for solar energy conversion, SWNTs could play a role as photosensitizers, photogenerators of charge carriers, or charge transport materials. The goal of this project is to develop a more complete understanding of the optical properties of SWNTs, in particular those that are especially relevant to solar photochemistry.

Despite recent interest in the optical properties of SWNTs, large gaps in the fundamental understanding of their photophysical characteristics remain. In particular, an accurate value for the SWNT fluorescence efficiency has not yet been determined. For an ensemble of nanotubes, the fluorescence quantum yield (QY) is extremely low, typically less than 0.1%. On the other hand, the brightest individual SWNTs have a QY ~ 3-8 %, almost two orders of magnitude larger than when determined in ensemble measurements. We have recently discovered that the QY of individual SWNTs can be further enhanced up to 10-fold in the presence of antioxidant triplet state quenchers such as dithiothreitol (DTT) (Figure 1). Single nanotube QY measurements were obtained using confocal microscopy by simultaneously dispersing dilute suspensions of SWNTs and CdTe/ZnS quantum dots (QDs) onto a substrate and monitoring their respective emission intensity. We have also found that the fluorescence enhancement is reversible, decreasing when the additive is removed. When exposed to antioxidants, the QY increased to ~25%, and thus is the same order as fluorescent dye molecules. Consequently, our findings suggest that the maximum QY for SWNTs is much higher than previously thought. Mechanisms for the huge enhancement of the SWNT fluorescence intensity will be presented.

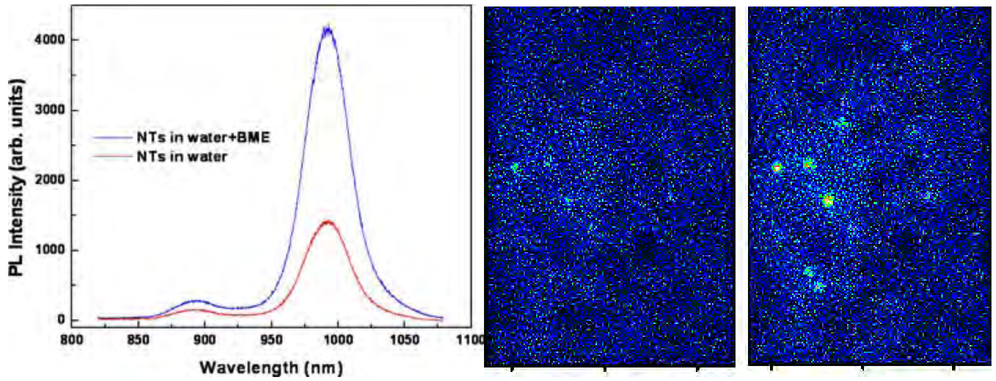

Figure 1. (Left) SWNT fluorescence spectra before (red) and after (blue) addition of beta-mercaptoethanol (BME). SWNTs were dispersed in D_2O with DNA. Single SWNT fluorescence images (20 x 20 μm^2) before (center) and after (right) addition of DTT. Fluorescence increase was 5-10 fold.

EFFICIENT CHARGE TRANSPORT IN DNA DIBLOCK OLIGOMERS

Frederick D. Lewis
Department of Chemistry
Northwestern University
Evanston, Il 60201

We have investigated the dynamics and efficiencies of charge separation in capped hairpins possessing polyG base pair domains (Chart 1b), diblock base pair domains consisting of 1-4 adenines followed by 1-7 guanines (Chart 1c), and several alternating base pair domains.[6] The results for several mono- and diblock polypurines are shown in Figure 1. Rate constants and quantum yields for charge separation in polyG sequences are strongly distance dependent, as previously observed for polyA sequences. However, charge separation efficiencies of ca. 25% over distances as large as 36 Å and the formation of long-lived charge separated states are observed for the diblock systems A_2G_n and A_3G_n possessing two or three adenines and as many as seven guanines, substantially higher than the efficiencies for either homopurine (polyA or polyG) or alternating (AG, CG, or AT) base sequences (Figure 1a).

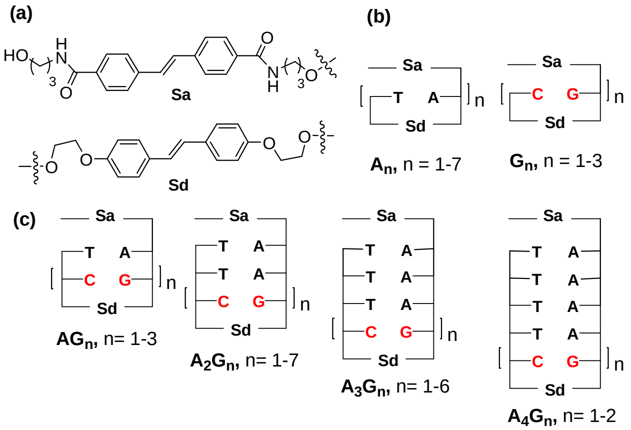

Chart 1. Structures for stilbenes Sa and Sd (a) and for capped hairpins possessing mono (b) and diblock (c) base pair sequences.

Rate constants for charge separation are only weakly distance dependent in the longer diblock systems and charge separation efficiencies are independent of the length of the guanine block (Figure 1b). Other sequences were less effective: values of Φ_{cs} = 0.15 for A_4G and A_4G_2 are intermediate between the values for A_n and A_3G_n systems having the same total number of base pairs, and values of Φ_{cs} for AG_n and several alternating base sequences including A_mGAGAG (m = 1-3) are lower than those for A_n sequences having the same total number of base pairs.

Figure 1. (a) Rate constants and (b) quantum yields for charge separation.

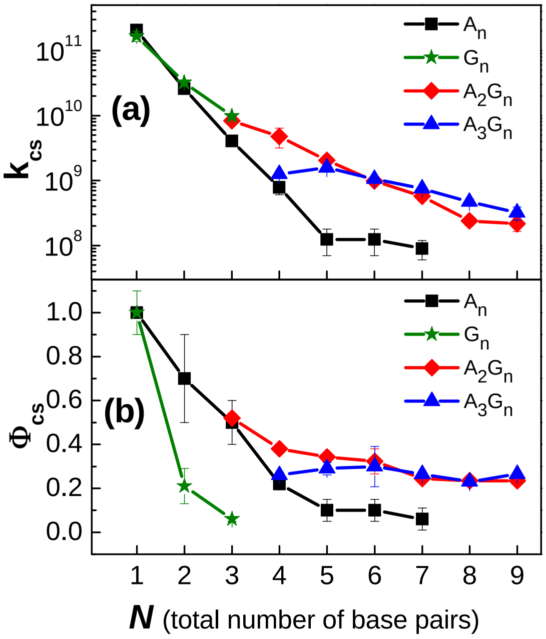

The fundamental principles governing long distance charge transport that are gleaned from these systems will more generally prove valuable in designing a wide variety of specialized charge transport oligomers.

INTERFACIAL CHARGE TRANSFER PROCESSES IN TiO_2-SENSITIZER- Ru-POM PHOTOCATALYTIC SYSTEMS FOR OXYGEN EVOLUTION FROM WATER

Zhuangqun Huang, Yurii V. Geletii, Yu Hou, Djamaladdin G. Musaev, Craig L. Hill, Tianquan Lian

Department of Chemistry and Emerson Center of Scientific Computing
Emory University
Atlanta, GA 30322

The overall goal of the project is to develop a solar-driven photocatalytic system for oxidizing water to generate O_2 and protons and to understand relevant fundamental processes. The photocatalytic system is based on an all-inorganic molecular (soluble) catalyst for H_2O oxidation, $[\{Ru_4O_4(OH)_2(H_2O)_4\}(\gamma\text{-}SiW_{10}O_{36})_2]^{10-}$ (or Ru-POM) and sensitized TiO_2 for efficient light-harvesting and charge separation. The Ru-POM complex has been shown to catalyze O_2 formation by stoichiometric one-electron oxidants, $[Ru(bpy)_3]^{3+}$ in the dark.[1]

This poster is focused on recent efforts to drive the above catalytic system using solar energy. In the first step, we have demonstrated that $[Ru(bpy)_3]^{3+}$ can be produced by photo-oxidation of $[Ru(bpy)_3]^{2+}$ in the presence of sacrificial electron donor ($S_2O_8^{2-}$) and the system can catalyze the oxidation of water to produce O_2 according to equation (1) with ~9% quantum efficiency.[2]

$$2S_2O_8^{2-} + 2H_2O + 2h\nu \xrightarrow{Ru-POM,[Ru(bpy)_3]^{2+}} 4SO_4^{2-} + O_2 + 4H^{+} \qquad (1)$$

In step 2, we are introducing TiO_2 as an electron acceptor to increase the quantum yield of $[Ru(bpy)_3]^{3+}$ generation. Femtosecond transient absorption and time-resolved fluorescence spectroscopy studies suggest that excited $[Ru(dcbpy)_3]$ is efficiently quenched by ultrafast electron transfer to TiO_2(see Fig.1). Ongoing studies are examining how charge recombination competes with the oxidation of RuPOM by the oxidized sensitizer and exploring various strategies for improving the yield of photo-oxidized catalyst.

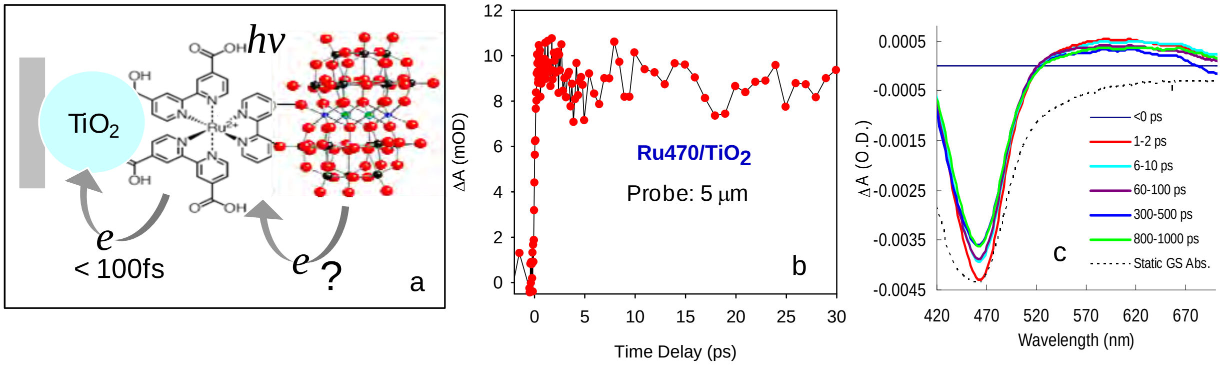

Figure 1. a) schematic view of the TiO_2-Ru470-RuPOM photocatalytic system and b) Electron injection kinetics from Ru470 to TiO_2 probed by transient IR spectroscopy; c) Charge recombination kinetics probed by ground state recovery of Ru470-TiO_2.

(1) Geletii, Y. V.; Botar, B.; Kögerler, P.; Hillesheim, D. A.; Musaev, D. G.; Hill, C. L. *Angew. Chem. Int. Ed.* **2008**, *47*, 3896-3899. (2) Geletii, Y. V.; Huang, Z.; Hou, Y.; Musaev, D. G.; Lian, T.; Hill, C. L. *J. Am. Chem. Soc.* **2009**, in revision.

CHLOROPHYLLS STRIPPED (ALMOST) NAKED BY DE NOVO SYNTHESIS

Olga Mass,[a] Masahiko Taniguchi,[a] Marcin Ptaszek,[a] David F. Bocian,[c] Dewey Holten,[b] and
Jonathan S. Lindsey[a]
[a]Department of Chemistry, North Carolina State University, Raleigh, NC 27695
[b]Department of Chemistry, Washington University, St. Louis, MO 63130
[c]Department of Chemistry, University of California Riverside, Riverside, CA 92521

Over the years we have been working to develop the synthetic chemistry of chlorins and bacteriochlorins so as to be able to prepare simple analogues of the natural hydroporphyrins as well as arrange the synthetic hydroporphyrins in a variety of 3-dimensional architectures. Here we have turned to a somewhat neglected question concerning chlorophyll chemistry and photochemistry, namely, what are the spectroscopic properties of the core chromophore itself, i.e., devoid of substituents at all sites around the perimeter of the macrocycle?

Chlorophylls are chlorins owing to the presence of one reduced pyrrole ring, yet the carbon skeleton of chlorophylls is not a mere tetrapyrrole but also contains an annulated five-membered ring equipped with a 13^1-keto group. Macrocycles with such a skeleton are known as 13^1-oxophorbines. The 13^1-keto group is conjugated with the π-system along the molecular y-axis, which is coincident with the long-wavelength Q_y transition. Given that the intensity and position of the Q_y band is central to the spectral and photochemical properties of chlorophylls, understanding the contributors to the Q_y band is of commensurate importance. Accordingly, we have developed rational (and relatively concise) syntheses from simple precursors to gain access to benchmark molecules such as the chlorin **ZnC** and the 13^1-oxophorbine **ZnOP**, and a series of analogues thereof with 1–3 auxochromes in distinct patterns. All such macrocycles are sparsely substituted, containing only the stabilizing *gem*-dimethyl group in the reduced ring and any specific groups at other designated sites in order to pinpoint the effects of substitution.

The absorption spectra of **ZnC**, **ZnOP**, and the zinc chelate of chlorophyll *a* (**Zn-Pheo *a***) are shown below. The chlorin alone is a poor surrogate for chlorophyll whereas the mere incorporation of the isocyclic ring (giving the 13^1-oxophorbine) provides an absorption spectrum that is a close mimic of that of the structurally more complex chlorophyll. The ability to capture the key spectral features of chlorophylls in simple synthetic structures, and to tune the spectral features through systematic structural alteration, together augurs well for the use of synthetic chlorophylls in fundamental studies as well as a variety of solar energy conversion approaches.

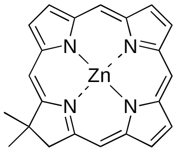
ZnC

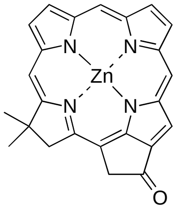
ZnOP

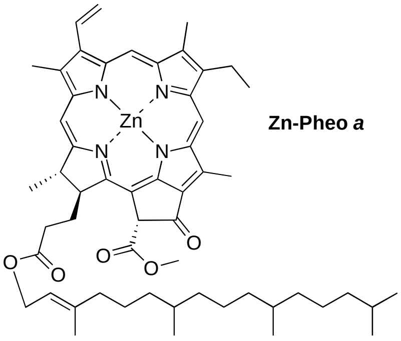
Zn-Pheo *a*

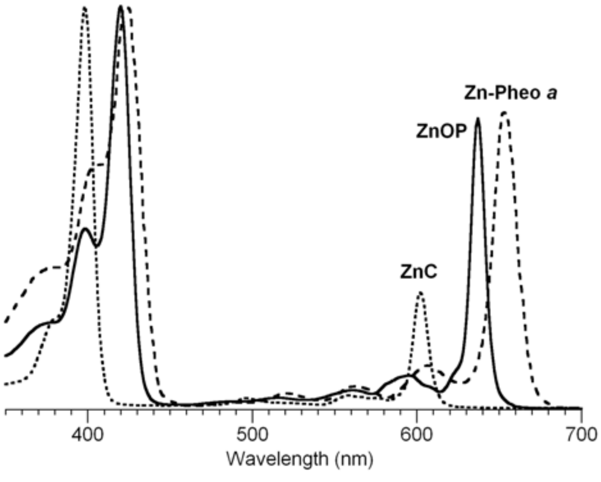

BENZYLIDENE MALONONITRILES AS PROBES OF LOCAL SOLVENT FRICTION

Hui Jin, Chet Swalina, Min Liang, Sergei Arzhantsev, Xiang Li, and Mark Maroncelli
Department of Chemistry
The Pennsylvania State University
University Park, PA 16802

Benzylidene malononitriles such as DMN and JDMN have been studied by various groups as nonlinear optical materials and as local friction probes in solutions, polymers, and biological systems. Large molecular hyperpolarizabilities of interest in nonlinear optics are the result of the charge-shift character of the $S_0 \rightarrow S_1$ transitions of these push-pull chromophores. Their use as friction probes results from environmentally sensitive nonradiative decay from S_1 as a result of some large-amplitude motion.

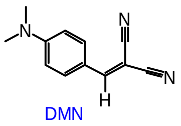
DMN

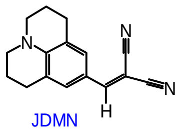
JDMN

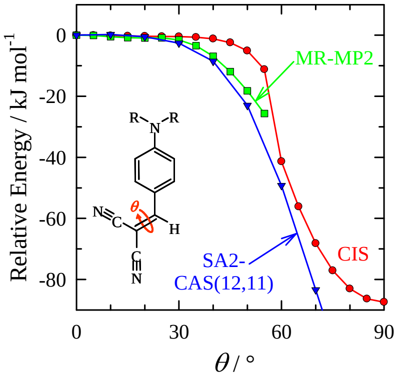

Fig. 1: Scans of the S_1 potential energy surface of DMN in the gas phase using various model chemistries (6-31G(d) basis set).

Despite long and widespread use of these molecules as fluorescence probes of fluidity, the precise nature of their solvent sensitivity, and the identity of the motion responsible for this sensitivity have remained poorly defined. We have been studying the photophysics of DMN and JDMN via both computation and experiment in order understand just what their nonradiative decay can reveal about local environment. Most researchers to date have assumed that that deactivation involves a (single bond) TICT process. In contrast, electronic structure calculations (Fig. 1) indicate that it is isomerization about the double bond, which results in a conical intersection with S_0, that leads to loss of fluorescence. These gas-phase calculations predict an unusually flat potential, implying that reaction occurs via an almost free rotation except for the friction imparted by the molecule's surroundings. An extensive survey of emission lifetimes in over 30 solvents (Fig. 2) shows that this reaction typically occurs in 1-10 ps with this time weakly correlated to solvent viscosity, $\tau \propto \eta^p$ with p =.13 (DMN) and 0.27 (JDMN). Contrary to the assumption made by most workers, the reaction rate is also significantly influenced by solvent polarity. We have yet to understand fully what features of the solvent determine these reaction rates; we hope to learn more using molecular dynamics simulations and semi-empirical S_1 surfaces.

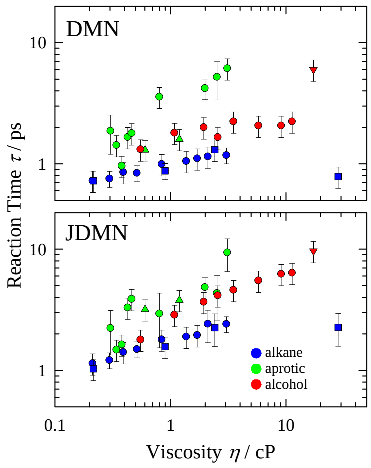

Fig. 1: Isomerization times measured using both emission quantum yield and lifetime data.

The high reaction rates in these molecules imparts a number of interesting features to their emission, for example non-exponential decay profiles, excitation-wavelength-dependent kinetics in high viscosity solvents, and retrograde spectral shifts as a function of temperature in certain cases. All of these features are understandable in terms of the relative rates of reaction and solvation under different conditions.

ELECTRON TRANSFER DYNAMICS IN EFFICIENT MOLECULAR ENHANCED SEMICONDUCTORS

Shane Ardo, Amanda J. Morris, and Gerald J. Meyer
Departments of Chemistry and Materials Science & Engineering,
Johns Hopkins University
Baltimore, MD 21218

Photo-initiated reactions that form chemical bonds are of considerable importance for the conversion and storage of solar energy.[1] For example, iodide oxidation to form I-I bonds is key to sensitizer regeneration in dye-sensitized solar cells. Mechanistic details of how iodide oxidation yields the I-I bonds present in $I_2^{-\bullet}$ and I_3^- reaction products remain speculative. Here direct evidence that electron transfer sensitized to visible light with metal-to-ligand charge transfer (MLCT) excited states directly yields iodine atoms that subsequently react to form an I-I chemical bond. The kinetic and mechanistic information to be reported are summarized in the Jablonski-type diagram shown in *Scheme 1*. The compound $[Ru(bpz)_2(deeb)](PF_6)_2$, where bpz is 2,2′-bipyrazine and deeb is 4,4’-$(CO_2Et)_2$-2,2’-bipyridine is abbreviated $Ru(bpz)^{2+}$. Excited state electron transfer to yield the iodine atom is favored by 430 mV. Reaction of the iodine atom with iodide to make an I-I bond lowers the free energy stored in the charge separated state by 110 mV. Charge recombination to yield ground state products, $Ru^+ + I_2^{-\bullet} \rightarrow Ru^{II} + 2I^-$ is thermodynamically downhill ($-\Delta G^o = 1.64$ eV) and occurs with a rate constant of $2.1 \times 10^{10}\ M^{-1}\ s^{-1}$, almost ten times larger than the $I_2^{-\bullet}$ disproportionation rate constant. Unwanted recombination to $I_2^{-\bullet}$ has been proposed to lower the efficiency of dye-sensitized solar cells and this data shows that it can be a very fast reaction.

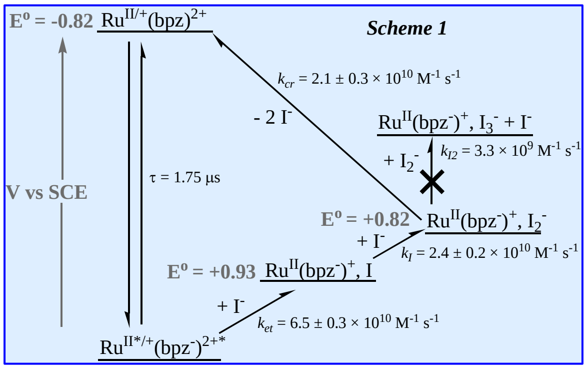

Scheme 1

$E^o = -0.82$ $Ru^{II/+}(bpz)^{2+}$
V vs SCE
τ = 1.75 μs
$k_{cr} = 2.1 \pm 0.3 \times 10^{10}\ M^{-1}\ s^{-1}$
- 2 I^-
$Ru^{II}(bpz^-)^+, I_3^- + I^-$
+ I_2^-
$k_{I2} = 3.3 \times 10^9\ M^{-1}\ s^{-1}$
$E^o = +0.82$ $Ru^{II}(bpz^-)^+, I_2^-$
+ I^-
$k_I = 2.4 \pm 0.2 \times 10^{10}\ M^{-1}\ s^{-1}$
$E^o = +0.93$ $Ru^{II}(bpz^-)^+$, I
+ I^-
$k_{et} = 6.5 \pm 0.3 \times 10^{10}\ M^{-1}\ s^{-1}$
$Ru^{II*/+}(bpz^-)^{2+*}$

Here we will also report that after rapid photo-induced electron injection into TiO_2 and regeneration by a donor, D, such as iodide or phenothiazine, sensitizers are present in an environment distinctly different from that prior to light absorption.[2] Significantly, the absorption spectrum of the Ru(II) sensitizer in this new environment is one that is known to be less favorable for excited-state electron injection. Transient stark-like behavior demonstrates that slow (μs to ms) cation transfer follows regeneration to yield the sensitizer that was initially photo-excited. This behavior has been observed with all Ru(II) sensitizers investigated in our laboratories and is now apparent in previously-published spectral data. Under air mass 1.5, 1 sun irradiation, the slow cation transfer is not expected to limit the efficiency of Grätzel solar cells as a typical Ru(II) sensitizer absorbs light approximately once every second. However, at higher irradiances or at planar TiO_2 surfaces this effect may limit light-to-electrical power conversion efficiency. In any case, this data shows that the operative sensitization mechanism put forth in review-type articles, where a Ru(II) sensitizer is regenerated to its *initial* state within 10 ns, needs to be modified.

[1] Gardner, J.M.; Giaimuccio, J.M.; Meyer, G.J. *I. Am. Chem. Soc.* **2008**, *130*, 17252. [2] Staniszewski, A.; Ardo, S.; Sun, Y.; Castellano, F.N.; Meyer, G.J. *J. Am. Chem. Soc.***2008**, *130*, 11586.

SURFACE AND SOLUTION WATER OXIDATION

Javier J. Concepcion, Jonah Jurss, M. Kyle Brennaman, John M. Papanikolas and Thomas J. Meyer
Department of Chemistry
University of North Carolina at Chapel Hill
Chapel Hill, NC 27599-3290

Mastering solar fuels production by Artificial Photosynthesis would be a considerable achievement, either water splitting into hydrogen and oxygen or reduction of CO_2 to methanol or hydrocarbons: $2\ H_2O + 4\ h\nu \rightarrow O_2 + 2\ H_2$; $2\ H_2O + CO_2 + 8\ h\nu \rightarrow 2\ O_2 + CH_4$. Water oxidation is an essential half reaction in either. Mechanistic studies have revealed important roles for Proton Coupled Electron Transfer (PCET), concerted electron-proton transfer (EPT), and peroxidic intermediates in water oxidation. For the blue Ru dimer, *cis,cis*-$[(bpy)_2(H_2O)Ru^{III}ORu^{III}(OH_2)(bpy)_2]^{4+}$, electrocatalytic water oxidation is inhibited by slow electron transfer at the electrode. The impact of electron transfer mediation by surface bound $Ru(bpy)((4,4'\text{-}PO_3H_2bpy))_2^{2+}$ is dramatic. With the surface bound complex on ITO (In_2O_3:Sn) or FTO (SnO_2:F) electrodes the characteristic $3e^-/3H^+$ oxidation wave, $(HO)Ru^{IV}ORu^{III}(OH_2)^{4+} \xrightarrow{-3e^-,-3H^+} \{(O)Ru^{V}ORu^{V}(O)\}^{4+}$, appears in cyclic voltammograms (CVs) inducing electrocatalytic water oxidation. Scans though this wave result in waves for the peroxidic intermediate $[(bpy)_2(HOO)Ru^{IV}ORu^{IV}(OH)(bpy)_2]^{4+}$ at 1.04 and 1.7 V vs NHE in 0.1 M HNO_3 followed by irreversible oxidation and oxygen evolution at ~2 V.

We have also developed new families of Ru-based monomeric catalysts for water oxidation examples being $Ru(tpy)(bpm)(OH_2)^{2+}$ and $Ru(tpy)(bpz)(OH_2)^{2+}$ (bpm is 2,2'-bipyrimidine, bpz is 2,2'-bipyrazine). This includes extensions to ligand-bridged complexes containing both electron transfer mediator and catalyst such as $[(bpy)_2Ru^{II}(bpm)Ru^{II}(tpy)(OH_2)]^{4+}$ and the surface-bound, phosphonated derivative shown below. A detailed kinetic study of Ce(IV) catalyzed water oxidation has demonstrated the stepwise mechanism below. The surface-bound complexes are impressive water oxidation electrocatalysts, in one case, undergoing more than 28,000 turnovers over a 13 hour period with a turnover rate of 0.6 s^{-1} with no sign of decrease in catalytic activity.

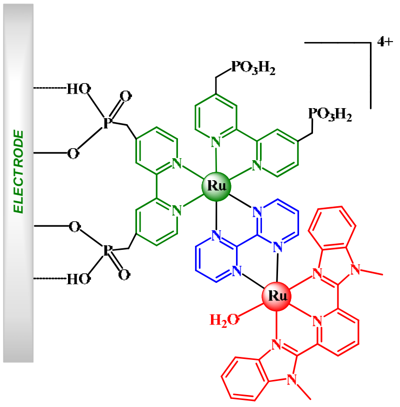

$$[Ru^{II}Ru^{II}{-}OH_2]^{4+} + Ce^{4+} \xrightarrow{k_1} \{Ru^{II}Ru^{III}{-}OH\}^{4+} + Ce^{3+} + H^+ \quad (a)$$

$$\{Ru^{II}Ru^{III}{-}OH\}^{4+} + Ce^{4+} \xrightarrow{rapid} [Ru^{II}Ru^{IV}{=}O]^{4+} + Ce^{3+} + H^+ \quad (b)$$

$$[Ru^{II}Ru^{IV}{=}O]^{4+} + Ce^{4+} \xrightarrow{k_2} [Ru^{III}Ru^{IV}{=}O]^{5+} + Ce^{3+} \quad (c)$$

$$[Ru^{III}Ru^{IV}{=}O]^{5+} + Ce^{4+} \xrightarrow{k_3} [Ru^{III}Ru^{V}{=}O]^{6+} + Ce^{3+} \quad (d)$$

$$[Ru^{III}Ru^{V}{=}O]^{6+} + H_2O \xrightarrow{k_{O\text{-}O}} \{Ru^{III}Ru^{III}{-}O_2H\}^{5+} + H^+ \quad (e)$$

$$\{Ru^{III}Ru^{III}{-}O_2H\}^{5+} + Ce^{4+} \xrightarrow{rapid} [Ru^{III}Ru^{IV}{-}O_2]^{5+} + Ce^{3+} + H^+ \quad (f)$$

$$[Ru^{III}Ru^{IV}{-}O_2]^{5+} + Ce^{4+} \xrightarrow{k_4} \{Ru^{III}Ru^{V}{-}O_2\}^{6+} + Ce^{3+} \quad (g)$$

$$\{Ru^{III}Ru^{V}{-}O_2\}^{6+} + H_2O \xrightarrow{rapid} \{Ru^{III}Ru^{III}{-}OH\}^{5+} + O_2 + H^+ \quad (h)$$

FAST ELECTRONS, FASTER EXCITONS
IN CONJUGATED "MOLECULAR WIRES"

John R. Miller, Andrew R. Cook, Paiboon Sreearunothai, Sadayuki Asaoka, Norihiko Takeda, Sean McIlroy, Julia M. Keller*and Kirk Schanze,* Yuki Shibano± and H. Imahori±
Chemistry Department, Brookhaven National Laboratory, Upton, NY 11973,
*University of Florida, Gainesville, FL. ±Kyoto University, Kyoto, Japan.

Organic photovoltaic (OPV) cells are a promising alternative for generation of electrical energy from sunlight. Exciton transport in OPV cells is characterized by short exciton diffusion lengths, typically 5-8 nm, which work to limit cell efficiencies. An important report in the literature on isolated chains with end-cap traps reinforced the idea that short diffusion lengths are the result of exciton transport being an "intrinsically slow process." Some other results support the view that exciton diffusion is "facile," but the belief that short diffusion lengths are an essential property of excitons in these materials is pervasive. Organic photovoltaic (OPV) cells are conceived and designed with this limitation in mind. Efforts to create OPV cells therefore focus on the heavily-interdigitated "bulk heterojunction" concept. Our experiments are examining this assumption along with measurements of electron and hole transport and the natures of the moving species.

Measurements described in this poster determine electron and exciton transport in polymers and oligomers having end-cap traps. Measurements of electron transport inject electrons into acceptor-capped oligomers or polymers in solution by ionizing the solvent with 7-10 ps, 9 MeV electron pulses at the Laser Electron Accelerator (LEAF). Subsequent detection of transient absorption uses the Optical Fiber Single-Shot detection system which enables experiments with 15 ps time resolution. The experiments find fast electron transport to end caps in oligomers of Platinum acetylides (Pt_nNDI2 shown at right). Transport of triplet excitons created by photoexcitation occurs with similar rates. In fluorene oligomers having C_{60} trap groups electron transport is also fast. Singlet excitons are not slow, but transport almost twenty times faster. They reach the C60 groups in ~10 ps in the $F_{16}(C_{60})_2$ molecule, shown below with a depiction of the electron or exciton as a polaron having a length of ~4 nm. If extensible to longer lengths, the exciton diffusion coefficient inferred from these measurements predict large exciton diffusion lengths that could support different, possibly more efficient, types of OPV structures.

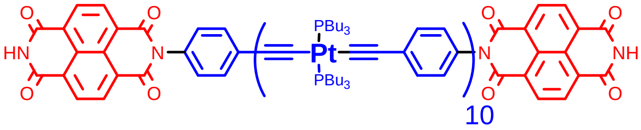

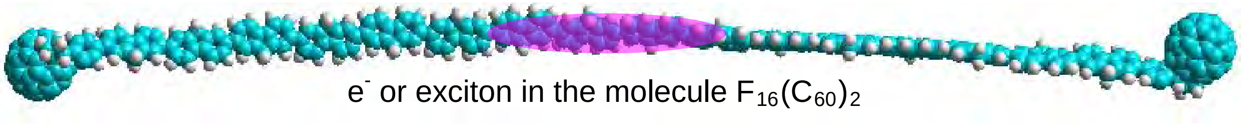

Recent publications

Takeda, N.; Asaoka, S.; Miller, J. R. "Nature and energies of electrons and holes in a conjugated polymer, polyfluorene" *J. Am. Chem. Soc.* **2006**, *128*, 16073-16082.

Cardolaccia, T.; Funston, A. M.; Kose, M. E.; Keller, J. M.; Miller, J. R.; Schanze, K. S."Radical ion states of platinum acetylide oligomers" *J. Phys. Chem. B* **2007**, *111*, 10871-10880.

Asaoka, S.; Takeda, N.; Iyoda, T.; Cook, A. R.; Miller, J. R. "Electron and hole transport to trap groups at the ends of conjugated polyfluorenes" *J. Am. Chem. Soc.* **2008**, *130*, 11912-11920.

CATALYST DESIGN AND ELECTRON TRANSFER MECHANISM BETWEEN THE MULTIPLE COMPONENTS OF A SOLAR ENERGY-DRIVEN WATER SPLITTING NANOSYSTEM

Aleksey E. Kuznetsov, Alexey L. Kaledin, Yurii Geletii, Tianquan Lian, Craig L. Hill,
Djamaladdin G. Musaev,

Emerson Center for Scientific Computation, and Department of Chemistry,
Emory University,
Atlanta, GA, 30322

The goal of our research project is to design stable nano-assembles for the efficient conversion of solar energy to fuel (H_2) by splitting water. Perhaps the most demanding aspect of this solar cell is to develop a robust and more efficient catalyst that captures the photogenerated hole to produce O_2 from H_2O. Previously, we have demonstrated [1] that Ru_2-substituted γ-Keggin polyoxotungstate complex, $\{\gamma\text{-}[(H_2O)Ru^{III}\text{-}(\mu\text{-}OH)_2\text{-}Ru^{III}(H_2O)][SiW_{10}O_{36}]\}^{4-}$, **1** could be such a catalyst. The stability and structure of **1** were predicted from computational studies and its Cs and TBA salts were prepared. However, in aqueous solution, **1** is not stable and rearranges to $[\{Ru_4O_4(OH)_2(H_2O)_4\}(\gamma\text{-}SiW_{10}O_{36})_2]^{10-}$, **2**, presumably via an oxidation mechanism.[2] Complex **2** is found to be very stable and capable of catalyzing the oxidation of water.

Computational results clearly demonstrate [3] that **1** can be easily oxidized. The reaction of **1** with O_2 is found to be highly exothermic, proceeds with a small energy barrier and leads to formation of $(H_2O)\{\gamma\text{-}[(O)Ru\text{-}(\mu\text{-}OH)_2\text{-}Ru(O)](H_2O)[SiW_{10}O_{36}]\}^{4-}$, **3**. The latter complex is better formulated as containing $Ru^{IV}{=}O\cdot$ units, rather than $Ru^{V}{=}O$ units. Water oxidation by **3** is found to be highly endothermic. The lack of reactivity of **3** towards the water molecule facilitates formation of the isolated [2] water oxidation catalyst, **2**.

Complex **2** catalyzes water oxidation using $[Ru(bpy)_3]^{2+}$ as a photosensitizer and persulfate as a sacrificial electron acceptor.[4] We examined the electron transfer mechanism between the visible photoexcited $[Ru(bpy)_3]^{2+*}$ and $S_2O_8^{2-}$, solvated in water, using the TD-DFT method.[5] The calculations support the existing experimental evidence for a short-lived, optically bright S_1 state (MLCT state) and its decay to lower-lying triplet states T_1/T_2. The lowest energy T_1 state leads to the observed products, i.e. $[Ru(bpy)_3]^{3+} + SO_4^{-} + SO_4^{2-}$. Detailed calculations of excited states, including spin-orbit coupling and bulk water effects, as well as use of an exciton interaction model, allow us to shed light on electron transfer dynamics and estimate the rate of transfer.

[1] D. Quiñonero, Y. Wang, K. Morokuma, L.A. Khavrutskii, B. Botar, Y.V. Geletii, C.L. Hill, D.G. Musaev, *J. Phys. Chem., B.* **2006**, *110*, 170-173.

[2] Y.V. Geletii, B. Botar, P. Kogerler, D.A. Hillesheim, D.G. Musaev, C.L. Hill, *Angew. Chem. Intern. Ed.* **2008**, *47,* 3896-3899

[3] A.E. Kuznetsov, Y.V. Geletii, C.L. Hill, K. Morokuma, D.G. Musaev, *J. Am. Chem. Soc.* **2009**, *ASAP*.

[4] Y.V. Geletii, Z. Huang, Y. Hou, D.G. Musaev, T. Lian, C.L. Hill, *J. Am. Chem. Soc.,* **2009**, *in revision*.

[5] A.L. Kaledin, Y.V. Geletii, C.L. Hill, T. Lian, D.G. Musaev, *J. Phys Chem. A.* **2009**, *submitted*

INFRARED LIGHT TRAPPING IN NANOCRYSTALLINE INVERSE OPAL PHOTOELECTRODES

Nathan R. Neale, Arthur J. Nozik, and Arthur J. Frank
Chemical & Biosciences Center
National Renewable Energy Laboratory
Golden, CO 80205

Research on sensitized photoelectrode materials as potential photoanodes and photocathodes in a tandem device for water electrolysis is presented. In this project, we have focused on developing porous conducting nanocrystalline semiconductor films to capture photogenerated charges from the photoactive electrode or from optically excited sensitizers (e.g., quantum dots and dyes) and transport them to the charge collecting substrate. We have explored inverse opals with the hope that they can enhance the optical absorption of the light-harvesting material by trapping otherwise weakly absorbed light near the inverse opal photonic band gap (PBG), a characteristic feature commonly observed in photonic crystals. Toward that end, we present the synthesis, characterization, and optoelectronic properties of CdSe inverse opal films.

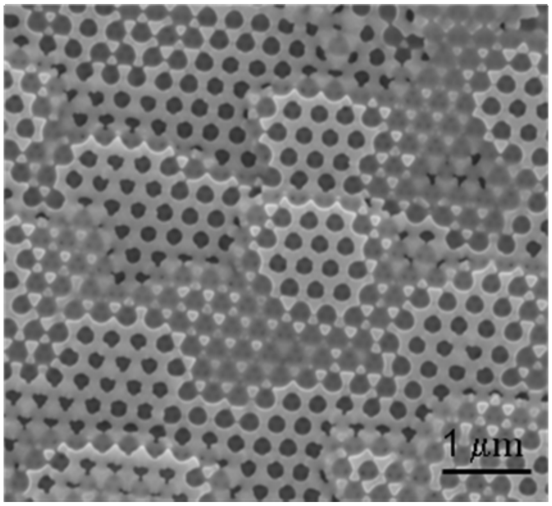

Figure 1: FE-SEM image of CdSe inverse opal film formed from 300 nm PS bead template.

CdSe films were prepared from electrodeposition within the pore space of self-assembled hexagonal close-packed polystyrene (PS) bead templates. After dissolving away the PS beads, the film pores replicate the size (300, 400, or 500 nm) and ordering of the template as shown in Figure 1. The as-deposited CdSe cubic crystallites making up the inverse opal architecture are 10–15 nm in diameter (cf. Bohr radius 5.4–7.0 nm) and thus exhibit a bulk band gap of ca. 1.75 eV.

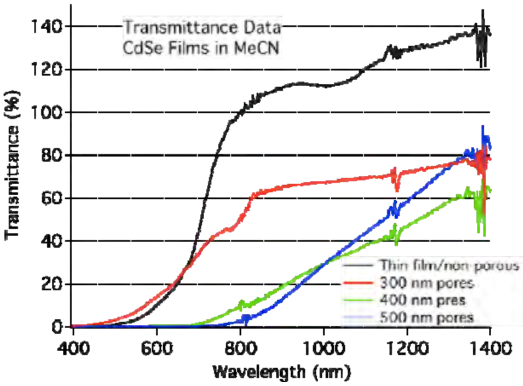

Figure 2: Transmittance data for non-porous and 300, 400 & 500 nm pore-sized inverse opal CdSe films in acetonitrile.

Interestingly, we find that the optoelectronic properties of the CdSe films are highly unusual. Typically, inverse opals display a strong PBG owing to the alternating pattern of high and low dielectric constant phases, which reflects light at the PBG and is observed as a dip in the transmittance spectrum. However, the data in Figure 2 show these CdSe inverse opal films exhibit only weak PBGs (e.g., 775 nm for the 300 nm pore size sample) and trap a significant degree of the infrared light, a phenomenon that can potentially be used to enhance the IR-absorption of low bandgap quantum dot or molecular sensitizers.

SENSITIZATION OF TITANIUM DIOXIDE SINGLE CRYSTALS WITH CdSe QUANTUM DOTS

Justin Sambur and B. A. Parkinson
Department of Chemistry and School of Energy Resources
University of Wyoming, Laramie WY 82071

Semiconductor quantum dots (QDs) have recently been employed as the light absorber in dye-sensitized solar cells (DSSCs). QDs are attractive sensitizers for several *possible* reasons including increased light absorption, the ability to tune the band gap(s) to effectively absorb the solar spectrum, increased stability and the possibility of realizing a quantum efficiency >1 via multiple exciton generation. However their potential as superior sensitizers has yet to be experimentally verified. Herein we directly compare the performance of the prototypical *cis*-di(thiocyanato)-bis(4,4′-di-carboxy-2,2′ bipyridine) ruthenium(II) dye (N3) and CdSe QDs adsorbed onto TiO_2 single crystal photoanodes, as well as provide evidence for the low QD surface coverages reported in the QD-sensitized nanocrystalline TiO_2 (nc-TiO_2) literature.

We determined that our inability to reproducibly measure electron injection from QDs on TiO_2 crystals, using sensitization procedures in the literature for binding CdSe QDs to nc-TiO_2, was primarily due to residual trioctylphosphine (TOP) which serves to passivate the surfaces of CdSe QDs but also strongly binds to the TiO_2 surface. Figure 1 demonstrates the detrimental effect on dye surface coverage due to the presence of excess capping molecules in the sensitization solution. Single crystal samples exposed to TOP or 3-mercaptopropionic acid (MPA is a bifunctional linker molecule commonly used to bind CdSe QDs to TiO_2) prior to dye adsorption showed greatly reduced sensitization current due to the competitive binding of surface sites by the excess capping agents. Therefore, we chose to avoid the use of bulky strongly surface-active organic surfactants in the QD sensitization solutions and instead synthesized CdSe QDs passivated with MPA directly in water. Although the QDs synthesized in water do not exhibit high mondispersity, we have observed reproducible sensitized photocurrents that are stable for weeks.

Figure 2 shows the direct comparison of CdSe QDs and N3 on the same rutile (110) single crystal using a Co(II) di-*tert*-butyl tris-bipyridine regenerator in acetonitrile electrolyte. AFM images indicate agglomeration of QDs, however a step height of ~3nm in AFM images indicates close to monolayer coverage. The benefit of using a semiconductor QD as a light-absorber is evident at blue wavelengths.

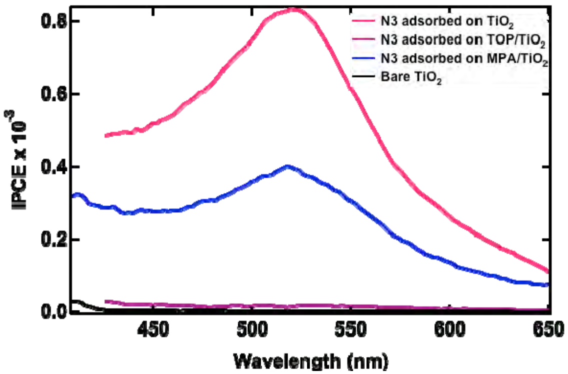

Figure 1. Sensitization spectra for N3 on anatase(101) single crystals were sensitized with on bare (pink), TOP-exposed (purple) and MPA-exposed surfaces.

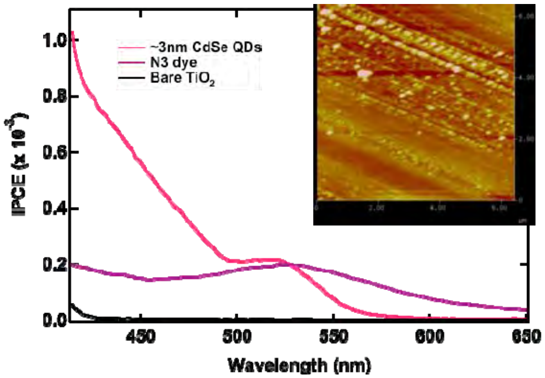

Figure 2. Rutile (110) single crystal sensitized with ~3nm CdSe QDs capped with MPA and N3 for comparison. Inset: AFM image of QDs on rutile where an intentional scratch was used to measure the stepheight of the monolayer.

FEMTOSECOND KERR-GATED FLUORESCENCE MICROSCOPY

Lars Gundlach and Piotr Piotrowiak
Department of Chemistry
Rutgers University
Newark, New Jersey 07102

A newly constructed Kerr-gated fluorescence microscope was applied to spatially, temporally, and spectrally resolve the early luminescence dynamics, charge transport and charge carrier localization in single CdSSe semiconductor nanobelts. Microscopic emission “movies” consisting of 100 fs frames, as well as time resolved luminescence spectra of individual nanobelts, were recorded. CdS_xSe_{1-x} alloys are important members of the family of ternary chalcogenides and are often investigated for potential photovoltaic applications. They exhibit a remarkably broad range of stoichiometries which allows materials with a continuous spectrum of bandgaps to be prepared. Their morphology can be also easily controlled. Q-dots, nanowires, nanobelts and other forms of CdSSe have been grown either in solution or by vapor deposition.

Our femtosecond microscopy experiments reveal complex, nonlinear carrier dynamics in the $CdS_{0.7}Se_{0.3}$ nanobelts. We were able to determine rates for relaxation pathways that are linear (Shockley-Read), quadratic (non-geminate), and cubic (Auger) in the carrier concentration. Such quantitative analysis would have been impossible on the basis of ensemble averaged measurements because the excitation cross-section of the nanobelts is strongly orientation dependent and the recombination dynamics depends on the shape of the particle. The dependence of carrier dynamics on the morphology of the particle is interesting in the context of the carrier multiplication (CM) or multiple exciton formation (MEF) reported for some of the heavier chalcogenides. The spatial distribution of the luminescence collected from larger nanobelts was highly structured (Fig.1b) and exhibited pronounced localization at the tip of the wedge-shaped nanobelt. This confinement effect is of purely classical nature as the dimensions of the investigated nanobelt are well above the onset of quantum size effects in CdS or CdSe. We tentatively ascribe it to the enhanced carrier recombination in the confined areas of the particle due to greater surface scattering and e-hole correlation.

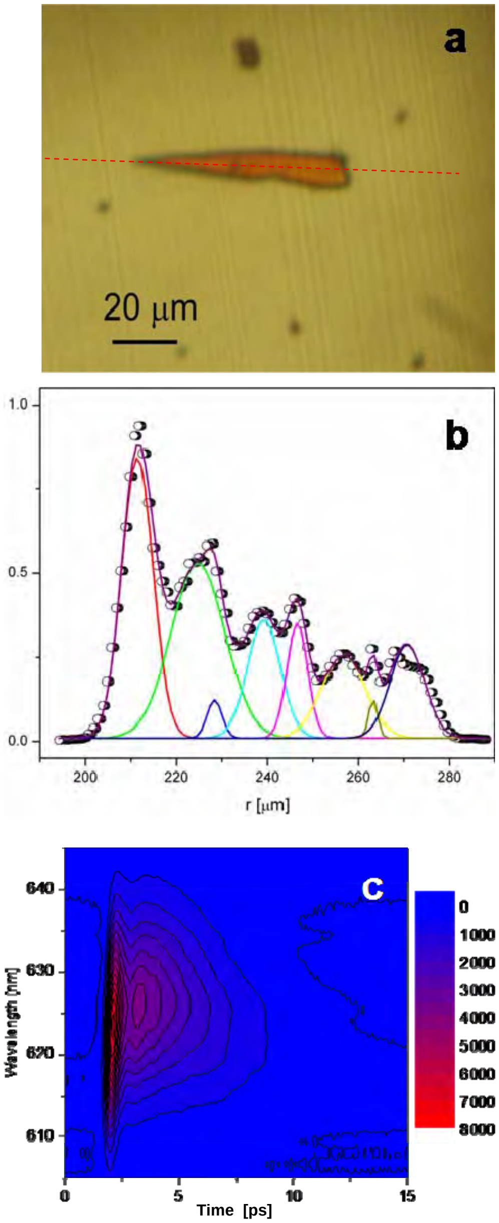

Fig.1. (a) A single 70×10 µm, 100 nm thick CdSSe nanobelt; **(b)** spatial emission cross-section collected 100 fs after the excitation; **(c)** spectrally and temporally resolved emission of the same nanobelt.

PHOTOINDUCED CHARGE SEPARATION IN POLYMER-C_{70}-FULLERENE COMPOSITES: HIGH-FREQUENCY PULSED EPR SPECTROSCOPY

Oleg Poluektov,[1] Juan Delgado,[2] Nazario Martín,[2] Andreas Sperlich,[3] Vladimir Dyakonov[3]
[1]Chemical Sciences and Engineering Division, Argonne National Laboratory,
9700 South Cass Avenue, Argonne, IL 60439, USA
[2]Department of Organic Chemistry, Universidad Complutense de Madrid,
28040, Madrid, Spain
[3]Experimental Physics VI, Physical Institute, Julius-Maximilians-University of Würzburg,
D-97074 Würzburg, Germany

Photovoltaic (PV) cells are the most promising man-made devices for solar energy utilization. As in natural photosynthesis, the most important step for PV solar energy conversion is the generation and separation of charges. PV systems can be classified into three major groups based on the active media: inorganic, hybrid, and organic devices. Although current organic based PVs do not exhibit high conversion efficiency, these systems have considerable potential because of their low-cost fabrication and tunability of the organic materials. Recently, a substantial improvement in efficiency has been demonstrated for PVs based on composites of conjugated polymers with fullerene C_{60}-derivatives. One of the downsides of C_{60}-PCBM acceptor material is a very low absorption coefficient in the visible region of the light, which can be considerably improved by replacement of C_{60} with C_{70} molecules. While the understanding of the elementary steps of efficient charge separation and charge dynamics in the organic photovoltaic materials is a prerequisite to be able to improve the efficiency of organic PV cells, not much is known about these processes in C_{70} containing composites.

Here we report on the investigation of charge polarons in thin films of polymer-fullerene composites by light-induced electron paramagnetic resonance (EPR) at 9.5 GHz (X-Band) and 130 GHz (D-Band). The materials studied were poly(3-hexylthiophene) (PHT) and soluble C_{70}- and C_{60}-derivates. Owing to the superior spectral resolution of the high-frequency D-band (130 GHz) EPR spectrometer we were able to differentiate light-induced signals from P^+ and P^-. Comparison of signals from C_{70}-derivatives with different side-chains allowed us, for the first time, to confirm that the polaron is localized on the cage of the C_{70} molecule. Considerable narrowing of the light-induced EPR lines were observed upon solvent removal and annealing of the blends. This reflects an increase in delocalization of the charges and is in agreement with the shortening of relaxation T_1-time in thin films.

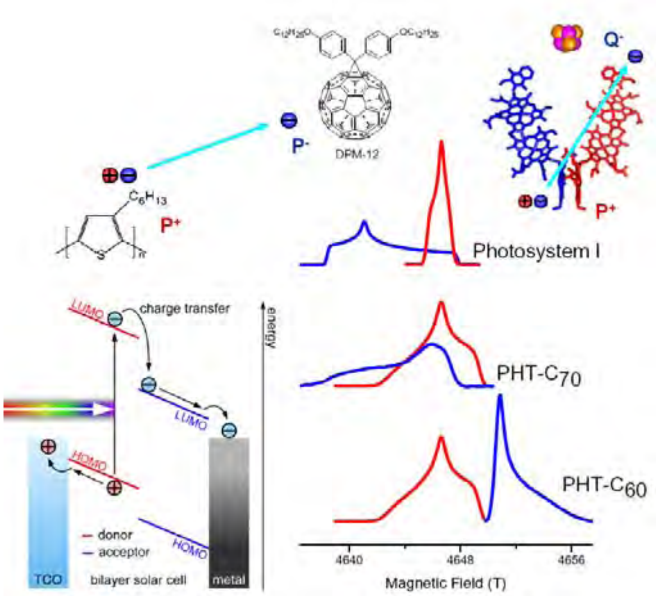

Figure 1. *Schematic representation of the charge separation process in polymer-fullerene composites in comparison with photosystem I. Related HF EPR spectra are shown for positive (red) and negative (blue) polarons.*

HIGH LEVEL AB INITIO CALCULATIONS OF PHOTOEXCITED STATES AND ELECTRON-PHONON INTERACTIONS IN SEMICONDUCTOR QUANTUM DOTS

Oleg. V. Prezhdo
Department of Chemistry
University of Washington
Seattle, WA 98195-1700

We demonstrated for the first time using a combination of the Hartree-Fock approximation and the symmetry adapted cluster theory with configuration interaction (SAC-CI) that multiple excitons (ME) in PbSe and CdSe QDs can be generated directly upon photoexcitation. At energies 2.5-3 times the lowest excitation, almost all optically excited states in Pb_4Se_4 become MEs, while both single excitons and MEs are seen in Cd_6Se6. We analyzed the high-level SAC-CI results of the small clusters based on the band structure and then extended our band structure analysis to $Pb_{68}Se_{68}$, $Pb_{180}Se_{180}$, $Cd_{33}Se_{33}$, and $Cd_{111}Se_{111}$. Our results explained the ultrafast generation of MEs without the need for the phonon-bottleneck and clarify why PbSe is particularly suitable for generation of MEs.

Further, using the same technique we showed that charging of small PbSe QDs greatly modifies their electronic states and optical excitations. Conduction and valence band transitions that are not available in neutral QDs dominate low energy electronic excitations and show weak optical activity. At higher energies these transitions mix with both single excitons (SEs) and MEs associated with transitions across the band-gap. As a result, both SEs and MEs are significantly blue-shifted, and ME generation is drastically hampered. The overall contribution of MEs to the electronic excitations of the charged NCs is small even at very high energies. The calculations support the recent view that the observed strong dependence of the ME yields on the experimental conditions is likely due to the effects of QD charging.

A dephasing mechanism of multiple exciton fission (MEF) in semiconductor quantum QDs was proposed, and dephasing times that govern luminescence linewidths, ME generation (MEG) and MEF were studied in a Si QD. MEF took hundreds of femtoseconds. In contrast, luminescence and MEG dephasing times were all sub-10fs. Generally, dephasing was faster for higher-energy and higher-order excitons, and increased temperatures. MEF was facilitated only by low-frequency acoustic modes, while luminescence and MEG coupled to both acoustic and optical modes. The detailed atomistic simulations of the photoexcitation and dephasing processes advance understanding of exciton dynamics in QDs for solar hydrogen production.

SYNTHESIS AND PHOTOPHYSICS OF LINEAR, BRANCHED AND DENDRIMERIC CONJUGATED POLYELECTROLYTES

Seoung Ho Lee, Xiaoyong Zhao, Prasad Tarenekar, Sevnur Kumurlu, Gustavo Moriena,
Quentin Bricaud, Valeria D. Kleiman, John R. Reynolds and Kirk S. Schanze
Department of Chemistry, University of Florida, Gainesville, FL, 32611-7200

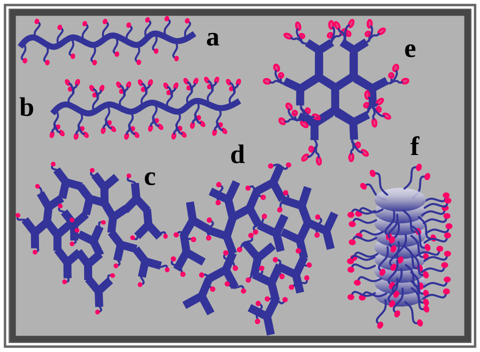

Variable band gap conjugated polyelectrolytes (CPEs) and conjugated polyelectrolyte dendrimers (CPDs) have been developed as energy and charge transporting materials that can be assembled into nanoscale structures with controllable architectures.(1) These materials have absorption and emission spectra that span the visible spectrum with structural architectures having disrupted inter- and intra-chain interactions which control exciton transport and amplified quenching phenomena. The extent of repeat unit ion density is compared in linear CPEs having single (**a**) and dendritic (**b**) appended pendant groups. Disrupted interactions are introduced through hyperbranching in which the ions can be placed as terminal units (**c**), or embedded internally (**d**) in the branched structure, along with fully dendrimeric polyelectrolytes (**e**) with exact molecular structures. Finally, helical CPEs (**f**) were developed to allow comparison of intra- and inter-chain energy and charge transport processes.

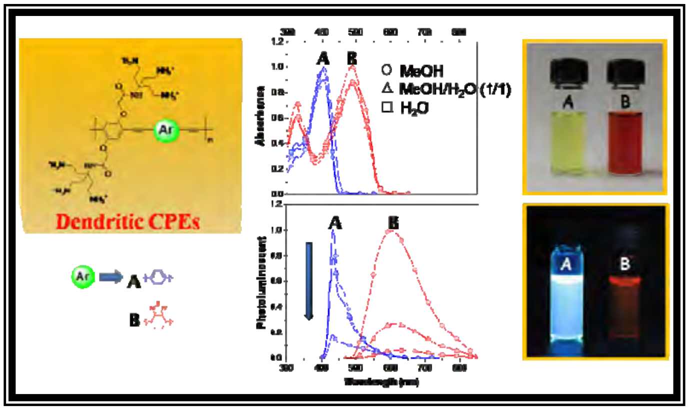

This approach is detailed by the results for two members of the cationic poly(*p*-phenylene ethynylene) (PPE) CPE family shown with phenylene (high gap) and benzothiadiazole (BTD) (low gap) linkages modifying the electronic structure. While the absorbance results demonstrate band gap narrowing (color change of yellow to red), aggregation effects are exemplified by the reduced fluorescence intensity as the solvent is changed from methanol to water.

The different CPE architectures lead to inter-chain aggregation, which controls exciton transport and amplified quenching phenomena. Aggregates were characterized by monitoring quenching efficiency under the influence of the aggregate-forming Ca^{2+} and by anisotropy experiments in H_2O/CH_3OH mixtures. Results show that linear and helical CPEs form π–π stacking aggregates. The aggregates formed with linear CPEs maintain the rigid rod structure of the isolated chains. Energy transfer was observed between isolated CPE chains and from the isolated chains to the aggregates on time scales shorter than 50 ps.(2) Ultrafast experiments with a donor CPE and ionic dye acceptors show the contribution to quenching from their strong ionic association and the amplification of quenching due to the intra-chain exciton transport.

1. Jiang, H.; Taranekar, P.; Reynolds, J. R.; Schanze, K. S. *Angew. Chem.*, in press.
2. Hardison, L. M. *et.al. J. Phys. Chem. C* **2008**, *112*, 16140–16147.

CONJUGATED POLYELECTROLYTE FILMS:
MORPHOLOGY, ENERGY TRANSPORT AND CHARGE INJECTION

Jarrett Vella[†], Quentin Bricaud[†], Hui, Jiang[†], Justin Sambur[§], Derek LaMontagne[†], Bruce A. Parkinson[§], Valeria D. Kleiman[†], John R. Reynolds[†] and Kirk S. Schanze[†]
[§]Department of Chemistry, University of Wyoming, Laramie, WY 82071 and
[†]Department of Chemistry, University of Florida, Gainesville, FL, 32611-7200

Conjugated polyelectrolytes (CPEs) are soluble in water and polar organic solvents and their comparatively high carbon atom:ionic charge ratio induces an ability to adsorb on oxide surfaces and makes them amphiphilic giving them a strong tendency to self-assemble into aggregates and other self-organizing structures in aqueous solution. Because of their polyelectrolyte nature, CPEs can also be deposited as nanostructured films via the layer-by-layer (LbL) polyelectrolyte deposition method. Here, the photophysical properties of molecularly dissolved CPE chains are contrasted with those of CPEs adsorbed on glass, quartz, and ITO/glass, along with single crystal (sc) and nanocrystalline (nc) TiO_2 surfaces, along with LbL films designed for vectorial energy and charge transport characteristics.

In one line of investigation, a series of carboxylate functionalized variable gap poly(p-phenylene ethynylene) (PPE) and polyfluorene (PF) based CPEs have been utilized. The HOMO-LUMO gap is varied across the series with absorption maxima ranging from 400 to 500 nm. The CPEs adsorb effectively from solution onto nc-TiO_2 films, giving rise to TiO_2/CPE films that absorb ~90% of the incident light at the absorption band maximum.[1] The photocurrent generation efficiency of the TiO_2/CPE films using an I_3^-/I^- propylene carbonate electrolyte and Pt/FTO counter electrode shows most of the films exhibit peak quantum efficiency ~50% at wavelengths corresponding to the polymers' absorption band maximum. The photocurrent generation efficiency for the lowest band gap polymer linked with a benzothiadiazole unit is reduced due to efficient non-radiative decay of excitons at trap sites arising from inter-chain contacts distal from the TiO_2/CPE interface. Ongoing studies are exploring the structure of the adsorbed CPE films on single crystal TiO_2 surfaces, and this work will shed light on the mechanism for exciton transport to the polymer-semiconductor interface.

Turning attention to LbL films, it is commonly assumed that a linear increase in light absorption as a function of the number of bilayers deposited suggests a uniform structure. Careful analysis of the fluorescence characteristics of LbL films using CPEs co-deposited with non-conjugated polyelectrolytes shows an initial increase in emission, followed by a decrease as the number of bilayers is increased. This is attributed to aggregate formation (as opposed to discrete layering) inducing a quenching of the CPE emission.

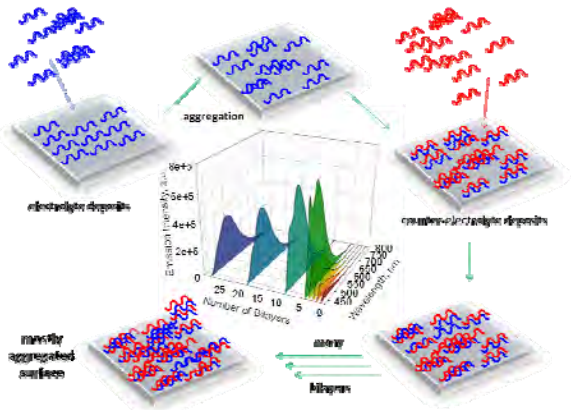

---

1. Jiang, H.; Zhao, X.; Shelton, A. H.; Lee, S. H.; Reynolds, J. R.; Schanze, K. S. *Appl. Mater. & Inter*, **2009**, *1*, 381-387.

LONG WAVELENGTH VISIBLE LIGHT ABSORBING CHROMOPHORES WITH LIFETIMES EXTENDED *VIA* REVERSIBLE ENERGY TRANSFER

Jing Gu, Jin Chen and Russell Schmehl
Department of Chemistry
Tulane University
New Orleans, LA 70118

The development of transition metal complex chromophores that absorb significantly in the green and red portions of the visible often results in complexes with very short excited state lifetimes. This is especially true for complexes having metal-to-ligand charge transfer excited states, where synthetic manipulation to generate longer wavelength charge transfer absorption is generally accompanied by a concomitant lowering of ligand field excited states that result in facile paths for nonradiative relaxation. Thus, while $[(bpy)_3Ru(II)]^{2+}$ (bpy = 2,2'-bipyridine) has absorption at 450 nm and a 2 eV excited state with a nearly 1μs lifetime, $[(bpy)_2Ru(II)Cl_2]$ has a MLCT maximum at 550 nm (in acetonitrile) but the lower energy excited state is very short lived (< 5 ns) in solution at room temperature and also in low temperature matrices (no luminescence is observed).

One approach to exploiting the longer wavelength MLCT absorption of such complexes is to employ diimine ligands that have substituents with localized excited states lower in energy than the MLCT state. For example, the triplet energies of bpy, 4-(1-pyrenyl)-bpy (bpy-pyr) and 4-(2-(1-pyrenyl)vinyl)-bpy (bpy-v-pyr) are 2.8, 2.0 and 1.8 eV, respectively. For the complexes $[(L)_2RuCl_2]$, the only complex that has an excited state lifetime in excess of 10 ns is the bpy-v-pyr complex, which has a lifetime of several hundred nanoseconds (see figure below). In addition, the $[(bpy\text{-}v\text{-}pyr)_2RuCl_2]$ complex has a very low one electron oxidation potential (+0.1 V vs SCE) and, given the calculated energy of the ligand (bpy-v-pyr) triplet excited state, the photoexcited complex should be a very strong one electron reducing agent.

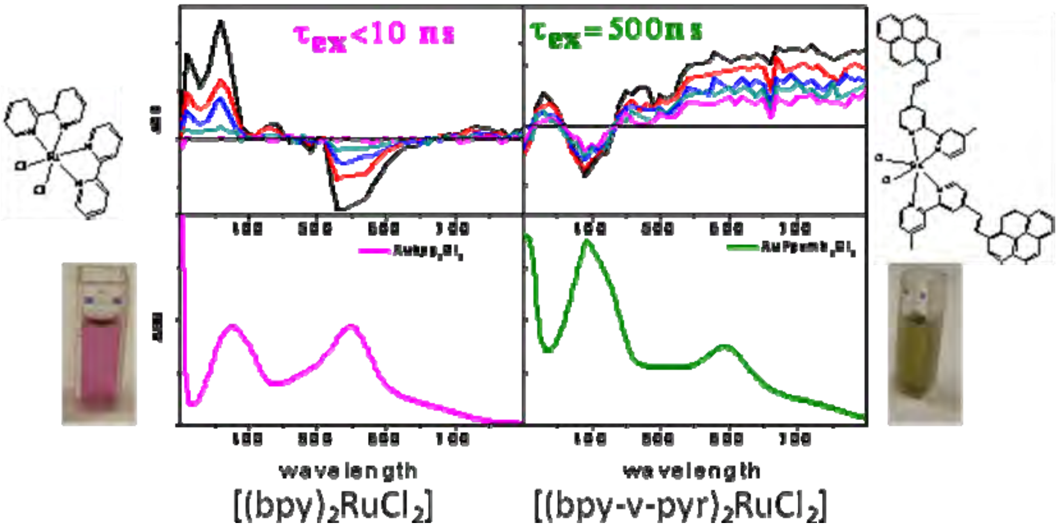

The work has been expanded to include a variety of other spectator ligands.

PROBING INTERFACIAL ELECTRON TRANSFER USING THz SPECTROSCOPY

C. P. Richter, R. L. Milot, Gonghu Li, R. H. Crabtree, G. W. Brudvig,
V. S. Batista and C. A. Schmuttenmaer
Department of Chemistry
Yale University
225 Prospect St. P.O. Box 208107, New Haven, CT 06520-8107

Nanocrystalline wide-band gap semiconductors such as TiO_2 have shown great promise in the areas of dye-sensitized solar cells and photocatalytic materials. Optimization of these devices requires an understanding of each of the individual processes that contribute to the overall efficiency: Photon capture, electron injection, electron transport within the nanocrystalline material, minimization of charge recombination and charge trapping, to name a few. A significant advantage of probing charge injection with THz spectroscopy compared to measuring overall efficiencies is that it focuses solely on charge injection and carrier mobility of the injected electrons.

To this end, this poster builds on our recent efforts in which experimental and computational techniques verify charge injection and separation from sensitizers into TiO_2 nanoparticles (NPs). We have characterized a variety of anchors, linkers, and types of TiO_2 NPs, and show how a combination of THz spectroscopy, UV/vis studies, and low-temperature EPR spectroscopy can provide a full picture of the charge injection process.

We have found that THz measurements of charge injection and carrier mobility often, but not always, correlate strongly with overall performance. We present new results for anchor/linker systems such as hydroxamate-functionalized terpyridine and *p*-methyl red, and the influence of $TiCl_4$ treatment prior to sensitization. In addition to the THz measurements and overall efficiencies, a detailed study of the general light-harvesting ability of these compounds has been carried out *via* their UV-vis absorption, reflection, and transmission properties.

An illustrative example of this approach is found in mixtures of ~100 nm diameter TiO_2 anatase NPs with ~20 nm × ~100 nm TiO_2 rutile nanorods (NRs). It is found that a relatively small fraction of the rutile NRs greatly enhances both the overall efficiency of a dye-sensitized solar cell in which this mixture makes up the photoanode, as well as the injection and mobility dynamics as measured with THz spectroscopy. Figure 1 presents a schematic of this arrangement as well as the measured results. We see that at ~10% rutile content, the performance is far better than can be expected from influences such as exposed surface area or dye concentration. The underlying reasons for this behavior will be discussed.

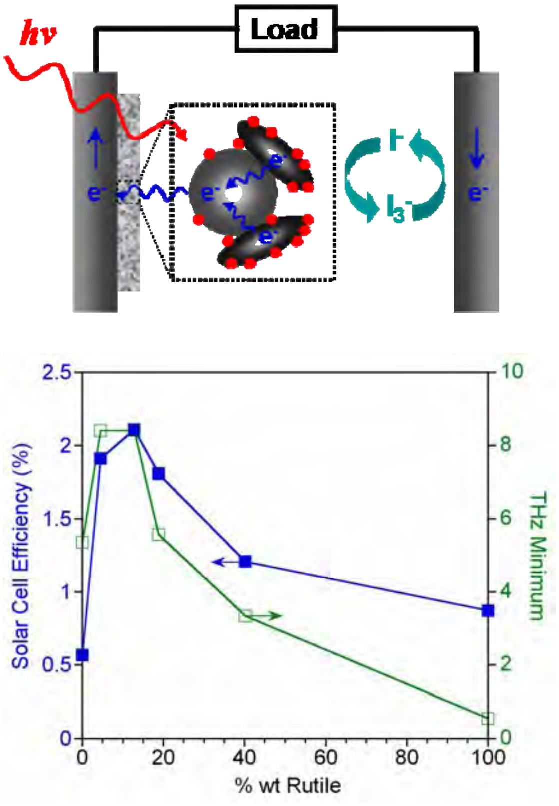

Figure 1. Top: Schematic representation of mixture of dye-sensitized anatase NPs with rutile NRs. Bottom: Overall cell efficiency and THz injection efficiency as a function of rutile NR fraction.

SINGLE-CHAIN, HELICAL WRAPPING OF INDIVIDUALIZED, SINGLE-WALLED CARBON NANOTUBES BY IONIC POLY(ARYLENEETHYNYLENE)S PROVIDE DIVERSE ORGANIC SOLVENT SOLUBILITY

Pravas Deria,[a,c] Youn K. Kang,[a] One-Sun Lee,[a] Sang Hoon Kim,[b] Tae-Hong Park,[a] Dawn A. Bonnell,[b] Jeffery G. Saven,[a] and Michael J. Therien[c]

[a]*Department of Chemistry, University of Pennsylvania, 231 South 34th Street, Philadelphia, PA 19104*
[b]*Department of Materials Science and Engineering, University of Pennsylvania, 3231 Walnut Street, Philadelphia, PA 19104;*
[c]*Department of Chemistry, French Family Science Center, 124 Science Drive, Duke University, Durham, NC 27708*

Amphiphilic, linear conjugated poly[*p*-{2,5-bis(3-propoxysulfonicacidsodiumsalt)} phenylene]ethynylene (**PPES**) and poly[2,6-{1,5-bis(3-propoxysulfonicacidsodiumsalt)} napthylene]ethynylene (**PNES**) efficiently disperse single-walled carbon nanotubes (SWNTs) under ultra-sonication conditions into the aqueous phase. Vis-NIR absorption spectroscopy, atomic force microscopy (AFM), and tunneling electron microscopy (TEM) demonstrate that these solubilized SWNTs are individualized. AFM and TEM data reveal that the interaction of **PPES** and **PNES** with SWNTs gives rise to a self-assembled superstructures in which a polymer monolayer helically wraps the nanotube surface; the observed **PPES** and **PNES** pitch lengths confirm structural predictions made via MD simulations. Following appropriate metathesis reactions, these self-assembled polymer-nanotube systems can be dissolved in organic solvents; AFM and TEM data confirm that the **PNES** helical wrapping structure observed for individualized SWNTs in aqueous solution persists in nonaqueous media. Pump-probe transient absorption spectroscopy reveals that the excited state lifetimes and exciton binding energies of these structurally well-defined nanotube-semiconducting polymer hybrid structures remain unchanged relative to benchmark data acquired previously for standard sodium dodecylsulfate (SDS)-SWNT suspensions, regardless of solvent. These results demonstrate that single-chain, helical wrapping of single-walled carbon nanotubes by ionic poly(aryleneethynylene)s provides a well-defined structural motif that solubulizes SWNTs in wide range of dielectric media while preserving established nanotube semi-conducting and conducting properties.

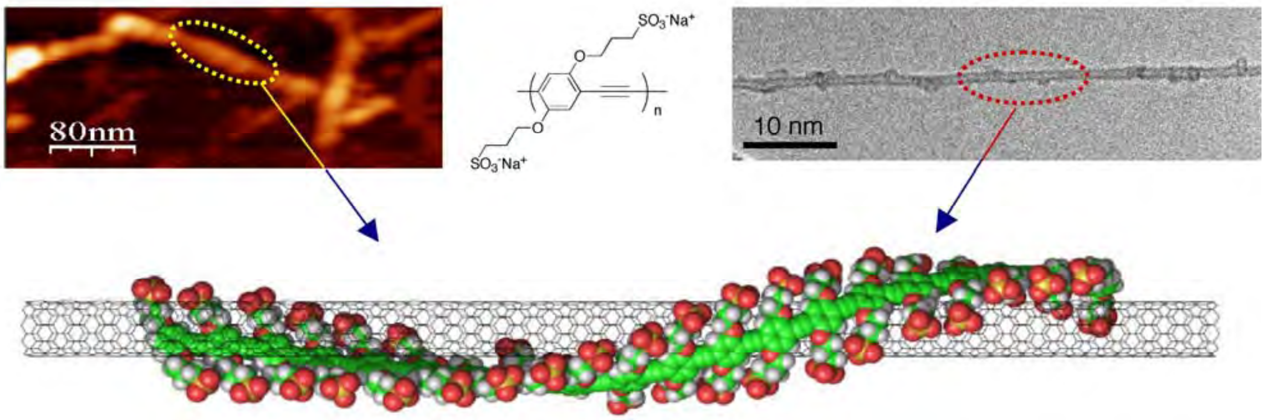

NANOCRYSTAL-BASED DYADS FOR SOLAR TO ELECTRIC ENERGY CONVERSION

M. Wu[a], G. Gotesman[b], P. Mukherjee[a], R. Naaman[b] and D.H. Waldeck[a]
a: Chemistry Department, University of Pittsburgh, Pittsburgh PA 15260
b: Chemical Physics Department, Weizmann Institute of Science, Rehovot ISRAEL

This project aims to develop a systematic and modular approach to creating a new generation of Grätzel-inspired solar energy conversion devices with the following novel advantages: ability to capture the entire available range of solar irradiance by employing sets of linked nanoparticles, fabrication accessible via self-assembly, enhanced robustness and lowered cost through use of nanostructured, rather than molecular, charge transfer elements. We will describe our progress toward creating and characterizing linked-nanoparticle aggregates that undergo vectorial charge transfer, with the ultimate aim of using them as the charge separation "engine" in new generation solar cells.

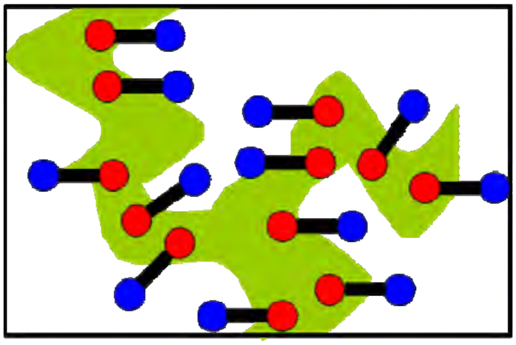

Figure 1. This cartoon illustrates localization of the dyads (red and blue dumbbells) between two phases, which form the anode (green) and cathode (white) of a photoelectric device that can be optically thick but physically thin.

The directional nature of the electron transfer is defined by the energy band alignment of the nanoparticles that are linked together by organic tethers. We report on the use of a model system of monolayer and bilayer assemblies of nanoparticles to quantify the Type II energy alignment of CdSe/CdTe nanoparticles by both UV photoemission spectroscopy and 'dark' electrochemistry. For example, Figure 2 plots the HOMO energies and LUMO energies as a function of the nanoparticle diameter.

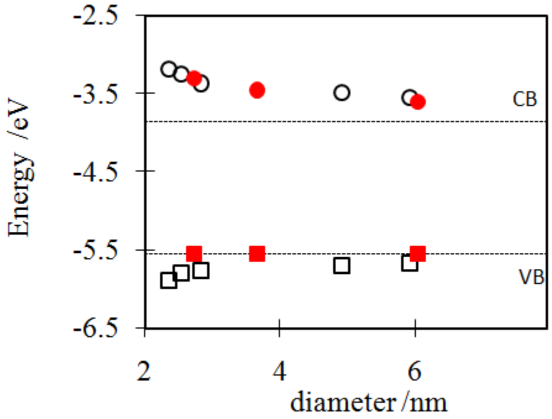

Figure 2. The graph plots the HOMO energies (open squares from electrochemistry and filled squares from photoemission measurements) and LUMO energies (open circles from electrochemistry and filled circles from photoemission measurements) of the different CdSe NPs as a function of their diameter. The dashed lines mark the bulk CdSe band positions, assuming that its valence band is pinned at 1.25 eV below the Fermi level of Au.

In addition, we report on the electron transfer between the CdSe and CdTe nanoparticles in aggregates (dimers and higher multimers) by way of time-resolved spectroscopy.

DIRECT MEASUREMENT OF PHOTOINDUCED CHARGE SEPARATION DISTANCES IN DONOR-ACCEPTOR SYSTEMS FOR ARTIFICIAL PHOTOSYNTHESIS

Raanan Carmieli, Annie Butler Ricks, Qixi Mi, Emilie M. Giacobbe, Sarah M. Mickley, and
Michael R. Wasielewski
Department of Chemistry and Argonne-Northwestern Solar Energy Research (ANSER) Center,
Northwestern University, Evanston, IL 60208

The distance over which two photogenerated charges are separated in electron donor-acceptor systems for artificial photosynthesis depends on the structure of the system, while the lifetime of the charge separation, and ultimately its ability to carry out useful redox chemistry, depend on the electronic coupling between the oxidized donor and reduced acceptor. The radical ions produced by charge separation are frequently delocalized over the π systems of the final oxidized donor and reduced acceptor, so that there is often significant uncertainty as to the average distance between the separated charges, especially in low dielectric constant media, where the Coulomb attraction of the ions may be significant and the charge distribution of the ions may be distorted, so that the average distance between them may be shorter than that implied by their chemical structures. The charge separation distances between photogenerated radical ions in three donor-acceptor molecules having different donor-acceptor distances were measured directly from their dipolar spin-spin interactions (D) using out-of-phase electron spin echo envelope modulation (OOP-ESEEM). The measured distances in toluene at 85K compare favorably to the calculated distances between the centroids of the spin distributions of the radical ions within the radical ion pairs. These results show that despite the intrinsically nonpolar nature of medium, the spin (and charge) distributions of the RPs are not significantly distorted by Coulomb attraction over these long distances. This study shows that OOP-ESEEM is well-suited for probing the detailed structural features of charge-separated intermediates that are essential to understanding how to design molecular structures that prolong and control charge separation for

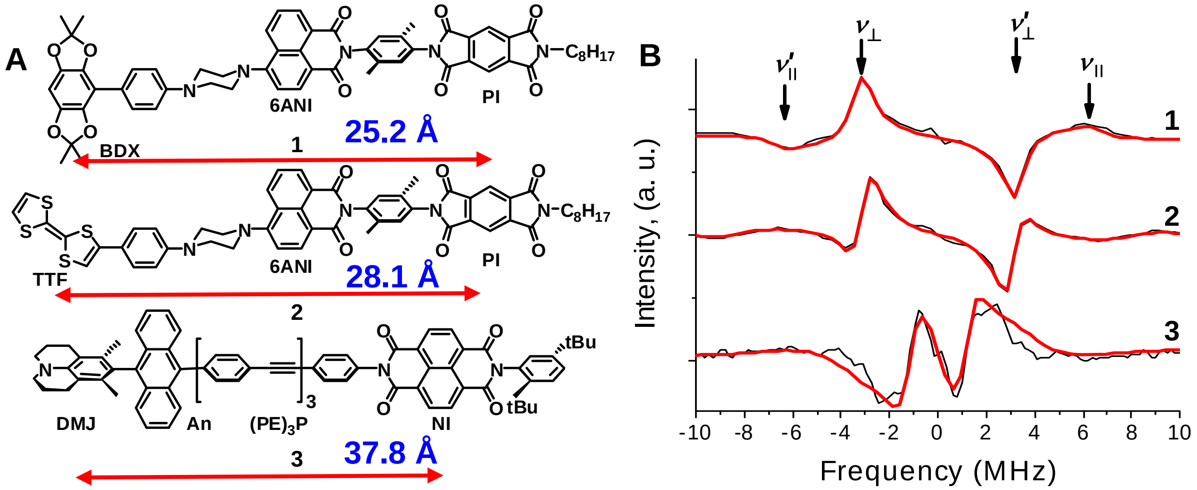

A) Structures of donor-acceptor triads. **B)** Sine Fourier transformation (SFT) of the time domain OOP-ESEEM data for **1-3**. The smooth curves superimposed on the experimental spectra are the SFT of the fit function. The value of D can be determined from $\nu_\perp$ and $\nu_\|$ (or $\nu'_\perp$ and $\nu'_\|$) using $D = (\nu_\perp - \nu_\|)/2$. The RP distances were calculated using the point dipole approximation, $D = -2785\ \text{mT}\cdot\text{Å}/r^3$

MULTISTAGE PHOTOCELL FOR WATER SPLITTING

Marye Anne Fox, James K. Whitesell, and Xuebin Shao
Department of Chemistry and Biochemistry
University of California, San Diego
La Jolla, CA and 92039

We are in the process of constructing a practical photolytic system for quantum efficient production of hydrogen. Our approach is based on the assembly of a multi-component integrated system for direct photocatalytic splitting of water for the efficient production of hydrogen. We propose to produce hydrogen as an energy source that is cost competitive with fossil fuels and without the concommitant production of greenhouse gases.

The concept is quite straight forward. In order to achieve the over potential required for direct water splitting, the device is composed of multiple dye-sensitzed cells directly linked in series, as illustrated in the figure below. The advantage of this concept is that each cell need contribute only a fraction of the overall potential required for water splitting, thus permitting device engineering to maximized efficiently without regard to electric potential.

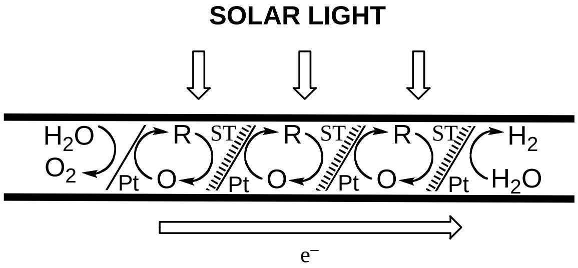

ST = Sensitizer dispersed on metal oxide or polymer support
Pt = Platinum
R = Reduced Species
O = Oxidized Species

A multipanel dye-sensitized water-splitting device composed of three such panels arranged in series.

Krishnan, M.; White, J.R.; Fox, M.A.; Bard, A.J. *J. Am. Chem. Soc.* **1983**, *105,*7002.

Smotkin, E. Bard, A.J.; Campion, A.; Fox, M.A.; Mallouk, T.; Webber, S.E.; White, J.M. *J. Phys. Chem.* **1986**, *90,* 4604.

Smotkin, E. Bard, A.J.; Campion, A.; Fox, M.A.; Mallouk, T.; Webber, S.E.; White, J.M. *J. Phys. Chem.* **1987**, *91,* 6.

Dabestani, R.; Bard, A.J.; Campion, A.; Fox, M.A.; Mallouk, T.; Webber, S.E.; White, J.M. *J. Phys. Chem.* **1988**, *92,* 1872.

METAL-LINKED ARTIFICIAL OLIGOPEPTIDES AS PHOTOINITIATED MOLECULAR WIRES

Carl P. Myers, Lauren A. Levine, Joy A. Gallagher, Richard M. Kelly, and Mary Elizabeth Williams*
Department of Chemistry
The Pennsylvania State University
University Park, PA 16802

The controlled assembly of multimetallic artificial oligopeptides using modular, interchangeable units provides a library of architectures for photoinitiated charge separation. Similar to nucleic acid recognition in DNA, artificial oligopeptides are cross-linked by metal bonds, thereby acting as scaffolds for heterofunctional inorganic molecular antennas. We synthesize artificial oligomeric peptides that use transition metal coordination to self-assemble multimetallic, polyfunctional double stranded duplexes. Our synthetic strategies use modular amino acid units linked by amide bonds to construct multimetallic oligopeptides with unique sequences. Directed self-assembly of the peptides using metal chelation will ultimately be employed to construct useful supramolecular structures for photochemical conversion of energy. In the metal-linked duplexes, the oligopeptide scaffold directs and enforces the arrangement of inorganic chromophores, donors and acceptors to enable charge and energy transfers: these assemblies are multimetallic, photoinitiated molecular wires.

Our group has begun to synthesize metal-linked artificial peptide duplexes with the two general structures in Figure 1. Both molecules are designed to reduce the number of possible structural isomers. The top structure is a $Ru(bpy)_3^{2+}$ molecule that has been synthesized to contain two attached oligopeptide chains bearing pendant bipyridine ligands for coordination to another transition metal ion. Metal binding crosslinks the two chains in a loop analogous to nucleic acid hairpins. Our initial studies have investigated the impact of Cu^{2+} binding to a series of these hairpin structures that vary the number and distances of the pendant bpy complexes. Figure 2 contains a representative emission spectrum for one of these complexes, and shows how this changes during titration of Cu^{2+} into the solution.

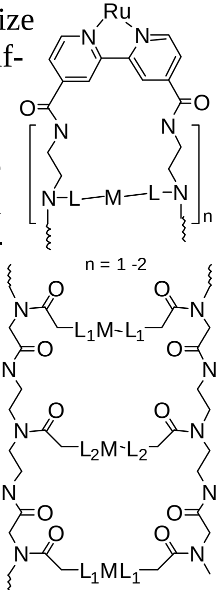

Figure 1. Two general structural motifs in the proposed experiments are (top) palindomic sequences and (bottom) hairpins, where M is Cu (II), L is bpy, and n is the number of repeat units on the chain.

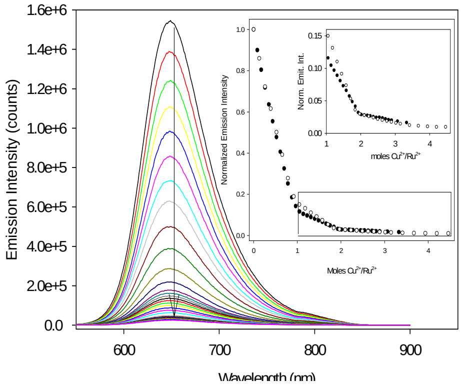

Figure 2. Spectrophotometric titration of Cu^{2+} into an acetonitrile solution of the Ru-$(bpy\text{-}bpy)_2$ hairpin.

The lower structure in Figure 1 is a new structural motif that uses symmetrical chains and palindromic sequences, which are designed to cross-link by coordination to three tetra-coordinate metal ions. Our initial studies have focused on preparation of a bpy-containing tripeptide as a starting point, and most recently the py-bpy-py and tpy-bpy-tpy tripeptides. This series is being used to demonstrate our ability to control duplex formation with two separate chains so that more complex and photoactive structures can be made.

EXPLORING COMPLEX OXIDES AND GRAPHENE FOR DYE-SENSITIZED SEMICONDUCTORS: SYNTHESIS, ASSEMBLY AND PHOTOELECTROCHEMISTRY

Yiying Wu, Mario A. Alpuche, Panitat Hasin, Gayatri Natu
Department of Chemistry
Ohio State University
Columbus, Ohio 43210

(1) Complex oxides for dye-sensitized solar cells (DSC). DSC is a promising alternative to the conventional Si p-n junction cells. An important component in DSC is the porous anode made of a wide-band-gap oxide for supporting sensitizers and conducting electrons. Previous efforts have been limited to binary oxides such as anatase TiO_2, ZnO and SnO_2 with little attention on complex oxides. However, complex oxides can provide the flexibility in tuning chemical and physical properties for dye anchoring and energy alignment. Complex oxides are also interesting for photocatalysis and transparent conducting electrodes. Therefore, a systematic study on complex oxides will have significant impact on photovoltaics and solar fuels.

In this poster we will report Zn_2SnO_4-based DSC and discuss its advantages and limitation in comparison with TiO_2, ZnO and SnO_2. We have also developed photoelectrochemical methods to measure the band structure of Zn_2SnO_4 (Fig. 1). We have established the band gap and the positions of conduction band edge, E_{CB}, and valence band edge, E_{vB}. We have also observed novel binding geometry of dye molecules based on the ATR-FTIR measurements. Other oxides such as Cd_2SnO_4 and $CdSnO_3$ are under investigation, and promising preliminary results have been obtained.

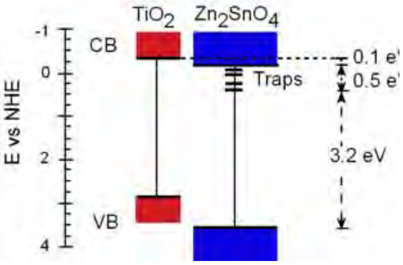

Figure 1. Comparative energy diagram of TiO_2 and Zn_2SnO_4 in aqueous solution at pH 4.8.

(2) Graphene: assembly and electrocatalytic performance. Graphene has been used as transparent conductor to replace FTO or ITO in DSC. At the anode, it is desirable to minimize the electron recombination with tri-iodide (I_3^-). Interestingly, graphite and carbon black have also been used for DSC cathode, which requires fast electrocatalytic reduction of I_3^-. These opposite requirements on the same material motivate us to investigate the fundamental electrocatalytic property of graphene films obtained from reduction of graphene oxide. In addition, we have also made an interesting discovery that graphene oxide nanosheets can be used for large-area, unidirectional alignment of nanowires (Fig. 2). The observation and detailed mechanism will be described in the poster.

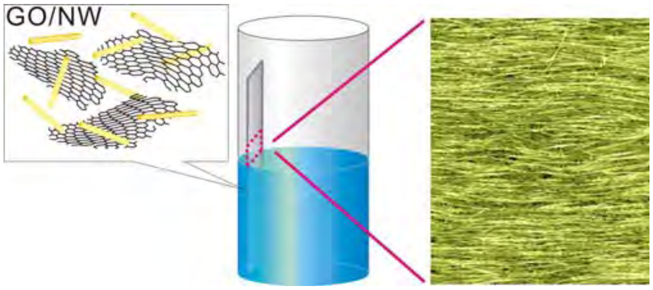

Figure 2: Coassembly of graphene oxide (GO) nanosheets and nanowires (NW) for nanowire alignment.

(3) Low-cost electrocatalysts for counter electrodes in dye cells. In this part, we will report the improved the electrocatalytic activity of Pt nanoparticles by using Nb-doped mesoporous TiO_2 as the support.

List of Participants

Participants List - 31st DOE Solar Photochemistry Research Meeting

Neal Armstrong
University of Arizona
Department of Chemistry
Tucson, AZ 85721
Phone: 520-621-8242
E-Mail: nra@email.arizona.edu

Paul Barbara
University of Texas
Austin, TX 78712
Phone: 512-471-2053
E-Mail: p.barbara@mail.utexas.edu

Matt Beard
NREL
1617 Cole Blvd.
Golden, CO 80020
Phone: 303-384-6781
E-Mail: matt.beard@nrel.gov

Jeffrey Blackburn
National Renewable Energy Laboratory (NREL)
1617 Cole Boulevard
Golden, CO 80401
Phone: 303-384-6649
E-Mail: jeffrey.blackburn@nrel.gov

Andrew Bocarsly
Princeton University
Frick Laboratory
Princeton, NJ 08544
Phone: 609-258-3888
E-Mail: bocarsly@princeton.edu

James Brainard
National Renewable Energy Laboratory (NREL)
1617 Cole Boulevard
Golden, CO 80401
Phone: 303-384-6462
E-Mail: james.brainard@nrel.gov

Gary Brudvig
Yale University
Department of Chemistry
New Haven, CT 06520-8107
Phone: 203-432-5202
E-Mail: gary.brudvig@yale.edu

Marc Baldo
MIT
77 Massachusetts Ave.
Cambridge, MA 02139
Phone: 617-452-5132
E-Mail: baldo@mit.edu

Victor Batista
Yale University
P.O. Box 208107
New Haven, CT 06520-8107
Phone: 203-432-6672
E-Mail: victor.batista@Yale.edu

David Beratan
Duke University
Box 90346
Durham, NC 27708
Phone: 919-660-1526
E-Mail: david.beratan@duke.edu

David Blank
University of Minnesota
207 Pleasant St. SE
Minneapolis, MN 55455
Phone: 612-624-0571
E-Mail: blank@umn.edu

David Bocian
University of California, Riverside
Chemistry, U. C. Riverside
Riverside, CA 92521
Phone: 951-827-3660
E-Mail: David.Bocian@ucr.edu

Karen Brewer
Virginia Tech
Department of Chemistry
Blacksburg, VA 24061-0212
Phone: 540-231-6579
E-Mail: kbrewer@vt.edu

Louis Brus
Chemistry Department, Columbia Univ.
3000 Broadway
New York, NY 10027
Phone: 212-854-4041
E-Mail: leb26@columbia.edu

Participants List - 31st DOE Solar Photochemistry Research Meeting

Emilio Bunel
Argonne National Laboratory
9700 South Cass Avenue
Argonne, IL 60439
Phone: 630-252-4309
E-Mail: ebunel@anl.gov

Ian Carmichael
Notre Dame Radiation Laboratory
University of Notre Dame
Notre Dame, IN 46556
Phone: 574-631-4502
E-Mail: carmichael.1@nd.edu

Michael Casassa
Basic Energy Sciences, US Dept of Energy
19901 Germantown Road
Germantown, MD 20874
Phone: 301-903-0448
E-Mail: michael.casassa@science.doe.gov

Lin Chen
Argonne National Lab/Northwestern Univ.
Building 200, 9700 S. Cass Ave.
Argonne, IL 60439
Phone: 630-252-3533
E-Mail: lchen@anl.gov

Kyoung-Shin Choi
Purdue University
Department of Chemistry
West Lafayette, IN 47907
Phone: 765-494-0049
E-Mail: kchoi1@purdue.edu

Philip Coppens
University at Buffalo, SUNY
732 NSc Complex
Buffalo, NY 14221
Phone: 716-645-6800
E-Mail: coppens@buffalo.edu

Carol Creutz
BNL Chemistry
P. O. Box 204
East Moriches, NY 11940
Phone: 631-878-1954
E-Mail: ccreutz@gmail.com

Niels Damrauer
University of Colorado at Boulder
Campus Box 215
Boulder, CO 80309
Phone: 303-335-1280
E-Mail: niels.damrauer@colorado.edu

Prabir Dutta
The Ohio State University
120 West 18th Avenue
Columbus, OH 43210
Phone: 614-292-4532
E-Mail: dutta.1@osu.edu

Richard Eisenberg
University of Rochester
Department of Chemistry
Rochester, NY 14627
Phone: 585-275-5573
E-Mail: eisenberg@chem.rochester.edu

Richard Eisenberg
University of Rochester
Department of Chemistry
Rochester, NY 14627
Phone: 585-275-5573
E-Mail: eisenberg@chem.rochester.edu

Randy Ellingson
The University of Toledo
2801 W. Bancroft St.
Toledo, OH 43606
Phone: 419-530-2648
E-Mail: randy.ellingson@utoledo.edu

C Michael Elliott
Department of Chemistry
Colorado State University
Fort Collins, CO 80523
Phone: 970-491-5204
E-Mail: Elliott@lamar.colostate.edu

Graham Fleming
Berkeley Lab & Univ. of California, Berkeley
1145 Contra Costa Drive
El Cerrito, CA 94530
Phone: 510-643-2735
E-Mail: grfleming@lbl.gov

Participants List - 31st DOE Solar Photochemistry Research Meeting

Marye Anne Fox
UCSD
1530 Soledad Ave.
La Jolla, CA 92037
Phone: 858-534-3136
E-Mail: mafox@ucsd.edu

Heinz Frei
Lawrence Berkeley National Laboratory
1 Cyclotron Road
Berkeley, CA 94720
Phone: 510-486-4325
E-Mail: HMFrei@lbl.gov

Etsuko Fujita
Brookhaven National Laboratory
Chemistry Department
Upton, NY 11973-5000
Phone: 631-344-4356
E-Mail: fujita@bnl.gov

Wayne Gladfelter
University of Minnesota
Department of Chemistry
Minneapolis, MN 55455
Phone: 612-624-4391
E-Mail: wlg@umn.edu

Richard Greene
Basic Energy Sciences, US Dept of Energy
19901 Germantown Road
Germantown, MD 20874
Phone: 301-903-6190
E-Mail: Richard.Greene@science.doe.gov

Mary Gress
DOE Retired
107 Biltmore
St. Simons Island, GA 31522
Phone: 912-638-8907
E-Mail: marygress@bellsouth.net

Craig Grimes
Penn State University
217 MRL
University Park, PA 16827
Phone: 814-865-9142
E-Mail: cgrimes@engr.psu.edu

Arthur Frank
National Renewable Energy Laboratory
1617 Cole Blvd.
Golden, CO 80401
Phone: 303-384-6262
E-Mail: afrank@nrel.gov

Richard Friesner
Columbia University, Dept. of Chemistry
3000 Broadway, MC 3110
New York, NY 10027
Phone: 212-854-7606
E-Mail: ec31@columbia.edu

Elena Galoppini
Rutgers University
73 Warren Street
Newark, NJ 07102
Phone: 973-353-5317
E-Mail: galoppin@rutgers.edu

Ian Gould
Arizona State University
Dept. of Chemistry and Biochemistry
Tempe, AZ 85281
Phone: 480-965-7278
E-Mail: igould@asu.edu

Brian Gregg
National Renewable Energy Laboratory
1617 Cole Blvd.
Golden, CO 80401
Phone: 303-384-6635
E-Mail: brian.gregg@nrel.gov

David Grills
Brookhaven National Laboratory
PO Box 5000
Upton, NY 11973
Phone: 631-344-4332
E-Mail: dcgrills@bnl.gov

Devens Gust
Department of Chemistry
Arizona State University
Tempe, AZ 85287-1604
Phone: 480-965-4547
E-Mail: gust@asu.edu

Participants List - 31st DOE Solar Photochemistry Research Meeting

Alexander Harris
Brookhaven National Laboratory
Chemistry Dept, Building 555
Upton, NY 11973
Phone: 631-344-4301
E-Mail: alexh@bnl.gov

Michael Henderson
PNNL
PO Box 999, MS K8-87
Richland, WA 99352
Phone: 509-371-6527
E-Mail: ma.henderson@pnl.gov

Dewey Holten
Washington University
Chemistry, One Brookings Dr.
St. Louis, MO 63130
Phone: 314-935-6502
E-Mail: holten@wustl.edu

Libai Huang
Notre Dame Radiation Laboratory
University of Notre Dame
Notre Dame, IN 46615
Phone: 574-631-2657
E-Mail: lhuang2@nd.edu

James Hurst
Washington State University
301 Fulmer Hall
Pullman, WA 99164-4630
Phone: 509-432-3194
E-Mail: hurst@wsu.edu

David Jonas
University of Colorado
215 UCB
Boulder, CO 80309-0215
Phone: 303-492-3818
E-Mail: david.jonas@colorado.edu

David Kelley
University of California, Merced
5200 N. Lake Rd.
Merced, CA 95344
Phone: 209-228-4354
E-Mail: dfkelley@ucmerced.edu

Michael Heben
The University of Toledo
2600 Dorr St.
Toledo, OH 43607
Phone:
E-Mail: michael.heben@utoledo.edu

Craig Hill
Emory University
1515 Dickey Dr. NE
Atlanta, GA 30322
Phone: 404-727-6611
E-Mail: chill@emory.edu

Michael Hopkins
Department of Chemistry, 929 E. 57th Street
The University of Chicago
Chicago, IL 60637
Phone: 773-702-6490
E-Mail: mhopkins@uchicago.edu

Joseph Hupp
Northwestern University
2145 Sheridan Road
Evanston, IL 60208
Phone: 847-491-3504
E-Mail: j-hupp@northwestern.edu

Justin Johnson
National Renewable Energy Laboratory
1617 Cole Boulevard
Golden, CO 80401
Phone: 303-384-6190
E-Mail: justin.johnson@nrel.gov

Prashant Kamat
University of Notre Dame
Radiation Laboratory
Notre Dame, IN 46556
Phone: 574-631-5411
E-Mail: pkamat@nd.edu

Lowell Kispert
The University of Alabama
Dept. of Chemistry
250 Hackberry Lane
Tuscaloosa, AL 35487-0336
Phone: 205-348-7134
E-Mail: lkispert@bama.ua.edu

Participants List - 31st DOE Solar Photochemistry Research Meeting

Valeria Kleiman
University of Florida
PO BOX 117200
Gainesville, FL 32605
Phone: 352-392-4656
E-Mail: kleiman@chem.ufl.edu

Bern Kohler
The Ohio State University
100 W. 18th Ave.
Columbus, OH 43210
Phone: 614-688-3944
E-Mail: kohler@chemistry.ohio-state.edu

Frederick Lewis
Northwestern University
Department of Chemistry
Evanston, IL 60208
Phone: 847-491-3441
E-Mail: fdl@northwestern.edu

Tianquan Lian
Emory University
1515 Dickey Drive
Atlanta, GA 30322
Phone: 404-727-6649
E-Mail: tlian@emory.edu

Mark Lonergan
University of Oregon
1253 Department of Chemistry
Eugene, OR 97403-1253
Phone: 541-344-1253
E-Mail: lonergan@uoregon.edu

Paul Maggard
North Carolina State University
532 Cayman Avenue
Holly Springs, NC 27540
Phone: 919-557-4814
E-Mail: paul_maggard@ncsu.edu

Kent Mann
University of Minnesota
Chemistry Department
Minneapolis, MN 55455
Phone: 651-484-3792
E-Mail: krmann@umn.edu

Victor Klimov
Los Alamos National Laboratory
MS-J567
Los Alamos, NM 87545
Phone: 505-665-8284
E-Mail: klimov@lanl.gov

Todd Krauss
University of Rochester
120 Trustee Road
Rochester, NY 14726-0216
Phone: 585-275-5093
E-Mail: krauss@chem.rochester.edu

Nathan Lewis
California Institute of Technology
1200 E. California Bl-mc 127-72
Pasadena, CA 91125
Phone: 626-395-6335
E-Mail: nslewis@caltech.edu

Jonathan Lindsey
North Carolina State University
CB8204
Raleigh, NC 27695-8204
Phone: 919-515-6406
E-Mail: jlindsey@ncsu.edu

Margaret Lyday
ORAU
PO Box 117
Oak Ridge, TN 37830
Phone: 865-576-2922
E-Mail: Margaret.Lyday@orise.orau.gov

Thomas Mallouk
The Pennsylvania State University
104 Chemistry Building
University Park, PA 16802
Phone: 814-863-9637
E-Mail: tom@chem.psu.edu

Marie Mapes
DOE Solar Energy Technologies Program
1000 Independence Ave.
Washington, DC 20585
Phone: 202-586-3765
E-Mail: marie.marie@ee.doe.gov

Diane Marceau
Basic Energy Sciences, US Dept of Energy
19901 Germantown Road
Germantown, MD 20874
Phone: 301-903-0235
E-Mail: diane.marceau@science.doe.gov

Dmitry Matyushov
Arizona State University
PO Box 871604
Tempe, AZ 85287
Phone: 480-965-0057
E-Mail: dmitrym@asu.edu

James McCusker
Michigan State University
Department of Chemistry
East Lansing, MI 48824-1322
Phone: 517-355-9715
E-Mail: jkm@chemistry.msu.edu

Dan Meisel
University of Notre Dame
Radiation Lab
Notre Dame, IN 46556
Phone: 574-631-5457
E-Mail: dani@nd.edu

Gerald Meyer
Johns Hopkins University
3400 N Charles St
Baltimore, MD 21218
Phone: 410-516-7319
E-Mail: meyer@jhu.edu

Thomas Moore
Center for Bioenergy and Photosynthesis
Arizona State University
Tempe, AZ 85287
Phone: 480-965-3308
E-Mail: tmoore@asu.edu

James Muckerman
Brookhaven National Laboratory
Chemistry Department
Upton, NY 11973-5000
Phone: 631-344-4368
E-Mail: muckerma@bnl.gov

Mark Maroncelli
Penn State
104 Chemistry Building
University Park, PA 16802
Phone: 814-865-0898
E-Mail: maroncelli@psu.edu

Jeffrey Mazer
DOE Solar Energy Technologies Program
1000 Independence Ave., SW
Washington, DC 20585
Phone: 202-586-2455
E-Mail: jeffrey.mazer@ee.doe.gov

Gail McLean
Basic Energy Sciences, US Dept of Energy
19901 Germantown Road
Germantown, MD 20874
Phone: 301-903-7807
E-Mail: Gail.McLean@science.doe.gov

Thomas Meyer
University of North Carolina at Chapel Hill
Department of Chemistry
Chapel Hill, NC 27599-3290
Phone: 919-843-8313
E-Mail: tjmeyer@unc.edu

John Miller
Brookhaven National Lab
Chemistry 555
Upton, NY 11973
Phone: 631-344-4354
E-Mail: jrmiller@bnl.gov

Ana Moore
Center for Bioenergy and Photosynthesis
Arizona State University
Tempe, AZ 85287
Phone: 480-965-2953
E-Mail: amoore@asu.edu

Djamaladdin Musaev
Emory University
1515 Dickey Dr., Department of Chemistry
Atlanta, GA 30322-2210
Phone: 404-727-2382
E-Mail: dmusaev@emory.edu

Participants List - 31st DOE Solar Photochemistry Research Meeting

Nathan Neale
National Renewable Energy Laboratory (NREL)
1617 Cole Boulevard
Golden, CO 80401
Phone: 303-384-6165
E-Mail: nathan.neale@nrel.gov

Marshall Newton
Brookhaven National Laboratory
Chemistry Department
Upton, NY 11973
Phone: 631-751-6580
E-Mail: newton@bnl.gov

Daniel Nocera
Massachusetts Institute of Technology
77 Massachusetts Avenue
Cambridge, MA 02139
Phone: 617-253-5537
E-Mail: nocera@mit.edu

Arthur Nozik
NREL
1617 Cole Blvd.
Golden, CO 80401
Phone: 303-384-6603
E-Mail: anozik@nrel.gov

John Papanikolas
University of North Carolina at Chapel Hill
Department of Chemistry
Chapel Hill, NC 27599
Phone: 919-962-1619
E-Mail: john_papanikolas@unc.edu

Bruce Parkinson
University of Wyoming
Department of Chemistry
Laramie, WY 82071
Phone: 307-766-9891
E-Mail: bparkin1@uwyo.edu

Mark Pederson
Basic Energy Sciences, US Dept of Energy
SC-22.1/Germantown Building
Washington, DC 20585-1290
Phone: 301-903-9956
E-Mail: mark.pederson@science.doe.gov

Piotr Piotrowiak
Rutgers University
73 Warren Street
Newark, NJ 07102
Phone: 973-353-5318
E-Mail: piotr@andromeda.rutgers.edu

Oleg Poluektov
Argonne National Laboratory
9700 South Cass Ave.
Argonne, IL 60439
Phone: 630-252-3546
E-Mail: Oleg@anl.gov

Oleg Prezhdo
University of Washington
Department of Chemistry
Seattle, WA 98195
Phone: 206-354-5341
E-Mail: prezhdo@u.washington.edu

Jeff Pyun
University of Arizona
1306 E. University Blvd.
Tucson, AZ 85721
Phone: 520-626-1834
E-Mail: jpyun@email.arizona.edu

Larry Rahn
Basic Energy Sciences, US Dept of Energy
19901 Germantown Road
Germantown, MD 20874-1920
Phone: 301-903-2508
E-Mail: larry.rahn@science.doe.gov

John Reynolds
University of Florida
PO Box 117200
Gainesville, FL 32611
Phone: 352-392-9151
E-Mail: cgoogins@chem.ufl.edu

Dean Roddick
University of Wyoming, Chemistry Dept.
1000 E. University Ave.
Laramie, WY 82071
Phone: 307-766-2535
E-Mail: dmr@uwyo.edu

Participants List - 31st DOE Solar Photochemistry Research Meeting

Garry Rumbles
National Renewable Energy Lab.
1617 Cole Boulevard
Golden, CO 80401-3393
Phone: 303-384-6502
E-Mail: garry.rumbles@nrel.gov

Kirk Schanze
University of Florida
Chemistry/UF POB 117200
Gainesville, FL 32608-4141
Phone: 352-336-5630
E-Mail: kschanze@chem.ufl.edu

Charles Schmuttenmaer
Yale University, Department of Chemistry
225 Prospect St., PO Box 20810
New Haven, CT 06520-8107
Phone: 203-432-5049
E-Mail: charles.schmuttenmaer@yale.edu

Robert Stack
Basic Energy Sciences, US Dept of Energy
19901 Germantown Rd.
Germantown, MD 20874
Phone: 301-903-5652
E-Mail: robert.stack@science.doe.gov

Randolph Thummel
University of Houston
136 Fleming
Houston, TX 77204-5003
Phone: 713-743-2734
E-Mail: thummel@uh.edu

Lisa Utschig
Argonne National Laboratory
9700 S. Cass Ave.
Argonne, IL 60439
Phone: 630-252-3544
E-Mail: utschig@anl.gov

David Waldeck
University of Pittsburgh
329 Parkman Avenue
Pittsburgh, PA 15260
Phone: 412-624-8430
E-Mail: dave@pitt.edu

S. Scott Saavedra
Univ. of Arizona, Department of Chemistry
1306 E University
Tucson, AZ 85721-0041
Phone: 520-751-1457
E-Mail: saavedra@u.arizona.edu

Russell Schmehl
Tulane University
Department of Chemistry
New Orleans, LA 70118
Phone: 504-862-3566
E-Mail: russ@tulane.edu

Mark Spitler
Basic Energy Sciences, US Dept of Energy
18327 Tapwood Road
Boyds, MD 20841
Phone: 301-903-4568
E-Mail: mark.spitler@science.gov

Michael Therien
Duke University
124 Science Drive
Durham, NC 27708-0346
Phone: 919-660-1670
E-Mail: michael.therien@duke.edu

David Tiede
Argonne National Laboratory
9700 South Cass Avenue
Argonne, IL 60439
Phone: 630-252-3539
E-Mail: tiede@anl.gov

Jao van de Lagemaat
NREL
1617 Cole Blvd.
Golden, CO 80401
Phone: 303-384-6143
E-Mail: jao_vandelagemaat@nrel.gov

Michael Wasielewski
Northwestern University, Dept. of Chemistry
2145 N. Sheridan Rd.
Evanston, IL 60208-3113
Phone: 847-467-1423
E-Mail: m-wasielewski@northwestern.edu

Participants List - 31st DOE Solar Photochemistry Research Meeting

James Whitesell
UCSD
1530 Soledad Ave.
La Jolla, CA 92037
Phone: 858-349-3182
E-Mail: jkwhitesell@mac.com

Mary Beth Williams
Penn State
Department of Chemistry
University Park, PA 16801
Phone: 814-865-8859
E-Mail: mbw@chem.psu.edu

Yiying Wu
Ohio State University
100 W18th Avenue
Columbus, OH 43210
Phone: 614-247-7810
E-Mail: wu@chemistry.ohio-state.edu

Xiaoyang Zhu
University of Minnesota
Department of Chemistry
Minneapolis, MN 55455
Phone: 612-624-7849
E-Mail: zhu@cm.utexas.edu

Author Index

Ahn, T. 123
Akdag, A. 136
Allen, L. 116
Alpuche, M. A. 163
Arachchige, S. 111
Ardo, S. 145
Armstrong, N. R. 86
Arzhantsev, S. 144
Asaoka, S. 147
Ashbrook, L. 122
Attenkofer, K. 113
Baker, D. 137
Balamurugan, D. 108
Baldo, M. 105
Bang, J. H. 137
Barbara, P. F. 106
Batista, V. S. 53, 116, 157
Beard, M. C. 107, 131
Bender, S. 31
Benedict, J. 115
Beratan, D. N. 108
Besson, C. 7
Blackburn, J. L. 99, 109, 131
Blank, D. A. 67
Bocian, D. F. 110, 132, 143
Bolinger, J. C. 106
Bonnell, D. A. 158
Bovachevarov, A. 126
Brennaman, M. K. 146
Brennan, B. 130
Brennessel, W. 120
Brewer, K. J. 111
Bricaud, Q. 154, 155
Bridgewater, J. 130
Brown, A. 70
Brudvig, G. W. 53, 116, 157
Brus, L. 112, 126
Cabelli, D. 117
Calhoun, T. 123
Cao, R. 7
Cape, J. L. 135
Carlson, L. J. 140
Carmieli, R. 160
Chambers, S. A. 45
Chen, J. 156
Chen, L. X. 31, 35, 113
Cheng, Y.-C. 123
Cho, B. 77
Choi, K.-S. 114
Coffey, D. 99
Cohen, B. W. 117
Concepcion, J. J. 146
Cook, A. R. 147
Coppens, P. 115
Crabtree, R. H. 53, 116, 157
Creutz, C. 117
Damrauer, N. H. 118
Deason, B. 25
Delgado, J. 152
Deng, Z. 10
Deria, P. 109, 158
Diers, J. R. 110
Difley, S. 105
Doherty, M. D. 128
Du, P. 120
Du, Y. 45
Dutta, P. 119
Dyakonov, V. 152
Eguchi, M. 83
Eisenberg, R. 120
Ellingson, R. J. 107, 121
Elliott, C. M. 122
Engtrakul, C. 131
Feng, X. 129
Ferguson, A. 99, 109
Fleming, G. R. 123
Focsan, A. L. 139
Fox, M. A. 161
Frank, A. J. 125, 149
Frei, H. 56
Friesner, R. A. 126
Fujita, E. 13, 59, 128
Gallagher, J. A. 162
Galoppini, E. 127
Geletii, Y. V. 7, 142, 148
Gervaldo, M. 130
Giacobbe, E. M. 160
Gladfelter, W. L. 67
Gotesman, G. 159
Gould, I. R. 25
Gregg, B. A. 93
Grills, D. C. 128
Grimes, C. A. 129
Grumstrup, E. M. 118
Gu, J. 156
Gundlach, L. 151
Guo, D. 70
Gust, D. 83, 130

Hardcastle, K. I. 7
Hasin, P. 163
Hata, H. 83
Heben, M. J. 99, 109, 131
Heidel, T. 105
Henderson, M. A. 45
Hill, C. L. 7, 142, 148
Hill, R. 77
Hoertz, P. G. 83
Holten, D. 110, 132, 143
Hopkins, M. D. 18
Hou, Y. 7, 142
Huang, L. 31, 133
Huang, Z. 7, 142
Hupp, J. T. 134
Hurst, J. K. 135
Imahori, H. 147
Ishizaki, A. 123
Ito, N. 25
Jamula, L. 70
Jarosz, P. 120
Jellison, L. 83
Jennings, G. 113
Jiang, H. 155
Jin, H. 144
Johnson, J. C. 136
Jonas, D. M. 77
Jurss, J. 146
Kaledin, A. L. 7, 148
Kamat, P. V. 137
Kang, Y. K. 158
Keller, J. M. 147
Kelley, D. F. 138
Kelly, R. M. 162
Khvorostov, A. 127
Kim, I. 31
Kim, S. H. 158
Kimball, G. M. 41
King, P. W. 131
Kispert, L. D. 139
Kleiman, V. D. 154, 155
Klimov, V. 75
Kobayashi, Y. 83
Kodis, G. 130
Kohler, B. 119
Konovalova, T. A. 139
Kopidakis, N. 99
Krauss, T. D. 140
Kumurlu, S. 154
Kuznetsov, A. E. 7, 148
Lackowski, W. M. 106
Lair, D. 138
LaMontagne, D. 155
Larsen, B. 109
LaTempa, T. J. 129
Law, M. 107
Lazarides, T. 120
Lazorski, M. 122
Lee, A. J. 140
Lee, C. H. 127
Lee, K. J. 106
Lee, O.-S. 158
Lee, S. H. 154
Lee, S.-H. A. 83
Levine, L. A. 162
Lewis, F. D. 141
Lewis, N. S. 41
Li, G. 157
Li, X. 144
Lian, T. 7, 142, 148
Liang, M. 144
Liang, Z. 93
Liddell, P. A. 130
Lindsey, J. S. 110, 132, 143
Lockard, J. V. 31, 35, 113
Lonergan, M. C. 96
Lovaasen, B. M. 18
Luo, G. 120
Lyubinetsky, I. 45
Ma, R. 83
Maeda, K. 83
Maggard, P. A. 48
Mallouk, T. E. 83
Mann, K. R. 67
Maroncelli, M. 144
Martin, N. 152
Mass, O. 143
Matyushov, D. V. 25
McCormick, T. 120
McCusker, J. K. 70
McDonald, K. J. 114
McIlroy, S. 147
McNamara, B. 116
Meisel, D. 88
Meyer, G. J. 145
Meyer, T. J. 146
Mi, Q. 160
Michl, J. 136

Mickley, S. M. 160
Midgett, A. 107
Milikisiyants, S. 35
Miller, J. R. 147
Milot, R. L. 157
Mirafzal, H. 138
Molnár, P. 139
Montgomery, M. A. 118
Moore, A. L. 83, 130
Moore, T. A. 83, 130
Moriena, G. 154
Morris, A. J. 145
Muckerman, J. T. 13, 59
Mukherjee, P. 159
Mulder, C. 105
Mulfort, K. L. 31
Musaev, D. G. 7, 142, 148
Myers, C. P. 162
Naaman, R. 159
Natu, G. 163
Neale, N. R. 125, 149
Newton, M. D. 23
Nozik, A. J. 107, 136, 149
O'Hanlon, D. 18
Ohsawa, T. 45
Palacios, R. E. 106
Papanikolas, J. M. 146
Park, T.-H. 158
Parkinson, B. A. 150, 155
Paulose, M. 129
Peters, W. K. 77
Piotrowiak, P. 127, 151
Poluektov, O. G. 31, 35, 152
Polyakov, N. E. 139
Polyansky, D. E. 13
Postnikoff, C. 133
Prezhdo, O. V. 153
Ptaszek, M. 143
Pyun, J. 86
Rangan, K. 111
Reusswig, P. 105
Reynolds, J. R. 154, 155
Richert, R. 25
Richter, C. P. 157
Ricks, A. B. 160
Rocha, J.-D. 109
Rodriguez, J. A. 59
Romero, M. 79
Rumbles, G. 99, 109
Saavedra, S. S. 86
Sambur, J. 150, 155
Saven, J. G. 158
Schanze, K. S. 147, 154, 155
Schlau-Cohen, G. 123
Schmehl, R. 156
Schmuttenmaer, C. A. 53, 116, 157
Schneider, J. 120
Semonin, O. 107
Shao, X. 161
Shibano, Y. 147
Skourtis, S. S. 108
Smeigh, A. 70
Song, H. 132
Speckbacher, M. 132
Sperlich, A. 152
Spray, R. L. 114
Sreearunothai, P. 147
Steigerwald, M. 126
Stickrath, A. B. 113
Svedruzic, D. 131
Swalina, C. 144
Takeda, N. 147
Taniguchi, M. 110, 132, 143
Tarenekar, P. 154
Tenent, R. C. 131
Therien, M. J. 109, 158
Thummel, R. 10
Tiede, D. M. 31, 35
Traub, M. C. 41
Tseng, H.-W. 10
Tvrdy, K. 137
Utschig, L. M. 31, 35
Van de Lagemaat, J. 79
Van Voorhis, T. 105
Vella, J. 155
Waldeck, D. H. 159
Wang, D. 93
Wang, Q. 125
Wang, T. 126
Wang, X. 140
Wasielewski, M. R. 160
White, T. 111
Whitesell, J. K. 161
Wiederrecht, G. 31
Williams, M. E. 162
Woodhouse, M. 93
Wu, M. 159
Wu, Y. 163

Yin, Q. 7
Youngblood, W. J. 83
Yu, L. 132
Zhang, G. 10
Zhang, X. 113
Zhao, X. 154
Zhu, K. 125
Zhu, X. 3
Zigler, D. 111
Zong, R. 10